OPTIMISED MULTI-MARKET FRAMEWORK FOR ELECTRICITY WITH EMISSION MECHANISMS, RENEWABLE ENERGY CERTIFICATES, AND ANCILLARY SERVICES

PRAKAIPETCH MUANGKHIEW

A Thesis Submitted in Partial Fulfillment of the Requirements for
the Degree of Doctor of Philosophy in Electrical Engineering
Suranaree University of Technology
Academic Year 2025

การเพิ่มประสิทธิภาพของกรอบการดำเนินงานหลายตลาดสำหรับตลาดไฟฟ้า พร้อมกลไกการปล่อยมลพิษ ใบรับรองพลังงานหมุนเวียน และบริการเสริมความมั่นคง

นางสาวประกายเพชร ม่วงเขียว

วิทยานิพนธ์นี้เป็นส่วนหนึ่งของการศึกษาตามหลักสูตรปริญญาปรัชญาดุษฎีบัณฑิต
สาขาวิชาวิศวกรรมไฟฟ้า
มหาวิทยาลัยเทคโนโลยีสุรนารี
ปีการศึกษา 2568

OPTIMISED MULTI-MARKET FRAMEWORK FOR ELECTRICITY WITH EMISSION MECHANISMS, RENEWABLE ENERGY CERTIFICATES, AND ANCILLARY SERVICES

Suranaree University of Technology has approved this thesis submitted in partial fulfillment of the requirements for the Degree of Doctor of Philosophy.

Thesis Examining Committee

....

(Assoc. Prof. Dr. Naebboon Hoonchareon)

Chairperson

....

(Assoc. Prof. Dr. Keerati Chayakulkheeree)

Member (Thesis Advisor)

S. NIRUKKANAPORN ....

(Asst. Prof. Dr. Supattana Nirukkanaporn)

Member

....

(Prof. Dr. Thanatchai Kulworawanichpong)

Member

Tosaphol Ratniyomchai ....

(Asst. Prof. Dr. Tosaphol Ratniyomchai)

Member

....

(Assoc. Prof. Dr. Yupaporn Ruksakulpiwat)

Acting Vice Rector for Academic Affairs and Quality Assurance

....

(Assoc. Prof. Dr. Pornsiri Jongkol)

Dean of Institute of Engineering

ประกายเพชร ม่วงเขียว : การเพิ่มประสิทธิภาพของกรอบการดำเนินงานหลายตลาดสำหรับตลาดไฟฟ้า พร้อมกลไกการปล่อยมลพิษ ใบรับรองพลังงานหมุนเวียน และบริการเสริมความมั่นคง (OPTIMISED MULTI-MARKET FRAMEWORK FOR ELECTRICITY WITH EMISSION MECHANISMS, RENEWABLE ENERGY CERTIFICATES, AND ANCILLARY SERVICES)

อาจารย์ที่ปรึกษา : รองศาสตราจารย์ ดร.กีรติ ชยะกุลคีรี, 200 หน้า

คำสำคัญ : บริการเสริมความมั่นคงระบบไฟฟ้า, กลไกราคาคาร์บอน, ตลาดไฟฟ้าแบบบูรณาการ, การส่งกำลังไฟฟ้าเชิงเหมาะที่สุด, ใบรับรองพลังงานหมุนเวียน, ระบบไฟฟ้าของประเทศไทย

ภาคพลังงานไฟฟ้าเป็นแหล่งปล่อยก๊าซคาร์บอนไดออกไซด์จากการใช้พลังงานคิดเป็นสัดส่วนเกือบ 40% ของการปล่อยทั่วโลก ซึ่งสะท้อนถึงความจำเป็นเร่งด่วนของการกำหนดนโยบายเพื่อสนับสนุนการลดคาร์บอนในภาคพลังงาน กลไกการกำหนดราคาคาร์บอน การสร้างรายได้จากใบรับรองพลังงานหมุนเวียน และตลาดบริการเสริมความมั่นคงระบบไฟฟ้าได้รับการนำมาใช้โดยหน่วยงานกำกับดูแลและรัฐบาลเพื่อสร้างแรงจูงใจในการลดการปล่อยและเพิ่มความมั่นคงของระบบ อย่างไรก็ตามการดำเนินงานของแต่ละกลไกอย่างแยกส่วนก่อให้เกิดความซ้ำซ้อน การประสานงานที่ไม่มีประสิทธิภาพ และการจัดสรรทรัพยากรที่ไม่เหมาะสม

งานวิจัยนี้เสนอกรอบการดำเนินงานของการส่งกำลังไฟฟ้าเชิงเหมาะที่สุดแบบบูรณาการ ซึ่งผสานตลาดไฟฟ้าเข้ากับกลไกราคาคาร์บอน รายได้จากใบรับรองพลังงานหมุนเวียน และการจัดหาบริการเสริมความมั่นคงระบบไฟฟ้าภายใต้แบบจำลองการเหมาะที่สุดเพียงหนึ่งเดียว การวิเคราะห์ในรูปแบบหลายสถานการณ์ถูกนำมาใช้เพื่อประเมินผลกระทบจากการบูรณาการตลาดอย่างเป็นลำดับ เริ่มจากการศึกษาปฏิสัมพันธ์ระหว่างการส่งกำลังไฟฟ้าและการจัดเก็บภาษีคาร์บอนภายใต้กลไกราคาแบบสปอต จากนั้นได้ขยายไปสู่การพิจารณาแหล่งพลังงานหมุนเวียนและการซื้อขายใบรับรองพลังงานหมุนเวียนเพื่อประเมินผลเชิงเสริมของกลไกด้านสิ่งแวดล้อมคู่ขนาน ก่อนจะเพิ่มเติมตลาดบริการเสริม โดยให้ความสำคัญกับโปรแกรมตอบสนองด้านความต้องการพลังงานที่สามารถให้บริการสำรองกำลังหมุนได้เมื่อไม่อยู่ในช่วงลดโหลด สุดท้ายจึงนำเสนอกรอบการดำเนินงานตลาดแบบหลายมิติที่ผสานตลาดไฟฟ้า กลไกราคาคาร์บอน ตลาดพลังงานหมุนเวียน และตลาดบริการเสริมความมั่นคงระบบไฟฟฟ้าให้ทำงานร่วมกัน

ผลการวิจัยมีส่วนสำคัญสามประการ ได้แก่ ประการแรกการพัฒนาแบบจำลองทางคณิตศาสตร์เชิงบูรณาการเพื่อประสานกลไกตลาดหลายมิติ ประการที่สองการลดต้นทุนการดำเนินงานระบบรวมภายใต้กรอบการประมูลทางเดียวโดยคำนึงถึงภาษีคาร์บอน รายได้จากใบรับรอง

พลังงานหมุนเวียนและข้อกำหนดของบริการเสริม และประการสุดท้ายการเพิ่มค่าสวัสดิการทางสังคมภายใต้กรอบการประมูลสองทางที่ทั้งผู้ผลิตและผู้จัดจำหน่ายไฟฟ้ามีบทบาทเป็นผู้เข้าร่วมตลาดอย่างแข็งขัน นอกจากนี้ ยังมีการเปรียบเทียบระหว่างการดำเนินตลาดแบบแยกส่วนและแบบบูรณาการเพื่อประเมินประสิทธิผลของกรอบที่เสนอ พร้อมประยุกต์ใช้เทคนิคการหาคำตอบเชิงเหมาะที่สุดที่หลากหลาย ทั้งวิธีเชิงกำหนดแบบดั้งเดิม วิธีเชิงสุ่มแบบเมตาฮิวริสติก รวมถึงวิธีแบบผสมผสานที่ผนวกความสามารถในการค้นหาคำตอบเชิงโลกของเมตาฮิวริสติกเข้ากับความแม่นยำในการปรับแต่งเชิงเฉพาะที่ของวิธีเชิงคณิตศาสตร์ เพื่อเพิ่มคุณภาพและประสิทธิภาพของการคำนวณ

การตรวจสอบเชิงตัวเลขได้ดำเนินการบนระบบทดสอบ IEEE 30 บัสเพื่อยืนยันความถูกต้องของอัลกอริทึม และระบบไฟฟ้าเทียบเท่า 160 บัสของประเทศไทยเพื่อประเมินความเป็นไปได้ในการประยุกต์ใช้จริง ระบบไฟฟ้าของประเทศไทยถือเป็นกรณีศึกษาที่มีความสำคัญ เนื่องจากตลาดการส่งกำลังไฟฟ้า การบัญชีคาร์บอน กลไกพลังงานหมุนเวียน และตลาดบริการเสริมยังคงดำเนินงานแยกจากกัน ผลการจำลองแสดงให้เห็นว่ากรอบแบบบูรณาการสามารถลดการปล่อยคาร์บอนได้เกือบ 5% สร้างการกระจายผลประโยชน์อย่างเป็นธรรมระหว่างผู้บริโภค ผู้ผลิต รัฐบาล และผู้ผลิตพลังงานหมุนเวียน รวมทั้งเพิ่มความมั่นคงของระบบเมื่อเทียบกับแนวทางตลาดแยกส่วน นอกจากนี้ การบูรณาการตลาดยังช่วยเพิ่มประสิทธิภาพของกลไกราคาคาร์บอนและส่งเสริมความคุ้มค่าทางเศรษฐกิจของพลังงานหมุนเวียนผ่านการซื้อขายใบรับรองพลังงานหมุนเวียนที่มีการประสานงานอย่างเหมาะสม อีกทั้งการวิเคราะห์ความไวนั้นยืนยันว่าการประสานกลไกตลาดแบบหลายมิติสามารถลดข้อจำกัดและความขัดแย้งระหว่างประสิทธิภาพทางเศรษฐกิจ ความยั่งยืนด้านสิ่งแวดล้อม และความมั่นคงของระบบได้อย่างมีประสิทธิผล อันจะนำไปสู่แนวทางการเปลี่ยนผ่านสู่ระบบไฟฟ้าคาร์บอนต่ำของประเทศไทยที่ยั่งยืนและมีประสิทธิภาพยิ่งขึ้น

สาขาวิชาวิศวกรรมไฟฟ้า ลายมือชื่อนักศึกษา..

ปีการศึกษา 2568 ลายมือชื่ออาจารย์ที่ปรึกษา ....

PRAKAIPETCH MUANGKHIEW : OPTIMISED MULTI-MARKET FRAMEWORK FOR ELECTRICITY WITH EMISSION MECHANISMS, RENEWABLE ENERGY CERTIFICATES, AND ANCILLARY SERVICES

THESIS ADVISOR : ASSOC. PROF. DR. KEERATI CHAYAKULKHEEREE, D.Eng., 200 PP.

Keyword : ancillary services, carbon pricing mechanism, integrated electricity market, optimal power dispatch, renewable energy certificates, Thai power system

The power sector accounts for nearly 40% of global energy-related carbon dioxide emissions, underscoring the need for urgent policy interventions to support decarbonisation. Carbon pricing mechanisms, renewable energy certificates revenue, and ancillary service markets have been introduced by governments and regulators to incentivise emission reductions and enhance system reliability. However, market fragmentation, coordination inefficiencies, and suboptimal resource allocation result from the independent operation of these mechanisms.

This research proposes a unified optimal power dispatch framework integrating electricity markets with carbon pricing mechanisms, REC revenue, and ancillary service procurement within a single optimisation model. A progressive multi-scenario analysis is employed to evaluate the impacts of market integration systematically. The fundamental interaction between energy dispatch and carbon taxation under spot-pricing mechanisms is examined first. Renewable energy sources and REC trading are subsequently incorporated to assess the synergies from dual environmental incentives. Ancillary service markets are then introduced, with particular emphasis on incentive-based demand response programmes capable of providing spinning reserves when not actively curtailing load. Finally, a comprehensive multi-dimensional market-clearing framework simultaneously coordinating the electricity market, carbon pricing mechanism, renewable energy market, and ancillary services market is presented.

Three principal research contributions are established through this investigation. A unified mathematical optimisation model coordinating multiple market dimensions is formulated. Total system operational costs under single-sided auction frameworks are minimised whilst accounting for carbon tax liabilities, REC revenues, and ancillary service requirements. Social welfare is maximised under double-sided auction frameworks, where both generation companies and distribution companies participate as active market agents. A comparative analysis of segregated and integrated market-clearing approaches is conducted to demonstrate the framework's effectiveness. Multiple optimisation techniques are employed to ensure robust solutions and computational efficiency. Classical deterministic methods provide baseline solutions with guaranteed optimality for convex formulations. Stochastic optimisation algorithms are applied to handle non-convex problem characteristics and explore diverse solution spaces. A hybrid PSO-QP approach combining the global search capability of metaheuristics with the local refinement precision of classical methods is developed, offering improved solution quality and computational performance.

Numerical validation is conducted using the IEEE 30-bus test system for algorithmic verification and the 160-bus equivalent Thai power system for practical applicability assessment. The Thai system represents a particularly relevant case study, given that energy dispatch, carbon accounting, renewable energy incentives, and ancillary service procurement currently operate as segregated mechanisms. Substantial emission reductions approaching 5%, equitable welfare distribution among consumers, producers, government, and renewable energy participants, and enhanced system reliability compared to fragmented market approaches are demonstrated through simulation results. The environmental effectiveness of carbon pricing is amplified, and the economic viability of renewable energy deployment through coordinated REC trading is strengthened by market integration, as confirmed through sensitivity analyses. The inherent trade-offs between economic efficiency, environmental sustainability, and system security that characterise isolated policy instruments can be resolved through multi-dimensional market coordination, thereby supporting more effective pathways toward carbon neutrality in Thailand’s power sector.

School of Electrical Engineering — Student’s Signature ....

Academic Year 2025 — Advisor’s Signature ....

ACKNOWLEDGEMENT

The completion of this doctoral thesis has been intellectually demanding and profoundly rewarding. Its realisation has been made possible through the support, guidance, and encouragement of numerous individuals and institutions, to whom I am deeply indebted.

My sincere and utmost appreciation is extended to my supervisor, Assoc. Prof. Dr. Keerati Chayakulkheeree, whose expert guidance, steadfast support, and thoughtful advice have been central to the development of this research. His academic insight and dedicated mentorship have significantly shaped the direction and quality of this work. I am equally grateful to the thesis examination committee. I offer my appreciation to Assoc. Prof. Dr. Naebboon Hoonchareon, Chair of the committee, for his constructive comments and discerning observations. I further acknowledge the valuable scholarly contributions of Prof. Dr. Thanatchai Kulworawanichpong, Asst. Prof. Dr. Supattana Nirukkanaporn, and Asst. Prof. Dr. Tosaphol Ratniyomchai, whose expertise strengthened the academic rigour and clarity of this thesis. My thanks are also extended to Dr. Nan Zhao of Lancaster University for his academic guidance and professional support during my research placement in the United Kingdom; his insights contributed meaningfully to the refinement of this research.

This research benefitted from the generous support of several funding bodies. I gratefully acknowledge the financial assistance provided by the Suranaree University of Technology Research and Development Fund, which supported the core development of this work. Additional funding was received through Research ID 204158, supported by (i) Suranaree University of Technology (SUT), (ii) Thailand Science Research and Innovation (TSRI), and (iii) the National Science, Research and Innovation Fund (NSRF). I am also profoundly grateful to the National Research Council of Thailand (NRCT) for supporting my doctoral studies under Contract No. N41A670289, which encompassed tuition fees, research expenses, overseas research activities, and a stipend throughout the duration of the programme. I further acknowledge Suranaree

University of Technology for providing an excellent academic environment, advanced research facilities, and continuous opportunities for professional and intellectual development.

Finally, I extend my deepest gratitude to my family, friends, and those whose encouragement and unwavering support have sustained me throughout this academic endeavour. Their confidence in me has been an enduring source of strength. I also acknowledge, with humility, the perseverance and resilience that enabled me to overcome the challenges encountered over the course of this doctoral journey.

PRAKAIPETCH MUANGKHIEW

TABLE OF CONTENTS

Page

TABLE OF CONTENTS (Continued)

Page

TABLE OF CONTENTS (Continued)

Page

TABLE OF CONTENTS (Continued)

TABLE OF CONTENTS (Continued)

LIST OF TABLES

Table | Page

LIST OF TABLES (Continued)

Table Page

LIST OF TABLES (Continued)

LIST OF FIGURES

Figure Page

LIST OF FIGURES (Continued)

LIST OF ABBREVIATIONS

Abbreviation

AGC	= automatic generation control
AS	= ancillary service
ASM	= ancillary services market
BWO	= black widow optimisation
CAGC	= cost of automatic generation control
CCE	= cost of carbon emission
CDR	= cost of demand response
CE	= carbon emissions
CECPS	= competitive electricity-carbon prices scheme
CECRPS	= competitive electricity-carbon-REC prices scheme
CEPS	= competitive electricity price scheme
CG	= cost of generation
CM	= carbon pricing mechanism
CMC	= co-optimised market clearing
CMC-DR	= co-optimised market clearing with demand response
CRE	= cost of renewable energy
CS	= consumer surplus
CSR	= cost of spinning reserve
DISCOs	= distribution companies
DR	= demand response
DSA	= double-sided auction
EM	= electricity market
ETS	= emission trading scheme
GENCOs	= generation companies

LIST OF ABBREVIATIONS (Continued)

GHG = global greenhouse gas
GWO = grey wolf optimisation
ISO = independent system operator
KKT = Karush-Kuhn-Tucker
LMP = locational marginal price
LP = linear programming
MBECPS = market-based electricity-carbon prices scheme
MBECRPS = market-based electricity-carbon-REC prices scheme
MBEPS = market-based electricity price scheme
OPF = optimal power flow
PS = producer surplus
PSO = particle swarm optimisation
QP = quadratic programming
REC = renewable energy certificate
RECR = renewable energy certificate revenue
REM = renewable energy market
RES = renewable energy source
SMC = sequential market clearing
SMC-DR = sequential market clearing with demand response
SR = spinning reserve
SSA = single-sided auction
SW = social welfare
TC = total cost
TCC = total cost to consumer (from spot price)
WOA = whale optimisation algorithm

LIST OF ABBREVIATIONS (Continued)

Symbol

a_i, b_i and c_i	= the coefficients that depend on the GENCOs' willingness to sell behaviours
a_{li}	= the line l sensitivity factor to the active injection power at bus i
AGC_i	= the activated automatic generation control capacity at bus i (MW)
$AGCP_i$	= the automatic generator control price ($ or THB/MWh)
B_{ij}	= the susceptance of the entry in the bus admittance matrix (Y bus)
$B_j(P_{D,j})$	= the consumers willing to buy at the price of the load bus j
c_1 and c_2	= the acceleration constants of PSO
$C_i(P_{G,i})$	= the suppliers willing to sell at the price of the generator bus i.
C_{tax}	= the carbon tax rate ($ or THB/tonCO_2)
$CAGC(P_{G,i})$	= the cost of automatic generation control at bus i ($ or THB/h)
$CCE(P_{G,i})$	= the cost of carbon emission at bus i ($ or THB/h)
$CDR(\delta_{i,j})$	= the cost of demand response for step i by demand response participant j ($ or THB/h)
$CE(P_{G,i})$	= the carbon emission at bus i (ton/h)
$CG(P_{G,i})$	= the cost of generation at bus i ($ or THB/h)
$CRE(P_{RE,r})$	= the cost of renewable energy at bus r ($ or THB/h)
$CSR(P_{G,i})$	= the cost of spinning reserve at bus i ($ or THB/h)
d_j, e_j and k_j	= the non-negative coefficients of the benefit function for the load at bus j from consumer bidding behaviour
EC_i^w	= the electricity cost with carbon emission cost spot pricing ($/h)
EC_i^{wo}	= the electricity cost without carbon emission cost spot pricing ($/h)
f_i, g_i, and h_i	= the coefficients that determine the shape of RE the quadratic curve
$g(x,u)$	= the equality constraint
G_{ij}	= the conductance of the entry in the bus admittance matrix (Y bus)
$h(x,u)$	= the inequality constraint
ITL_i	= the incremental transmission loss

LIST OF ABBREVIATIONS (Continued)

nl = the number of transmission lines

NB = the total number of buses in the power system

NC = the total number of shunt reactors or capacitors

ND = the total number of loads in the power system

NDR = the total number of pricing steps in the demand response program

NG = the total number of generating units in the power system

NP = the number of particles in the population

NRE = the number of renewable energy sources

NT = the total number of transformers with controllable taps

$P_{D,j}$ = the active power demand at bus j

$P_{G,i}$ = the active power output of the generator at bus i (MW)

$P_{G,i}^{\min}$ and $P_{G,i}^{\max}$ = the minimum and maximum active power output limit for the generator bus i, respectively (MW)

P_{loss} = the total active power loss in the transmission network (MW)

$P_{L,j}$ = the active power demand at bus j (MW)

$P_{RE,r}$ = the active renewable energy power output RE at bus r (MW)

$Q_{C,i}^{\max}$ = the minimum and maximum reactive power compensation limits for the shunt device, respectively (MVar)

$Q_{G,i}$ = the reactive power generation at bus i (MVar)

$Q_{G,i}^{\min}$ and $Q_{G,i}^{\max}$ = the minimum and maximum reactive power output limits for the generator bus i, $Q_{C,i}^{\min}$ respectively (MVar)

$Q_{L,j}$ = the reactive power load at bus j (MVar)

r_1 and r_2 = the random values of PSO

R_{total} = the total revenue ($ or THB/h)

$R_{i,j}$ = the price per unit of electricity reduction for step i by demand response participant j ($/MWh)

$RECP$ = the renewable energy certificate price ($ or THB/MWh)

$RECR(P_{RE,r})$ = the renewable energy certificate revenue ($ or THB/h)

S_i = the complex power at bus i

LIST OF ABBREVIATIONS (Continued)

SR_i = the spinning reserve utilisation at bus i (MW)

SRP_i = the spinning reserve price ($ or THB/MWh)

SW = the social welfare ($ or THB/h)

SW_{eco} = the economic social welfare ($ or THB/h)

SW_{post} = the post-transfer social welfare ($ or THB/h)

T_i = the tap setting limits for the transformer i (p.u.)

$T_i^{\min}$ and $T_i^{\max}$ = the minimum and maximum tap setting limits for the transformer, respectively (p.u.)

TC = the total cost ($ or THB/h)

TCC = the total cost to consumer ($ or THB/h)

u = the dependent variable

$V_{G,i}$ = the voltage magnitude for the generator bus i

$V_{G,i}^{\min}$ and $V_{G,i}^{\max}$ = the minimum and maximum voltage magnitude limits for the generator bus i, respectively

w = the inertia weight factor of PSO

x = the control variable

$X_{C,i}$ = the reactance control setting of the shunt reactor i

X_{ij} = the reactance of the transmission line between buses i and j

α_i, β_i and ω_i = the coefficients of carbon emission at bus i

$\delta_{i,j}$ = the amount of load reduction achieved within step i by demand response participant j (MW)

$\delta_{i,j}^{\max}$ = the maximum allowable reduction in step i by demand response participant j (MW)

$\eta_{L,i}$ = the marginal transmission loss at bus i ($/MWh)

$\eta_{QS,i}$ = the network quality of supply at bus i ($/MWh)

λ = the system marginal price ($/MWh)

λ_{AGC} = the automatic generation control marginal price ($/MWh)

λ_{CG} = the energy marginal price ($/MWh)

λ_{CCE} = the carbon emission marginal price ($/MWh)

LIST OF ABBREVIATIONS (Continued)

λ_{SR} = the spinning reserve marginal price ($/MWh)

μ = the penalty factor

μ_l = the reduction in supply cost that results from an incremental relaxation of constraint l ($/MWh)

θ_i and θ_j = the phase angles at buses i and j, respectively

ρ_i = the spot price at bus i ($/MWh)

ρ_i^w = the spot price with carbon emission cost at bus i ($/MWh)

ρ_i^{wo} = the spot price without carbon emission cost at bus i ($/MWh)

$\%AGCR_i$ = the percentage of automatic generator control requirement

$\%SRR_i$ = the percentage of spinning reserve requirement

CHAPTER I

INTRODUCTION

1.1 Background and Significance of the Research Problem

The power sector significantly contributes to global greenhouse gas (GHG) emissions, accounting for nearly 40% of energy-related carbon dioxide emissions worldwide. To mitigate climate change, governments and energy regulators are implementing strategies to reduce emissions from power generation sources. These strategies include clean energy incentives, carbon pricing mechanisms, renewable energy mandates, and emission standards. Collectively, these measures drive emissions reduction efforts and promote investment in low-carbon technologies (IEA, 2022). In competitive electricity markets, independent system operators (ISOs) play a vital role in managing wholesale energy markets and ensuring a secure power supply (Kirschen & Strbac, 2004). The optimal energy dispatch schedules and locational marginal prices (LMPs) are determined by ISOs, reflecting the real-time cost of meeting additional demand at specific nodes within the transmission network (Litvinov, 2010). Energy trading occurs through various auction mechanisms, including single-sided auctions (SSAs), where electricity is offered by generation companies (GENCOs), and double-sided auctions (DSAs), where bids for electricity demand are submitted by distribution companies (DISCOs) (Fu et al., 2023; Wood & Wollenberg, 2014).

In addition to energy market operations, ISOs procure ancillary services to maintain grid reliability and balance supply and demand in real time (Zhou et al., 2016). Services such as regulation reserves, spinning reserves, and non-spinning reserves ensure system stability, especially as renewable energy integration increases (Banshwar et al., 2017; Reddy et al., 2015). Short-term supply-demand imbalances are managed through regulation reserves, while backup capacity in case of sudden generation or transmission outages is provided by spinning and non-spinning reserves. In power pool markets, energy production is optimised by the ISO, with consumption levels and pricing for producers and consumers determined to pass generation costs to consumers reasonably and efficiently (Yang et al., 2021). The importance of ancillary services has been heightened by the increasing penetration of renewable energy sources (RES), such as wind and solar power. While renewable generation is vital for achieving carbon neutrality, grid stability is challenged by the variability and unpredictability inherent in these sources, requiring more flexible, responsive reserves. However, ancillary services are still procured separately from energy markets in many electricity systems, resulting in inefficiencies, higher costs, and a lack of coordination between energy generation and grid reliability needs (Banshwar et al., 2017). To further incentivise renewable energy adoption, renewable energy certificates (RECs) have been introduced (Tao et al., 2021). Market-based rewards for renewable energy generation are provided through these certificates, similar to carbon trading mechanisms. However, REC trading, carbon pricing, and ancillary services often operate independently of energy market functions, leading to suboptimal market outcomes. Cost reduction, increased renewable energy deployment, and enhanced system reliability could be achieved through market integration, as recent research suggests (Hustveit et al., 2017).

This thesis proposes a comprehensive framework to address market fragmentation challenges through a progressive, multi-stage analysis. The fundamental interaction between the energy market and carbon taxation mechanisms is examined in Chapter 3, using a spot-pricing approach to assess the immediate impact of carbon taxes on system operations and market outcomes. The baseline effects of carbon pricing on generation dispatch and electricity costs are established through this foundational analysis. The analysis is extended in Chapter 4 to incorporate renewable energy sources into the system. This chapter examines how carbon taxation interacts with renewable generation and explores the additional economic benefits from REC trading. The synergistic effects of integrating environmental pricing mechanisms with clean energy deployment are revealed by examining the dual incentive structure of carbon costs and renewable certificates. The framework is advanced further in Chapter 5 by introducing the ancillary services market dimension. This chapter examines the integration of energy markets, carbon pricing mechanisms, and ancillary service procurement, with particular emphasis on incentive-based demand response programmes. A key innovation explored in this chapter involves the dual-use capability of demand response resources, which can provide spinning reserves when not actively engaged in load curtailment. System flexibility and security are thereby enhanced while resource utilisation is optimised.

A co-optimised electricity market-clearing framework that simultaneously coordinates four distinct market components is presented in Chapter 6, including electricity market (EM), carbon pricing mechanism (CM), renewable energy market (REM), and ancillary services market (ASM). This integrated optimisation approach addresses the inherent inefficiencies of fragmented market operations by simultaneously optimising electricity dispatch decisions, carbon costs, renewable incentives, and reliability requirements. The computational framework for this integrated approach is illustrated in Figure 1.1. Superior economic efficiency, enhanced environmental performance, and improved system security can be achieved through market integration, as demonstrated by this progressive analytical structure. The proposed framework provides policymakers and system operators with valuable insights for modernising electricity market structures in the context of ambitious decarbonisation targets and increasing renewable energy penetration.

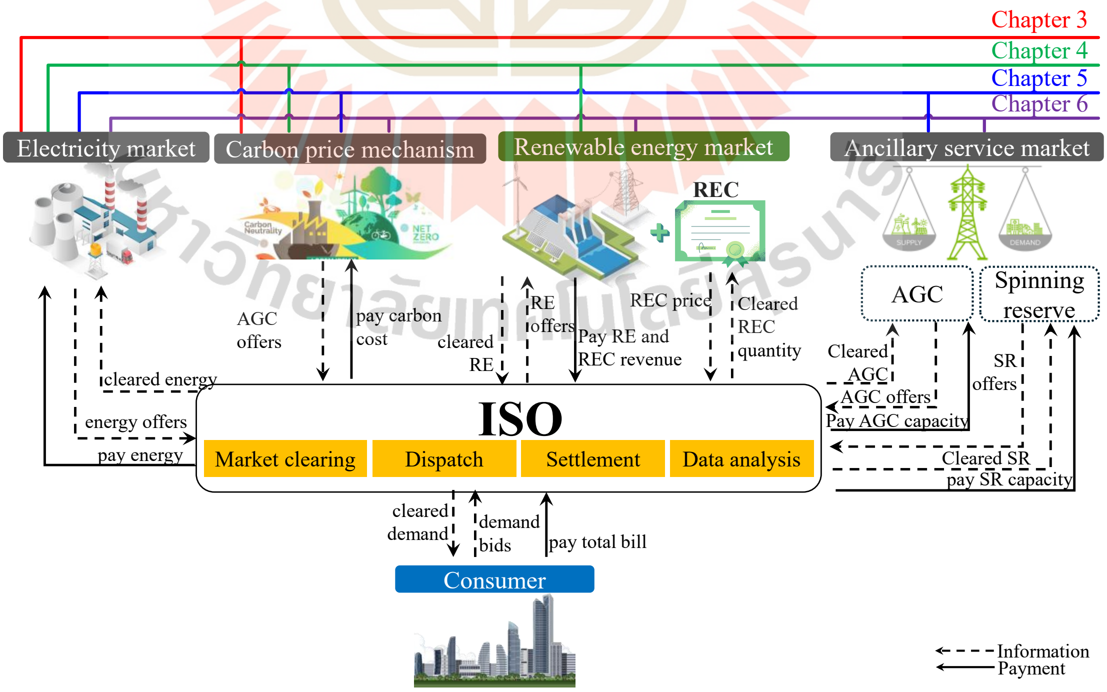

Figure 1.1 The coupling mechanism of the co-optimised market mechanism

1.2 Research Objectives

The main objective of this research is to develop an integrated optimal power dispatch framework that simultaneously considers the interactions among the electricity market, the carbon pricing mechanism, renewable energy sources, renewable energy certificate revenue, and ancillary service markets. The overall aim is to improve market efficiency, environmental performance, and system security through coordinated market clearing. So, to achieve this objective, the study pursues the following specific objectives:

(1) To formulate a co-optimised mathematical optimisation model that coordinates electricity market operations with carbon emission costs, renewable energy certificate revenue, and ancillary service requirements, thereby addressing the inefficiencies inherent in fragmented market structures.

(2) To minimise total system operational costs under a single-sided auction framework where generation companies submit supply offers, with explicit consideration of carbon tax implications, renewable energy certificate revenues, and ancillary service capacity constraints.

(3) To maximise social welfare under a double-sided auction framework where both generation companies and distribution companies participate as market agents, while simultaneously accounting for carbon emission externalities, renewable energy incentives, and system security requirements through ancillary service provision.

(4) To evaluate and compare the economic efficiency, environmental performance, and system security outcomes across different market structures and integration scenarios, providing quantitative evidence for the benefits of multi-dimensional market coordination.

These objectives aim to demonstrate that co-optimised market-clearing mechanisms can achieve superior outcomes in economic efficiency, environmental sustainability, and grid reliability compared to conventional segregated market approaches, thereby providing practical insights for electricity market design and regulatory policy development.

1.3 Scope and Limitations

The scope and limitations of this research are defined as follows:

(1) This research develops an OPF model that integrates the electricity market, carbon pricing mechanism, renewable energy generation, renewable energy certificate trading, and ancillary service requirements within a unified optimisation framework.

(2) The research considers only the carbon tax scheme as the carbon pricing mechanism. Other approaches, such as cap-and-trade systems or emission permit trading, are beyond the scope of this research.

(3) Renewable energy sources are modelled as dispatchable generation units, with analysis focused exclusively on the actual dispatched output quantities. Variability and intermittency associated with renewable generation are not explicitly modelled.

(4) Renewable energy certificate revenues are calculated based on the actual dispatched renewable energy generation, with the assumption that all dispatched renewable energy output is eligible for REC sales.

(5) The study examines two distinct market-clearing schemes: single-sided auctions, where only generation companies submit supply offers, and double-sided auctions, where both generation companies and distribution companies participate as active bidders. The analyses of these auction schemes are conducted to evaluate their impacts on market efficiency and social welfare.

(6) Ancillary services are limited to AGC for frequency regulation and spinning reserve (SR) for contingency response. The analysis focuses solely on the procurement quantities and market-clearing prices of these services. The operational control mechanisms, real-time deployment strategies, and dynamic performance characteristics of ancillary services are beyond the scope of this study. Other ancillary services, such as black-start capability, reactive power support, voltage control, and energy imbalance services, are excluded, as these are typically procured through long-term bilateral contracts and allocated to consumers based on proportional energy consumption.

(7) The research performs a comparative evaluation between separated market mechanisms and the proposed integrated market-clearing framework that combines energy, carbon pricing mechanisms, RES, REC revenue, and ancillary services.

(8) Numerical simulations and validation are conducted using two power system models, including the IEEE 30-bus test system for fundamental analysis and algorithm verification and the 160-bus equivalent Thai power system for practical application.

(9) The research investigates and compares four optimisation algorithms, including particle swarm optimisation (PSO), black widow optimisation (BWO), grey wolf optimiser (GWO), and whale optimisation algorithm (WOA).

These scope definitions ensure focused research development while acknowledging the boundaries within which the proposed framework operates and the simplifying assumptions adopted for tractable mathematical formulation and computational implementation.

1.4 Research Benefit

This study offers several key benefits:

(1) The research develops a novel mathematical framework for simultaneous market-clearing across multiple dimensions, including electricity dispatch, carbon pricing mechanism, renewable energy certificate revenue, and ancillary service procurement. This integrated optimisation approach addresses the theoretical gap in coordinating interdependent market mechanisms that have traditionally operated in isolation and provides a foundation for future research in multi-dimensional electricity market design.

(2) The research demonstrates quantifiable reductions in total system operational costs through the formulation of an integrated optimisation model under single-sided auction structures. By explicitly incorporating carbon tax obligations, renewable energy certificate revenues, and ancillary service requirements within the dispatch optimisation, the proposed mechanism enables system operators to identify cost-effective generation schedules that simultaneously satisfy energy demands, emission constraints, renewable energy targets, and reliability standards. The findings provide practical guidance for independent system operators seeking to enhance economic efficiency whilst managing increasingly complex operational requirements.

(3) The research establishes an integrated market-clearing mechanism for double-sided auction environments that maximises social welfare, defined as the sum of consumer surplus and producer surplus. By coordinating electricity market transactions with carbon pricing, renewable incentives, and ancillary service procurement, the proposed framework ensures that market outcomes reflect the actual economic value and environmental externalities of electricity generation. This approach promotes allocative efficiency and equitable distribution of benefits between supply-side and demand-side market participants, offering valuable insights for regulatory authorities designing competitive electricity markets.

(4) Validation using both the IEEE 30-bus test system and the 160-bus equivalent Thai power system confirms the framework's scalability and practical applicability, offering a methodological reference for real-world implementation in systems with diverse operating conditions. In particular, Thailand's power sector currently functions through segregated mechanisms for electricity dispatch, carbon pricing, renewable incentives, and ancillary service procurement. The proposed integrated market-clearing framework demonstrates that unified coordination across these mechanisms can significantly enhance economic efficiency, reduce operational costs, and improve environmental performance. These results provide evidence-based insights for Thai regulatory authorities seeking to advance market integration reforms amid ongoing electricity transition, decarbonisation, and renewable expansion efforts.

1.5 Thesis Outline

This thesis is organised into six chapters, as shown in Figure 1.2. Chapter 1 introduces the research background, motivation, objectives, and scope of the study, highlighting the necessity of integrating multiple market mechanisms, namely electricity market, carbon pricing mechanism, renewable energy certificates, and ancillary services, within a unified optimisation framework. Chapter 2 presents the theoretical background and literature review relevant to optimal power flow, spot electricity pricing, ancillary service management, carbon pricing mechanisms, and renewable energy certificates. The review establishes the conceptual foundation for developing integrated market-clearing mechanisms and identifies key research gaps addressed in the subsequent chapters.

Chapters 3 to 6 constitute the simulation and analysis components of the study, each addressing a specific aspect of the proposed integrated electricity market framework and its optimisation methodologies. Chapter 3 focuses on integrating the electricity market with a carbon pricing mechanism under both single-sided and double-sided auction schemes. The models are tested on the IEEE 30-bus test system, and optimisation is performed using four stochastic algorithms. Chapter 4 extends the framework by incorporating renewable energy sources and revenue from renewable energy certificates into the joint EM-CM structure. Both single-sided and double-sided auction mechanisms are analysed to examine the influence of renewable participation and REC revenue on market equilibrium. The IEEE 30-bus test system is again employed, and optimisation is performed using the PSO algorithm to determine the optimal dispatch under multiple market configurations.

Chapter 5 introduces ancillary services into the market framework, with a particular emphasis on incentive-based demand response schemes. Two operational approaches, sequential and co-optimised, are modelled under scenarios with and without DR participation. The IEEE 30-bus test system is utilised for simulation, and solutions are derived using quadratic programming and a combined QP-LP approach. Finally, Chapter 6 presents the comprehensive multi-dimensional market-clearing framework under a double-sided auction scheme. The model is applied to the 160-bus equivalent Thai power system to assess real-world applicability. Comparative analyses are performed using deterministic and hybrid PSO-QP optimisation approaches to evaluate performance across economic, environmental, and reliability dimensions.

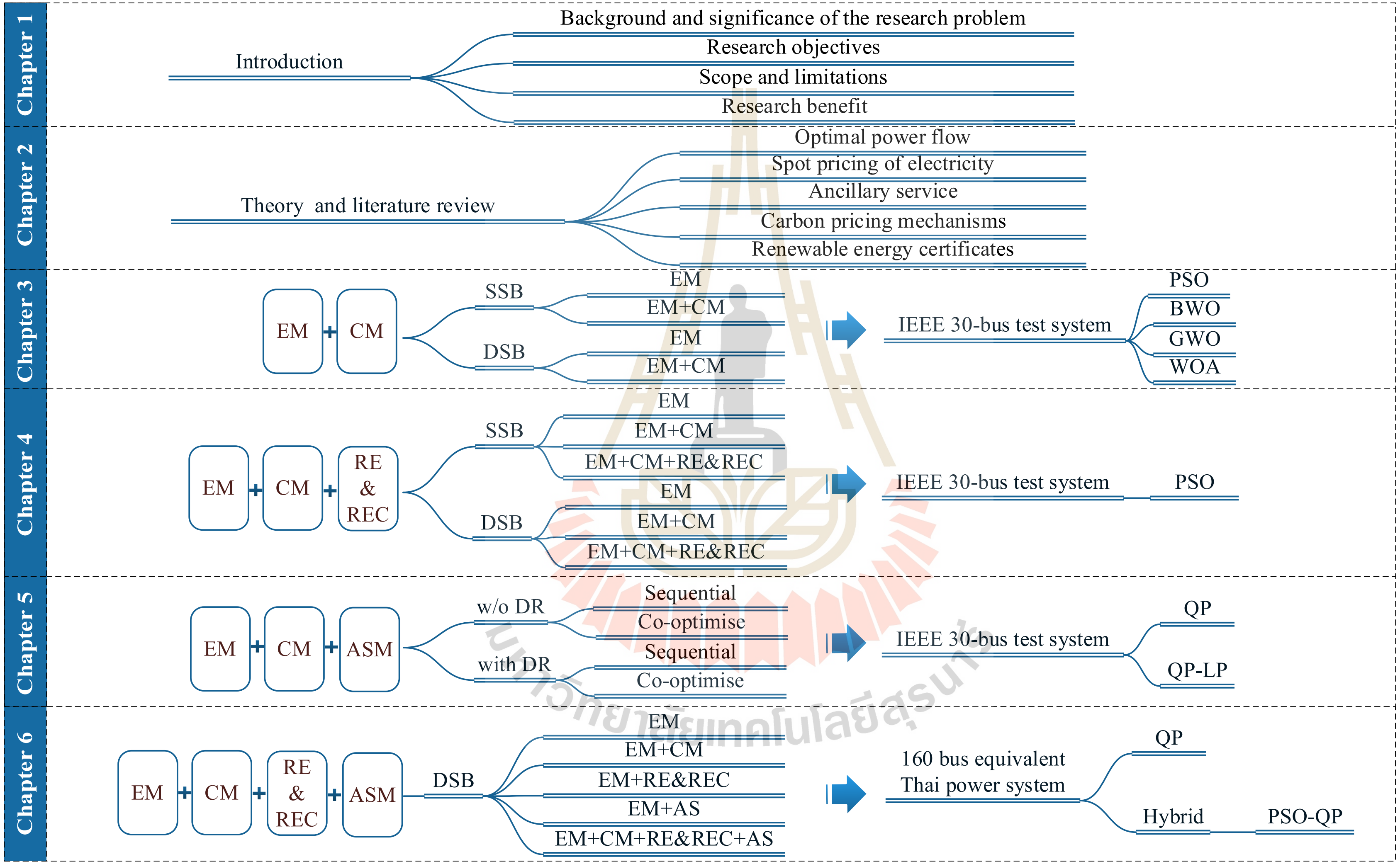

Figure 1.2 Outline of Thesis

CHAPTER II
THEORY AND LITERATURE REVIEW

2.1 Chapter Overview

A competitive electricity market involves multiple suppliers or generators competing to sell their electricity to various customers, including large consumers or retailers who distribute it to smaller end-users. Although electric energy can technically be stored in batteries, doing so on a large scale is economically impractical, rendering electricity a real-time commodity that must be produced and consumed instantly. Electric demand exhibits substantial daily, weekly, and seasonal variations, compounded by a significant random component (Bunn, 2000). The primary commodity traded in these markets is energy; however, additional services such as reserves, reactive power, and automatic generation control (AGC) are essential to maintaining system security (Gjengedal et al., 1998). The AGC is essential for maintaining grid safety and reliability, particularly in regulating frequency deviations and supporting commercial transactions. AGC systems automatically adjust the output of generating units in response to changes in system frequency, ensuring the real-time balance between supply and demand. In deregulated power markets, designing effective mechanisms for procuring and pricing AGC services is a key challenge. AGC services can be secured through negotiations between market operators, generation companies, or specialised auctions. The demand for AGC capacity significantly impacts market outcomes, as generation units in AGC mode automatically adjust their output to correct mismatches between planned production and actual system load. Efficient pricing mechanisms ensure that AGC resources are compensated fairly while maintaining economic efficiency and system security (Zhao et al., 2004). To ensure efficient trading, these ancillary services must be accommodated within the market structure (Singh & Papalexopoulos, 1999). Moreover, the geographical distribution of generators and consumers, coupled with the principles of Kirchhoff's laws, dictates the paths power takes across transmission systems, leading to potential congestion issues. Alleviating such congestion requires adjusting supply (generator outputs) and demand (customer consumption), which can constrain competition (Gedra, 1999). The interdependence of energy, ancillary services, transmission, and real-time stochastic nature of electricity demand presents significant challenges in designing efficient electricity markets.

2.2 Optimal Power Flow

Optimal power flow (OPF) is a fundamental and complex challenge in power system operation, typically characterised by its large-scale, highly constrained, nonlinear, and non-convex nature. This complexity necessitates using sophisticated solution techniques for optimal and reliable system performance. The primary objective of OPF is to minimise the cost of active power generation within an interconnected power system, where controllable variables such as active and reactive power outputs, transformer tap settings, and phase-shift angles are adjusted within the bounds of various operational constraints. The OPF procedure integrates power flow methodologies with economic dispatch strategies, systematically tuning control variables to optimise objective functions like minimising active power generation costs or power losses. Economic dispatch is also constrained by transmission system limits, including MW and MVA flow limits at buses. These limits ensure that the resulting generation dispatch achieves the minimum total generation cost and satisfies the power flow equations at the optimal point. This optimisation process ensures compliance with physical and operational limits imposed on control variables, dependent variables, and their functional relationships. Consequently, OPF is crucial in ensuring the economic efficiency and reliability of power system operations.(Wood & Wollenberg, 2014).

The standard OPF problem aims to minimise the total cost of active power generation across multiple units while satisfying operational constraints. The objective function quantifies the total production cost, considering factors such as fuel expenses and generation efficiency, and is optimised subject to constraints, including generation limits and system balance requirements.

Objective function:

minimise $$\sum_{i=1}^{NG} C_i(P_{G,i}) . \tag{2.1}$$

The OPF problem is subject to several constraints that reflect the physical and operational limits of the power system.

Generator limit inequality constraints:

$$P_{G,i}^{\min} \le P_{G,i} \le P_{G,i}^{\max} \quad ,i = 1,\dots,NG . \tag{2.2}$$

Power balance constraints:

$$\sum_{i=1}^{NG} P_{G,i} = \sum_{j=1}^{ND} P_{L,j} + P_{loss} , \tag{2.3}$$

In OPF solution, AC power flow is used to confirm the steady-state operation of the power system using non-linear equations. These equations relate the voltage magnitudes and angles to the active and reactive power injections at each bus.

AC power flow equations:

$$S_i = V_i \sum_{j=1}^{N} Y_{ij} V_j^* . \tag{2.4}$$

where S_i is the complex power at bus i, which consists of active power P_i and reactive power Q_i, expressed as $S_i = P_i + jQ_i$, V_i is the voltage at bus i, represented as a complex number $V_i = |V_i| \angle \theta_i$, Y_{ij} is the admittance between buses i and j, representing the combined effects of conductance G_{ij} and susceptance B_{ij} of the transmission line, V_j^* denote the complex conjugate of the voltage at bus j. Hence, separate equations for active power P_i and reactive power Q_i:

$$P_i = \sum_{j=1}^{NB} V_i V_j [G_{ij} \cos(\theta_i - \theta_j) + B_{ij} \sin(\theta_i - \theta_j)], \quad i = 1, \ldots, NB, \tag{2.5}$$

$$Q_i = \sum_{j=1}^{NB} V_i V_j [G_{ij} \sin(\theta_i - \theta_j) - B_{ij} \cos(\theta_i - \theta_j)], \quad i = 1, \ldots, NB. \tag{2.6}$$

The AC power flow equations are nonlinear due to the trigonometric functions involved, making them more complex to solve than the linear DC power flow equations. Typically, numerical methods such as Newton-Raphson or Gauss-Seidel are used to solve these equations iteratively. Constraints are as follows:

(1) Power balance constraints (active and reactive power)

(2) Voltage magnitude and phase angle constraints

(3) Generation limits

(4) Line flow limits

2.3 Spot Pricing of Electricity

Spot pricing is the foundation of deregulated electricity markets, facilitating efficient short-term operations and providing crucial signals for long-term investments. By accurately reflecting the balance of supply and demand, spot prices assist in optimising the use of existing resources while leading potential trends that enhance social welfare. The concept of spot pricing in electricity markets was first introduced by Schweppe et al. (1988), who proposed that the optimal electricity price should vary across space and time. This pricing mechanism accounts for the variable costs of electricity production at the time of consumption, adjustments needed to offset transmission losses, delivery costs, and any constraints related to generation or transmission capacity that might affect supply availability. The foundational theory of real-time pricing has since been expanded to address additional considerations.

Over the past decades, this foundational theory has been significantly expanded to include broader considerations, particularly for system security. Caramanis et al. (1987) pioneered integrating system security into the pricing framework, underscoring the necessity of a pricing mechanism that balances economic efficiency with grid reliability. This conceptual advancement laid the groundwork for further refinements in real-time pricing models, which increasingly accounted for the complexities of operational constraints. Alvarado et al. (1991) and Kaye et al. (1995) further enhanced the modelling of security constraints, ensuring that real-time pricing could effectively maintain grid stability while optimizing economic outcomes. Berger and Schweppe (1989) explored the potential of real-time pricing to support load frequency control, demonstrating how dynamic pricing can be a tool for maintaining system stability. Extending the theory's application, Baughman and Siddiqi (1991) addressed the real-time pricing of reactive power, a crucial component in voltage control, while Siddiqi and Baughman (1995) examined the pricing mechanisms for spinning reserves, which are essential for system reliability. Building on these foundational works, Baughman et al. (1997) introduced an advanced pricing theory that integrates these diverse elements into a cohesive framework. By employing Lagrange decomposition, this approach effectively navigates the complexities inherent in modern electricity markets, addressing the additional constraints and requirements imposed by an increasingly interconnected and sophisticated grid.

This evolution in spot pricing theory has not only built upon the foundational contributions of Schweppe et al. (1988) but has also significantly advanced the practical applicability of these concepts within contemporary electricity markets, ensuring that pricing mechanisms are robust enough to address emerging challenges. Central to this modern theory is the LMP concept, which deconstructs the electricity price at any location into three primary components: marginal energy, congestion, and losses. These components are derived from the least-cost, security-constrained dispatch of system resources, which aims to meet system demand as efficiently as possible. Marginal energy represents the incremental cost of producing electricity at the reference bus, with prices fluctuating based on load distribution across the network. Congestion reflects the additional costs incurred when transmission constraints prevent the delivery of the least-cost energy to all locations. At the same time, marginal losses account for the energy dissipated due to resistance in transmission lines. The integration of these components, marginal energy, congestion, and losses, provides a nuanced and comprehensive framework for understanding energy pricing, highlighting the economic implications of transmission constraints and the overall efficiency of the electricity system.

The LMP is the most widely adopted pricing scheme in contemporary electricity markets. Numerous studies have explored various pricing schemes, emphasising the importance of competitive equilibrium, revenue adequacy, and consumer payment minimisation. For instance, Y. Wang et al. (2023) proposed an optimization-based partial marginal pricing model that introduces discriminatory price components to manage the price coupling among market participants while ensuring both competitive equilibrium and revenue adequacy. This model effectively transforms a bi-level strategic bidding problem into a mixed-integer linear programming problem, enabling a comprehensive analysis of strategic bidding behaviours under different pricing schemes. Additionally, M. Wang et al. (2022) examined the practical experience of foreign electricity markets' settlement mechanisms, specifically investigating the effects of bidding procedures and the fairness of outcomes for both generators and consumers under three different settlement mechanisms: LMP, zonal pricing, and average system pricing. Their study developed a spot market clearing and settlement model to quantitatively assess the impact of zonal settlement mechanisms on the interests of various market participants within China's evolving electric spot market environment, ultimately enhancing market efficiency and fairness.

LMP, by definition, corresponds to the dual multiplier of the nodal active power balance constraint in the OPF model and can be implemented using both AC and DC OPF models. Yang et al. (2017) introduced a linear model for calculating loss-embedded LMP, beginning with an analysis of the Karush-Kuhn-Tucker (KKT) conditions in a general OPF formulation. This analysis provided critical insights into the interrelationships among LMP, reactive power marginal cost, and congestion cost, leading to the development of an iterative algorithm for solving the loss-embedded LMP. In a related study, Liu et al. (2009) explored the use of AC and DC OPF models for deriving LMP, with particular emphasis on the equivalence between full-structured and reduced-form models. They substantiated their theoretical findings with a three-bus system case study, illustrating the practical application of both OPF models and demonstrating that LMP results are consistent across both full-structured and reduced-form DC OPF models. Furthermore, Yang et al. (2021) compared loss factor-based LMP methods using IEEE 5-bus and 39-bus systems. They found that marginal loss factor-based LMP methods produce higher market settlement surpluses but lower generation income. Consequently, the study recommended OPF-based methods for calculating loss factors over PF-based methods, as the latter's larger variations could negatively impact market stability. Table 2.1 presents a summary of selected literature on the spot pricing of electricity, providing a concise overview of key contributions in this field.

Table 2.1 The summary of selected literature on the spot pricing of electricity

Ref.	Method	Description
Schweppe et al. (1988)	DC load flow	• Introduced the concept of spot pricing in electricity markets • Proposed that optimal electricity prices should vary across space and time, accounting for marginal energy, marginal loss, and congestion relaxation
Baughman et al. (1997)	Hamiltonian function (the dynamic equivalent of a Lagrangian)	• Utilizes Lagrangian decomposition to address complex constraints in modern electricity markets • Key Components of Pricing: - Active power, including marginal energy, marginal loss, congestion relaxation, marginal outage cost, and constraint terms - Reactive power, including marginal energy, congestion relaxation, marginal outage cost, voltage security, and constraint terms

Table 2.1 The summary of selected literature on the spot pricing of electricity (Continued)

Ref.	Method	Description
Wang et al. (2023)	Optimization-based partial marginal pricing model	• Introduces an optimization-based partial marginal pricing model with discriminatory price components • Ensures the PMP model maintains competitive equilibrium and revenue adequacy while managing price coupling among market participants • The bi-level strategic bidding problem is transformed into a mixed integer linear programming problem for thorough analysis
Wang et al. (2022)	A multi-agent-based electricity market simulation	• Investigates the effects of bidding procedures and fairness on the generator and consumption sides under three settlement mechanisms: LMP, zonal pricing, and ASP • A multi-agent-based electricity market simulation establishes a spot market clearing and settlement model
Liu et al. (2009)	AC and DC optimal power flow	• AC and DC OPF models to derive LMP. • Full-structured and reduced-form models to understand their equivalence in LMP calculations. • Illustrate the derivation of LMP solutions using a three-bus system • They show the same results, reinforcing the reliability of the models used: the LMP solutions derived from the full-structured and reduced-form DC OPF models

Table 2.1 The summary of selected literature on the spot pricing of electricity (Continued)

Ref.	Method	Description
Yang et al. (2021)	MLF-based LMP methods	• Compared loss factor-based LMP methods in electricity markets • Used IEEE 5-bus and 39-bus systems for testing • Found marginal loss factors-based LMP methods: -Produce higher market settlement surpluses - Lead to lower generation income • Recommended OPF-based methods over PF-based methods for loss factor calculation
Yang et al. (2017)	Optimal Power Flow	• Introduced a linear model for loss-embedded LMP calculation • Analyzed KKT conditions in general OPF formulation • Revealed relationships among LMP, reactive power marginal cost, and congestion cost • Developed an iterative algorithm to solve loss-embedded LMP • Improved accuracy in representing true marginal electricity costs at different network locations

2.4 Ancillary Service

The primary service in power systems is generating and delivering real power. However, ensuring this power is reliable, high-quality, and efficiently produced requires ancillary services. These services are organised by their time scales, ranging from real-power balancing, which demands constant attention and immediate response, to black-start services, which are rarely needed but crucial for system recovery after a blackout (NERC, 1996). Ancillary services provided by the system operator are essential to maintaining grid stability and supporting electricity dispatch, trade, and delivery. While services are critical, exclude activities such as investment in generation and transmission infrastructure, which, although important, are not classified as ancillary services. The specific services offered and definitions can vary across markets. However, market operators typically procure ancillary services from participants in accordance with reliability standards established by the North American Electric Reliability Corporation (NERC) and regional Coordinating Councils, such as the Western Electricity Coordinating Council (WECC).

While energy and ancillary services are procured separately, a generator can receive compensation for both as long as the capacities allocated to each service do not overlap within the same period. This mutual exclusivity ensures that resources are efficiently utilised without double-counting capacity. A significant subset of these ancillary services is procured through market-based mechanisms, notably regulation reserves, spinning reserves, and non-spinning reserves (Zhou et al., 2016).

(1) Regulation services are regarded as essential mechanisms for maintaining the real-time equilibrium between electricity supply and demand by compensating for minor fluctuations. Generation units that provide such services are required to respond to AGC signals issued by the system operator, enabling output adjustments over very short time intervals, typically from one to several seconds. Depending on the market design, regulation services are commonly categorised into regulation-up (capacity available to increase output) and regulation-down (capacity available to reduce production). In some markets, a fast-frequency regulation product has also been introduced, primarily supported by energy storage systems and demand response resources, which can modify their output more rapidly than conventional generators. Within competitive electricity markets, the procurement of AGC services has attracted considerable attention from both researchers and practitioners. These services are generally procured either through direct contractual arrangements between market operators and generating companies or via auction-based mechanisms (Rebours et al., 2007). An optimal dispatch algorithm for AGC was developed by Chen et al. (2007) to address capacity requirements for regulation dispatch under uncertain demand conditions, highlighting the stochastic nature of these requirements.

(2) Spinning reserves, also referred to as synchronised reserves, are recognised as vital for enabling the power system to respond promptly to forced outages or other

contingency events. These reserves are provided by online generating units that are synchronised to the grid but not operating at full capacity, thereby allowing a rapid increase in generation output when required. Units participating in spinning reserve provision are generally expected to be capable of ramping up their generation within 10 to 15 minutes of receiving instructions. Demand-side resources may also contribute to spinning reserves by curtailing their consumption within the same timeframe.

(3) Non-spinning reserves, also termed supplementary reserves, are intended to facilitate system recovery following unexpected contingencies, serving a function similar to that of spinning reserves. However, these reserves may also be supplied by offline generating units, provided that such units can be started and reach the required output level within a specified period, typically ranging from 10 to 30 minutes, depending on the market. Online units with surplus capacity may likewise contribute to non-spinning reserves. In many cases, the total available non-spinning reserve capacity encompasses surplus capacity from spinning reserves. Both spinning and non-spinning reserves are commonly classified as primary, supplemental, or contingency reserves.

(4) Other Ancillary Servicesare also considered indispensable for the secure and efficient operation of the power system, including black start capability, reactive power support, voltage control, and energy imbalance services. Black-start capability is fundamental for system restoration following a total blackout, typically relying on small diesel generators or energy storage systems to provide the initial energy needed to restart larger generating units. Reactive power provision and voltage control are required to maintain system voltages within acceptable limits and to mitigate transmission congestion caused by reactive power flows, thereby enhancing active power transfer capacity. Jay and Swarup (2021) examined the complexities associated with establishing a reactive power market, with particular attention to uncertainties and the non-convex nature of AC optimal power flow (AC-OPF). Their findings suggest that effective pricing may be achieved by determining nodal prices corresponding to the Lagrangian dual variables of the AC-OPF, thereby incorporating system operating conditions into the pricing mechanism.

Table 2.2 Ancillary services offered by ISO/RTO markets in the United States

	Product	Description
CAISO	• Regulation-up	• Must immediately increase output in response to automated signals • In the Day-Ahead Market and Hour-Ahead Market
	• Regulation-down	• Must immediately decrease output in response to automated signals
	• Regulation Mileage-up/down	• The absolute change in output between four-second set points
	• Spinning Reserves	• Synchronized to the grid • Must respond within 10 minutes • Must run for at least two hours
	• Non-spinning	• Must respond within 10 minutes • Must run for at least two hours
ERCOT	• Regulation-up	• must immediately increase output in response to automated signals
	• Regulation-down	• Must immediately decrease output in response to automated signals
	• Responsive Reserves	• Must respond within "the first few minutes of an event that causes a significant deviation from the standard frequency"
	• Non-spinning Reserves:	• Must respond within 30 minutes; must run for at least one hour
ISO-NE	• Regulation	• Must immediately increase or decrease output in response to automated signals
	• TMSR	• Synchronized to the grid; must respond within 10 minutes
	• TMNSR	• Must respond within 10 minutes
	• TMOR	• Must respond within 30 minutes

Table 2.2 Ancillary services offered by ISO/RTO markets in the United States (Continued)

Product		Description
MISO	• Regulation	• Must respond fully within five minutes • Online and synchronized with the grid • Able to respond to automated signals
	• Spinning Reserve	• Synchronized to the grid • Must respond within 10 minutes
	• Supplemental Reserve	• Not necessarily synchronized to the grid • Must respond within 10 minutes
NYISO	• Regulation	• Must immediately increase or decrease output in response to automated signals
	• TMSR	• Synchronized to the grid • Must respond within 10 minutes
	• TMNSR	• Must respond within 10 minutes
	• Thirty-minute Spinning Reserves	• Synchronized to the grid • Must respond within 30 minutes
	• Thirty-minute Non-synchronized Reserves	• Must respond within 30 minutes
PJM	• Regulation	• Must immediately increase or decrease output in response to automated signals
	• Synchronized Reserves	• Synchronized to the grid • Must respond within 10 minutes
	• Primary Reserves	• Must respond within 10 minutes • Includes Synchronized Reserves
SPP	• Regulation	• Must immediately increase or decrease output in response to automated signals
	• Spinning Reserves	• Synchronized to the grid • Must respond within 10 minutes
	• Non-spinning Reserves	• Not necessarily synchronized to the grid • Must respond within 10 minutes

Energy imbalance services address mismatches between scheduled and actual energy delivery during a given operational period and may be provided by both supply- and demand-side resources. Although dedicated markets for such services are not operated across most U.S. power systems, resource adequacy is ensured through internal requirements and other procurement mechanisms. In the United States, seven independent power markets administered by ISOs or regional transmission organisations (RTOs) are responsible for managing transmission networks, administering energy and ancillary service markets, and ensuring compliance with reliability standards established by the North American Electric Reliability Corporation (NERC), except for the Electric Reliability Council of Texas (ERCOT), which operates outside the jurisdiction of the Federal Energy Regulatory Commission (FERC). Across these markets, ancillary services are generally organised into the categories of regulation, spinning reserves, and non-spinning reserves. Table 2.2 shows ancillary services offered by ISO/RTO markets in the United States.

The increasing integration of RES into electricity generation has substantially increased demand for ancillary services (AS) to maintain power system stability. This transition has stimulated extensive research into market mechanisms and optimisation strategies aimed at addressing the challenges associated with renewable energy integration, operational reliability, and cost efficiency. Reddy et al. (2015) developed a market-clearing mechanism for wind-thermal power systems to manage the stochastic nature of wind generation. This framework incorporated both thermal and demand-side reserves while accounting for wind volatility within energy and spinning reserve markets. Optimal scheduling was achieved by combining a genetic algorithm with a two-point estimate method for probabilistic real-time OPF. The approach, validated on the IEEE 30-bus system, demonstrated the potential to minimise day-ahead and real-time adjustment costs when benchmarked against Monte Carlo simulations.

Building on this foundation, Banshwar et al. (2017) introduced a market-based approach enabling renewable power producers to participate simultaneously in energy and ancillary service markets within a disaggregated day-ahead framework. The sequential clearing of these markets was performed using AC-OPF techniques, ensuring feasibility under transmission and power flow constraints. The study, which focused on the ten-minute spinning reserve (TMSR) and thirty-minute replacement reserve (TMRR), demonstrated that the joint participation of renewable producers in energy and reserve markets could significantly enhance market efficiency while reducing total operational costs. Similarly, Lin et al. (2021) addressed unit commitment challenges in ancillary service optimisation by integrating Discrete Particle Swarm Optimisation and Sequential Quadratic Programming (DPSO–SQP). This model incorporated AGC and real spinning reserve (RSR), achieving optimal energy supply scheduling while satisfying energy balance and operational constraints. Comparative analyses with Genetic Algorithm (GA), Evolutionary Programming (EP), PSO, and Simulated Annealing (SA) confirmed the robustness of the proposed hybrid method in minimising day-ahead market operating costs.

At the distribution level, the proliferation of distributed energy resources and uncontrollable loads has further amplified the necessity for ancillary services. In response, He et al. (2023) developed a bi-level game-theoretic model for multi-agent load aggregators to participate in ancillary service markets and maximise their respective profits. The model was reformulated as a single-level structure using Karush-Kuhn-Tucker (KKT) conditions and strong duality theory. In contrast, PSO was used to determine the Nash equilibrium arising from non-cooperative interactions among aggregators. This approach underscored the increasing importance of decentralised coordination in distribution-level ancillary service provision. More recently, Lu et al. (2024) introduced a Convex Hull (CH) pricing-based frequency regulation (FR) market aimed at enhancing stability, flexibility, and cost-effectiveness in low-carbon systems. The CH pricing scheme, derived through the sub-gradient surrogate Lagrangian method, enabled efficient joint market clearing while minimising uplift payments. The results demonstrated notable improvements in frequency performance, alongside reductions in total operating costs, uplift payments, and carbon emissions.

Parallel to the development of new optimisation frameworks, contemporary studies have highlighted the growing operational challenges in low-inertia systems. Baig et al. (2021) employed an inertia-dependent stochastic unit commitment (SUC) model to demonstrate that ancillary service costs in Great Britain could increase by up to 165% if inertia levels were not explicitly integrated into market design. The findings emphasised the critical linkage between inertia and frequency response provision, reinforcing the need for restructured ancillary service markets under conditions of reduced synchronous generation. The evolution of market mechanisms and pricing models has also been a central research theme. Zheng and Litvinov (2006) proposed an ex post pricing framework for co-optimised electricity and reserve products in ISO New England's market, simplifying the pricing process through a decoupled approach that maintained consistency between electricity and reserve prices while avoiding the complexity of conventional heuristic methods. Complementarily, Wang et al. (2005) presented a cost-benefit-based clearing model for operating reserve markets, which simultaneously determined the optimal reserve capacity under both uniform-price and pay-as-bid auction mechanisms. Together, these studies laid the analytical groundwork for modern reserve market structures that balance economic efficiency with system reliability.

Comprehensive reviews of ancillary service market evolution have been conducted. Pollitt and Anaya (2021) traced the transformation of ancillary services from by-products of conventional generation to independent market products increasingly shaped by renewable integration. Meanwhile, Viola et al. (2024) expanded on this perspective through a systematic review of ancillary service markets in the United States and Europe, developing a standard taxonomy of AS products and identifying key design principles to support systems with high shares of variable renewable energy (VRE). The review proposed potential solutions to remaining technical and regulatory challenges, emphasising the importance of adaptive, technology-neutral market frameworks that can maintain reliability in fully decarbonised systems.

Beyond pricing and optimisation, research attention has also focused on zonal coordination, active network participation, and demand-side flexibility. Dutta et al. (2024) examined zonal reserve pricing under transmission congestion and contingency scenarios, revealing that system reliability and market efficiency can be improved through optimised reserve procurement. Jin et al. (2015) explored the participation of active distribution networks (ADNs) in ancillary service provision through a bilevel coordinated dispatch model that captures the interaction between distribution-level decision-making and main-grid market clearing. The results demonstrated that balanced participation between electricity and ancillary service markets could be achieved through decentralised optimisation strategies. The contribution of demand-side participation has been further established as a critical element of ancillary service markets (Rahmani et al., 2024). The research investigated the impact of demand response (DR) programmes on reserve costs, demonstrating that consumption management and load-shifting strategies can significantly reduce generation and reserve costs during peak demand periods. The findings reaffirmed the essential role of consumer flexibility in ensuring economic and operational efficiency in restructured electricity markets.

Advancements in strategic bidding mechanisms have continued to refine the design of the ancillary service market. Maneesha and Swarup (2022) formulated a convex joint double-auction strategy integrating wind power plants, pumped storage hydro plants, and demand response resources within day-ahead electricity and ancillary service markets. By incorporating both upward- and downward-spinning reserves, the model effectively mitigated output imbalances and improved overall market performance. Complementary insights into market behaviour were analysed in heterogeneous consumer responses to ancillary service subscription models. The study demonstrated that subscription-based pricing can enhance market competitiveness while enabling more effective price discrimination among consumers with varying usage patterns and willingness to pay (Wang et al., 2019). The literature consistently emphasises that as renewable integration deepens, ancillary service markets must be restructured to achieve operational resilience, economic efficiency, and equitable participation across both supply and demand sides, thereby ensuring the long-term stability of future low-carbon power systems. So, the summary of selected literature on ancillary services in the energy sector is shown in Table 2.3.

Table 2.3 The selected literature on ancillary services in the energy sector

Ref.	Method	Description
Chen et al. (2007)	The optimal AGC dispatching model	• Focus on the optimal dispatch algorithm for AGC - Capacity requirements for regulation dispatch - Uncertain demand conditions • Objectives of the algorithm: - Minimise opportunity costs - Minimise uplift costs - Minimise regulation costs • Constraints considered: - Operating constraints - AGC capacity requirements - Generator ramping rate limitations - Regulation capacity constraints
Jay and Swarup (2021)	AC-OPF	• Analyze the complexities of implementing a reactive power market, emphasising uncertainty in system conditions and non-convexity of the AC-OPF problem. • Propose that nodal prices, linked to the Lagrangian dual variables of AC-OPF, offer an effective pricing mechanism by incorporating system operating conditions.
Reddy et al. (2015)	• GA - based scheduling • a two-point estimate method - based probabilistic real-time OPF	• Considering generator spinning reserve and demand-side reserve constraints • Propose a market-clearing mechanism for wind-thermal systems • Models wind volatility impact on energy and spinning reserve markets • Validates approach on IEEE 30-bus system • Compares results with Monte Carlo Simulation

Table 2.3 The selected literature on ancillary services in the energy sector (Continued)

Ref.	Method	Description
Banshwar et al. (2017)	AC OPF	• Propose a market-based approach for renewable power producers to participate in energy and ancillary service markets in a disaggregated day-ahead framework. • The method sequentially clears the EM and ASM to optimize costs and ensure feasible solutions. • Focuses on RM, specifically TMSR and TMRR. Demonstrates that RPP participation in EM and RM can lead to cost savings and effective market clearing.
Lin et al. (2021)	DPSO and SQP	• Integrates DPSO and SQP for unit commitment with ancillary services in power market. • Analyze AGC, RSR, and SR for the day-ahead power market cost model. • Comparison with GA, EP, PSO, and SA for effectiveness • Lower costs with ancillary services in power market operations.
He et al. (2023)	Bi-level game model for multi-agent load aggregators Nash equilibrium calculation using particle swarm optimization algorithm	• Proposed a bi-level game model for multi-agent load aggregators • The model aims to participate in the ancillary service market and maximize profit for each aggregator. • The bi-level model was transformed into a single-level model using the KKT condition and strong duality theory. • The non-cooperative game relationship exists between load aggregators • Nash equilibrium of the market calculated using particle swarm optimization algorithm

Table 2.3 The selected literature on ancillary services in the energy sector (Continued)

Ref.	Method	Description
Lu et al. (2024)	Convex Hull (CH) pricing	• Propose a CH pricing-based FR ancillary services market. • The market aims to enhance stability, support, and flexibility, especially from low-carbon sources. • Develop an exact CH pricing scheme using the sub-gradient surrogate Lagrangian method. • Finding improved system frequency performance, Reduced total operation costs, Lower uplift payments, and Decreased carbon emissions
Baig et al. (2021)	Inertia-dependent stochastic unit commitment (SUC) model	• Finding: AS costs in GB could rise 165% if inertia is not explicitly market-integrated. • Emphasised the critical link between inertia and frequency response.
Zheng & Litvinov (2006)	Ex post pricing framework	• Proposed for co-optimised energy and reserve (ISO New England). • Simplified pricing using a decoupled approach.
Wang et al. (2005)	Cost-benefit-based clearing model	• Determined optimal operating reserve capacity. • Assessed uniform-price and pay-as-bid auction mechanisms.
Pollitt & Anaya (2021)	Comprehensive review	• Traced the evolution of ancillary services from by-products to independent market products. • Analysed the impact of renewable integration.
Viola et al. (2024)	Systematic review (US & Europe)	• Developed a standard taxonomy for AS products. • Identified design principles for high VRE systems. • Advocated for adaptive, technology-neutral frameworks.

Table 2.3 The selected literature on ancillary services in the energy sector (Continued)

Ref.	Method	Description
Dutta et al. (2024)	Analysis of zonal reserve pricing	• Examined pricing under transmission congestion and contingencies. • Showed optimised procurement improves reliability and efficiency.
Jin et al. (2015)	Bilevel coordinated dispatch model	• Explored AS provision from active distribution networks (ADNs). • Demonstrated viability of decentralised optimisation strategies.
Rahmani et al. (2024)	Investigation of demand-side participation	• Assessed the impact of DR programmes on reserve costs. • Finding: Load-shifting strategies significantly reduce generation/reserve costs.
Maneesha & Swarup (2022)	Convex joint double-auction strategy	• Integrated wind, pumped storage, and DR in day-ahead markets. • Mitigated output imbalances by including upward/downward reserves.
Wang et al. (2019)	Analysis of consumer response models	• Studied subscription-based pricing for ancillary services. • Showed it enhances market competitiveness and price discrimination.

2.5 Carbon Pricing Mechanisms

Global climate change is one of the most pressing concerns of our time, prompting international organisations to adopt a range of mitigation policies. In 2015, countries reaffirmed their commitment to the Paris Agreement, which aims to limit the global temperature rise to below 2 degrees Celsius above pre-industrial levels, with efforts to restrict it further to 1.5 degrees Celsius. Despite these commitments, recent developments in social and industrial productivity have led to a continued increase in GHG emissions, exacerbating environmental problems. A significant contributor to this issue is the substantial GHG emissions from the consumption of fossil fuels for electricity generation, which is a primary driver of climate change and a major contributor to a country's overall carbon footprint.

GHG emissions from organisational activities are categorised into three scopes: Scope 1 includes direct emissions from an organisation's activities under its control; Scope 2 encompasses indirect emissions associated with the purchase of electricity, steam, heating, or cooling; and Scope 3 covers all other indirect emissions related to the organisation's activities but originating from sources not owned or controlled by the organisation. In the electricity sector, GHG emissions arise from consumer electricity consumption (Scope 2) and from the burning of fossil fuels to generate electricity (Scope 1). Notably, over 40% of all carbon dioxide emissions from energy are linked to burning fossil fuels for electricity production, making this sector a crucial focus for reducing carbon emissions to meet climate change goals.

To address these challenges, carbon pricing mechanisms, including carbon taxes and cap-and-trade systems, have emerged as prominent policies for reducing GHG emissions. The design of institutions plays a significant role in determining the selection and feasibility of these policy options, as well as the sustainable financing of mitigation measures. Institutions that encourage participation by representatives from emerging industries and technologies can facilitate the transition to low-GHG-emission pathways. However, implementing various policies requires different levels of institutional innovation. For instance, carbon taxation can often leverage existing tax infrastructures, making it administratively simpler to implement than cap-and-trade systems. This may necessitate more complex institutional capabilities, particularly in developing countries.

Several studies have examined integrating carbon-emission costs into the optimal power dispatch framework, exploring their impact on generator schedules, system costs, and emission profiles. It is essential to use it to ensure the electrical grid remains reliable, especially as RESs are added and carbon emissions are reduced. However, these existing studies concentrate on decreasing carbon emissions without integrating carbon pricing mechanisms into single- and multi-objective OPF problems (G. Wang et al., 2022; G. Wang et al., 2023). Several methods have been proposed for an efficient method for optimising control variables in power systems with distributed RESs to minimise carbon emissions (Ilyas et al., 2020; Li et al., 2022).

Carbon pricing mechanisms, including carbon tax and cap-and-trade systems, are two of the most prominent policies for reducing GHG emissions and mitigating global climate change. The design of institutions significantly influences the selection and feasibility of policy options, as well as the sustainable financing of mitigation measures. Institutions that encourage participation by representatives from emerging industries and technologies can facilitate the transition to low-GHG-emissions pathways. The implementation of various policies differs regarding the new institutional capabilities they necessitate. Carbon taxation, for instance, can often leverage existing tax infrastructure, making it administratively simpler to implement than alternatives such as cap-and-trade systems.

Policies GHG emissions have increasingly relied on market-based instruments such as emission trading schemes (ETS) and carbon taxation, both of which aim to internalise the external costs of carbon emissions and promote cost-effective mitigation. In the power sector, these mechanisms have been widely adopted to encourage low-carbon generation and to influence investment decisions towards cleaner technologies. Under assumptions of rational market behaviour and complete markets, GHG pricing instruments are theoretically capable of achieving emission reduction targets at minimal economic cost. Carbon taxes are particularly valued for their administrative simplicity and broad applicability across sectors, as they can be levied upstream at production or import points, ensuring comprehensive coverage of carbon-intensive fuels. In most cases, such taxes are imposed on power generators, with the resulting cost burden subsequently reflected in higher wholesale electricity prices.

Empirical analyses have provided substantial evidence of the effectiveness of carbon taxation in reducing emissions within the power sector. Gugler et al. (2023) employed a regression discontinuity-in-time approach to evaluate the causal impact of the United Kingdom’s carbon tax, revealing a substantial decline in power-sector emissions between 2012 and 2016, with approximately 60% of the reduction directly attributable to the tax. Comparable outcomes were reported in Sweden, where a similar carbon pricing policy achieved significant emission abatement (Andersson, 2019). Complementing this evidence, Fang et al. (2012) developed an economic dispatch model that integrated wind power uncertainty and carbon taxation in the Australian power system. The framework minimised total operational costs, including fuel and emission expenses, while satisfying power balance and system constraints. Subsequent studies, such as that by Xuan et al. (2023), extended this line of research by incorporating carbon price uncertainty and varying carbon tax levels into investment planning for carbon capture, utilisation, and storage (CCUS) technologies. The findings revealed that increased carbon taxation levels, combined with moderate carbon price signals, can incentivise greater investment in decarbonisation technologies and accelerate emission reduction pathways.

The broader implications of carbon taxation have also been examined in the context of energy efficiency and sustainable energy system design. Zeng et al. (2019) proposed an integrated framework that combines combined cooling, heating, and power (CHP) systems with ground-source heat pumps (GSHPs), utilising carbon taxation as an incentive to enhance energy efficiency and reduce emissions. The proposed system demonstrated significant potential to align energy consumption with environmental targets. Similarly, Deng et al. (2024) investigated the integration of carbon taxation with dynamic electricity pricing mechanisms, illustrating how the coordination of economic and regulatory instruments can facilitate low-carbon transitions in the power sector. While carbon taxes provide strong and predictable price signals, ETS have emerged as flexible market-based tools that cap total emissions while allowing trading among emitters. Lin and Jia (2019) employed a dynamic recursive computable general equilibrium model to analyse the effects of ETS price levels on China’s economy and energy consumption. The results indicated that higher ETS prices can lead to deeper emission reductions but impose significant economic costs, particularly on energy-intensive industries. The analysis suggested that maintaining ETS prices between \$10 and \$20 would achieve meaningful emission reduction without undermining economic stability, especially when complemented by subsidies for renewable generation.

Analyses of the socio-economic implications of carbon pricing have emphasised its distributional and welfare effects across income groups and regions. Using a meta-analytical approach covering 53 empirical studies in 39 countries, Ohlendorf et al. (2021) demonstrated that progressive distributional outcomes are more likely in low-income countries and in the transport sector, particularly when indirect effects and consumer demand adjustments are incorporated into the modelling. Similarly, Dorband et al. (2019) assessed carbon pricing incidence across 87 low- and middle-income countries, revealing that moderate carbon prices can exhibit progressive characteristics in economies with per capita incomes below \$15,000. These findings suggest that carbon pricing can simultaneously achieve emission mitigation, revenue generation, and inequality reduction when accompanied by appropriate fiscal frameworks.

Chen and Nie (2016) provided an economic theoretical perspective on carbon taxation by constructing a social welfare model under oligopolistic electricity market conditions. The results indicated that imposing a modest carbon tax on production links enhances social welfare, whereas taxes applied to consumption and redistribution stages can diminish welfare outcomes. The analysis underscored the need for carefully designed carbon tax structures that consider sectoral characteristics and redistribution effects. Aggarwal et al. (2025) further examined the short-term welfare implications of carbon pricing in Uganda, employing a consumer demand system for food and energy commodities. The analysis showed that a carbon price of \$40 per tonne of CO_2 would reduce household welfare by 0.2-12% of total expenditure, primarily through higher electricity and fuel prices. However, the study highlighted that complementary social protection measures, such as targeted cash transfers, could mitigate adverse effects on low-income households and enhance policy acceptability. Beyond fiscal and welfare considerations, the role of carbon pricing in shaping low-carbon transition pathways has been explored through integrated modelling approaches. Yang et al. (2025) developed a cyber-physical-social system framework that co-optimises carbon reduction and carbon sequestration strategies in China's power sector. The study employed clustering and optimisation methods to construct and evaluate diverse carbon neutrality pathways, identifying co-optimised strategies that minimise cumulative economic costs by leveraging spatiotemporal complementarities between renewable substitution and carbon capture retrofitting.

Earlier works have also addressed the broader policy and institutional challenges of carbon market design. Wang et al. (2017) examined China's carbon market mechanisms in the context of renewable energy applications in building projects, proposing a programmatic clean development mechanism (CDM) framework to facilitate the inclusion of building portfolios in carbon trading. The study identified modified volume verification as a core methodological adaptation, which enables building projects to participate effectively in carbon markets. Khastar et al. (2020) conducted an evaluative study of Finland's carbon tax policy using a computable general equilibrium model, concluding that although the tax effectively reduced emissions, it negatively affected social welfare, thereby emphasising the importance of setting an optimal carbon price that balances environmental and social objectives.

Cap-and-trade, also known as emissions trading, is a market-based mechanism for pricing greenhouse gas emissions. In this system, the government establishes an emissions cap, requiring emitters to purchase allowances for each ton of carbon dioxide equivalent released. Entities are allocated specific allowances, each representing one ton of emissions over a set period. Those exceeding their limit can purchase additional allowances from entities that emit less, creating a trading system among participants. Allowance prices are determined by market supply and demand, analogous to stock trading. This approach ensures cost-effective emissions reductions while providing certainty over the total reductions achieved. The cap-and-trade scheme thus incentivises emissions reductions and promotes economically efficient ways to meet environmental goals, balancing ecological concerns with economic considerations.

In recent literature, various models and strategies have been proposed to address the challenges of carbon pricing and its impact on economic and environmental outcomes. Lou (2023) introduced pricing models that explore how the collection ratio and carbon cap influence a manufacturer's decision-making, emphasising profit optimisation within the complexities of carbon emissions and trading mechanisms. In addition, Ouyang et al. (2024) also developed a low-carbon economic dispatch strategy for integrated power systems, leveraging the substitution effects of carbon taxes and carbon trading to enhance economic and environmental benefits. In a comparative analysis, Chen et al. (2020) evaluated carbon tax and cap-and-trade systems concerning their effectiveness, efficiency, and environmental impact. Their findings suggest that while a carbon tax is more effective in reducing emissions, a cap-and-trade system offers higher economic efficiency. This body of work collectively underscores the nuanced trade-offs between different carbon pricing mechanisms and their implications for policy and practice.

2.6 Renewable Energy Certificates

Renewable energy certificates (RECs) have emerged as a pivotal element in market-based strategies to combat climate change, gaining substantial momentum since the early 2000s. Each REC certifies that one megawatt-hour (MWh) of electricity has been generated from renewable sources and supplied to the power grid, effectively decoupling the environmental attributes of clean energy from the physical electricity produced. Ownership of a REC enables entities to claim these environmental benefits, such as reduced carbon footprint, supporting their sustainability objectives regardless of the actual energy sources used in their operations.

The REC system functions through certification by approved authorities, ensuring credibility for both electricity generators and consumers in declaring their production and usage of renewable energy. This mechanism not only facilitates the transition to sustainable energy infrastructure by converting renewable sources into tradable assets but also provides additional revenue streams for renewable energy projects through the sale of these certificates. The trading process initiates when a buyer expresses intent to purchase RECs from a seller (registrant), followed by verification and certification from an authorised REC issuer. A standardised registry system transfers the REC to the buyer upon validation, and the seller receives payment commensurate with the REC’s value, as illustrated in Figures 2.1 and 2.2.

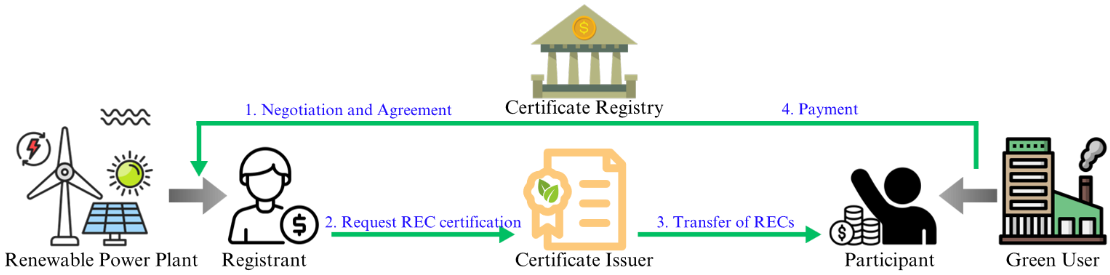

Figure 2.1 Schematic diagram of RECs trading process

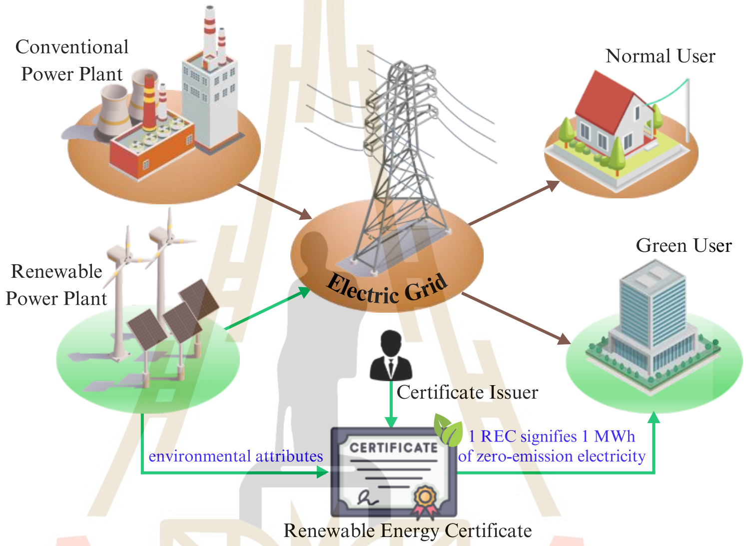

Figure 2.2 Schematic diagram of RECs trading process in the power system

The current REC issuance and tracking system is centralised, highly regulated, and operationally expensive. Further research has explored the institutional and policy dimensions of carbon markets. Ying and Xin-gang (2021) developed a system dynamics model to evaluate the interaction between renewable portfolio standards (RPS), electricity market reform, and carbon emission trading (CET) in China. The findings demonstrated that electricity market liberalisation enhances trading activity and demand for emission allowances, while the introduction of RPS may reduce the demand for emission rights and power generation from carbon-intensive sources. Yu et al. (2021) examined the integration of the tradable green certificate (TGC) market with CET in the Chinese power sector, concluding that combined implementation of these mechanisms supports emission control, optimises the generation mix, and enhances national progress toward carbon neutrality. Similarly, Tan et al. (2021)

analysed the combined effects of carbon trading and RPS within China's multi-energy dispatching systems, demonstrating that carbon trading is more effective in emission reduction when the share of renewable generation is high, while RPS contributes more substantially to energy saving.

Zuo (2022) proposed a blockchain-based, decentralised platform for REC issuance and trading that would allow greater traceability and transparency in transactions and reduce the operational costs of REC exchanges. Additionally, Tao et al. (2021) emphasised the importance of a quantitative, balanced approach to designing REC multipliers, suggesting that such an approach can effectively support renewable energy goals by considering economic and social factors. This strategy is particularly relevant for fostering more stable and consistent energy policies, as demonstrated in the context of South Korea. Further research has also been directed towards improving the low-carbon efficiency of integrated energy systems by leveraging carbon markets and green certificate markets. Tian et al. (2023) proposed an integrated energy trading strategy incorporating the interaction between carbon emissions and green certificates. This approach has been shown to effectively reduce both operating costs and carbon emissions within an integrated energy system. Hence, the summary of the selected literature on carbon pricing mechanism and renewable energy certificates are shown in Table 2.4.

Table 2.4 The selected literature on carbon pricing mechanisms and renewable energy certificates

Ref.	Objective	Method	Description
G. Wang et al. (2022)	• Minimise generation cost • Minimise active power loss • Minimise carbon emissions	• NSGA2 algorithm • TOPSIS	• AC-OPF with carbon emissions reduction using NSGA2 algorithm • TOPSIS method for obtaining optimal solutions in multi-objective optimisation • Tested on IEEE 14-bus system
G. Wang et al. (2023)	• Minimise generation cost • Minimise active power loss • Minimise carbon emissions	• AC-OPF • NSGA-III algorithm	• Constructed OPF calculation model considering carbon emission intensity • Tested on modified IEEE 39-bus system
Ilyas et al., (2020)	• Minimise generation cost • Minimise active power loss • Minimise carbon emissions	• AC-OPF • PSO	• Integration of renewable energy sources in power flow optimisation • Use of fuzzy membership function for compromise solution extraction • Penalty function approach for constraint satisfaction • Tested on Modified IEEE 30-bus system
Li et al. (2022)	• Minimise generation cost • Minimise active power loss • Minimise voltage deviation • Minimise carbon emissions	• AC-OPF • Adaptive crossover non-dominated sorting differential evolution	• Enhances renewable energy integration in power systems • Improves decision-making for multi-objective optimal power flow • Tested on Modified IEEE 30-bus and IEEE 57-bus systems

Table 2.4 The selected literature on carbon pricing mechanisms and renewable energy certificates (Continued)

Ref.	Objective	Method	Description
Gugler et al. (2023)	• Estimate the causal effects of Britain's carbon tax on emissions in the power sector	• Regression discontinuities in time • Causal evidence for carbon tax effects	• Carbon tax led to a significant emissions decline in the British power sector • Coal was replaced by gas due to the impact of carbon pricing
Andersson (2019)	• Analyse the impact of carbon taxes on CO2 emissions in Sweden	• A synthetic control method for comparison	• Establish a causal relationship between implementing a carbon tax and the observed decline in emissions • Evaluate the effectiveness of carbon taxes relative to price elasticities
Fang et al. (2012)	• Minimise generation cost • Minimise carbon emission cost	• Quantum-Inspired Particle Swarm Optimization	• Integrates wind power uncertainty and carbon tax in economic dispatch • Carbon tax reduces emissions and impacts fossil-based generation enterprises.
Xuan et al. (2023)	• Minimise costs associated with CCUS, including investment, operational, carbon capture and storage costs, carbon taxes, and revenues from carbon pricing	• Piecewise Linearisation Method	• Considered carbon price uncertainty and varying carbon tax levels • Rising carbon taxes resulting in increased investment in technologies increases • Tested on a modified IEEE 24-bus system

Table 2.4 The selected literature on carbon pricing mechanisms and renewable energy certificates (Continued)

Ref.	Objective	Method	Description
Zeng et al. (2019)	• Minimise generation cost • Minimise carbon emission cost	• PSO combined with fish swarm algorithm	• Energy consumption, environmental pollution, and operation expense reduction • The coupling CHP-GSHP system outperforms the reference system in energy, cost, and emissions • Flexible energy output provided by the coupled system
Deng et al. (2024)	• Maximise social welfare by integrating a carbon tax	• Differential evolution algorithm combined with CPLEX solver	• Integrated energy prices with a carbon tax. • Tested on an industrial park in northern China
Lin and Jia (2019)	• To analyse the impact of different ETS price levels on the economy, energy consumption, and CO_2 emissions.	• Computable General Equilibrium (CGE) model	• Analyzes the impact of ETS price levels. • Findings: Higher prices reduce GDP and emissions; current pilot prices are too low ($10-$20 suggested) • Tested on China's ETS.
Ohlendorf et al. (2021)	• To determine the sources of variation in the distributional impacts of carbon pricing.	• Ordered Probit Meta-analysis	• Analyzes distributional impacts of carbon pricing. • Findings: Progressive outcomes are more likely in lower-income countries, the transport sector, and when indirect effects are included.

Table 2.4 The selected literature on carbon pricing mechanisms and renewable energy certificates (Continued)

Ref.	Objective	Method	Description
Dorband et al. (2019)	• To assess the distributional incidence of carbon pricing across income groups.	• Incidence Assessment and Decomposition Technique.	• Assesses distributional effects in low/middle-income countries.
Chen and Nie (2016)	• Maximise social welfare	• Classification method	• Evaluates social welfare effects of carbon in China. • Finding: A small tax on the production link raises social welfare.
Aggarwal et al. (2025)	• Maximise social welfare	• Exact Affine Stone Index demand system	• Assesses welfare and demand impacts of a \$40/tCO_2 carbon price in Uganda. • Findings: Significant welfare losses, adverse nutritional impacts, and shifts in consumption. • Recommends complementary social protection.
Yang et al. (2025)	• Minimise economic costs	• Co-optimisation framework (CPSSE & WRT)	• Develops a pathway for power sector carbon neutrality. • Focus: Co-optimisation of carbon reduction (RE) and carbon sequestration (CCS) to minimise economic costs.
Wang et al. (2017)	• To establish a feasible mechanism for RE in building projects to participate in the carbon market.	• Volume verifying method	• Focus: Integrating RE in Chinese building projects into the carbon trading market. • Recommends Programmatic CDM with a modified verification method.

Table 2.4 The selected literature on carbon pricing mechanisms and renewable energy certificates (Continued)

Ref.	Objective	Method	Description
Khastar et al. (2020)	• Maximise social welfare	• Computable General Equilibrium (CGE) Model	• To analyse the impact of Finland's carbon tax on social welfare and emission reduction. • Assesses carbon tax impacts in Finland. • Findings: The tax successfully reduced emissions but had negative effects on social welfare.
Lou (2023)	• Maximise social welfare considering production costs, demand, and carbon trading implications	• Stackelberg game model	• Analyses carbon cap-and-trade impacts on decision-making • Higher collection ratio potentially reduces emissions • A lower ratio may incentivise new product manufacturing, increasing emissions • Demonstrates interplay between remanufacturing practices and environmental outcomes
Ouyang et al. (2024)	• Minimise generation cost • Minimise carbon emission	• Monte Carlo method • Grey Wolf Optimization	• Carbon trading and renewable energy generation involve inherent uncertainties • Monte Carlo method used to analyse carbon trading price uncertainty • Long Short-Term Memory method forecasts renewable energy power and electricity load

Table 2.4 The selected literature on carbon pricing mechanisms and renewable energy certificates (Continued)

Ref.	Objective	Method	Description
Chen et al. (2020)	• Compare carbon tax and cap-and-trade systems	-	• Finding carbon tax more effective in reducing emissions than cap-and-trade. • A cap-and-trade system leads to higher economic efficiency than a carbon tax.
Ying and Xin-gang (2021)	• To simulate and evaluate the impact of RPS and electricity marketisation on CET.	• System Dynamics (SD) evaluation model	• Simulates the impact of RPS on China's CET. • Findings: Marketisation is positive for CET; RPS implementation harms CET demand.
Yu et al. (2021)	• To analyse the integrated impact of TGC and CET on the power industry.	• SD Simulation Model	• Analyses the integrated impact of TGC and CET in China's power industry. • Findings: Both mechanisms control emissions; RE investment is profitable.
Tan et al. (2021)	• To evaluate the impact mechanism of CET and RPS on a multi-energy power-dispatching system.	• Cost-accounting Models	• Compares CET and RPS. • Findings: CET is more effective with high RE; RPS is better for energy saving.

Table 2.4 The selected literature on carbon pricing mechanisms and renewable energy certificates (Continued)

Ref.	Objective	Method	Description
Zuo (2022)	• Developing a blockchain-based system for managing and trading renewable energy certificates	• Blockchain Technology	• Implementing a blockchain-based system is anticipated to lower the operational costs of REC issuance and trading
Tao et al. (2021)	• optimal REC multipliers	• LCOE-integrated AHP model	• Develop an LCOE-integrated AHP model for REC multiplier analysis • Focuses on cost-effectiveness and social concerns in determining REC multipliers • Revised REC multipliers in Korean market
Tian et al. (2023)	• Minimise generation cost	• Mixed integer linear programming problem	• Integrated energy trading strategy based on carbon emissions/green certificates • The simulation results indicate a significant reduction in operating costs and carbon emissions

2.6 Conclusion

The literature review encompasses several critical topics for studying power systems and electricity markets. It begins with exploring OPF, a fundamental concept aimed at optimising the operation of electrical power systems to minimise costs while satisfying operational constraints. This is followed by examining the spot pricing of electricity, which addresses the dynamic pricing mechanisms that reflect real-time supply and demand conditions in electricity markets. The review then examines the role of ancillary services, which are crucial for maintaining grid stability and reliability.

Furthermore, the review explores market-based emission strategies to reduce carbon emissions within the energy sector. These strategies are categorised into three main areas: carbon tax, a fiscal approach that imposes a fee on carbon emissions to incentivise lower emissions; emission trading, also known as cap-and-trade, which allows companies to buy and sell emission allowances under a capped total limit; and RECs, which provide a market-based instrument to promote renewable energy generation. These strategies are increasingly relevant in global efforts to mitigate climate change. An overview of existing literature review topics is presented in Table 2.5.

Table 2.5 The summary of selected research

Ref.	EM	CM	RES	ASM	Contribution
Schweppe et al. (1988)	✓				Spot pricing
Baughman et al. (1997)	✓				Spot pricing
Wang et al. (2023)	✓				Spot pricing
Wang et al. (2022)	✓				Spot pricing
Liu et al. (2009)	✓				Spot pricing
Yang et al. (2021)	✓				Spot pricing
Yang et al. (2017)	✓				Spot pricing
Jay and Swarup (2021)	✓			✓	Reactive power market
Chen et al. (2007)	✓			✓	AGC
Reddy et al. (2015)	✓		✓	✓	Spinning reserve
Banshwar et al. (2017)	✓		✓	✓	TMSR and TMRR
Lin et al. (2021)	✓			✓	AGC, RSR, and SR
Lu et al. (2024)	✓			✓	Frequency regulation
He et al. (2023)	✓			✓	Ancillary service market
Baig et al. (2021)	✓		✓	✓	Inertia-dependent SUC/AS costs
Zheng et al. (2006)	✓			✓	Ex-post pricing for co-optimised
Wang et al. (2005)				✓	Cost-benefit clearing for reserve
Pollitt & Anaya (2021)			✓	✓	Review of AS evolution with RE
Viola et al. (2024)			✓	✓	AS taxonomy for high-VRE systems
Dutta et al. (2024)				✓	Zonal reserve pricing
Jin et al. (2015)	✓		✓	✓	Bilevel AS dispatch from ADNs
Rahmani et al. (2024)	✓			✓	DR impact on reserve costs
Maneesha et al. (2022)	✓		✓	✓	Joint auction with wind/storage/DR
Wang et al. (2019)				✓	Subscription-based AS pricing
G. Wang et al. (2023)	✓	✓			Carbon emissions reduction
Ilyas et al. (2020)	✓	✓	✓		Carbon emissions
Li et al. (2022)	✓	✓	✓		Carbon emissions

Table 2.5 The summary of selected research (Continued)

Ref.	EM	CM	RES	ASM	Contribution
Gugler et al. (2023)	✓	✓			Carbon tax
Andersson (2019)	✓	✓			Carbon tax
Fang et al. (2012)	✓	✓			Carbon tax
Xuan et al. (2023)	✓	✓			Carbon tax
Zeng et al. (2019)	✓	✓			Carbon tax
Deng et al. (2024)	✓	✓			Carbon tax
Lin and Jia (2019)	✓		✓		CGE analysis of ETS price levels
Ohlendorf et al. (2021)	✓				Meta-analysis of carbon price distribution
Dorband et al. (2019)	✓				Distributional effects of carbon price
Chen and Nie (2016)	✓				SW model for carbon tax
Aggarwal et al. (2025)	✓				SW impact of carbon price
Yang et al. (2025)	✓		✓		Co-optimisation of RE and CCS
Wang et al. (2017)	✓		✓		Programmatic CDM for RE
Khastar et al. (2020)					CGE analysis of carbon tax
Lou (2023)	✓	✓			Carbon cap-and-trade
Ouyang et al. (2024)	✓	✓	✓		Carbon trading and RES
Chen et al. (2020)	✓	✓			Carbon tax and carbon trading
Zuo (2022)		✓	✓		REC trading Blockchain
Tao et al. (2021)	✓	✓	✓		REC
Ying et al. (2021)	✓		✓		Impact of RPS on CET market
Yu et al. (2021)	✓		✓		Integrated impact of TGC and CET
Tian et al. (2023)	✓	✓	✓		REC
Proposed method	✓	✓	✓	✓	Maximise social welfare for integrated EM, CM, REC, and ASM

CHAPTER III

CO-OPTIMISED FRAMEWORK AND SPOT PRICING FOR COMBINED ELECTRICITY MARKET AND EMISSION MECHANISMS[1]

3.1 Chapter Overview

This chapter presents a comprehensive carbon-accounted dispatch and pricing framework that explicitly embeds short-run carbon emission costs into the electricity market-clearing process. The proposed model directly integrates environmental externalities into the objective function, enabling market prices to reflect economic and environmental costs simultaneously. The framework introduces a unified mathematical formulation applicable to single-sided and double-sided auction mechanisms, aiming to optimise power generation, minimise total system costs, and maximise social welfare while internalising carbon emission costs. The model is implemented on the IEEE 30-bus test system and solved using stochastic optimisation algorithms, PSO, BWO, GWO, and WOA.

Comparative analyses are conducted among algorithms to evaluate convergence performance, stability, and computational efficiency. Simulation results demonstrate that incorporating carbon costs within the dispatch framework leads to significant reductions in total emissions and consumer expenditures, alongside improvements in system-wide social welfare. Figure 3.1 illustrates the conceptual framework of the proposed carbon-accounted optimal power dispatch and spot pricing model, highlighting the interconnections among market participants, carbon taxation, and the optimisation process. This conceptual diagram visually summarises how the system operator incorporates carbon costs into market-clearing to derive environmentally informed spot prices.

---

[1] A portion of this chapter has been published in the *IEEE Transactions on Industry Applications (P. Muangkhiew & K. Chayakulkheeree, 2024; Muangkhiew & Chayakulkheeree, 2025).*

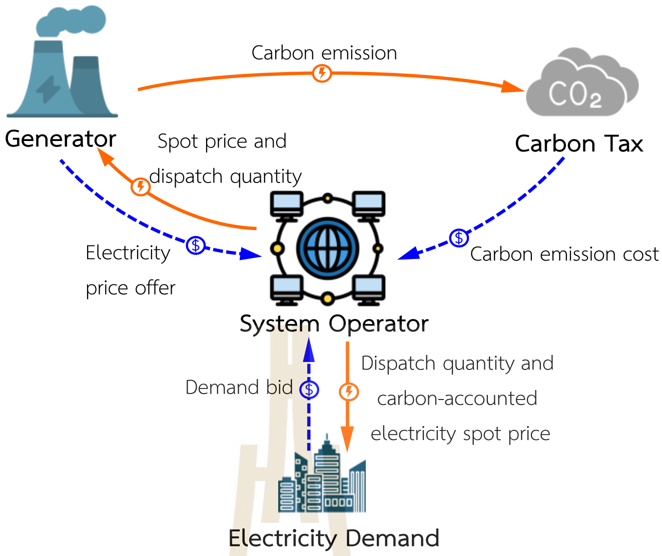

Figure 3.1 Schematic diagram of carbon-accounted optimal power dispatch and spot pricing

3.2 Mathematical Formulation

The OPF problem is a non-linear, non-convex optimisation challenge aimed at minimising specific objectives within the power system while adhering to numerous equality and inequality constraints. Mathematically, the objective function can be represented in general form as follows:

$$\text{minimise} \qquad f_i(x,u), \tag{3.1}$$

$$\text{subject to} \qquad g_i(x,u)=0, \tag{3.2}$$

$$h_i(x,u)\leq 0, \tag{3.3}$$

where $f_i(x,u)$ is the objective function to minimised.

In Equation (3.2), the equality constraints $g_i(x,u)$ represent the general power flow equations, which ensure the balance between power generation and demand as follows:

$$P_{G,i}-P_{L,j}-\sum_{j=1}^{NB}V_iV_j[G_{ij}\cos(\theta_i-\theta_j)+B_{ij}\sin(\theta_i-\theta_j)]=0 \quad , i=1,\ldots,NB, \tag{3.4}$$

$$Q_{G,i} - Q_{L,j} - \sum_{j=1}^{NB} V_i V_j [G_{ij} \sin(\theta_i - \theta_j) - B_{ij} \cos(\theta_i - \theta_j)] = 0 \quad , i = 1,...,NB . \tag{3.5}$$

Also, Equation (3.3) represents the inequality constraints $h_i(x,u)$ as follows:

(1) Generation constraints: Bus voltage limits $(V_{G,i})$, active power output limit $(P_{G,i})$, and reactive power output limit $(Q_{G,i})$ are restricted by their lower and upper limits as follows:

$$V_{G,i}^{\min} \le V_{G,i} \le V_{G,i}^{\max} \quad , i = 1,...,NG \ , \tag{3.6}$$

$$P_{G,i}^{\min} \le P_{G,i} \le P_{G,i}^{\max} \quad , i = 1,...,NG \ , \tag{3.7}$$

$$Q_{G,i}^{\min} \le Q_{G,i} \le Q_{G,i}^{\max} \quad , i = 1,...,NG \ . \tag{3.8}$$

(2) Transformer constraints: Transformer tap settings (T_i) are restricted by their limits as follows:

$$T_i^{\min} \le T_i \le T_i^{\max} \quad , i = 1,...,NT \ . \tag{3.9}$$

(3) Shunt reactor adjustments constraints: Shunt reactor adjustments $(Q_{C,i})$ are bouned as follows:

$$Q_{C,i}^{\min} \le Q_{C,i} \le Q_{C,i}^{\max} \quad , i = 1,...,NC \ . \tag{3.10}$$

(4) Security constraints: Voltages at load buses and line flow limit constraints are as follows:

$$V_{L,i}^{\min} \le V_{L,i} \le V_{L,i}^{\max} \quad , i = 1,...,NL \ , \tag{3.11}$$

$$S_{l,i} \le S_{l,i}^{\max} \quad , i = 1,...,nl \ . \tag{3.12}$$

The state variables are the dependent variables u that define the distinct state of the power system. The state variables of the OPF include the active power output of the slack bus $(P_{G,1})$, generator reactive power outputs $(Q_{G,i})$, bus voltage of load bus (V_L) , and loads of transmission line $(S_{l,i})$. The control variables or decision variables are independent variables x that can coordinate the solution of power flow equations. The control variables related to OPF are generator active power outputs $(P_{G,i})$, voltage magnitudes of generators $(V_{G,i})$, transformer tap settings (T_i), adjustment of capacitive reactance $(X_{C,i})$, and active power load $(P_{D,i})$.

3.2.1 Cost of Generation

The cost of generation (CG) can be determined as the sum of power generation in the power system using the quadratic equation. Equation (3.13) describes the generators' energy cost function regarding active power output.

$$CG(P_{G,i}) = \sum_{i=1}^{NG} (a_i P_{G,i}^2 + b_i P_{G,i} + c_i), \tag{3.13}$$

where a_i, b_i and c_i are coefficients that depend on the GENCOs' willingness to sell behaviours, NG represents number of generators, $P_{G,i}$ is the active power of generators at bus i.

3.2.2 Cost of Carbon Emission

Fossil-fired generating units are significant sources of carbon emissions (CE), primarily in the form of carbon dioxide, which contributes to the accumulation of greenhouse gases and exacerbates climate change. There is a direct correlation between the power generated (in per unit MW) and the CE produced (in tons per hour, t/h) as follows:

$$CE(P_{G,i}) = \sum_{i=1}^{NG} (\alpha_i P_{G,i}^2 + \beta_i P_{G,i} + \omega_i). \tag{3.14}$$

Consequently, the cost of carbon emission (CCE) for a fossil-fired generation unit can be expressed as the product of a carbon tax (C_{tax}) in dollars per ton and the total carbon emissions. This formulation reflects the actual societal cost of carbon emissions, accounting for the adverse impacts of climate change on the environment and public health. Therefore, the CCE can be mathematically represented as the product of the C_{tax} and the corresponding CE as follows:

$$CCE(P_{G,i}) = C_{tax} \times \sum_{i=1}^{NG} CE(P_{G,i}), \tag{3.15}$$

where α_i, β_i and γ_i are the coefficients of carbon emission at bus i.

3.2.3 Demand benefit

The demand benefit represents the economic value or utility that consumers derive from the consumption of electrical energy. In market models, this is often quantified by the consumers' willingness to pay. The aggregate benefit for all loads in the system can be modelled as a function of power consumption. Equation (3.16) describes the consumers' benefit function, which is commonly represented by a quadratic equation.

$$B_j(P_{D,j}) = \sum_{j=1}^{ND} (d_j P_{D,j}^2 + e_j P_{D,j} + k_j), \tag{3.16}$$

where d_j, e_j and k_j are the non-negative coefficients of the benefit function for the load at bus j, which are derived from consumer bidding behaviour. ND represents the total number of load buses, $P_{D,j}$ is the active power consumed by the load at bus j.

3.2.4 Spot Pricing of Electricity

In electricity markets, spot prices are determined using a methodology that incorporates key pricing characteristics, mainly incremental transmission losses and transmission line constraint relaxation. These factors are essential for reflecting the physical realities and limitations of the power grid and can be accurately calculated using power system sensitivity techniques (Wood & Wollenberg, 2014). Therefore, the spot price considered in this work includes the market-clearing price (MCP), marginal transmission loss, and network quality of supply, all of which can be calculated as follows (Schweppe et al., 1988):

$$\rho_i = \lambda + \eta_{L,i} + \eta_{QS,i}, \quad i = 1,\ldots, NB, \tag{3.17}$$

$$\eta_{L,i} = \lambda \times (-ITL_i), \quad i = 1,\ldots, NB, \tag{3.18}$$

$$\eta_{QS,i} = -\sum_{l=1}^{NB} \mu_l (a_{li}), \quad i = 1,\ldots, NB, \tag{3.19}$$

where ρ_i is the spot price at bus i (\$/MWh); λ is the system marginal price (\$/MWh); $\eta_{L,i}$ is marginal transmission loss at bus i (\$/MWh); $\eta_{QS,i}$ is network quality of supply at bus i (\$/MWh); ITL_i is the incremental transmission loss; μ_l is the reduction in supply cost that results from an incremental relaxation of constraint l (\$/MWh); a_{li} is the line l sensitivity factor to the active injection power at bus i, NB is the total number of buses.

The marginal loss component is calculated using the Jacobian matrix from the Newton-Raphson power flow (NRPF) method. In this method, the changes in active and reactive power injections are determined by analysing the power flow equations as follows:

$$\begin{bmatrix} dP \\ dQ \end{bmatrix} = \begin{bmatrix} \frac{\partial P}{\partial \delta} & \frac{\partial P}{\partial v} \\ \frac{\partial Q}{\partial \delta} & \frac{\partial Q}{\partial v} \end{bmatrix} \begin{bmatrix} d\delta \\ dv \end{bmatrix}. \tag{3.20}$$

Specifically, the change in injection power at the S-th slack bus as follows:

$$dP_S = \left[\frac{\partial P_S}{\partial \delta}\right][d\delta], \tag{3.21}$$

since $\frac{\partial P}{\partial v} \approx 0$ and $\frac{\partial Q}{\partial \delta} \approx 0$, so

$$dP_S = \left[\frac{\partial P_S}{\partial \delta}\right]\left[\frac{\partial P}{\partial \delta}\right]^{-1}[dP] = [\gamma_1, \gamma_2, \ldots, \gamma_{S-1}, \gamma_{S+1}, \ldots, \gamma_{NB}][dP]. \tag{3.22}$$

The change in total active power loss can be derived from these calculations as follows:

$$dP_{loss} = dP_S + \sum_{\substack{i=1 \\ i \neq S}}^{NB} dP_i = \sum_{\substack{i=1 \\ i \neq S}}^{NB} (1-\gamma_i) dP_i \,. \tag{3.23}$$

The incremental transmission loss (ITL_i) is a sensitivity factor that quantifies the impact of incremental changes in active power injection at bus i on the total system losses. Mathematically, ITL_i is defined as the partial derivative of the total system losses for the active power injection at bus i. This relationship is expressed in the following equation.

$$ITL_i = \frac{dP_{loss}}{dP_i} = 1 + \gamma, \quad i = 1, \ldots, S-1, S+1, \ldots, NB \tag{3.24}$$

and $ITL_S = 0$.

Consequently, the change in system losses due to a variation in active power load $(P_{D,i})$ at bus i can be formulated as follows:

$$\frac{dP_{loss}}{dP_{D,i}} = -ITL_i \,, \tag{3.25}$$

where P_{loss} represents the total system active power loss.

3.2.5 Social Welfare Formulation

Social welfare (SW) within electricity markets encapsulates the holistic societal advantage of energy production and consumption. It is represented as the disparity between the value of energy to society, gauged by society's willingness to pay for its demand, and the expenses incurred in energy production and distribution. SW is a composite of generation costs and consumer benefits. Maximising SW necessitates optimising consumer benefits while concurrently minimising power generation costs. So, the general form of SW is formulated as:

$$SW = \sum_{j=1}^{ND} B_j(P_{D,j}) - \sum_{i=1}^{NG} C_i(P_{G,i}), \tag{3.26}$$

where $B_j(P_{D,j})$ denotes the consumers willing to buy at the price at load bus j, ND represents the total number of loads.

3.3 Objective Function and Study Cases

The study investigates two different auction schemes: single-sided auction (SSA) and double-sided auction (DSA). The SSA scheme investigates the impact of integrating carbon emission costs into the spot pricing of electricity. On the other hand, the DSA scheme evaluates the effects of carbon emission costs on the welfare of society. This study aims to provide a comprehensive analysis of the impact of carbon emission costs on the electricity market, considering supply-side and demand-side behaviour by implementing these two auction mechanisms. The summary of case studies in this chapter is shown in Table 3.1.

Table 3.1 The summary of case studies in Chapter 3

Cases	Spot pricing		Demand-side bidding	Social welfare
	Electricity	*Carbon emission*		
Case 3.1a	✓			
Case 3.1b	✓	✓		
Case 3.2a	✓		✓	✓
Case 3.2b	✓	✓	✓	✓

3.3.1 Scheme 1: Single-Side Auction Scheme

Case 3.1a: Conventional Single-Side Auction Scheme

This case study involves the conventional electricity spot market, which determines electricity pricing without accounting for carbon emissions pricing mechanisms. Consequently, the objective function to be minimised is formulated as follows:

minimise $$f_{3.1\mathrm{a}}(x,u)=\sum_{i=1}^{NG}CG(P_{G,i})+\mu\cdot\left[g(x,u)\right]^2, \tag{3.27}$$

subject to equality and inequality constraints as in Equations (3.4)-(3.12), where $CG(P_{G,i})$ is formulated as shown in Equation (3.13), μ denotes the penalty factor, and $\left[g(x,u)\right]^2$ represents the quadratic penalty term.

Case 3.1b: Carbon-accounted Single-Side Auction Scheme

In this case, the pricing mechanism for electricity incorporates a cost component that accounts for the carbon emissions associated with power generation. Thus, the objective function for this case can be formulated as follows:

minimise $$f_{3.1\mathrm{b}}(x,u)=\left[\sum_{i=1}^{NG}CG(P_{G,i})+\sum_{i=1}^{NG}CCE(P_{G,i})\right]+\mu\cdot\left[g(x,u)\right]^2, \tag{3.28}$$

subject to equality and inequality constraints as in Equations (3.4)-(3.12), where $CCE(P_{G,i})$ is formulated as shown in Equation (3.15).

3.3.2 Scheme 2: Double-Side Auction Scheme

Case 3.2a: Conventional Double-Side Auction Scheme

This case aims to maximise the overall social welfare, disregarding the CCE associated with power generation. The formulation incorporates the electricity offer prices submitted by GENCOs and the demand-side bidding (DSB) mechanism facilitated by DISCOs. Hence, the objective function can be expressed as follows:

maximise $$f_{3.2\mathrm{a}}=\left[\sum_{j=1}^{ND}B_j(P_{D,j})-\sum_{i=1}^{NG}CG(P_{G,i})\right]+\mu\cdot[g(x,u)]^2, \tag{3.29}$$

subject to equality and inequality constraints as in Equations (3.4)-(3.12).

Case 3.2b: Carbon-accounted Double-Side Auction Scheme

This case aims to maximise the overall social welfare for electricity offer prices, accounting for CCE and the demand-side bidding mechanism. Hence, the objective function can be formulated as follows:

maximise $$f_{3.2b} = \left[\sum_{j=1}^{ND} B_j(P_{D,j}) - \sum_{i=1}^{NG} CG(P_{G,i}) - \sum_{i=1}^{NG} CCE(P_{G,i}) \right] + \mu \cdot \left[g(x,u) \right]^2 , \quad (3.30)$$

subject to equality and inequality constraints as in Equations (3.4)-(3.12).

For Cases 3.1a and 3.2a, the spot prices are determined based on electricity generation costs, excluding costs associated with carbon emissions, which can be calculated as Equation (3.31). Additionally, the CCE calculated using Equation (3.15) is combined with the products of electricity consumption and spot prices, which can be formulated as Equation (3.32).

$$\rho_i^{wo} = \lambda_{CG} + \eta_{L,i} + \eta_{QS,i} \quad , i = 1, \ldots, NB , \quad (3.31)$$

$$EC_i^{wo} = (\rho_i^{wo} \times P_{D,i}) + CCE(P_{G,i}) \quad , i = 1, \ldots, NB . \quad (3.32)$$

Conversely, in Cases 3.1b and 3.2b, the carbon emissions cost was incorporated into the spot pricing mechanism, which can be calculated as Equation (3.33). Under carbon-accounted spot pricing, the electricity cost (EC) is the power product and the corresponding carbon-accounted spot price. Mathematically, it can be expressed in Equation (3.34).

$$\rho_i^{w} = (\lambda_{CG} + \lambda_{CCE}) + \eta_{L,i} + \eta_{QS,i} \quad , i = 1, \ldots, NB , \quad (3.33)$$

$$EC_i^{w} = \rho_i^{w} \times P_{D,i} \quad , i = 1, \ldots, NB . \quad (3.34)$$

Therefore, the total cost to consumers (TCC) can be formulated in general terms as follows:

$$TCC = \sum_{i=1}^{NB} EC_i^{wo} \text{ or } \sum_{i=1}^{NB} EC_i^{w} . \quad (3.35)$$

3.4 Methodology

The proposed optimisation algorithm incorporates carbon emission prices into the OPF framework. The primary goal is to maximise electricity generation, reduce environmental costs, and maximise social welfare while assessing the effectiveness of various auction schemes and optimisation approaches. The PSO (Kennedy & Eberhart, 1995) results are compared with those from BWO (Hayyolalam & Pourhaji Kazem, 2020), GWO (Mirjalili et al., 2014), and WOA (Mirjalili & Lewis, 2016). The proposed approach's conceptual flowchart, illustrated in Figure 3.2, is based on carbon-accounted optimal power dispatch and spot pricing approach.

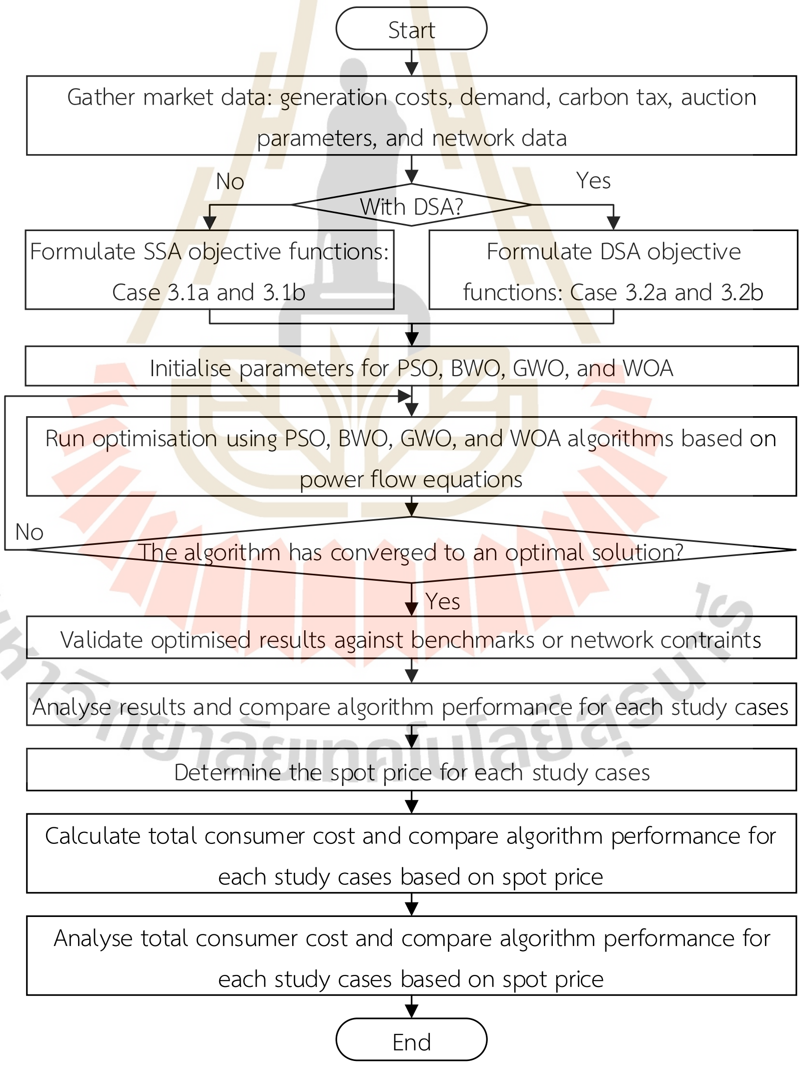

Figure 3.2 The proposed carbon-accounted optimal power dispatch and spot pricing flowchart

The vector population, representing the control variables x, for the single-side auction and double-side auction schemes, are defined to enhance the search for the best value as:

$$\mathbf{x} = [x_1,\ x_2,\ \dots,\ x_{NP}]\ ,\ i = 1,\dots,NP\ , \tag{3.36}$$

where NP is the number of particles in the population.

The Variable search boundaries include generation limits, voltage constraints, transformer tap settings, and reactive power compensation ranges, all defined based on IEEE standard test systems.

From the formulation,

(1) Single-Side Auction Scheme

$$\mathbf{x} = [P_{G,2} \dots P_{G,NG},\ V_{G,1} \dots V_{G,NG},\ T_1 \dots T_{NT},\ X_{C,1} \dots X_{C,NC}], \tag{3.37}$$

(2) Double-Side Auction Scheme

$$\mathbf{x} = [P_{G,2} \dots P_{G,NG}, V_{G,1} \dots V_{G,NG}, T_1 \dots T_{NT}, X_{C,1} \dots X_{C,NC}, P_{D,j} \dots P_{D,ND}], \tag{3.38}$$

where $P_{G,i}$ denotes active power output of the generator at bus i, $V_{G,i}$ is voltage magnitude for the generator bus i, T_i is tap setting limits for the transformer i, $X_{C,i}$ is reactance control setting of the shunt reactor i, and $P_{D,j}$ is active power demand at bus j.

The boundaries of the Variables are the power generation limit, voltage limit, transformer tap settings, and reactive power compensation ranges. For the IEEE 30-bus test system, the power generation limits are provided in Table A.1, while the transformer tap settings and voltage levels are constrained within the range of [0.90 1.10]. This chapter compares PSO proposed method to BWO, GWO, and WOA, so the computation algorithms are as follows:

Step computation of PSO

Step 1: Initialise a swarm of particles with random positions and velocities according to Equation (3.36). Each particle represents a candidate solution within the search space.

Step 2: Evaluate the fitness value of each particle using the objective function.

Step 3: Assign each particle's current position as its personal best ($pbest$), and determine the global best position ($gbest$) among all particles.

Step 4: Update the velocity of each particle based on the cognitive and social components that depend on $pbest$ and $gbest$.

Step 5: Update each particle's position using the newly computed velocity.

Step 6: Recalculate the fitness value of each particle and update both $pbest$ and $gbest$ better solutions are found.

Step 7: Repeat Steps 4-6 until the predefined stopping criterion, such as the maximum number of iterations, is satisfied.

Step 8: Return the final $gbest$ as the optimal solution.

Step computation of BWO

Step 1: Initialise the population of search agents randomly using Equation (3.36).

Step 2: Set the maximum number of iterations and initialise pheromone values for all agents.

Step 3: Randomly generate two control Variables: $m \in [0.4, 0.9]$ and $\beta \in [-1.0, 1.0]$

Step 4: For each search agent, update its position based on a random probability threshold (0.3).

- If $rand < 0.3$, update position using the first update rule.
- Otherwise, update position using the second update rule.

Step 5: Compute the pheromone value for each agent based on its fitness.

Step 6: Identify and update agents with $pheromone \leq 0.3$ to enhance exploration.

Step 7: Evaluate the fitness of all agents after position updates.

Step 8: Apply the survival (σ) procedure:

- If $rand \leq 0.5$, discard the agent; otherwise, retain it.

Step 9: Update the best agent if a better fitness value is obtained.

Step 10: Repeat Steps 3-9 until the maximum iteration limit is reached.

Step 11: Return the best agent as the final optimal solution.

where m is a mating ratio, a randomly chosen value between 0.4 and 0.9 that determines the offspring creation; $pheromone_i$ is a fitness indicator used to evaluate the quality of a solution. β is a random number in the range [-1, 1] used for updating the positions in oscillation-based movements. σ is the survival probability, deciding whether offspring survive or are eliminated.

<u>Step computation of GWO</u>

Step 1: Initialise a population of wolves with random positions using Equation (3.36).

Step 2: Evaluate the fitness of all wolves and identify the three best individuals, denoted as x_α (best), x_β (second best), and x_γ (third best).

Step 3: For each iteration, update the coefficient vectors and compute the distance of each wolf relative to x_α, x_β, and x_γ using the GWO position update equations.

Step 4: Update each wolf's position based on the encircling and hunting behaviour determined by x_α, x_β, and x_γ.

Step 5: Evaluate the updated fitness values of all wolves and adjust x_α, x_β, and x_γ according to the new rankings.

Step 6: Repeat Steps 3-5 until the termination criterion, such as the maximum iteration limit, is satisfied.

Step 7: Return the position of x_α as the final optimal solution.

where x_α is the position of the alpha wolf, representing the best solution. x_β is the position of the beta wolf, representing the second-best solution. x_δ is the position of the delta wolf, representing the third-best solution. A is a coefficient vector that decreases linearly from 2 to 0, balancing exploration and exploitation. C is a coefficient vector with random values in the range [0, 2], controlling the influence of leader wolves on the rest.

<u>Step computation of WOA</u>

Step 1: Initialise the whale population randomly using Equation (3.36).

Step 2: Evaluate the fitness of each whale and identify the best whale as the leader.

Step 3: For each iteration, update the control Variables a, A, C, l and p.

Step 4: If $p < 0.5$:

- If $|A|<1$, update each whale's position toward the best solution (exploitation phase).
- If $|A|\geq 1$, select a random whale and update the position to explore new regions (exploration phase).

Step 5: If $p\geq 0.5$, update the whale's position using a spiral motion toward the best solution, mimicking bubble-net hunting behaviour.

Step 6: Evaluate the fitness of all whales and update the best whale if a superior solution is found.

Step 7: Repeat Steps 3-6 until the maximum iteration criterion is satisfied.

Step 8: Return the final leader whale's position as the optimal solution.

where A is a coefficient vector updated at each iteration, controlling the encircling mechanism. C is a coefficient vector that determines the weight of the leader's position in updating other whales. b is spiral shape constant, used to model the spiral position update. l is a random number in [-1, 1], defining the logarithmic spiral's randomness. p is a probability value in [0, 1], controlling the balance between encircling prey and the spiral movement.

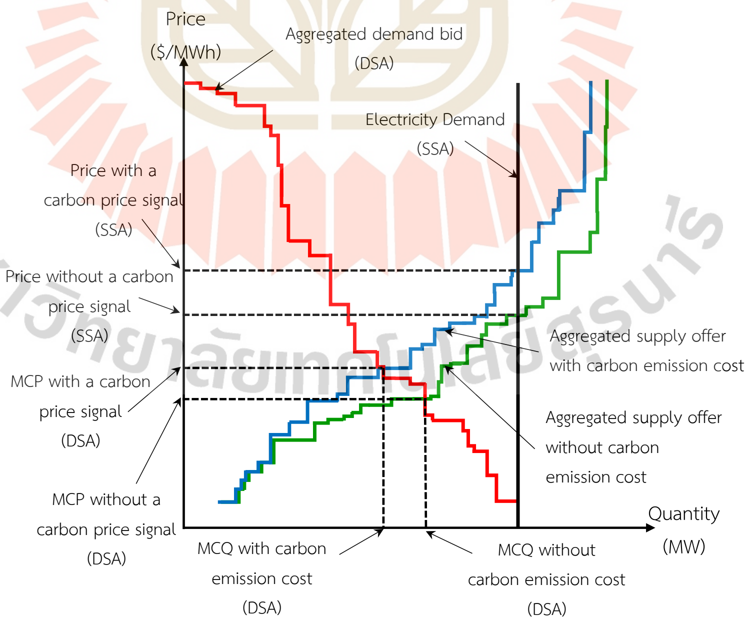

Figure 3.3 Aggregated bid curve and electricity demand

The relation between the supply and demand curves for each scheme in SSA and DSA is shown in Figure 3.3. The increased marginal costs of power generation, considering carbon emissions, are shown in the aggregated carbon-accounted supply curve. The possible differences in market-clearing prices and quantities when carbon emission costs are internalised within the electricity market are highlighted explicitly by the divergence between the demand curve's intersections and the two supply curves.

3.5 Simulation Results and Discussions

The chapter model has been tested on the IEEE 30-bus system, which includes seventeen control variables: four transformer tap settings, two shunt VAR compensators, five active power outputs of generators, and six voltage magnitudes of generators. The generation cost and carbon emission coefficients are detailed in Table A.1. In this chapter, the economic impact of greenhouse gas emissions is assessed by assuming a carbon tax (C_{tax}) of \$31 per metric ton. This subsection presents a comparative analysis of results obtained through four optimisation algorithms: PSO, BWO, GWO, and WOA, focusing on both SSA and DSA schemes.

This chapter analyses the four algorithms by comparing SSA and DSA results, followed by a statistical evaluation and case-specific analyses. The detailed parameter adjustments for each algorithm are presented in Table 3.2. Specifically, for PSO, the inertia weight (w) varied from 0.1 to 1.1, and the swarm size was set to 500. All four stochastic algorithms employed the same maximum iteration number of 1500 to ensure fair comparisons. After these analyses, optimal hyperparameters that provided the best balance of accuracy, convergence speed, and robustness were selected. Each algorithm was then executed 30 times using these optimal hyperparameters to validate the consistency and stability of the obtained solutions. The detailed parameter adjustments for each algorithm are shown in Figure B.1.

Table 3.3 presents the results of four optimisation algorithms, including PSO, BWO, GWO, and WOA, applied to the SSA scheme. The comparison shows that PSO performs most efficiently across objective functions, achieving the lowest generation cost of 799.31549 \$/h in Case 3.1a, which does not account for carbon emissions. As a result, the TCC is \$ 1,140.1179 /h. While carbon emission costs are incorporated in

Case 3.1b, PSO maintains its lead with an objective value of \$809.40759/h, reducing TCC by \$1,135.6748/h and simultaneously lowering carbon emissions compared to Case 3.1a.

Table 3.2 The best optimal hyperparameters

Algorithm	The Best Optimal Hyperparameters			
	Case 3.1a	Case 3.1b	Case 3.2a	Case 3.2b
PSO	c_1=2, c_2=1.49	c_1=1.49, c_2=1	c_1=1.49, c_2=1.49	c_1=1.49, c_2=1.49
BWO	Population size=100	Population size=80	Population size=80	Population size=80
GWO	Population size=40	Population size=40	Population size=50	Population size=40
WOA	Population size=50	Population size=60	Population size=40	Population size=60

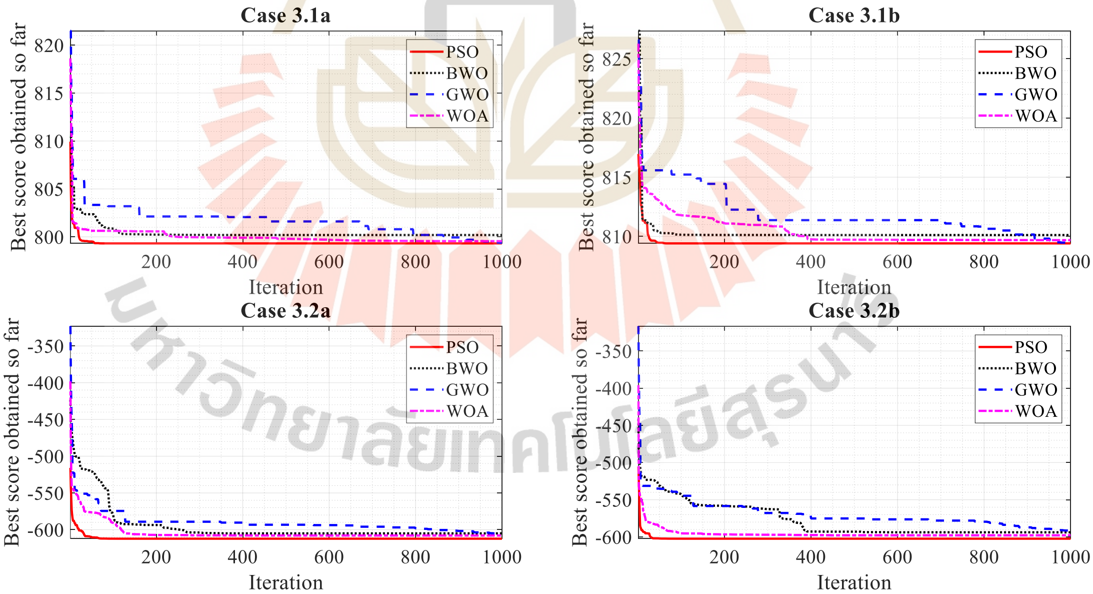

Figure 3.4 The convergence plot of the proposed method across different case studies

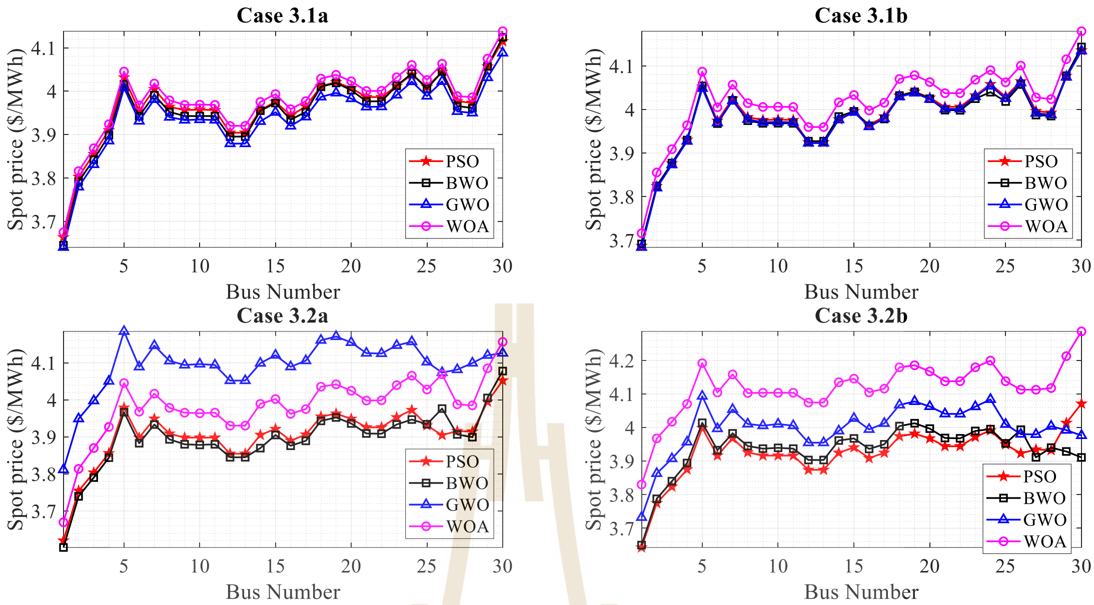

Figure 3.5 Comparison of spot prices across different case studies

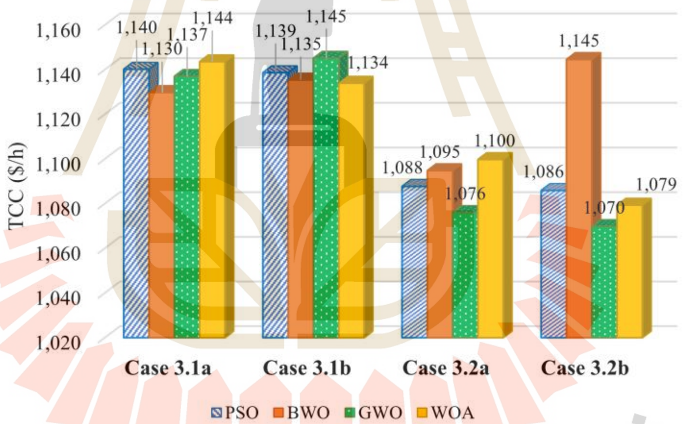

Figure 3.6 Electricity prices in different market mechanisms

Table 3.4 compares the DSA schemes of four optimisers. In this scheme, demand and supply bids are considered, and carbon costs are integrated. In Case 3.2a, which does not include carbon cost, PSO achieves the highest SW of 612.25805. Case 3.2b, accounting for carbon emissions, demonstrates significant emission reductions, with PSO registering 0.31577 tons/h of CE. This results in a TCC of 1,083.0282 $/h, lower than that of Case 3.2a. While PSO again emerges as the best-performing algorithm in the objective function of cost, emissions, and social welfare, BWO and GWO show more competitive results in terms of TCC, which indicates that these algorithms may offer slight advantages in different market conditions.

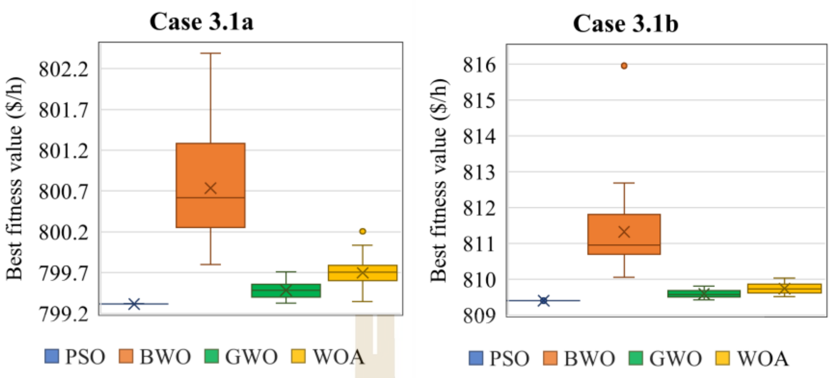

(a) Box plots for different optimisation algorithms of SSA

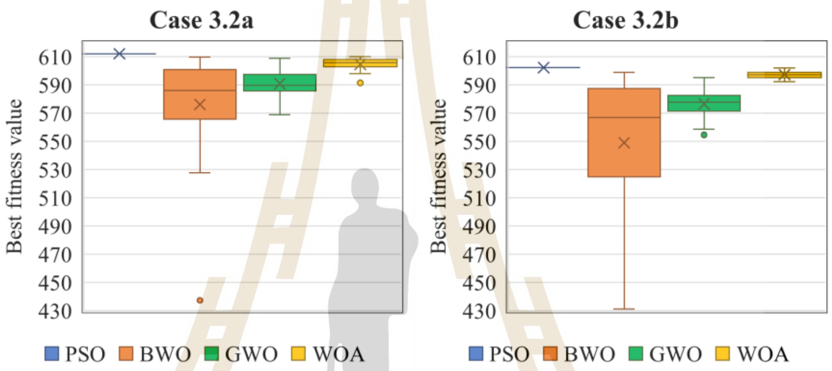

(b) Box plots for different optimisation algorithms of DSA

Figure 3.7 Statistical comparison of case studies in different optimisation algorithms

Table 3.5 summarises the best, worst, average, median, and standard deviation results for each algorithm under the SSA and DSA schemes. PSO consistently yields the best results across both auction types, particularly in minimising costs and maximising social welfare. The standard deviations of the results for PSO are the lowest, and it significantly outperforms other algorithms, further highlighting its reliability. In contrast, BWO and WOA exhibit higher variability, especially in Case 3.2b, where the worst outcomes notably impact TCC and CE. The results underline PSO's robustness for optimising power dispatch when considering carbon emissions and spot pricing.

Figure 3.4 illustrates the convergence plots of the proposed method across different case studies. PSO demonstrates rapid convergence in all cases, comparing BWO, GWO, and WOA, typically reaching near-optimal solutions within the first 50-100 iterations. This fast convergence is particularly evident in the SSA cases (3.1a and 3.1b).

The DSA cases (3.2a and 3.2b) show slightly slower convergence, which can be attributed to the increased complexity of the problem due to the inclusion of DSB. Figure 3.5 compares spot prices across different case studies and shows the impact of carbon accounting on electricity pricing. The carbon-accounted cases (3.1b and 3.2b) generally show higher spot prices compared to their non-carbon-accounted counterparts (3.1a and 3.2a). This increase reflects the internalisation of environmental costs into the electricity market. The DSA scheme (Cases 3.2a and 3.2b) tends to result in lower and more stable spot prices compared to the SSA, likely due to the increased competition and flexibility introduced by DSB. Figure 3.6 demonstrates the effects of carbon pricing and different market mechanisms on electricity prices.

The main driver of cost optimisation in this chapter framework is the electricity price, which is influenced by various market factors, including generation costs, carbon pricing, and supply-demand dynamics. To illustrate this, a figure is provided that shows electricity price variations across different scenarios, highlighting the impact of carbon accounting and optimisation strategies on market-clearing prices. The effects of carbon pricing and other market mechanisms on electricity prices are demonstrated in Figure 3.7.

The interplay between optimisation algorithms, auction mechanisms, and carbon accounting, as revealed in these results, underscores the complex dynamics in modern electricity markets. The superior performance of PSO in terms of convergence speed suggests its potential as an efficient tool for market clearing in real-time operations. Meanwhile, the observed price differentials between carbon-accounted and non-carbon-accounted scenarios emphasise the significant role of environmental policy in shaping market outcomes. The stabilising effect of DSA on spot prices further underscores the potential benefits of increased demand-side participation in electricity markets, indicating a more balanced and efficient market design. Figure 3.8 shows the average computation times across 30 trials for each algorithm in all four scenarios. PSO required the quickest calculation time while maintaining an excellent solution quality, exceeding BWO, GWO, and WOA.

The interplay between optimisation algorithms, auction procedures, and carbon accounting, as demonstrated by these findings, highlights the complex dynamics of modern power markets. PSO's superior convergence speed shows that it could be an effective instrument for market clearing in real-time operations. Meanwhile, the observed price differences between carbon-accounted and non-carbon-accounted scenarios highlight the importance of environmental policy in determining market results. DSA's stabilising effect on spot prices emphasises the potential benefits of expanded demand-side participation in electricity markets, implying a more balanced and efficient market design.

The detailed comparison analysis confirms this, demonstrating that the suggested technique consistently produces high-quality solutions with competitive performance across various case studies. Furthermore, the consistency of the results was checked across numerous runs to reduce the impact of random fluctuation. While exact global optimality is not guaranteed due to the nature of heuristic approaches, the close performance of this solution to the theoretical optimal and its stability across trials strongly suggest that the method achieves near-global optimal solutions.

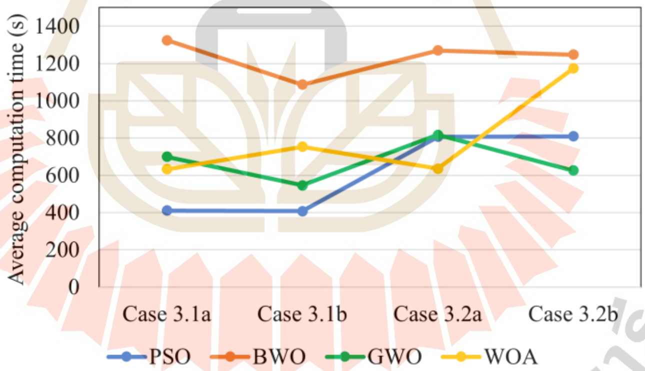

Figure 3.8 The average computation times of case studies with different optimisation algorithms

Table 3.3 Comparing the best results in different optimisation algorithms of SSA scheme

Single-Side Auction Scheme									
Variable	*Case 3.1a*				*Variable*	*Case 3.1b*			
	PSO	*BWO*	*GWO*	*WOA*		*PSO*	*BWO*	*GWO*	*WOA*
$P_{G,1}$ (MW)	177.07365	179.59219	177.96393	177.75830	$P_{G,1}$ (MW)	173.49890	169.24676	173.06652	174.13876
$P_{G,2}$ (MW)	48.70373	48.87309	48.51264	48.84775	$P_{G,2}$ (MW)	49.42987	48.99243	49.43309	49.48108
$P_{G,5}$ (MW)	21.30557	21.15851	21.12053	21.39806	$P_{G,5}$ (MW)	21.57253	21.06155	21.54725	21.80406
$P_{G,8}$ (MW)	21.10103	18.66231	20.77375	21.13008	$P_{G,8}$ (MW)	22.75124	26.78892	23.08085	21.73904
$P_{G,11}$ (MW)	11.91005	11.66530	11.76984	11.03133	$P_{G,11}$ (MW)	12.59854	12.88982	12.66577	12.54806
$P_{G,13}$ (MW)	12.00000	12.56332	12.03073	12.04303	$P_{G,13}$ (MW)	12.00001	12.68169	12.03379	12.25912
$V_{G,1}$ (p.u.)	1.10000	1.10000	1.10000	1.10000	$V_{G,1}$ (p.u.)	1.10000	1.10000	1.10000	1.10000
$V_{G,2}$ (p.u.)	1.08781	1.09872	1.08760	1.08919	$V_{G,2}$ (p.u.)	1.08802	1.08687	1.08799	1.08957
$V_{G,5}$ (p.u.)	1.06176	1.07048	1.06121	1.06191	$V_{G,5}$ (p.u.)	1.06210	1.06498	1.06218	1.06558
$V_{G,8}$ (p.u.)	1.06920	1.07725	1.06814	1.07215	$V_{G,8}$ (p.u.)	1.06984	1.07157	1.07000	1.06866
$V_{G,11}$ (p.u.)	1.10000	1.10000	1.06330	1.08498	$V_{G,11}$ (p.u.)	1.10000	1.09999	1.10000	1.08957
$V_{G,13}$ (p.u.)	1.10000	1.05514	1.10000	1.09036	$V_{G,13}$ (p.u.)	1.10000	1.10000	1.09978	1.08957
T_1 (p.u.)	1.08107	1.10000	1.09555	0.99843	T_1 (p.u.)	1.08333	0.98480	1.02594	0.98422
T_2 (p.u.)	0.91209	1.07594	0.92279	0.99790	T_2 (p.u.)	0.90944	1.02770	0.99774	1.05383
T_3 (p.u.)	0.96816	1.05666	0.94297	0.99613	T_3 (p.u.)	0.96747	1.05219	0.98649	1.05332
T_4 (p.u.)	0.95808	1.02773	0.95060	0.99844	T_4 (p.u.)	0.95801	1.01302	0.97227	0.98983

Table 3.3 Comparing the best results in different optimisation algorithms of SSA scheme (Continued)

Single-Side Auction Scheme									
Variable	*Case 3.1a*				*Variable*	*Case 3.1b*			
	PSO	*BWO*	*GWO*	*WOA*		*PSO*	*BWO*	*GWO*	*WOA*
$X_{C,1}$ (p.u.)	-3.71260	-11.33756	-2.28701	-7.75570	$X_{C,1}$ (p.u.)	-3.71014	-22.04395	-4.24223	-8.75058
$X_{C,2}$ (p.u.)	-9.88323	-8.19291	-7.78196	-8.25301	$X_{C,2}$ (p.u.)	-9.90088	-20.33743	-10.09805	-11.32186
$\boldsymbol{f_{3.1a}}$ *($/h)*	**799.31549**	800.19211	799.37519	799.55243	$\boldsymbol{f_{3.1b}}$ *($/h)*	**809.40759**	810.11192	809.43595	809.68000
CE (t/h)	0.32904	0.33390	0.33078	0.33053	*CE (t/h)*	0.32216	0.31408	0.32133	0.32329
CCE ($/h)	10.20031	10.35105	10.25421	10.24650	*CCE ($/h)*	9.98693	9.73650	9.96115	10.02194
TCC ($/h)	1,140.1178	1,137.3258	1,133.4391	1,144.3921	*TCC ($/h)*	1,135.6747	1,135.1834	1,134.5692	1,145.2994

Table 3.4 Comparing the best results in different optimisation algorithms of DSA scheme

Double-Side Auction Scheme									
Variable	*Case 3.2a*				*Variable*	*Case 3.2b*			
	PSO	*BWO*	*GWO*	*WOA*		*PSO*	*BWO*	*GWO*	*WOA*
$P_{G,1}$ (MW)	172.47011	170.24654	166.50682	175.33804	$P_{G,1}$ (MW)	168.98342	168.31714	162.57575	159.17631
$P_{G,2}$ (MW)	47.59365	48.32202	45.90390	48.68086	$P_{G,2}$ (MW)	48.29905	47.94210	45.42560	45.71099
$P_{G,5}$ (MW)	20.96051	20.42179	19.41160	21.35615	$P_{G,5}$ (MW)	21.21893	21.27578	19.09130	20.51258
$P_{G,8}$ (MW)	18.38719	19.70981	12.99476	17.86595	$P_{G,8}$ (MW)	20.00595	12.18542	12.24699	35.00000
$P_{G,11}$ (MW)	10.94443	10.54262	11.25003	11.59527	$P_{G,11}$ (MW)	11.61811	12.59673	10.43534	10.00000
$P_{G,13}$ (MW)	12.00000	12.02866	16.23014	12.00000	$P_{G,13}$ (MW)	12.00000	13.14655	14.89551	12.00000
$V_{G,1}$ (p.u.)	1.10000	1.10000	1.09964	1.10000	$V_{G,1}$ (p.u.)	1.10000	1.10000	1.10000	1.10000
$V_{G,2}$ (p.u.)	1.08793	1.10000	1.08818	1.10000	$V_{G,2}$ (p.u.)	1.08814	1.10000	1.08708	1.10000
$V_{G,5}$ (p.u.)	1.06202	1.10000	1.06263	1.10000	$V_{G,5}$ (p.u.)	1.06235	1.10000	1.06228	1.08132
$V_{G,8}$ (p.u.)	1.06985	1.10000	1.07274	1.10000	$V_{G,8}$ (p.u.)	1.07048	1.10000	1.06995	1.10000
$V_{G,11}$ (p.u.)	1.09995	1.10000	1.00070	1.10000	$V_{G,11}$ (p.u.)	1.09125	1.10000	1.07253	1.10000
$V_{G,13}$ (p.u.)	1.10000	1.10000	1.09543	1.10000	$V_{G,13}$ (p.u.)	1.10000	1.10000	1.06448	1.10000
T_1 (p.u.)	1.05675	1.10000	1.07627	1.10000	T_1 (p.u.)	1.05505	1.10000	1.03733	1.10000
T_2 (p.u.)	0.93730	1.10000	0.92813	1.10000	T_2 (p.u.)	0.94329	1.10000	0.97980	1.10000
T_3 (p.u.)	0.96778	1.10000	1.09474	1.10000	T_3 (p.u.)	0.96721	1.10000	1.05536	1.10000
T_4 (p.u.)	0.95984	1.10000	1.02986	1.10000	T_4 (p.u.)	0.95982	1.10000	1.02457	1.10000

Table 3.4 Comparing the best results in different optimisation algorithms of DSA scheme (Continued)

Double-Side Auction Scheme									
Variable	*Case 3.2a*				*Variable*	*Case 3.2b*			
	PSO	*BWO*	*GWO*	*WOA*		*PSO*	*BWO*	*GWO*	*WOA*
$X_{C,1}$ (p.u.)	-3.72698	-45.00000	-6.14379	-5.77242	$X_{C,1}$ (p.u.)	-3.37395	-4.09873	-6.74545	-6.50684
$X_{C,2}$ (p.u.)	-10.02087	-45.00000	-18.26346	-8.00074	$X_{C,2}$ (p.u.)	-10.02062	-33.86133	-7.93134	-7.96603
$P_{D,2}$ (MW)	21.70000	21.70000	21.69906	21.70000	$P_{D,2}$ (MW)	21.70000	21.70000	21.70000	21.70000
$P_{D,3}$ (MW)	2.40000	2.39999	2.35116	2.40000	$P_{D,3}$ (MW)	2.40000	2.40000	2.26811	2.40000
$P_{D,4}$ (MW)	7.60000	7.59686	7.59693	7.60000	$P_{D,4}$ (MW)	7.60000	7.60000	7.59965	7.60000
$P_{D,5}$ (MW)	94.20000	94.20000	94.20000	94.20000	$P_{D,5}$ (MW)	94.20000	94.20000	94.20000	94.20000
$P_{D,7}$ (MW)	22.80000	22.80000	22.80000	22.80000	$P_{D,7}$ (MW)	22.80000	22.80000	22.79939	22.80000
$P_{D,8}$ (MW)	30.00000	30.00000	29.98738	30.00000	$P_{D,8}$ (MW)	30.00000	30.00000	30.00000	30.00000
$P_{D,10}$ (MW)	0.00000	0.13230	0.69572	0.10162	$P_{D,10}$ (MW)	0.00000	0.00000	0.95975	0.25024
$P_{D,12}$ (MW)	11.20000	11.20000	11.20000	11.20000	$P_{D,12}$ (MW)	11.20000	11.20000	11.20000	11.20000
$P_{D,14}$ (MW)	6.20000	0.83952	4.34958	6.20000	$P_{D,14}$ (MW)	6.20000	6.20000	3.01190	6.20000
$P_{D,15}$ (MW)	8.20000	8.19998	8.19873	8.20000	$P_{D,15}$ (MW)	8.20000	8.20000	8.19035	8.20000
$P_{D,16}$(MW)	3.50000	3.50000	3.49289	3.50000	$P_{D,16}$(MW)	3.50000	3.50000	3.49857	3.50000
$P_{D,17}$ (MW)	9.00000	9.00000	8.50449	9.00000	$P_{D,17}$ (MW)	9.00000	9.00000	5.88710	9.00000
$P_{D,18}$ (MW)	3.20000	3.20000	3.19213	3.20000	$P_{D,18}$ (MW)	3.20000	3.20000	3.19193	3.20000

Table 3.4 Comparing the best results in different optimisation algorithms of DSA scheme (Continued)

Double-Side Auction Scheme									
Variable	*Case 3.2a*				*Variable*	*Case 3.2b*			
	PSO	*BWO*	*GWO*	*WOA*		*PSO*	*BWO*	*GWO*	*WOA*
$P_{D,19}$ (MW)	9.50000	9.50000	9.46147	9.50000	$P_{D,19}$ (MW)	9.50000	9.50000	9.48952	9.50000
$P_{D,20}$ (MW)	2.20000	2.20000	2.19730	2.20000	$P_{D,20}$ (MW)	2.20000	2.20000	1.79252	2.20000
$P_{D,21}$ (MW)	17.50000	17.50000	17.16364	17.50000	$P_{D,21}$ (MW)	17.50000	17.50000	17.49509	17.50000
$P_{D,23}$ (MW)	3.20000	3.19998	3.17082	3.20000	$P_{D,23}$ (MW)	3.20000	3.20000	3.19496	3.20000
$P_{D,24}$ (MW)	8.70000	8.70000	8.70000	8.70000	$P_{D,24}$ (MW)	8.70000	8.70000	8.66107	8.70000
$P_{D,26}$ (MW)	0.00000	3.50000	0.13525	3.50000	$P_{D,26}$ (MW)	0.00000	3.50000	0.00221	0.34170
$P_{D,29}$ (MW)	2.40000	2.40000	2.38302	2.40000	$P_{D,29}$ (MW)	2.40000	2.40000	2.12447	2.40000
$P_{D,30}$ (MW)	10.60000	10.59999	3.05175	10.60000	$P_{D,30}$ (MW)	10.60000	0.07398	0.00000	10.60000
$f_{3.2a}$	**612.25805**	605.03273	605.73541	607.94252	$F_{3.2b}$	**602.36894**	593.78702	591.58698	597.80657
SW	**596.48420**	595.45684	596.37060	596.20107	***SW***	**602.36894**	593.78702	591.58698	597.80657
CE (t/h)	0.32233	0.31859	0.31263	0.32687	*CE (t/h)*	0.31577	0.31573	0.30763	0.29888
CCE ($/h)	9.99208	9.87640	9.69167	10.13300	*CCE ($/h)*	9.78887	9.78772	9.53667	9.26518
TCC ($/h)	**1,087.7486**	1,077.7954	1,101.4281	1,122.1867	***TCC ($/h)***	**1,083.0282**	1,058.8616	1,038.3661	1,138.7365

Table 3.5 Statistical comparison of case studies in different optimisation algorithms

Single-Side Auction Scheme								
Function	*Case 3.1a*				*Case 3.1b*			
Algorithm	*PSO*	*BWO*	*GWO*	*WOA*	*PSO*	*BWO*	*GWO*	*WOA*
Best	799.31549	800.19211	799.37519	799.55243	809.40759	810.11192	809.43595	809.68000
Worst	799.31552	803.75838	799.75972	800.53869	809.40763	819.88613	809.83685	810.78174
Average	799.31550	801.81634	799.52234	799.92350	809.40760	811.92861	809.63245	810.15134
Median	799.31550	801.84923	799.50325	799.90403	809.40760	811.47729	809.60973	810.10677
S.D.	0.00001	0.84418	0.11379	0.24268	0.00001	1.85885	0.10460	0.28039

Double-Side Auction Scheme								
Function	*Case 3.2a*				*Case 3.2b*			
Algorithm	*PSO*	*BWO*	*GWO*	*WOA*	*PSO*	*BWO*	*GWO*	*WOA*
Best	612.25805	605.03273	605.73541	607.94252	602.36894	593.78702	591.58698	597.80657
Worst	612.25775	437.43270	546.01117	576.92913	602.36832	431.38744	556.79640	558.24406
Average	612.25792	562.46385	583.00927	602.10967	602.36880	549.25934	576.03255	592.12092
Median	612.25792	576.79175	585.90390	603.55496	602.36885	560.70859	575.56178	594.60615
S.D.	0.00071	44.17016	14.18606	6.00640	0.00014	40.92580	9.99768	7.81242

3.6 Conclusion

This chapter introduces an enhanced optimal power dispatch and spot pricing framework that explicitly incorporates short-run carbon emission costs into the electricity market structure. The proposed model was rigorously tested on the IEEE 30-bus system using stochastic optimisation algorithms, namely PSO, BWO, GWO, and WOA. The findings reveal that embedding carbon emission costs directly into electricity spot pricing (Cases 3.1b and 3.2b) leads to a substantial reduction in carbon emissions compared to conventional pricing approaches (Cases 3.1a and 3.2a). In particular, the carbon-accounted scenarios resulted in lower carbon emissions and total consumer costs compared to the traditional cases, thereby validating the economic and environmental effectiveness of the proposed framework. Furthermore, the integration of the DSA scheme enhanced social welfare outcomes, highlighting the benefits of incorporating demand-side participation within carbon-aware market mechanisms. Among the optimisation techniques evaluated, PSO consistently exhibited superior performance, yielding lower objective function values, faster convergence, and greater computational efficiency compared to BWO, GWO, and WOA. These results underscore the robustness and applicability of PSO for real-time carbon-conscious electricity market dispatch.

CHAPTER IV
CO-OPTIMISED FRAMEWORK FOR COMBINED ELECTRICITY MARKET AND EMISSION MECHANISMS WITH RENEWABLE ENERGY CERTIFICATES[2]

4.1 Chapter Overview

This chapter introduces a novel integrated energy trading mechanism that unifies the RECs mechanism, CCE, and the conventional electricity market. Traditionally, REC trading has been conducted separately from electricity trading, with limited integration of carbon emissions into the core functions of electricity markets. The proposed approach incorporates an OPF model with a unified market-clearing mechanism that minimises CG, accounts for CE, and captures renewable energy benefits through REC earnings while maintaining system reliability.

By embedding carbon pricing mechanisms, generators can internalise the cost of carbon emissions within their electricity prices, thereby addressing environmental externalities. The framework also merges carbon pricing and REC trading by comparing SSA and DSA mechanisms, enabling generators to submit integrated energy bids that account for CCE and potential REC revenues. Simultaneously, consumers can purchase electricity and RECs based on their valuation of renewable energy's environmental benefits. This double-sided market framework enhances economic efficiency and environmental sustainability by maximising social welfare through the seamless integration of the REC price and CCE, as illustrated in Figure 4.1.

[2] A portion of this chapter has been published in the *Journal of Renewable and Sustainable Energy (Muangkhiew & Chayakulkheeree, 2024).*

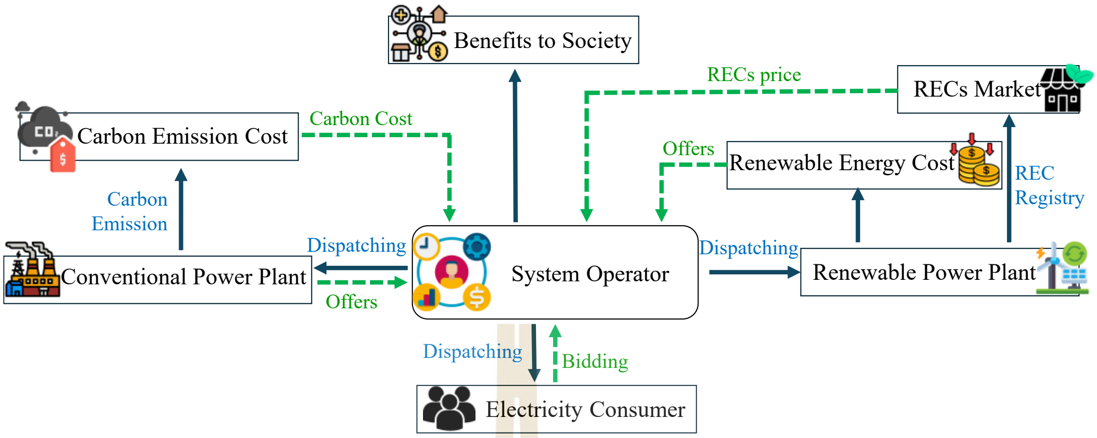

Figure 4.1 The coupling mechanism of the electricity-carbon-REC market

4.2 Mathematical Formulation

The proposed optimisation model minimises the total system operating cost, which includes generation cost (CG), carbon emissions cost (CCE), renewable energy cost (CRE), and renewable energy certificate revenue (RECR). This formulation is subject to equality and inequality constraints. Equations (3.13) and (3.14) define the calculations for CG and CCE, respectively.

4.2.1 Cost of Renewable Energy

In the SSA scheme, control variables x within the PSO population are represented by Equation (3.36). Dispatchable RES are vital for addressing the variability and intermittency of renewable technologies, providing reliable power that aids in reducing fossil fuel dependency. However, integrating renewable energy requires careful consideration of both environmental benefits and economic costs. The cost of renewable energy (CRE), expressed in dollars per hour ($/h), is often linked to power output in megawatts (MW) through a quadratic relationship. This nonlinear cost-power dynamic is crucial for optimising renewable integration and ensuring economic viability within the energy mix. Mathematically, the CRE can be represented as:

$$CRE(P_{RE,r}) = \sum_{r=1}^{NRE} (f_r P_{RE,r}^2 + g_r P_{RE,r} + h_r), \qquad (4.1)$$

where $P_{RE,r}$ denotes the active renewable energy power output RE at bus r (MW), f_r, g_r, and h_r are the coefficients that determine the shape of RE the quadratic curve, NRE is the number of renewable energy sources.

4.2.2 Renewable Energy Certificate Revenue

In the SSA scheme, control variables x within the PSO population are represented by Equation (3.35). Renewable energy projects can generate additional income through the sale of RECs, which represent their certified clean energy production. Each REC corresponds to the generation of one megawatt-hour (MWh) of electricity from a renewable source, making it a tradable asset in the electricity market. The REC revenue (RECR), therefore, reflects the economic value of this certified renewable energy. Mathematically, the REC revenue can be expressed as the product of the REC price (RECP), measured in dollars per hour, and the corresponding RE output, as follows:

$$RECR(P_{RE,r}) = RECP \times \sum_{r=1}^{NRE} P_{RE,r}\ , \tag{4.2}$$

where $RECP$ denotes renewable energy certificate price ($/MWh).

4.3 Objective Function and Study Cases

This chapter investigates two different auction schemes: single-sided auction (SSA) and double-sided auction (DSA).

4.3.1 Scheme 1: Single-Side Auction Scheme

In the SSA scheme, control variables x within the PSO population are represented by Equation (3.36) as follows:

$$\mathbf{x} = [P_{G,2},\ldots,P_{G,NG},\ V_{G,1},\ldots,V_{G,NG},\ T_1,\ldots,T_{NT},\ X_{C,1},\ldots,X_{C,NC},\ P_{RE,1},\ldots,P_{RE,NRE}]. \tag{4.3}$$

<u>Case 4.1a</u>: Competitive Electricity Price Scheme (CEPS)

This scheme dispatches the generation power of GENCOs by minimising the CG offered by GENCOs, regardless of the CCE from power generation, CRE, RECR, and DSB. Then, the CE and CCE are obtained and included in the total operating cost to compute the carbon accounted for electricity, including the RECR from RE. Hence, the objective function is to be described as:

minimise $$f_{4.1\mathrm{a}}(x,u)=\sum_{i=1}^{NG}CG(P_{G,i})+\mu\cdot\left[g(x,u)\right]^2, \tag{4.4}$$

subject to equality and inequality constraints as in Equations (3.4)-(3.12), where $CG(P_{G,i})$ is formulated as shown in Equation (3.13).

Case 4.1b: Competitive Electricity-Carbon Prices Scheme (CECPS)

This scheme dispatches the power from GENCOs by minimising the total cost offered by GENCOs, considering the CCE from power generation as a resultant aggregated supply curve without CRE, RECR, and DSB. As a result, this scheme's total operating cost incorporates electricity and carbon prices. The objective function is formulated:

minimise $$f_{4.1b}(x,u)=\left[\sum_{i=1}^{NG}CG(P_{G,i})+\sum_{i=1}^{NG}CCE(P_{G,i})\right]+\mu\cdot\left[g(x,u)\right]^2, \tag{4.5}$$

subject to equality and inequality constraints as in Equations (3.4)-(3.12), where $CCE(P_{G,i})$ is formulated as shown in Equation (3.15).

Case 4.1c: Competitive Electricity-Carbon-REC Prices Scheme (CECRPS)

This scheme dispatches the power from GENCOs by minimising the total cost offered by GENCOs, considering the CCE from power generation, CRE, and RECR, in an aggregated supply curve without DSB. This scheme's total operational cost includes electricity, CCE, CRE, and RECR. The objective function is formulated:

minimise $$f_{4.1\mathrm{c}}(x,u)=\left[\sum_{i=1}^{NG}CG(P_{G,i})+\sum_{i=1}^{NG}CCE(P_{G,i})+\sum_{r=1}^{NRE}CRE(P_{RE,r})-\sum_{r=1}^{NRE}RECR(P_{RE,r})\right]+\mu\cdot\left[g(x,u)\right]^2, \tag{4.6}$$

subject to:

$$\sum_{i=1}^{NG} P_{G,i} + \sum_{r=1}^{NRE} P_{RE,r} = \sum_{j=1}^{ND} P_{D,j} \,, \tag{4.7}$$

$$P_{RE,r}^{\min} \leq P_{RE,r} \leq P_{RE,r}^{\max} \,, \tag{4.8}$$

and as in Equation (3.5). Moreover, inequality constraints are as in Equations (3.6)-(3.12), where $CRE(P_{RE,r})$ and $RECR(P_{RE,r})$ are formulated as shown in Equations (4.1) and (4.2), respectively.

For Cases 4.1a to 4.1c, the study compares the total cost (TC) to society, including electricity production and environmental costs, which are computed as follows:

$$TC = \sum_{i=1}^{NG} CG(P_{G,i}) + \sum_{i=1}^{NG} CCE(P_{G,i}) + \sum_{r=1}^{NRE} CRE(P_{RE,r}) - \sum_{r=1}^{NRE} RECR(P_{RE,r}) \,. \tag{4.9}$$

4.3.2 Scheme 2: Double-Side Auction Scheme

In the DSA scheme, the control variables x within the PSO population are represented by Equation (3.36), as follows:

$$\mathbf{x} = [P_{G,2},\ldots,P_{G,NG},V_{G,1},\ldots,V_{G,NG},T_1,\ldots,T_{NT},X_{C,1},\ldots,X_{C,NC},P_{RE,1},\ldots,P_{RE,NRE},P_{D,1},\ldots,P_{D,ND}] \tag{4.10}$$

<u>Case 4.2a</u>: Market-Based Electricity Price Scheme (MBEPS)

This scheme aims to maximise social welfare for market participants by considering electricity offer prices and DSB; however, it disregards the CCE, CRE, and RECR. After that, the CCE, CRE, and RECR are calculated and coupled with all operating expenses to determine the MBEPS. The objective function is thus:

maximise $$f_{4.2a}(x,u) = \left[\sum_{j=1}^{ND} B_j(P_{D,j}) - \sum_{i=1}^{NG} CG(P_{G,i}) \right] + \mu \cdot \left[g(x,u) \right]^2 \,, \tag{4.11}$$

subject to equality and inequality constraints as in Equations (3.4)-(3.12), where $B_j(P_{D,j})$ is formulated as shown in Equation (3.16).

Case 4.2b: Market-Based Electricity-Carbon Prices Scheme (MBECPS)

This scheme aims to maximise the overall welfare of market participants, in which electricity offer prices consider CCE (as a resulting aggregated supply curve) and DSB without considering the CRE and RECR. Thus, all this scheme's benefits and operating costs are considered in terms of carbon and electricity prices. Hence, the objective function provides the following description:

$$\text{maximise} \quad f_{4.2b}(x,u) = \left[\sum_{j=1}^{ND} B_j(P_{D,j}) - \sum_{i=1}^{NG} CG(P_{G,i}) - \sum_{i=1}^{NG} CCE(P_{G,i})\right] + \mu \cdot \left[g(x,u)\right]^2 \quad (4.12)$$

subject to equality and inequality constraints as in Equations (3.4)-(3.12).

Case 4.2c: Market-Based Electricity-Carbon-REC Prices Scheme (MBECRPS)

This scheme aims to maximise market participants' overall welfare, where electricity prices consider CCE, CRE, RECR (as defined by the aggregated supply curve), and DSB. Thus, this scheme's operating costs, integrated CCE, CRE, and benefits regarding RECR are assessed. So, the objective function explains:

$$\text{maximise} \quad f_{4.2c}(x,u) = \left[\sum_{j=1}^{ND} B_j(P_{D,j}) - \sum_{i=1}^{NG} CG(P_{G,i}) - \sum_{i=1}^{NG} CCE(P_{G,i}) - \sum_{r=1}^{NRE} CRE(P_{RE,r}) + \sum_{r=1}^{NRE} RECR(P_{RE,r})\right] + \mu \cdot \left[g(x,u)\right]^2, \quad (4.13)$$

subject to equality and inequality constraints as in Equations (4.7)-(4.8), (3.5)-(3.12).

For Cases 4.2a to 4.2c, the comparison of the overall SW that incorporates economic and environmental aspects is investigated by the following equation:

$$SW=\sum_{j=1}^{ND}B_j(P_{D,j})-\sum_{i=1}^{NG}CG(P_{G,i})-\sum_{i=1}^{NG}CCE(P_{G,i})-\sum_{r=1}^{NRE}CRE(P_{RE,r})+\sum_{r=1}^{NRE}RECR(P_{RE,r}) \tag{4.14}$$

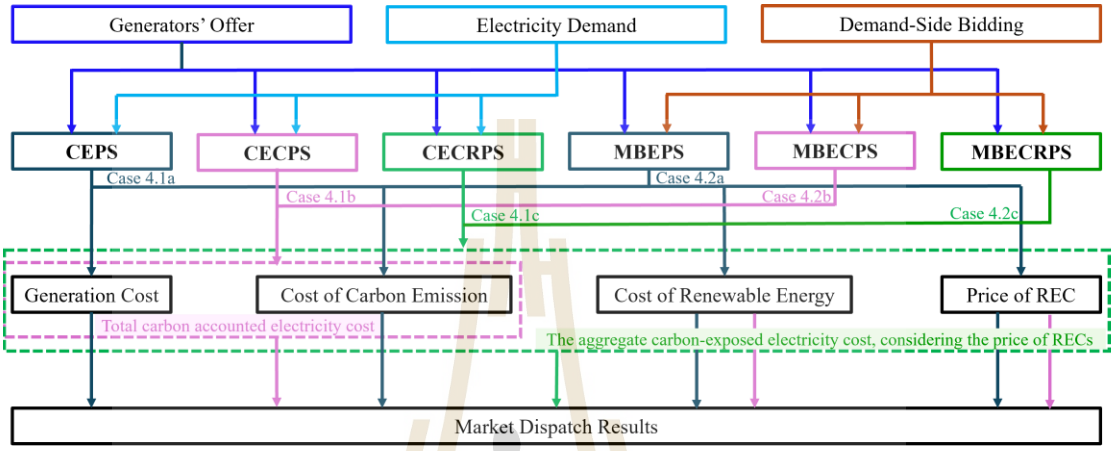

Figure 4.2 Summary of the case study schematic diagram

Figure 4.2 depicts a schematic diagram summarising various pricing mechanisms (cases) for electricity generation and DSBs, considering carbon accounting, CRE, and RECR. Case 4.1a (CEPS) shows that the traditional power pricing system is based purely on CG. Case 4.1b (CECPS) adds CCE to CG to calculate the carbon-accounted electricity cost. Case 4.1c (CECRPS) adds the CG and CCE to CRE and RECR. Regarding demand, Case 4.2a (MBEPS) represents the market-based electricity pricing scheme. In the context of DSB, Case 4.2b (MBECPS) incorporates CCE. In contrast, Case 4.2c (MECRPS) considers CRE and corresponding RECR. The lower row illustrates the market dispatch results, indicating the most significant societal benefit that incorporates the relevant cost elements derived from the various pricing methods described in the scenarios above.

4.4 Methodology

This chapter details the proposed framework for achieving an optimal and efficient clearing of the electricity market, utilising a metaheuristic approach, specifically PSO algorithm. PSO is selected for its proven robustness and efficiency in navigating complex search spaces to find a near-global optimum solution. The computational procedure is structured as follows:

Inputs: Power system data and PSO parameters.

Outputs: Optimal power dispatch, total cost to society, and social welfare.

Step 1: Initialise the PSO parameters.

Step 2: Initialise the particle positions and velocities randomly within the search space, considering the system operating constraints.

Step 3: Formulate the PSO populations for the SSA and DSA schemes defined by Equations (4.3) and (4.10), respectively.

Step 4: Run power flow for all populations and compute the objective function value.

Step 5: Check for constraint violations in the population.

Step 6: Compute the objective function for SSA by Equations (4.4)-(4.6) and DSA by Equations (4.11)-(4.13), incorporating the relevant terms and constraints.

Step 7: Initialise $pbest$ position and fitness for each particle and $gbest$ position and fitness across the entire swarm.

Step 8: Update the particle's velocity and particle's position for SSA and DSA schemes.

Step 9: Check for convergence. If convergence is reached or the maximum number of iterations is completed, proceed to step 10. Otherwise, return to step 4.

Step 10: Designate the global best position as the optimal power dispatch solution.

Step 11: Calculate the carbon emissions associated with the optimal power dispatch using the OPF model.

Step 12: Determine the TC and SW based on the optimal power dispatch and carbon emissions for SSA and DSA, respectively.

4.5 Simulation Results and Discussions

The simulation is on a modified version of the IEEE 30-bus system designed for this study. The generation cost and carbon emission coefficients are shown in Table A.1. The system includes six generators, four tap-changeable transformers, and two static VAR compensators. Moreover, this simulation involves two RES connected to buses 7 and 21, which are the buses connected with high demands as shown in Figure

4.3. The study defines CRE generation as aligning with the lowest price observed for fossil fuel-based generators. Also, the proposed method includes RECR, which is assessed at providing a spending of \$1.7 per MWh. In addition, it considers the economic impacts of greenhouse gas emissions, with a carbon tax (C_{tax}) of \$31 per ton. This analysis demonstrates the importance of environmental and financial factors in the research.

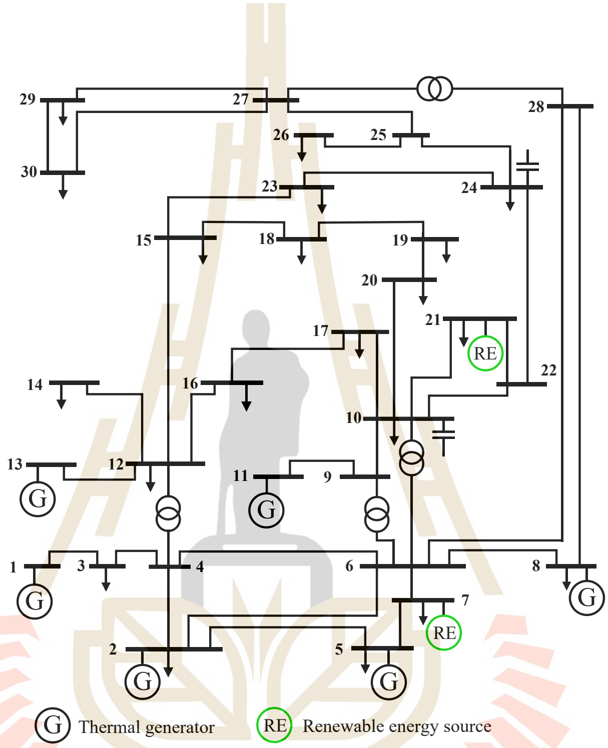

Figure 4.3 Schematic of the modified IEEE 30-bus system

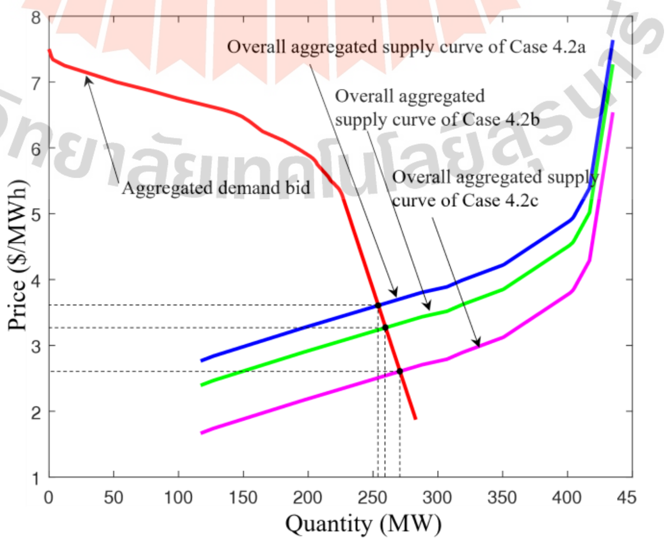

Figure 4.4 The concept of aggregated demand and supply curve

Figure 4.4 illustrates the procurement procedures employed across three distinct scenarios. The analysis begins with Case 4.2a, which serves as the reference scenario. The model considers only the essential costs associated with energy generation, as specified by Equation (4.9). In this scenario, the supply curve mirrors that of a conventional electricity market, where CCE, CRE, and RECR are treated as independent entities. The primary supply offer comprises several components that function independently of the objective function described in Equation (4.13). In Case 2b, the procurement framework integrates the CCE associated with energy generation into the objective function, as described in Equation (4.11). While the CRE and RECR components remain unchanged in the primary supply offer, the inclusion of the CCE leads to a downward shift in the supply curve compared to Case 4.2a. Finally, Case 4.2c adopts a more comprehensive approach by incorporating all cost factors related to carbon emissions, renewable energy generation, and the price of RECs into a unified supply curve, as outlined in Equation (4.12). This comprehensive integration results in a further downward shift in the curve of supply compared to both Cases 4.2a and 4.2b. Tables 4.1 and 4.3 provide a thorough examination of the simulation outcomes for each case study belonging to the SSA and DSA schemes, respectively. These tables provide a comprehensive summary of the main discoveries and practical observations obtained from the simulations. In Table 4.1, Case 4.1a, the GENCOs aim to minimise the CG while ensuring that the total electricity demand of 283.4 MW is met (excluding DSB). The costs of RE and RECR are disregarded. As a result, the CG is \$560.4716/h, corresponding to 0.2815 ton/h of carbon emissions, resulting in a CCE of \$8.7259/h. The combined cost of CG and CCE amounts to \$569.1959/h. When including the CRE and RECR of \$226.25/h and \$119/h, respectively, the TC reaches \$676.4459/h. Although this case minimises CG, leading to lower initial costs, the overall costs are higher due to the exclusion of CCE, CRE, and RECR.

Table 4.1 The simulation results of the single-side auction scheme

Single-Side Auction Scheme					
Variable	Case 4.1a	Variable	Case 4.1b	Variable	Case 4.1c
$P_{G,1}$ (MW)	131.1915	$P_{G,1}$ (MW)	129.7861	$P_{G,1}$ (MW)	136.3033
$P_{G,2}$ (MW)	37.66	$P_{G,2}$ (MW)	38.6909	$P_{G,2}$ (MW)	40.3185
$P_{G,5}$ (MW)	17.7328	$P_{G,5}$ (MW)	18.0543	$P_{G,5}$ (MW)	18.6249
$P_{G,8}$ (MW)	10	$P_{G,8}$ (MW)	10	$P_{G,8}$ (MW)	10
$P_{G,11}$ (MW)	10	$P_{G,11}$ (MW)	10	$P_{G,11}$ (MW)	10
$P_{G,13}$ (MW)	12	$P_{G,13}$ (MW)	12.0001	$P_{G,13}$ (MW)	12
$V_{G,1}$ (p.u.)	1.1	$V_{G,1}$ (p.u.)	1.1	$V_{G,1}$ (p.u.)	1.1
$V_{G,2}$ (p.u.)	1.0894	$V_{G,2}$ (p.u.)	1.0894	$V_{G,2}$ (p.u.)	1.0892
$V_{G,5}$ (p.u.)	1.0675	$V_{G,5}$ (p.u.)	1.0677	$V_{G,5}$ (p.u.)	1.0667
$V_{G,8}$ (p.u.)	1.0756	$V_{G,8}$ (p.u.)	1.0755	$V_{G,8}$ (p.u.)	1.0747
$V_{G,11}$ (p.u.)	1.0406	$V_{G,11}$ (p.u.)	1.0995	$V_{G,11}$ (p.u.)	1.0532
$V_{G,13}$ (p.u.)	1.1	$V_{G,13}$ (p.u.)	1.1	$V_{G,13}$ (p.u.)	1.1
T_1 (p.u.)	1.0057	T_1 (p.u.)	0.9691	T_1 (p.u.)	0.9836
T_2 (p.u.)	1.048	T_2 (p.u.)	1.0997	T_2 (p.u.)	1.0993
T_3 (p.u.)	0.9577	T_3 (p.u.)	0.9576	T_3 (p.u.)	0.9586
T_4 (p.u.)	0.9569	T_4 (p.u.)	0.9563	T_4 (p.u.)	0.9562
$X_{C,1}$ (p.u.)	-2	$X_{C,1}$ (p.u.)	-2.7089	$X_{C,1}$ (p.u.)	-2.0003
$X_{C,2}$ (p.u.)	-10.1685	$X_{C,2}$ (p.u.)	-10.1703	$X_{C,2}$ (p.u.)	-10.1672
$f_{4.1a}$ ($/h)	**560.4716**	CG($/h)	560.5064	CG ($/h)	587.0209
CE (t/h)	0.2815	CE (t/h)	0.2793	CE (t/h)	0.2883
CCE ($/h)	8.7259	CCE ($/h)	8.6589	CCE ($/h)	8.9364
$CG+CCE$ ($/h)	569.1959	**$f_{4.1b}$ ($/h)**	**569.1649**	$CG+CCE$ ($/h)	595.9573
CRE ($/h)	226.25	CRE ($/h)	226.2499	CRE ($/h)	180.7007
$RECR$ ($/h)	119	$RECR$ ($/h)	119	$RECR$ ($/h)	104.8712
TC ($/h)	**676.4459**	**TC ($/h)**	**676.4149**	**$f_{4.1c}$ ($/h)**	**671.7868**

Table 4.2 The best, worst, average, median and standard deviation of TC from 30 trial solutions of Case 4.1c

The proposed single-side auction scheme in Case 4.1c					
	Best	*Worst*	*Average*	*Median*	*S.D.*
TC ($/h)	671.78682	671.79634	671.79233	671.79433	0.00388

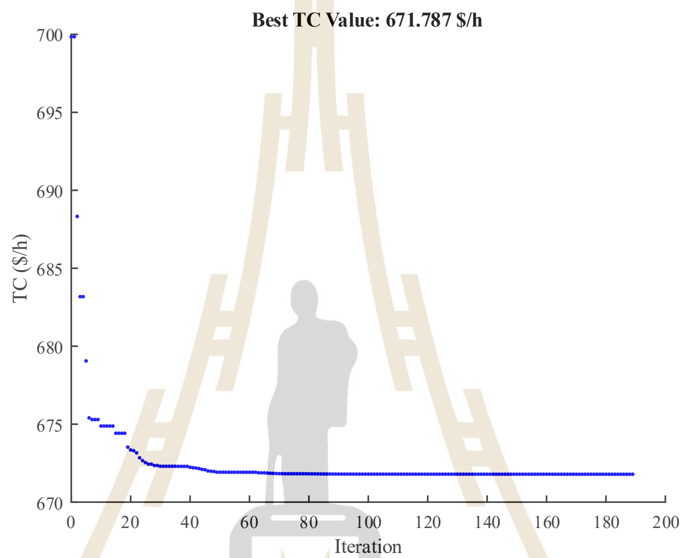

Figure 4.5 The convergence plot of the proposed method for Case 4.1c

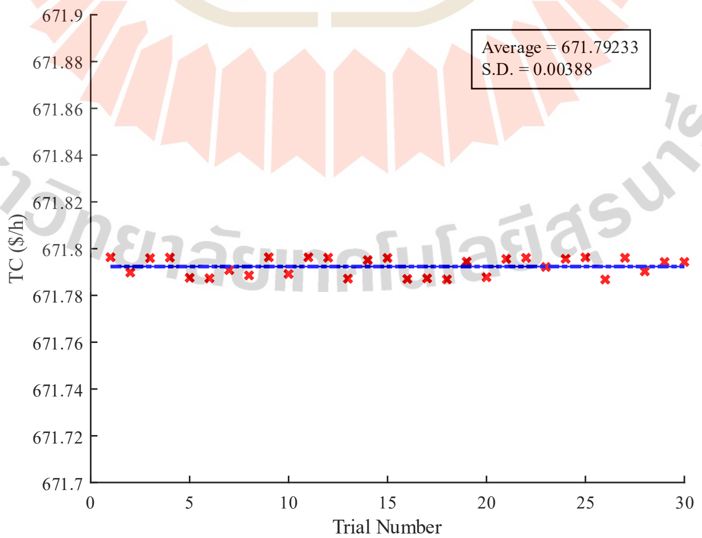

Figure 4.6 The solution with 30 trials of the proposed method run for Case 4.1c

Table 4.3 The simulation results of the double-side auction scheme

Double-Side Auction Scheme					
Variable	Case 4.2a	Variable	Case 4.2b	Variable	Case 4.2c
$P_{G,1}$ (MW)	160.7767	$P_{G,1}$ (MW)	157.0837	$P_{G,1}$ (MW)	157.0787
$P_{G,2}$ (MW)	44.7773	$P_{G,2}$ (MW)	45.6763	$P_{G,2}$ (MW)	45.6665
$P_{G,5}$ (MW)	20.0314	$P_{G,5}$ (MW)	20.3626	$P_{G,5}$ (MW)	20.3569
$P_{G,8}$ (MW)	11.7235	$P_{G,8}$ (MW)	13.9315	$P_{G,8}$ (MW)	13.9504
$P_{G,11}$ (MW)	10.0000	$P_{G,11}$ (MW)	10.0004	$P_{G,11}$ (MW)	10.0001
$P_{G,13}$ (MW)	12.0000	$P_{G,13}$ (MW)	12.0001	$P_{G,13}$ (MW)	12.0000
$V_{G,1}$ (p.u.)	1.1000	$V_{G,1}$ (p.u.)	1.1000	$V_{G,1}$ (p.u.)	1.1000
$V_{G,2}$ (p.u.)	1.0882	$V_{G,2}$ (p.u.)	1.0884	$V_{G,2}$ (p.u.)	1.0884
$V_{G,5}$ (p.u.)	1.0631	$V_{G,5}$ (p.u.)	1.0637	$V_{G,5}$ (p.u.)	1.0638
$V_{G,8}$ (p.u.)	1.0711	$V_{G,8}$ (p.u.)	1.0715	$V_{G,8}$ (p.u.)	1.0716
$V_{G,11}$ (p.u.)	1.1000	$V_{G,11}$ (p.u.)	1.0992	$V_{G,11}$ (p.u.)	1.0434
$V_{G,13}$ (p.u.)	1.1000	$V_{G,13}$ (p.u.)	1.1000	$V_{G,13}$ (p.u.)	1.1000
T_1 (p.u.)	1.0478	T_1 (p.u.)	1.0886	T_1 (p.u.)	0.9955
T_2 (p.u.)	0.9000	T_2 (p.u.)	0.9017	T_2 (p.u.)	1.0810
T_3 (p.u.)	1.0089	T_3 (p.u.)	0.9646	T_3 (p.u.)	0.9670
T_4 (p.u.)	0.9769	T_4 (p.u.)	0.9595	T_4 (p.u.)	0.9606
$X_{C,1}$ (p.u.)	-44.9998	$X_{C,1}$ (p.u.)	-3.8756	$X_{C,1}$ (p.u.)	-2.0011
$X_{C,2}$ (p.u.)	-8.9948	$X_{C,2}$ (p.u.)	-10.1110	$X_{C,2}$ (p.u.)	-10.0668
$P_{RE,7}$ (MW)	12.0000	$P_{RE,7}$ (MW)	12.0000	$P_{RE,7}$ (MW)	12.0000
$P_{RE,21}$ (MW)	10.0000	$P_{RE,21}$ (MW)	10.0000	$P_{RE,21}$ (MW)	10.0000
$P_{D,2}$ (MW)	21.7000	$P_{D,2}$ (MW)	21.7000	$P_{D,2}$ (MW)	21.7000
$P_{D,3}$ (MW)	2.4000	$P_{D,3}$ (MW)	2.4000	$P_{D,3}$ (MW)	2.4000
$P_{D,4}$ (MW)	7.6000	$P_{D,4}$ (MW)	7.6000	$P_{D,4}$ (MW)	7.6000
$P_{D,5}$ (MW)	94.2000	$P_{D,5}$ (MW)	94.2000	$P_{D,5}$ (MW)	94.2000
$P_{D,7}$ (MW)	22.8000	$P_{D,7}$ (MW)	22.8000	$P_{D,7}$ (MW)	22.8000
$P_{D,8}$ (MW)	30.0000	$P_{D,8}$ (MW)	30.0000	$P_{D,8}$ (MW)	30.0000
$P_{D,10}$ (MW)	0.0000	$P_{D,10}$ (MW)	0.0000	$P_{D,10}$ (MW)	0.0000
$P_{D,12}$ (MW)	11.2000	$P_{D,12}$ (MW)	11.2000	$P_{D,12}$ (MW)	11.2000
$P_{D,14}$ (MW)	6.2000	$P_{D,14}$ (MW)	6.2000	$P_{D,14}$ (MW)	6.2000
$P_{D,15}$ (MW)	8.2000	$P_{D,15}$ (MW)	8.2000	$P_{D,15}$ (MW)	8.2000

Table 4.3 The simulation results of the double-side auction scheme (Continued)

Double-Side Auction Scheme					
Variable	Case 4.2a	Variable	Case 4.2b	Variable	Case 4.2c
$P_{D,16}$(MW)	3.5000	$P_{D,16}$(MW)	3.5000	$P_{D,16}$(MW)	3.5000
$P_{D,17}$ (MW)	9.0000	$P_{D,17}$ (MW)	9.0000	$P_{D,17}$ (MW)	9.0000
$P_{D,18}$ (MW)	3.2000	$P_{D,18}$ (MW)	3.2000	$P_{D,18}$ (MW)	3.2000
$P_{D,19}$ (MW)	9.5000	$P_{D,19}$ (MW)	9.5000	$P_{D,19}$ (MW)	9.5000
$P_{D,20}$ (MW)	2.2000	$P_{D,20}$ (MW)	2.2000	$P_{D,20}$ (MW)	2.2000
$P_{D,21}$ (MW)	17.5000	$P_{D,21}$ (MW)	17.5000	$P_{D,21}$ (MW)	17.5000
$P_{D,23}$ (MW)	3.2000	$P_{D,23}$ (MW)	3.2000	$P_{D,23}$ (MW)	3.2000
$P_{D,24}$ (MW)	8.7000	$P_{D,24}$ (MW)	8.7000	$P_{D,24}$ (MW)	8.7000
$P_{D,26}$ (MW)	0.0000	$P_{D,26}$ (MW)	0.0000	$P_{D,26}$ (MW)	0.0000
$P_{D,29}$ (MW)	2.4000	$P_{D,29}$ (MW)	2.4000	$P_{D,29}$ (MW)	2.4000
$P_{D,30}$ (MW)	10.6000	$P_{D,30}$ (MW)	10.6000	$P_{D,30}$ (MW)	10.6000
CG (\$/h)	688.3934	CG (\$/h)	688.4189	CG (\$/h)	698.4132
CE (t/h)	0.3307	CE (t/h)	0.3225	CE (t/h)	0.3225
TC (\$/h)	698.4948	TC (\$/h)	698.2676	TC (\$/h)	698.2632
$\boldsymbol{f_{4.2a}}$	**565.7062**	$\boldsymbol{f_{4.2b}}$	**555.6818**	$\boldsymbol{f_{4.2c}}$	**555.8363**
$\boldsymbol{SW}$	**555.6048**	$\boldsymbol{SW}$	**555.8318**	$\boldsymbol{SW}$	**555.8363**

In Case 4.1b, GENCOs are allocated to minimise the aggregated supply curve, which includes CG and CCE generated by power generation. In this scenario, the total electricity demand is 283.4 MW (excluding DSB). CRE and RECR are disregarded. The calculated CG is \$560.5045/h, with a CE of 0.2793 ton/h and a CCE of \$8.6595/h. The per-hour cost of CG and CCE is \$569.1649 when combined. Considering that the CRE and RECR are \$226.2499/h and \$119/h, respectively, the TC is \$676.4149/h. Incorporating CCE results in a slight reduction in total costs relative to Case 4.1a, underscoring the importance of accounting for carbon emissions in the cost structure. In Case 4.1c, the GENCOs are dispatched to minimise the TC by considering an aggregated supply curve for a total electricity demand of 283.4 MW (excluding DSB). The CG is \$587.0209/h, with emissions of 0.2883 ton/h and a CCE of \$8.93564/h. The combined hourly cost of CG and CCE amounts to \$595.9573. The CRE and RECR are \$180.7007/h and \$104.8712/h, respectively, leading to a TC of \$671.7868/h.

A comparison of price-competition markets across the three case studies, excluding DSB, reveals that Case 4.1b achieves a marginally lower combined CG and CCE of 0.006% than Case 4.1a. Additionally, Case 4.1c demonstrates a significant reduction in TC of 0.6886% compared to both Cases 4.1a and 4.1b. The incorporation of CRE and RECR, along with CCE, presents a more holistic approach that encourages the use of renewable energy and provides a more accurate representation of societal costs, thereby enhancing long-term sustainability and economic efficiency.

Table 4.2 presents the results from 30 trials of the proposed method. In the single-sided auction in Case 4.1c, the best and worst TC values obtained by the PSO algorithm are \$671.7868/h and \$671.7963/h, respectively. The average and median of TC across 30 trials are \$671.7923/h and \$671.7943/h, respectively, with a standard deviation of 0.00388. The convergence diagram in Figure 4.5 demonstrates that the PSO algorithm consistently identifies the optimal solution within a reasonable number of iterations. Figure 4.6 shows the distribution of TC values across the 30 trial solutions for Case 4.1c.

For the DSA scheme shown in Table 4.3, in Case 4.2a, the SW value obtained is 555.6048, focusing solely on CG and DSB. This case optimises SW based on CG and DSB but excludes CCE, CRE, and RECR. Consequently, the initial SW values are lower. In Case 4.2b, the objective is to enhance supply-side performance by incorporating CCE into the aggregated supply curve alongside DSB, while omitting CRE and RECR. The resulting SW value is 555.8318. The inclusion of CCE results in a marginal SW increase of 0.04085% relative to Case 4.2a, highlighting the advantage of accounting for carbon costs. Case 4.2c aims to maximise supply-side profits by integrating CCE, CRE, RECR, and DSB into electricity offer prices. The SW value achieved in this case is 555.8346. Among the cases that consider DSB, Case 4.2c yields the highest SW, underscoring the benefits of a holistic approach that includes economic and environmental factors. Compared to Case 4.2a, the SW in Case 4.2c is 0.04135% higher.

Table 4.4 The best, worst, average, median and standard deviation of TC from 30 trial solutions of Case 4.2c

The proposed double-side auction scheme in Case 4.2c					
	Best	*Worst*	*Average*	*Median*	*S.D.*
SW ($/h)	555.8363	553.9136	555.7468	555.8343	0.3549

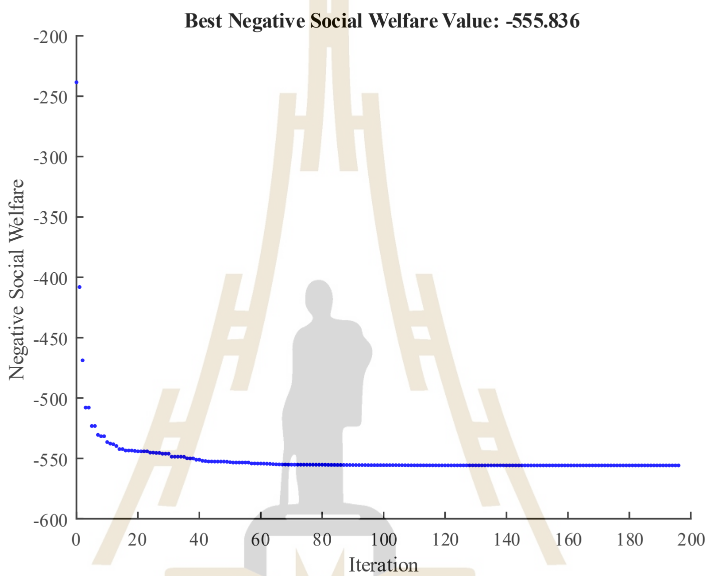

Figure 4.7 The convergence plot of the proposed method for Case 4.2c

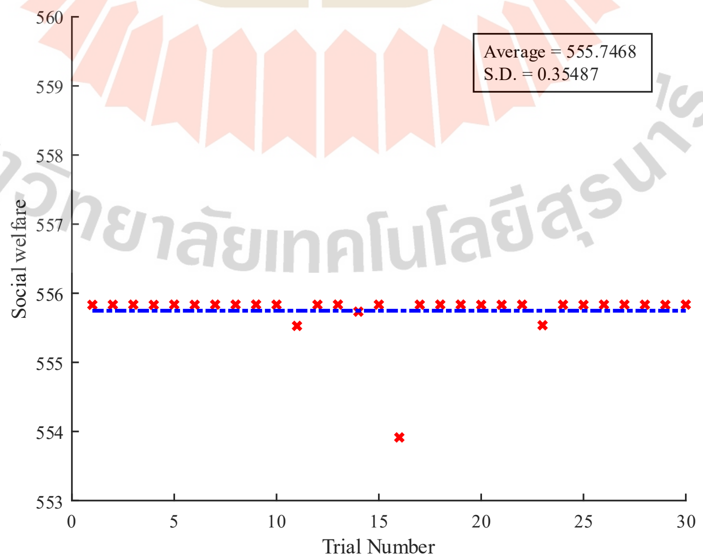

Figure 4.8 The solution with 30 trials of the proposed method run for Case 4.2c

Table 4.4 presents the results from 30 trials of the proposed method. For the double-sided auction in Case 4.2c, the best and worst SW values obtained using the PSO method are 555.8363 and 553.9136, respectively. The average and median of SW values across 30 trials are 555.7468 and 555.8343, with a standard deviation of 0.35487. Additionally, Figure 4.7 illustrates the convergence plot for Case 4.2c, while Figure 4.8 displays the distribution of SW values across the 30 trials.

4.6 Conclusion

This chapter examines the effect of several competitive pricing schemes on the economy and environment of low-carbonising strategies in power systems. The investigation focused on incorporating RECs and DSB using a PSO algorithm. The proposed approach has been applied to the modified IEEE 30-bus system. The occurrences under observation are:

(1) The combined supply offer, including CG, CCE, CRE, and RECR, without DSB, resulted in the most significant decrease in the overall total cost of electricity production, demonstrating the effectiveness of comprehensive optimisation methods.

(2) The DSB and competitive pricing schemes, including the CCE, CRE, and RECR, were considered the most advantageous models. The proposed model illustrates the significance of comprehensive optimisation methodologies for achieving maximum SW and promoting sustainable energy utilisation.

These results highlight the importance of integrating various economic and environmental variables into the optimisation frameworks of low-carbon power systems.

CHAPTER V

CO-OPTIMISED FRAMEWORK FOR COMBINED ELECTRICITY MARKET AND EMISSION MECHANISMS WITH COORDINATED DEMAND RESPONSE AND ANCILLARY SERVICES

5.1 Chapter Overview

This chapter presents a comprehensive evaluation of the novel integrated market-clearing framework to validate its performance and quantify its benefits in terms of economic efficiency, environmental outcomes, and grid security. This chapter empirically demonstrates the advantages of co-optimising energy, ancillary services, and demand-side flexibility within a unified market structure incorporating carbon pricing. The evaluation is conducted using the standard IEEE 30-bus test system, which serves as a benchmark for methodological validation. A range of simulation scenarios has been rigorously designed to test the model under various plausible conditions. These scenarios systematically vary key policy and operational parameters, including different carbon tax rates, tiered demand response (DR) incentive levels, and conditions of generator shortage, thereby allowing for a robust assessment of the framework's adaptability.

This chapter is the comparative analysis of different market-clearing strategies. The performance of the proposed integrated co-optimisation approach is benchmarked against a conventional sequential clearing mechanism. Furthermore, each clearing strategy is evaluated under two distinct schemes: a traditional generation-only case and the proposed DR-integrated case, which uniquely allows uncalled DR to serve as spinning reserve capacity. The results section provides a detailed analysis of key performance indicators, including total operational costs, reserve procurement costs, and system-wide carbon emissions. The findings reveal that the integrated DR scenario yields significant economic advantages, achieving cost savings of up to 6.1% and substantially reducing reserve procurement expenditures compared to conventional approaches. Critically, the analysis demonstrates that utilising DR as a co-optimised reserve resource enhances system flexibility and adaptability without adversely affecting environmental performance. The chapter concludes by discussing the implications of these findings and offering vital, policy-relevant insights to support the design of a scalable, economically efficient, and environmentally sustainable electricity market. Figure 5.1 illustrates the ISO's management of energy and reserves, implementation of carbon tax mechanism, and utilisation of active or standby demand response for real-time balancing, enhancing cost efficiency and environmental performance.

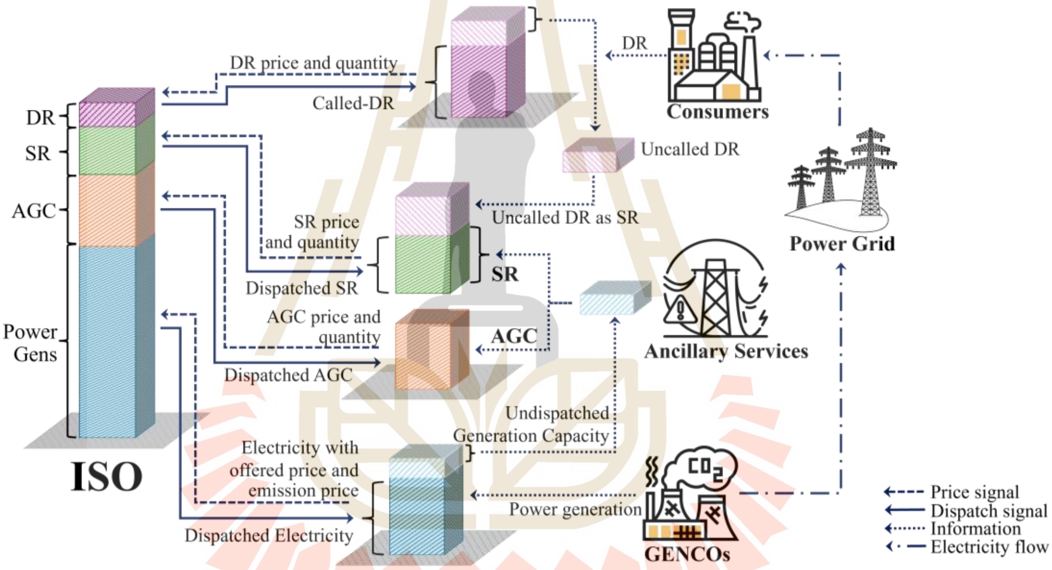

Figure 5.1 Schematic diagram of carbon-accounted optimal power dispatch and spot pricing

5.2 Mathematical Formulation

The proposed optimisation model minimises the total system operating cost, which includes CG, CCE, automatic generation control cost (CAGC), spinning reserve cost (CSR), and demand response cost (CDR). This formulation, containing both quadratic and linear components, is subject to constraints on power balance, generator and reserve capacity limits, and demand response. The calculations for CG and CCE are defined by Equations (3.13) and (3.14), respectively.

5.2.1 Cost of Automatic Generation Control

The cost of automatic generation control (CAGC) represents the financial cost incurred when generation units modulate their dispatch to provide frequency regulation and maintain grid security. The magnitude of this cost is influenced by the technical and economic characteristics of the generators, including their ramp rates and deviations from their optimal economic dispatch points. The CAGC, measured in dollars per hour ($/h), is determined by summing the costs from all participating units, where the cost for each unit i is the product of the market price for AGC service ($AGCP_i$ in $/MWh) and the amount of AGC capacity activated (AGC_i in MW):

$$CAGC(P_{G,i}) = \sum_{i=1}^{NG} AGCP_i \times AGC_i \text{ ,} \tag{5.1}$$

where $AGCP_i$ represents the price of automatic generation control at bus i ($/MWh) and AGC_i represents the activated automatic generation control capacity at bus i (MW).

5.2.2 Cost of Spinning Reserve

The spinning reserve utilisation is a critical component of power system reliability management, focusing on strategically activating reserve capacity to address emergent stability challenges. The economic aspect of spinning reserve services is defined by the cost structure of deploying this reserve capacity. Specifically, spinning reserve utilisation (SR_i) refers to the actual quantity of reserve capacity, measured in MW, that is dynamically activated during system contingencies. Meanwhile, the spinning reserve price (SRP_i) is expressed as the willingness to pay for activated services ($/MWh), at a designated bus i. The cost of spinning reserve (CSR) is calculated similarly to AGC, based on actual reserve deployed and its unit price defined as:

$$CSR(P_{G,i}) = \sum_{i=1}^{NG} SRP_i \times SR_i \text{ ,} \tag{5.2}$$

where SRP_i represents the unit price for spinning reserve ($/MWh), SR_i represents spinning reserve utilisation at bus i (MW).

5.2.3 Demand Response Cost

The DR cost incorporates incentive payments given to consumers who participate in load reduction under the DR programme. A progressive incentive system is used, with compensation increasing with the level of load reduction, expressed in \$/MWh, for participants in the demand response programme. For instance, early load reductions up to the first $\delta_{i,1}^{\max}$ MW receive \$ $R_{i,1}$ /MWh. Additional reductions beyond this threshold are rewarded at higher rates, at \$ $R_{i,2}$ /MWh and \$ $R_{i,3}$ /MWh, as shown in Figure 5.2. Therefore, the called-DR in step-based pricing, which represents the total cost incurred for reducing electricity consumption, can be described as follows:

$$CDR(\delta_{i,j}) = \sum_{i=1}^{ND} \sum_{j=1}^{NDR} R_{i,j} \times \delta_{i,j} \ , \tag{5.3}$$

subject to:

$$0 \le \delta_{i,j} \le \delta_{i,j}^{\max} \quad , i = 1, 2, ..., ND, \ j = 1, 2, ..., NDR \ , \tag{5.4}$$

where ND denotes the number of loads, NDR represents the number of pricing steps in the demand response program, $R_{i,j}$ is the price per unit of electricity reduction for step i by demand response participant j (\$/MWh), $\delta_{i,j}$ represents the amount of load reduction achieved within step i by demand response participant j (MW), $\delta_{i,j}^{\max}$ represents the maximum allowable reduction in step i by demand response participant j (MW).

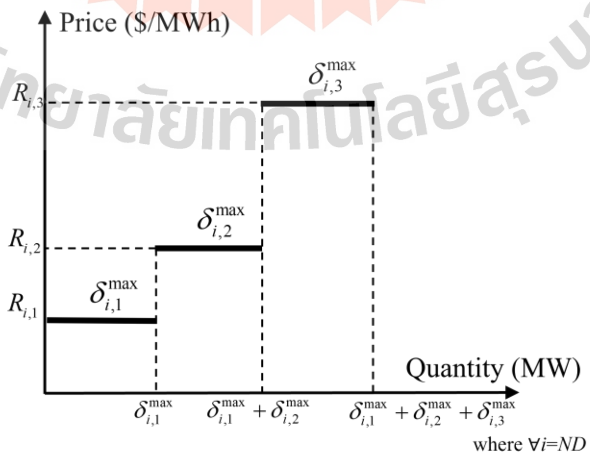

Figure 5.2 Incentive-based demand response with stepwise pricing

5.3 Objective Function and Study Cases

The proposed OPF framework simultaneously optimises economic generator dispatch and environmental objectives, the latter by limiting carbon emissions and incentivising renewable generation. System security is maintained through the integrated management of essential ancillary services, namely SR and AGC. The model internalises the cost of carbon emission, enabling it to identify dispatch portfolios that optimally balance operational expenditures against environmental externalities. Figure 5.3 demonstrates the effect of a demand response program on electricity market pricing and generation expenses. As power demand increases, the marginal cost of generation, which represents the aggregated generation cost, becomes apparent in the blue curve. Without a DR program, market-clearing prices and quantities are determined by the intersection of the demand curve and the aggregated generating cost, resulting in higher prices and quantities. However, implementing a DR programme reduces power demand and total electricity consumption. Market-clearing prices and amounts are reduced due to this decrease in demand. In addition, the market-clearing prices under the DR programme are calculated to reflect the associated DR costs, encompassing the financial incentives offered to participants.

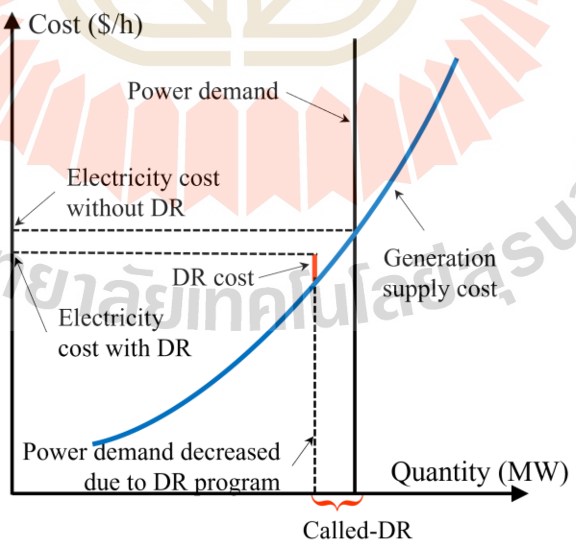

Figure 5.3 Demand response program on the electricity market pricing

To investigate the effects of DR integration, this chapter evaluates two market-clearing schemes: (1) a combined electricity-emission market without DR and (2) a combined electricity-emission market with DR. These schemes are assessed using both sequential and integrated clearing strategies, resulting in four distinct case studies: Sequential Market Clearing (SMC), Co-optimised Market Clearing (CMC), SMC with DR (SMC-DR), and CMC with DR (CMC-DR). Table 5.1 summarises the formulation of these four cases.

Table 5.1 Summary of market-clearing models

Scheme	Market Model	Market Clearing Approach		
		CM	*AS*	*DR*
1. Combined Electricity-Emission	SMC	Combined	Sequential	Without
	CMC	Combined	Co-optimised	Without
2. Combined Electricity-Emission with DR	SMC-DR	Combined	Sequential	Co-optimised
	CMC-DR	Combined	Co-optimised	Co-optimised

5.3.1 Scheme 1: Combined Electricity-Emission Scheme

Case 5.1a: Sequential Market Clearing (SMC)

In this case, energy dispatch is solved via quadratic programming-based OPF (QP-OPF), followed by separate linear programming-based (LP) procurement of ancillary services, reflecting traditional market operations. Hence, the primary objective function for this case can be formulated as follows:

minimise $$f_{5.1a,1}(x,u)=\left[\sum_{i=1}^{NG}CG(P_{G,i})+\sum_{i=1}^{NG}CCE(P_{G,i})\right]+\mu\cdot\left[g(x,u)\right]^2, \qquad (5.5)$$

subject to:

$$\sum_{i=1}^{NG}P_{G,i}=\sum_{j=1}^{ND}P_{D,j}\,. \qquad (5.6)$$

Sub-objective function can be described as follows:

minimise $$f_{5.1a,2}(x,u)=\sum_{i=1}^{NG} CAGC(P_{G,i})+\mu\cdot\left[g(x,u)\right]^2, \tag{5.7}$$

minimise $$f_{5.1a,3}(x,u)=\sum_{i=1}^{NG} CSR(P_{G,i})+\mu\cdot\left[g(x,u)\right]^2, \tag{5.8}$$

subject to:

$$\sum_{i=1}^{NG} AGC_i \geq \%AGCR\times\sum_{i=1}^{ND} P_{D,i}\ , \tag{5.9}$$

$$0\leq AGC_i \leq AGC_i^{\max},\quad i=1,2,\ldots,NG\ , \tag{5.10}$$

$$P_{G,i}+AGC_i\leq P_{G,i}^{\max},\quad i=1,2,\ldots,NG\ , \tag{5.11}$$

$$\sum_{i=1}^{NG} SR_i \geq \%SRR\times\sum_{i=1}^{ND} P_{D,i}\ , \tag{5.12}$$

$$0\leq SR_i \leq SR_i^{\max},\quad i=1,2,\ldots,NG\ , \tag{5.13}$$

$$P_{G,i}+AGC_i+SR_i\leq P_{G,i}^{\max},\quad i=1,2,\ldots,NG\ . \tag{5.14}$$

where $CG(P_{G,i})$, $CCE(P_{G,i})$, $CAGC(P_{G,i})$, and $CSR(P_{G,i})$ are formulated as shown in Equations (3.13), (3.15), (5.1), and (5.2), respectively.

Case 5.1b: Co-Optimised Market Clearing (CMC)

In this case, the proposed unified quadratic programming optimal power flow (QP-OPF) model co-optimises energy dispatch and ancillary services, thereby enabling operational synergies and enhancing cost-efficiency. So, the objective function for this case can be formulated as follows:

minimise $$f_{5.1b}(x,u)=\left[\sum_{i=1}^{NG}CG+\sum_{i=1}^{NG}CCE+\sum_{i=1}^{NG}CAGC+\sum_{i=1}^{NG}CSR\right]+\mu\cdot\left[g(x,u)\right]^2, \quad (5.15)$$

subject to:

$$\sum_{i=1}^{NG}P_{G,i}+\sum_{i=1}^{NG}AGC_i+\sum_{i=1}^{NG}SR_i=\sum_{j=1}^{ND}P_{D,j}, \quad (5.16)$$

and AGC and SR requirements are expressed in Equations (5.9)-(5.10) and (5.12)-(5.13), respectively.

5.3.2 Scheme 2: Combined Electricity-Emission with Demand Response Scheme

Case 5.2a: Sequential Market Clearing with demand response (SMC-DR)

In this case, a sequential optimisation approach is employed: an initial OPF-based dispatch is followed by a separate LP model for procuring DR and ancillary services. This decoupled methodology facilitates an assessment of its distinct market impacts. So, the primary objective function for this case can be formulated as follows:

minimise $$f_{5.2a,1}(x,u)=\left[\sum_{i=1}^{NG}CG+\sum_{i=1}^{NG}CCE+\sum_{i=1}^{ND}\sum_{j=1}^{NDR}CDR\right]+\mu\cdot\left[g(x,u)\right]^2, \quad (5.17)$$

subject to:

$$\sum_{i=1}^{NG}P_{G,i}=\sum_{j=1}^{ND}P_{D,j}-\underbrace{\sum_{i=1}^{ND}\sum_{j=1}^{NDR}\delta_{i,j}}_{\text{called DR}}. \quad (5.18)$$

Sub-objective function can be described as in Equations (5.7) and (5.8), subject to:

$$\sum_{i=1}^{NG}AGC_i\geq\%AGCR\times\left(\sum_{i=1}^{ND}P_{D,i}-\underbrace{\sum_{i=1}^{ND}\sum_{j=1}^{NDR}\delta_{i,j}}_{\text{called DR}}\right), \quad (5.19)$$

$$\sum_{i=1}^{NG} SR_i + \underbrace{\delta_{i,j}^{\max} - \sum_{i=1}^{ND}\sum_{j=1}^{NDR}\delta_{i,j}}_{\text{uncalled DR as SR}} \geq \%SRR \times \left(\sum_{j=1}^{ND} P_{D,j} - \underbrace{\sum_{i=1}^{ND}\sum_{j=1}^{NDR}\delta_{i,j}}_{\text{called DR}} \right), \tag{5.20}$$

and the active power generation limits of AGC are given in Equations (5.10) and (5.11), respectively. Likewise, the SR and active power generation limits of SR are used in Equations (5.13) and (5.14), respectively. The portion of DR capacity remains unused and is available as a reserve for system reliability.

Case 5.2b: Co-Optimised Market Clearing with DR (CMC-DR)

This case concurrently optimises energy, DR, and ancillary services within a single QP-OPF framework. Such a holistic formulation reflects an integrated, modern market design, thereby enabling the comprehensive utilisation of DR resources. Hence, the objective function can be formulated as follows:

minimise

$$f_{5.2b}(x,u) = \left[\sum_{i=1}^{NG} CG(P_{G,i}) + \sum_{i=1}^{NG} CCE(P_{G,i}) + \sum_{i=1}^{NG} CAGC(P_{G,i}) + \sum_{i=1}^{NG} CSR(P_{G,i}) + \sum_{i=1}^{ND}\sum_{j=1}^{NDR} CDR \right] + \mu \cdot \left[g(x,u)\right]^2, \tag{5.21}$$

subject to:

$$\sum_{i=1}^{NG} P_{G,i} + \sum_{i=1}^{NG} AGC_i + \sum_{i=1}^{NG} SR_i = \sum_{j=1}^{ND} P_{D,j} + P_{loss} - \underbrace{\sum_{i=1}^{ND}\sum_{j=1}^{NDR}\delta_{i,j}}_{\text{called DR}}, \tag{5.22}$$

and AGC and SR requirements are expressed in Equations (5.19) and (5.20), respectively. Moreover, variable limits are expressed in Equations (3.7), (5.10), (5.13), and (5.14).

A comparative analysis of Schemes 1 and 2 is conducted based on the total cost (TC), calculated as the summation of all cost components shown in Equation (5.23):

$$TC = \sum_{i=1}^{NG} CG(P_{G,i}) + \sum_{i=1}^{NG} CCE(P_{G,i}) + \sum_{i=1}^{NG} CAGC(P_{G,i}) + \sum_{i=1}^{NG} CSR(P_{G,i}) + \sum_{i=1}^{ND}\sum_{j=1}^{NDR} CDR(\delta_{i,j}). \tag{5.23}$$

For Scheme 1 (Cases 5.1a and 5.1b), which models a market without DR, the CDR component is inherently zero ($CDR = 0$).

5.4 Methodology

This chapter details the computational framework devised to evaluate the economic and environmental performance of the proposed market structures. The methodology is structured around the analysis of two primary schemes: (1) the combined electricity-emission scheme, detailed in Section 5.3.1, and (2) the combined electricity-emission with demand response scheme, presented in Section 5.3.2. To assess the impact of market design, each of these two schemes is implemented and compared using two distinct computational strategies: SMC and CMC. This structure yields four different case studies, including SMC, CMC, SMC-DR, and CMC-DR. The subsequent subsections will elaborate on the specific procedural steps and formulations adopted for each computational approach.

The control variables (x) are power generation, AGC, SR, and DR, which can be formulated as a quadratic function with linearised constraints. Therefore, the problem can be solved by QP. A standard quadratic programming problem can be expressed mathematically as follows:

$$\text{minimise} \quad \frac{1}{2}\mathbf{x}^T\mathbf{H}\mathbf{x} + \mathbf{f}^T\mathbf{x}, \tag{5.24}$$

subject to:

$$\mathbf{A}\mathbf{x} \le \mathbf{b},\ \mathbf{A}_{eq}\mathbf{x} \le \mathbf{b}_{eq},\ lb \le \mathbf{x} \le ub. \tag{5.25}$$

5.4.1 Scheme 1: Combined Electricity-Emission Scheme Computation

(1) <u>SMC</u>: The SMC employs a sequential optimisation approach to separately address energy dispatch, ancillary service, and spinning reserves procurement. The procedural steps are as follows:

Step 1: Gather all required system data, including bus data, branch data, generator Variables, and system constraints.

Step 2: Perform a power flow analysis to determine the total active power generation $(P_{G,i})$ and demand $(P_{D,j})$.

Step 3: The control variables are $P_{G,i}$, AGC_i, and SR_i as follows:

$$\mathbf{x}_{P_G} = \left[P_{G,1},\ldots,P_{G,NG}\right], \tag{5.26}$$

$$\mathbf{x}_{AGC} = \left[AGC_1,\ldots,AGC_{NG}\right], \tag{5.27}$$

$$\mathbf{x}_{SR} = \left[SR_1,\ldots,SR_{NG}\right]. \tag{5.28}$$

Step 4: Minimise the combined CG and CCE as in Equations (5.5) and (5.6), using QP formulation in Equation (5.24) as follows:

$$\mathbf{H}_{5.1a,1} = \begin{bmatrix} 2A_1 & 0 & \cdots & 0 \\ 0 & 2A_2 & \cdots & 0 \\ \vdots & \vdots & \ddots & \vdots \\ 0 & 0 & \cdots & 2A_{NG} \end{bmatrix}_{NG\times NG}, \tag{5.29}$$

$$\mathbf{f}_{5.1a,1} = [B_1 \ldots B_{NG}]^T, \tag{5.30}$$

where:

$$\mathbf{x}_{5.1a,1} = \mathbf{x}_{P_G}, \tag{5.31}$$

$$A_i = a_i + C_{Tax}(\alpha_i \times 0.01^2),\ B_i = b_i + C_{Tax}(b_i \times 0.01),\ i = 1,\ldots,NG. \tag{5.32}$$

Step 5: Compare the sum of $P_{G,i}$ from the QP solution with the initial power flow results. If the difference exceeds 0.001, recompute the QP until convergence.

Step 6: Minimise CAGC solving for AGC_i using LP as in Equations (5.7), (5.9), (5.10), and (5.11).

Step 7: Minimise CSR solving for SR_i using LP as in Equations (5.8), (5.12), (5.13) and (5.14).

Step 8: Calculate total operation cost, as in Equation (5.23).

Step 9: Verify all results against system constraints, including power balance, AGC and SR requirements, and operational limits.

(2) CMC: The CMC simultaneously integrates energy dispatch and AS procurement within a single optimisation framework. The procedural steps are as follows:

Step 1: Gather all required system data.

Step 2: Perform a power flow analysis to determine the $P_{G,i}$ and $P_{D,j}$.

Step 3: Define the control variables are $P_{G,i}$, AGC_i, and SR_i as in Equations (5.26)-(5.28).

Step 4: Minimise the objective function, as in Equations (5.15) and (5.16), using QP as follows:

$$\mathbf{H}_{5.1b} = \begin{array}{c} \begin{array}{ccc} \quad P_G \quad & \quad \overbrace{\qquad\quad}^{AGC} \quad & \quad \overbrace{\qquad\quad}^{SR} \end{array} \\ \begin{bmatrix} \mathbf{H}_{5.1a,1} & 0_{NG\times NG} & 0_{NG\times NG} \\ 0_{NG\times NG} & 0_{NG\times NG} & 0_{NG\times NG} \\ 0_{NG\times NG} & 0_{NG\times NG} & 0_{NG\times NG} \end{bmatrix}_{3\cdot NG\times 3\cdot NG} \end{array}, \tag{5.33}$$

$$\mathbf{f}_{5.1b} = [B_1 \ldots B_{NG} \quad AGCP_1 \ldots AGCP_{NG} \quad SRP_1 \ldots SRP_{NG}]^T, \tag{5.34}$$

where:

$$\mathbf{x}_{5.1b} = \left[\mathbf{x}_{P_G} \;\; \mathbf{x}_{AGC} \;\; \mathbf{x}_{SR}\right]. \tag{5.35}$$

Step 5: Verify that the optimised values satisfy the power balance constraint, reserve requirements, and operational limits for $P_{G,i}$, AGC_i, and SR_i. If any constraints are violated, refine the QP setup and resolve.

5.4.2 Scheme 2: Combined Electricity-Emission with Demand Response Scheme Computation

(1) SMC-DR: SMC-DR follows a sequential optimisation approach, incorporating DR explicitly in the process. The steps include:

Step 1: Gather all required system data.

Step 2: Perform a power flow analysis to determine $P_{G,i}$ and $P_{D,j}$.

Step 3: The control variables are $P_{G,i}$, AGC_i, SR_i and $\delta_{i,j}$ as in Equations (5.26)-(5.28) and

$$\mathbf{x}_{DR} = [\delta_{1,1} \ldots \delta_{ND,NDR}]. \tag{5.36}$$

Step 4: Minimise the combined CG, CCE, and CDR as in Equations (5.17) and (5.18) using QP as follows:

$$\mathbf{H}_{5.2a,1} = \begin{array}{c} \begin{array}{cc} \quad P_G \quad & \quad \overbrace{\quad}^{DR} \quad \end{array} \\ \begin{bmatrix} \mathbf{H}_{5.1a,1} & 0_{NG\times NDR} \\ 0_{NDR\times NG} & 0_{NDR\times NDR} \end{bmatrix}_{(NG+NDR)\times(NG+NDR)} \end{array}, \tag{5.37}$$

$$\mathbf{f}_{5.2a,1} = [B_1 \ldots B_{NG} \;\; R_1 \ldots R_{NDR}]^T, \tag{5.38}$$

where:

$$\mathbf{x}_{5.2a,1} = [\mathbf{x}_{P_G} \;\; \mathbf{x}_{DR}]. \tag{5.39}$$

Step 5: Compare the sum of $P_{G,i}$ from the QP solution with the initial power flow results. If the difference exceeds 0.001, recompute the QP until convergence.

Step 6: Minimise CAGC solving for AGC_i using LP as Equation (5.7), subject to as in Equations (5.10), (5.11), and (5.19).

Step 7: Minimise CSR solving for SR_i using LP as Equation (5.8), subject to as in Equations (5.13), (5.14), and (5.20).

Step 8: Calculate TC integrating DR as Equation (5.23).

Step 9: Verify all results against system constraints, including power balance with DR, AGC, and SR requirements and operational limits.

(2) CMC-DR: The CMC-DR adopts a fully integrated optimisation strategy incorporating DR into market-clearing. Procedural steps include:

Step 1: Gather all required data.

Step 2: Perform a power flow analysis to determine the $P_{G,i}$ and $P_{D,j}$.

Step 3: Define the decision variables are $P_{G,i}$, AGC_i, SR_i and $\delta_{i,j}$ as in Equations (5.26), (5.27), (5.28) and (5.36).

Step 4: Minimise the objective function as in Equation (5.21), subject to Equation (5.19), (5.20), and (5.22) using QP as follows:

$$\mathbf{H}_{5.2b} = \begin{bmatrix} \overbrace{\mathbf{H}_{5.1a,1}}^{P_G} & \overbrace{0_{NG\times NG}}^{AGC} & \overbrace{0_{NG\times NG}}^{SR} & \overbrace{0_{NG\times NDR}}^{DR} \\ 0_{NG\times NG} & 0_{NG\times NG} & 0_{NG\times NG} & 0_{NG\times NDR} \\ 0_{NG\times NG} & 0_{NG\times NG} & 0_{NG\times NG} & 0_{NG\times NDR} \\ 0_{NG\times NDR} & 0_{NG\times NDR} & 0_{NG\times NDR} & 0_{NDR\times NDR} \end{bmatrix}_{(3\cdot NG+NDR)\times(3\cdot NG+NDR)}, \tag{5.40}$$

$$\mathbf{f}_{5.2b} = [B_1 \ldots B_{NG} \quad AGCP_1 \ldots AGCP_{NG} \quad SRP_1 \ldots SRP_{NG} \quad R_1 \ldots R_{NDR}]^T, \tag{5.41}$$

where:

$$\mathbf{x}_{5.2b} = [\mathbf{x}_{P_G} \quad \mathbf{x}_{AGC} \quad \mathbf{x}_{SR} \quad \mathbf{x}_{DR}]. \tag{5.42}$$

Step 5: Verify that the optimised values satisfy the power balance constraint, reserve requirements, and operational limits for $P_{G,i}$, AGC_i, SR_i and $\delta_{i,j}$. If any constraints are violated, refine the QP setup and resolve the issue.

5.5 Simulation Results and Discussions

The proposed market-clearing framework is evaluated on the IEEE 30-bus test system to assess its performance in terms of cost efficiency, emission reduction, and system reliability under various market-clearing strategies and DR levels. The IEEE 30-bus system comprises 30 buses, 41 transmission lines, six generators, and 24 load buses. A baseline carbon tax of \$50/ton CO_2 is applied, while the requirements for AGC and SR are each set at 5% of the total active power dispatch. DR is implemented through a stepwise incentive structure, with incentive rates of \$2, \$4, and \$6/MWh corresponding to load reductions of 5 MW, 10 MW, and 15 MW, respectively. To examine the robustness of the proposed framework, additional sensitivity analyses are performed under varying generator availability conditions by systematically reducing the generation capacity of the Bus 2 generator $(P_{G,2})$ from 100% of its rated capacity to 75%, 60%, 50%, and 40%, simulating progressive capacity shortage scenarios. This subsection presents the simulation results from the IEEE 30-bus test system, analysing four market scenarios under two primary market schemes: the combined electricity–emission scheme (with and without DR). Each scheme is evaluated under both sequential (SMC and SMC-DR) and integrated (CMC and CMC-DR) clearing strategies. Simulations are conducted under progressively reduced generation availability at Bus 2, with $P_{G,2}$ outputs ranging from 100% to 40% of their maximum capacity.

The CMC consistently yields lower total operating costs compared with the SMC, particularly under conditions of limited generation availability as shown in Table 5.2. At 40% PG,2 capacity, the CMC approach achieves a 2.65% reduction in total system cost relative to SMC. Although SMC results in slightly lower emissions, the CMC scheme demonstrates greater stability in ancillary service procurement, especially in AGC and SR, thereby enhancing overall system security. Further improvements are observed when DR is incorporated, as summarised in Table 5.3. At 40% $P_{G,2}$ capacity, total operating cost decreases from \$966.01/h under SMC-DR to \$940.14/h under CMC-DR, representing a 2.68% cost reduction. The CMC-DR also eliminates the need for SR procurement by effectively utilising uncalled DR as reserve capacity, without compromising emission performance. The emission levels remain comparable between the sequential and integrated approaches, confirming that DR integration provides both economic and environmental benefits when co-optimised with other market components. Figure 5.4 illustrates the total cost performance across all simulation scenarios. DR-integrated strategies consistently yield lower system costs, while integrated clearing approaches outperform their sequential counterparts under all conditions. Among all configurations, CMC-DR delivers the most favourable outcomes in terms of cost reduction, reliability enhancement, and reserve optimisation. These findings substantiate the effectiveness of the proposed fully integrated market-clearing framework in co-optimising carbon pricing, ancillary services, and demand response to achieve sustainable, economically efficient electricity market operations.

Table 5.2 Comparison of combined electricity-emission scheme for IEEE 30-bus system

Variable	Scheme 1: Combined Electricity-Emission Scheme									
	Case 5.1a: SMC					Case 5.1b: CMC				
	$P_{G,2}$ *capacity (%)*					$P_{G,2}$ *capacity (%)*				
	100%	*75%*	*60%*	*50%*	*40%*	*100%*	*75%*	*60%*	*50%*	*40%*
$P_{G,1}$ (MW)	185.96	185.96	186.96	191.65	196.34	185.96	185.96	189.68	190	190
$P_{G,2}$ (MW)	49.71	49.71	48	40	32	49.71	49.71	43.36	35.36	27.35
$P_{G,5}$ (MW)	20.03	20.03	20.1	20.40	20.71	20.03	20.03	20.27	20.94	21.53
$P_{G,8}$ (MW)	15.00	15.00	15.48	17.72	19.98	15.00	15.00	16.79	21.69	26.11
$P_{G,11}$ (MW)	10.17	10.17	10.33	11.08	11.84	10.17	10.17	10.77	12.42	13.91
$P_{G,13}$ (MW)	12.00	12.00	12	12	12	12	12	12	12.46	13.94
AGC_1 (MW)	6.00	6.00	6	6	3.66	6	6	6	6	6
AGC_2 (MW)	4.64	4.64	0	0	0	4.64	4.64	4.64	4.64	4.64
AGC_5 (MW)	0	0	4.64	4.64	5	0	0	0	0	0
AGC_8 (MW)	0	0	0	0	1.98	0	0	0	0	0
AGC_{11} (MW)	0	0	0	0	0	0	0	0	0	0
AGC_{13} (MW)	4	4	4	4	4	4	4	4	4	4
SR_1 (MW)	4	4	4	2.35	0	4	4	4	4	4
SR_2 (MW)	0	0	0	0	0	0	0	0	0	0

Table 5.2 Comparison of combined electricity-emission scheme for IEEE 30-bus system (Continued)

Variable	Scheme 1: Combined Electricity-Emission Scheme									
	Case 5.1a: SMC					Case 5.1b: CMC				
	$P_{G,2}$ *capacity (%)*					$P_{G,2}$ *capacity (%)*				
	100%	*75%*	*60%*	*50%*	*40%*	*100%*	*75%*	*60%*	*50%*	*40%*
SR_5 (MW)	5	5	5	5	5	5	5	5	5	5
SR_8 (MW)	5.64	5.64	5.64	6	6	5.64	5.64	5.64	5.64	5.64
SR_{11} (MW)	0	0	0	0	0	0	0	0	0	0
SR_{13} (MW)	0	0	0	1.29	3.64	0	0	0	0	0
CG ($/h)	800.24	800.24	800.22	801.62	805.55	800.24	800.24	800.72	804.26	810.70
CE (t/h)	0.348	0.348	0.349	0.358	0.368	0.348	0.348	0.354	0.354	0.354
CCE ($/h)	17.38	17.376	17.464	17.91	18.400	17.376	17.376	17.714	17.700	17.688
CAGC ($/h)	113.08	113.08	117.72	117.72	131.4	113.08	113.08	113.08	113.08	113.08
CSR ($/h)	128.43	128.43	128.43	134.31	143.72	128.43	128.43	128.43	128.43	128.43
TC ($/h)	1,059.12	1,059.12	1,063.83	1,071.5	1,099.06	1,059.13	1,059.13	1,059.94	1,063.46	1,069.9

Table 5.3 Comparison of combined electricity-emission with demand response scheme for IEEE 30-bus system

Variable	Scheme 2: Combined Electricity-Emission with Demand Response Scheme									
	Case 5.2a: SMC-DR					Case 5.2b: CMC-DR				
	$P_{G,2}$ capacity (%)					*$P_{G,2}$ capacity (%)*				
	100%	*75%*	*60%*	*50%*	*40%*	*100%*	*75%*	*60%*	*50%*	*40%*
$P_{G,1}$ (MW)	183.23	183.23	183.93	188.72	193.41	185.76	185.76	189.45	194	194
$P_{G,2}$ (MW)	49.084	49.084	48	40	32	49.664	49.664	43.376	35.376	27.376
$P_{G,5}$ (MW)	19.854	19.854	19.899	20.210	20.515	20.018	20.018	20.258	20.575	21.208
$P_{G,8}$ (MW)	13.698	13.698	14.034	16.325	18.572	14.910	14.910	16.676	19.017	23.684
$P_{G,11}$ (MW)	10	10	10	10.614	11.371	10.136	10.136	10.732	11.521	13.095
$P_{G,13}$ (MW)	12	12	12	12	12	12	12	12	12	13.126
AGC_1 (MW)	6	6	6	6	6	6	6	6	6	6
AGC_2 (MW)	4.393	4.393	0	0	0	4.624	4.624	4.624	4.624	4.624
AGC_5 (MW)	0	0	4.393	4.393	4.393	0	0	0	0	0
AGC_8 (MW)	0	0	0	0	0	0	0	0	0	0
AGC_{11} (MW)	0	0	0	0	0	0	0	0	0	0
AGC_{13} (MW)	4	4	4	4	4	4	4	4	4	4
SR_1 (MW)	0	0	0	0	0.593	0	0	0	0	0
SR_2 (MW)	0	0	0	0	0	0	0	0	0	0

Table 5.3 Comparison of combined electricity-emission with demand response scheme for IEEE 30-bus system (Continued)

Variable	Scheme 2: Combined Electricity-Emission with Demand Response Scheme									
	Case 5.2a: SMC-DR					Case 5.2b: CMC-DR				
	$P_{G,2}$ capacity (%)					*$P_{G,2}$ capacity (%)*				
	100%	*75%*	*60%*	*50%*	*40%*	*100%*	*75%*	*60%*	*50%*	*40%*
SR_5 (MW)	4.393	4.393	4.393	4.393	3.800	0	0	0	0	0
SR_8 (MW)	0	0	0	0	0	0	0	0	0	0
SR_{11} (MW)	0	0	0	0	0	0	0	0	0	0
SR_{13} (MW)	0	0	0	0	0	0	0	0	0	0
δ_1 (MW)	5	5	5	5	5	0.38	0.38	0.38	0.38	0.38
δ_2 (MW)	0	0	0	0	0	0	0	0	0	0
δ_3 (MW)	0	0	0	0	0	0	0	0	0	0
CG ($/h)	783.09	783.09	783.05	784.26	788.01	798.95	798.95	799.41	802.28	808.39
CE (t/h)	0.343	0.343	0.344	0.353	0.363	0.347	0.347	0.354	0.363	0.363
CCE ($/h)	17.150	17.150	17.212	17.655	18.139	17.360	17.360	17.694	18.150	18.136
CAGC ($/h)	110.33	110.33	114.72	114.72	114.72	112.87	112.87	112.87	112.87	112.87
CSR ($/h)	35.146	35.146	35.146	35.146	35.146	0	0	0	0	0
CDR ($/h)	10	10	10	10	10	0.751	0.751	0.751	0.751	0.751
TC ($/h)	955.71	955.71	960.13	961.78	966.01	929.93	929.93	930.73	934.05	940.14

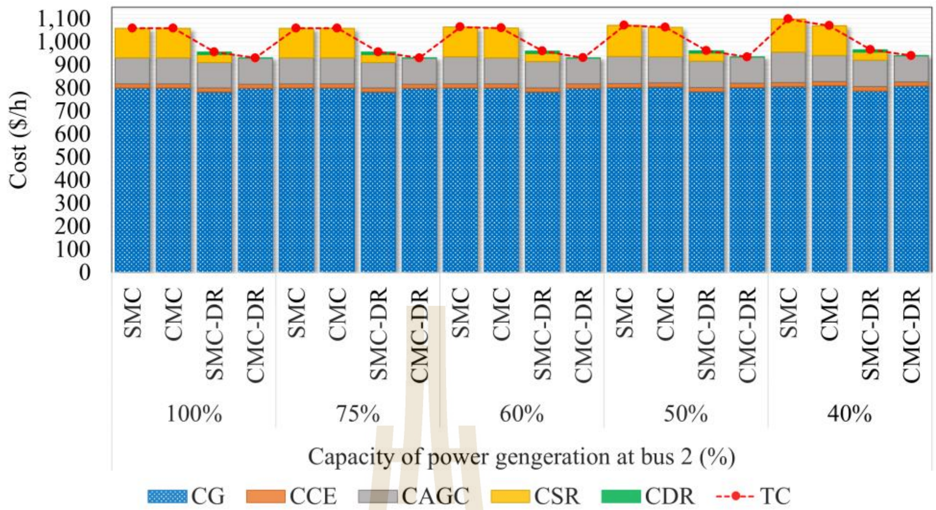

Figure 5.4 Comparison of cost across different scenarios under varying power generation capacity for IEEE 30-bus system

5.5.1 Sensitivity Analysis on Combined Electricity-Emission Scheme

This section investigates the influence of carbon pricing on system performance under the combined electricity-emission scheme (Scheme 1). The analysis evaluates how variations in the carbon tax rate affect total system cost (TC) and emission levels under two market-clearing strategies: the sequential market clearing (SMC) and the combined market clearing (CMC) approaches. The carbon tax rate is varied incrementally from \$10/ton CO_2 to \$90/ton CO_2, representing a wide range of potential policy scenarios for carbon regulation.

Table 5.4 summarises the outcomes of this sensitivity analysis. Increasing the carbon tax rate leads to a modest consistent reduction in total emissions, from 0.357 ton/h at the lowest tax level to 0.338 ton/h at the highest, indicating a gradual shift toward lower-emission generation units, even without the inclusion of demand response. This pattern underscores the effectiveness of carbon pricing in promoting cleaner generation dispatch. Conversely, total system cost rises steadily with increasing carbon tax rates in both SMC and CMC schemes. At \$10/ton, the TC is approximately \$1,046.5/h, whereas at \$90/ton, it reaches \$1,072.8/h, representing an overall increase of about 2.5%. Although the CMC approach consistently yields slightly lower costs than SMC across all tax levels, the results highlight the typical trade-off between emission reduction and operational expenditure associated with carbon pricing policies.

The carbon-emission component exhibits the greatest variation across tax levels, whereas the costs of AGC and SR remain constant at \$113.08/h and \$128.43/h, respectively. Notably, both SMC and CMC yield identical outcomes at all tax levels, indicating that in the absence of demand-side flexibility mechanisms such as DR, the advantages of integrated optimisation are minimal in terms of cost reduction when only carbon-related constraints are considered. These results imply that although carbon taxation leads to moderate emission reductions, its impact on total system cost is linear mainly, and the generation-only framework lacks sufficient operational flexibility to respond effectively to carbon pricing signals. Figure 5.5 illustrates the distribution of total cost components, including generation, emission, AGC, and SR costs, under five carbon tax levels within the combined electricity-emission scheme, comparing sequential and integrated clearing approaches. As the carbon tax rate increases, total cost rises gradually across both cases. However, the integrated clearing approach consistently maintains slightly lower or equivalent costs relative to the sequential method, reflecting enhanced coordination in reserve procurement and more efficient system operation.

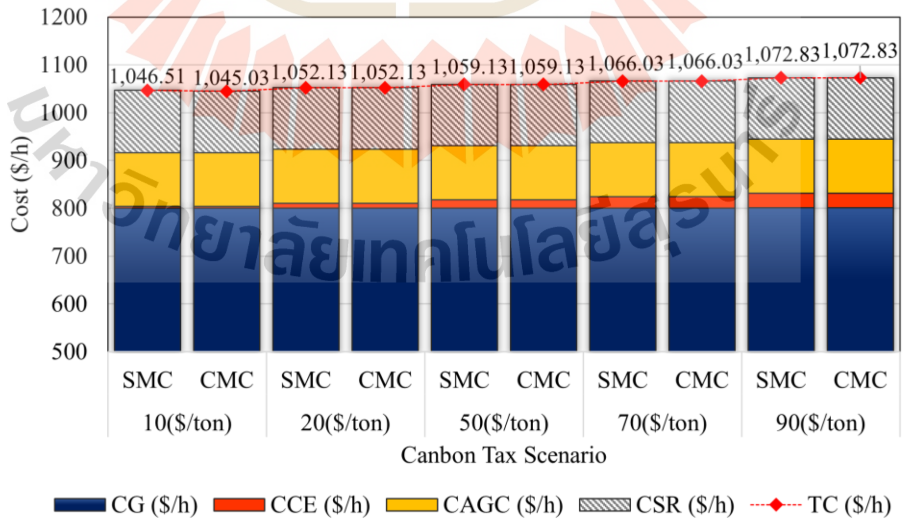

Figure 5.5 Impact of carbon tax on market-clearing costs in combined electricity-emission scheme

5.5.2 Sensitivity Analysis on Combined Electricity-Emission with Demand Response Scheme

This section investigates the influence of carbon pricing on combined electricity-emission with demand response scheme (Scheme 2). Table 5.5 presents the results of the sensitivity analysis conducted under the combined electricity-emission scheme with DR integration. The study explores the joint effects of varying carbon tax rates and DR incentive levels on overall system performance. Two market-clearing strategies, SMC-DR (sequential DR clearing) and CMC-DR (integrated DR clearing), are evaluated across nine scenarios corresponding to three DR incentive structures: [1, 2, 3], [2, 4, 6], and [3, 6, 9] $/MWh.

The results indicate that CMC-DR consistently achieves lower or equal total costs than SMC-DR across all carbon tax levels. The cost advantage of CMC-DR becomes increasingly evident as the DR incentive level rises. For instance, at a carbon tax of $90/ton, the total system cost in SMC-DR ranges from $969.24/h to $1,034.76/h, depending on the incentive level, whereas CMC-DR maintains a significantly lower range of $943.24/h to $943.99/h. Despite the higher DR payment rates, the CMC-DR framework preserves cost efficiency through more effective co-optimisation, selecting DR resources strategically to minimise overall system expenditure. Consequently, the DR cost (CDR) in CMC-DR is notably lower than in SMC-DR, reflecting superior utilisation of demand-side flexibility.

Emission reductions are moderate but consistent across all DR-inclusive scenarios, with average emission levels declining from approximately 0.357 t/h to 0.333 t/h as carbon tax rates and DR incentives increase. These results demonstrate the synergistic benefits of combining carbon pricing with incentive-based DR programs. The CMC-DR exhibits a stronger and more dynamic response to both carbon tax and DR price signals, effectively leveraging demand-side flexibility to reduce dependence on costly spinning reserves while maintaining cost-effectiveness under diverse policy conditions.

The sensitivity analysis confirms that carbon pricing alone produces limited impacts on system costs and emissions. However, integrating with structured DR incentives significantly enhances operational flexibility and economic performance.

The proposed integrated DR framework demonstrates strong robustness across varying policy parameters, offering a scalable, practical solution to improve the environmental and economic efficiency of electricity market operations. Figure 5.6 illustrates the distribution of total cost components under different combinations of carbon tax and DR incentive levels for the SMC-DR and CMC-DR cases. While SMC-DR is more sensitive to incentive variations, CMC-DR consistently achieves lower, more stable total costs, with notably reduced spinning reserve and DR procurement costs.

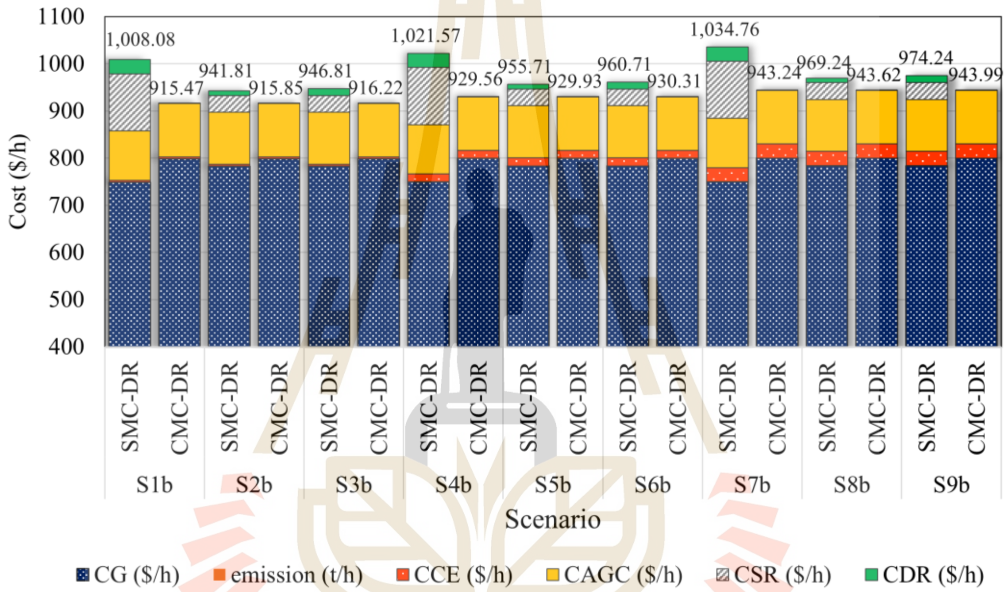

Figure 5.6 Combined impact of carbon tax and DR incentives on cost composition for combined electricity-emission with demand response scheme

Table 5.4 Sensitivity of carbon tax rates under the combined electricity-emission scheme for IEEE 30-bus system

Scheme 1: Combined Electricity-Emission Scheme								
Carbon tax ($/ton)	*Scenario*	*Case*	*CG ($/h)*	*CE (ton/h)*	*CCE ($/h)*	*CAGC ($/h)*	*CSR ($/h)*	*TC ($/h)*
10	S1a	SMC	799.950	0.357	3.574	113.076	129.916	1,046.515
		CMC	799.966	0.356	3.561	113.076	128.432	1,045.035
20	S2a	SMC	800.048	0.352	10.573	113.076	128.432	1,052.129
		CMC	800.048	0.352	10.573	113.076	128.432	1,052.129
50	S3a	SMC	800.245	0.348	17.376	113.076	128.432	1,059.129
	(Baseline)	CMC	800.245	0.348	17.376	113.076	128.432	1,059.129
70	S4a	SMC	800.550	0.342	23.970	113.076	128.432	1,066.028
		CMC	800.550	0.342	23.970	113.076	128.432	1,066.028
90	S5a	SMC	800.935	0.338	30.385	113.076	128.432	1,072.828
		CMC	800.935	0.338	30.385	113.076	128.432	1,072.828

Table 5.5 Sensitivity of carbon tax and DR incentives under the combined electricity-emission with demand response scheme for IEEE 30-bus system

Scenario 2: Combined Electricity-Emission with Demand Response Scheme										
Carbon tax ($/ton)	*DR Incentive ($/MW)*	*Scenario*	*Case*	*CG ($/h)*	*CE (t/h)*	*CCE ($/h)*	*CAGC ($/h)*	*CSR ($/h)*	*CDR ($/h)*	*TC ($/h)*
10	**1,2,3**	S1b	SMC-DR	748.930	0.340	3.396	104.826	120.932	30	1,008.084
			CMC-DR	798.659	0.357	3.570	112.869	0	0.376	915.473
	2,4,6	S2b	SMC-DR	782.811	0.352	3.523	110.326	35.146	10	941.806
			CMC-DR	798.659	0.357	3.570	112.869	0	0.751	915.849
	3,6,9	S3b	SMC-DR	782.811	0.352	3.523	110.326	35.146	15	946.806
			CMC-DR	798.659	0.357	3.570	112.869	0	1.127	916.224
50	**1,2,3**	S4b	SMC-DR	749.121	0.334	16.693	104.826	120.932	30	1,021.572
			CMC-DR	798.952	0.347	17.360	112.869	0	0.376	929.556
	2,4,6	S5b	SMC-DR	783.088	0.343	17.150	110.326	35.146	10	955.709
		(Baseline)	CMC-DR	798.952	0.347	17.360	112.869	0	0.751	929.932
	3,6,9	S7b	SMC-DR	783.088	0.343	17.150	110.326	35.146	15	960.709
			CMC-DR	798.952	0.347	17.360	112.869	0	1.127	930.307

Table 5.5 Sensitivity of carbon tax and DR incentives under the combined electricity-emission with demand response scheme for IEEE 30-bus system (Continued)

Scenario 2: Combined Electricity-Emission with Demand Response Scheme										
Carbon tax ($/ton)	*DR Incentive ($/MW)*	*Scenario*	*Case*	*CG ($/h)*	*CE (t/h)*	*CCE ($/h)*	*CAGC ($/h)*	*CSR ($/h)*	*CDR ($/h)*	*TC ($/h)*
90	**1,2,3**	S7b	SMC-DR	749.673	0.326	29.334	104.826	120.932	30	1,034.765
			CMC-DR	799.640	0.337	30.358	112.869	0	0.376	943.243
	2,4,6	S8b	SMC-DR	783.742	0.334	30.031	110.326	35.146	10	969.244
			CMC-DR	799.640	0.337	30.358	112.869	0	0.751	943.619
	3,6,9	S9b	SMC-DR	783.742	0.334	30.031	110.326	35.146	15	974.244
			CMC-DR	799.640	0.337	30.358	112.869	0	1.127	943.994

5.6 Conclusion

This study develops an integrated electricity market framework that jointly optimises generation dispatch, carbon pricing, ancillary services, and incentive-based DR. The proposed model, tested on the IEEE 30-bus system, demonstrates that integrated optimisation consistently outperforms conventional sequential market-clearing approaches regarding cost efficiency, system reliability, and environmental performance. In particular, the co-optimised scenario incorporating DR (CMC-DR) achieved the lowest total operating cost, reducing system expenditure by up to 6.1% compared with traditional generation-only models under generation shortage conditions. This improvement is primarily attributed to using uncalled DR capacity as spinning reserve, effectively minimising reliance on generation-based reserves without compromising reliability.

The simulation results also confirm the cost-effectiveness of implementing stepwise DR incentives. These incentives enable significant load reductions while maintaining economic efficiency. When combined with carbon pricing, DR further enhances emission-reduction outcomes, underscoring the synergies of integrating environmental and demand-side mechanisms. From a policy perspective, the findings advocate a transition from generation-centric market structures to more flexible, integrated frameworks. Such reforms would enable better coordination between energy, reserve, and environmental markets, supporting decarbonisation and operational efficiency.

This study demonstrates that an integrated operational approach is technically viable and economically advantageous. By co-optimising supply- and demand-side resources under carbon constraints, the framework offers a practical and scalable pathway for electricity market reform, enhancing system efficiency, environmental sustainability, and long-term energy security.

CHAPTER VI

CO-OPTIMISED FRAMEWORK FOR COMBINED ELECTRICITY MARKET AND EMISSION MECHANISMS WITH RENEWABLE ENERGY CERTIFICATES AND ANCILLARY SERVICES

6.1 Chapter Overview

Achieving carbon neutrality in the power sector requires market designs that align economic efficiency with environmental sustainability and system security. This chapter proposes a co-optimised framework for combined electricity market-clearing framework that includes the electricity market (EM), the carbon pricing mechanism (CM), the renewable energy market (REM), and the ancillary services market (ASM) procurement, advancing beyond fragmented market approaches that address these objectives separately. The proposed model is applied to a 160-bus equivalent Thai power system, which reflects Thailand's distinctive regulatory structure, rapidly growing electricity demand, and national commitment to carbon neutrality. This application addresses a significant gap in the literature, which has predominantly focused on developed markets while offering limited insights for emerging economies facing unique structural and regulatory challenges.

The chapter makes four principal contributions. First, it develops an integrated market-clearing model that optimises energy dispatch, carbon pricing, renewable energy utilisation, and ancillary service procurement, overcoming the limitations of existing fragmented approaches. Second, it provides a system-specific assessment of the Thai power system, capturing the country's unique operational and regulatory characteristics. Third, the model explicitly incorporates welfare optimisation across multiple stakeholder groups, consumers, producers, government, and renewable energy participants, offering insights into the distributional consequences of multi-dimensional market mechanisms. Finally, the findings provide evidence-based recommendations for Thailand's decarbonisation pathway, with broader implications for countries balancing emission reduction, energy security, and economic competitiveness.

The analysis compares five market mechanism scenarios, revealing that while carbon taxation reduces emissions and generates fiscal revenues, it imposes welfare losses. REC trading enhances producer viability but has limited operational effects, and ancillary service procurement strengthens reliability at added cost. By contrast, the integrated multi-dimensional market reduces emissions by nearly 5%, achieves more equitable welfare distribution among stakeholders, and mitigates the drawbacks of single-policy instruments. Sensitivity analyses confirm that market integration amplifies the environmental effectiveness of carbon pricing and enhances the welfare gains from REC trading. These results demonstrate that coordinated market mechanisms can simultaneously support emission reduction, system adequacy, and fair welfare allocation, providing timely insights for Thailand's energy transition and offering broader lessons for electricity market design in emerging economies pursuing sustainable development pathways. Figure 6.1 illustrates the conceptual framework underpinning this study, where the ISO coordinates energy, renewable, and ancillary service markets alongside carbon pricing mechanisms to achieve transparency, efficiency, and decarbonisation.

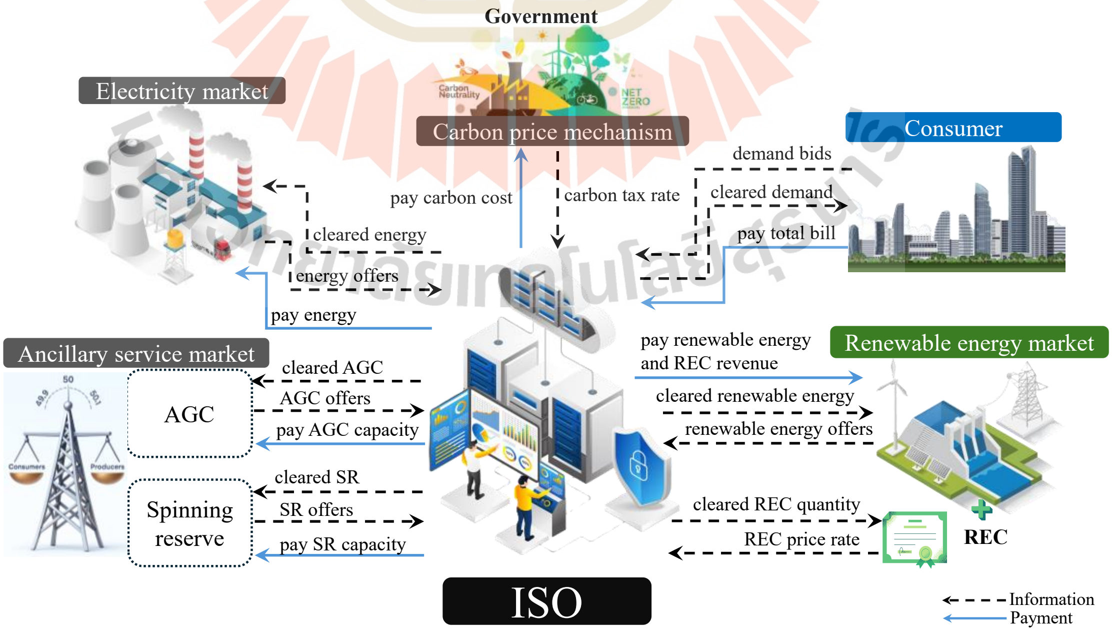

Figure 6.1 Framework of multi-dimensional markets

6.2 Economic and Market Performance Metrics

This section defines the economic and market performance metrics used to evaluate the outcomes of each market study case. These indicators measure the system's overall efficiency, welfare distribution, and the financial implications for key stakeholders. Specifically, the study employs welfare-based and revenue-based metrics to capture the economic interactions among consumers, producers, and the system operator. However, each metric is expressed in mathematical form, which collectively provides economic interpretations rather than purely mathematical constructs. Hence, this section focuses on the quantitative assessment of market efficiency, stakeholder welfare, and financial performance under different policy configurations.

6.2.1 Social Welfare

Social welfare (SW) represents a fundamental measure of market efficiency, capturing the balance between societal benefits from electricity consumption and the total system costs required to supply it. In general terms, SW is defined as the difference between the gross demand benefit, reflecting consumers' willingness to pay, and the aggregate supply costs, including generation costs, carbon emissions, renewable integration, and ancillary reserves. Two variants of social welfare to provide deeper analytical insight are considered in this study:

(1) Economic social welfare reflects the intrinsic efficiency of resource allocation by excluding financial transfers such as carbon tax payments and REC trading. This indicator isolates the pure economic outcome of market optimisation, focusing on the balance between demand benefits and real production costs, as formulated:

$$SW_{eco} = \sum_{j=1}^{ND} B_j(P_{D,j}) - \sum_{i=1}^{NG} CG(P_{G,i}) - \sum_{r=1}^{NRE} CRE(P_{RE,r}) - \sum_{i=1}^{NG} CAGC(P_{G,i}) - \sum_{i=1}^{NG} CSR(P_{G,i}). \tag{6.1}$$

(2) Post-Transfer Social Welfare, in contrast, incorporates monetary transfers arising from policy mechanisms, namely, carbon tax revenues and REC

payments, to capture the effective redistribution of welfare among market participants, including consumers, producers, and the government. This variant, therefore, represents the net financial outcome of all stakeholders after accounting for fiscal and incentive-based instruments, as defined:

$$SW_{post} = \sum_{j=1}^{ND} B_j(P_{D,j}) - \sum_{i=1}^{NG} CG(P_{G,i}) - \sum_{i=1}^{NG} CCE(P_{G,i}) - \sum_{i=1}^{NG} CAGC(P_{G,i}) - \sum_{i=1}^{NG} CSR(P_{G,i}) - \sum_{r=1}^{NRE} CRE(P_{RE,r}) + \sum_{r=1}^{NRE} RECR(P_{RE,r}), \tag{6.2}$$

where $B_j(P_{D,j})$, $CG(P_{G,i})$, $CCE(P_{G,i})$, $CAGC(P_{G,i})$, $CSR(P_{G,i})$, $CRE(P_{RE,r})$, and $RECR(P_{RE,r})$ are formulated as shown in Equations (3.16), (3.13), (3.15), (5.1), (5.2), (4.1), and (4.2), respectively.

6.2.2 Consumer Surplus

Consumer surplus (CS) measures the economic benefit that consumers receive from purchasing electricity at the market-clearing price, representing the difference between consumers' willingness to pay and the actual payment. This indicator reflects the affordability and efficiency of market outcomes from the consumer's perspective. A higher consumer surplus indicates improved welfare and competitive pricing conditions. The actual expenditures in the market, including payments for energy, reserves, and REC transfers, are defined as:

$$CS = \sum_{j=1}^{ND} B_j(P_{D,j}) - \left[\underbrace{\lambda_{CG} \sum_{j=1}^{ND} P_{D,j}}_{\text{energy revenue}} + \underbrace{\lambda_{AGC} \sum_{i=1}^{NG} AGC_i + \lambda_{SR} \sum_{i=1}^{NG} SR_i}_{\text{ancillary service revenue}} + \underbrace{\sum_{r=1}^{NRE} RECR(P_{RE,r})}_{\text{REC revenue}} \right], \tag{6.3}$$

where λ_{CG} is the energy marginal price obtained from the Lagrange multiplier of the power balance constraint, λ_{AGC} and λ_{SR} are market-clearing prices for AGC and SR, respectively.

6.2.3 Total Revenue

Total revenue quantifies the overall income generated from electricity sales and other market components, such as REC trading and ancillary service payments. This metric clearly indicates market liquidity, price signals, and financial performance under varying policy conditions, facilitating comparison across market cases to assess the impact of multi-dimensional integration on revenue generation. The mathematical representation is given by:

$$R_{total} = \underbrace{\lambda_{CG}\sum_{j=1}^{ND} P_{D,j}}_{\text{energy revenue}} + \underbrace{\lambda_{AGC}\sum_{i=1}^{NG} AGC_i + \lambda_{SR}\sum_{i=1}^{NG} SR_i}_{\text{ancillary service revenue}} + \underbrace{\sum_{r=1}^{NRE} RECR(P_{RE,r})}_{\text{REC revenue}}. \tag{6.4}$$

6.2.4 Producer Surplus

Producer surplus (PS) represents the total benefit to generation companies. It is calculated as the difference between market revenues and production costs, serving as a measure of producer profitability and market competitiveness. Changes in producer surplus across scenarios indicate that policy instruments, such as carbon pricing, renewable incentives, or ancillary service payments, affect generator welfare and market incentives. The producer surplus is expressed as:

$$\begin{aligned} PS = R_{total} - \Bigg[& \sum_{i=1}^{NG} CG(P_{G,i}) + \sum_{i=1}^{NG} CCE(P_{G,i}) + \sum_{i=1}^{NG} CAGC(P_{G,i}) + \sum_{i=1}^{NG} CSR(P_{G,i}) \\ & + \sum_{r=1}^{NRE} CRE(P_{RE,r}) \Bigg]. \end{aligned} \tag{6.5}$$

6.3 Objective Function and Study Cases

The proposed model evaluates the implications of different policy instruments within a double-side auction in five market study cases. Each case activates a subset of the available markets, including EM, CM, REM, and ASM, and defines a corresponding welfare-maximising objective function. Table 6.1 summarises market cases under a double-sided auction framework.

6.3.1 Case 6.0: Baseline Case

This case represents a conventional energy-only market, serving as the baseline for evaluating the impacts of subsequent policy interventions. Within the double-sided auction framework, the market-clearing process considers only the electricity market on the supply side, where generation companies submit energy offers while consumers submit demand bids. The corresponding objective function for this case is formulated to maximise the social welfare derived solely from energy transactions, without incorporating carbon pricing, renewable energy incentives, or ancillary service procurement as follows:

$$\text{maximise} \qquad f_{6.0}(x,u)=\left[\sum_{j=1}^{ND}B_j(P_{D,j})-\sum_{i=1}^{NG}CG(P_{G,i})\right]+\mu\cdot\left[g(x,u)\right]^2, \tag{6.6}$$

subject to equality and inequality constraints as in Equations (3.4)-(3.12).

6.3.2 Case 6.1: Carbon Pricing Mechanism

In this case, a carbon tax is introduced to internalise the environmental externalities associated with fossil-fuel-based generation. The carbon pricing mechanism directly influences generation dispatch decisions by adding a cost component proportional to each generator's carbon emission rate. Under the double-sided auction, this tax redistributes welfare through government revenue collection while incentivising cleaner generation choices. The objective function in this scenario includes the carbon cost term within the welfare optimisation problem, thereby reflecting both economic and environmental considerations in the market-clearing process as follows:

$$\text{maximise} \qquad f_{6.1}(x,u)=\left[\sum_{j=1}^{ND}B_j(P_{D,j})-\sum_{i=1}^{NG}CG(P_{G,i})-\sum_{i=1}^{NG}CCE(P_{G,i})\right]+\mu\cdot\left[g(x,u)\right]^2, \tag{6.7}$$

subject to equality and inequality constraints as in Equations (3.4)-(3.12).

6.3.3 Case 6.2: Renewable Energy Market

Case 6.2 extends the baseline framework to include renewable energy generation and REC trading. The objective of this case is to examine whether renewable incentives alter producer revenues, market equilibrium, and social welfare outcomes. Within the double-sided auction, renewable producers submit bids representing generation costs, while REC prices are endogenously determined based on demand from obligated entities or consumers seeking clean energy participation. The objective function, therefore, integrates REC revenue streams and renewable generation costs, allowing assessment of clean energy policies' effect on market efficiency and the financial viability of renewable producers. So, the objective function is defined as follows:

maximise $$f_{6.2}(x,u)=\left[\sum_{j=1}^{ND}B_j(P_{D,j})-\sum_{i=1}^{NG}CG(P_{G,i})-\sum_{r=1}^{NRE}CRE(P_{RE,r})+\sum_{r=1}^{NRE}RECR(P_{RE,r})\right] +\mu\cdot\left[g(x,u)\right]^2 \tag{6.8}$$

subject to equality as in Equations (4.7) and (3.5) and inequality constraints as in Equations (3.6)-(3.12).

6.3.4 Case 6.3: Ancillary Services Market

This case incorporates ancillary service co-optimisation alongside the electricity market to reflect system security requirements. Specifically, the model accounts for AGC and SR obligations. The double-sided auction structure is expanded to include bids for ancillary services from generation companies, with corresponding costs and benefits integrated into the market-clearing process. The objective function maximises social welfare by jointly optimising energy and ancillary service procurement, capturing the trade-offs between security enhancement and increased operational costs, as follows:

maximise $$f_{6.3}(x,u)=\left[\sum_{j=1}^{ND}B_j(P_{D,j})-\sum_{i=1}^{NG}CG(P_{G,i})-\sum_{i=1}^{NG}CAGC(P_{G,i})-\sum_{i=1}^{NG}CSR(P_{G,i})\right] +\mu\cdot\left[g(x,u)\right]^2, \tag{6.9}$$

subject to equality as in Equations (5.16) and (3.5) and inequality constraints as in Equations (5.9)-(5.14).

6.3.5 Case 6.4: Multi-Dimensional Market Mechanism

The final case represents the fully integrated market framework, in which all policy instruments, carbon pricing, renewable energy incentives, and ancillary services are co-optimised simultaneously. This configuration captures the interactive effects among environmental, renewable, and security objectives, offering the most comprehensive representation of a real-world multi-dimensional market. Within the double-sided auction, the ISO clears energy, REC, and ancillary service bids concurrently, ensuring consistency in price signals and welfare allocation across all market segments. The objective function combines all relevant cost and benefit components, enabling an integrated optimisation that balances economic efficiency, environmental sustainability, and system security. Hence, the objective function is formulated as follows:

maximise

$$f_{6.4}(x,u)=\left[\sum_{j=1}^{ND}B_j(P_{D,j})-\sum_{i=1}^{NG}CG(P_{G,i})-\sum_{i=1}^{NG}CCE(P_{G,i})-\sum_{i=1}^{NG}CAGC(P_{G,i})\right.$$
$$\left.-\sum_{i=1}^{NG}CSR(P_{G,i})-\sum_{r=1}^{NRE}CRE(P_{RE,r})+\sum_{r=1}^{NRE}RECR(P_{RE,r})\right]+\mu\cdot\left[g(x,u)\right]^2, \quad (6.10)$$

subject to:

$$\sum_{i=1}^{NG}P_{G,i}+\sum_{i=1}^{NG}AGC_i+\sum_{i=1}^{NG}SR_i+\sum_{r=1}^{NRE}P_{RE,r}=\sum_{j=1}^{ND}P_{D,j}\,, \quad (6.11)$$

$$P_{G,i}^{\min}\le P_{G,i}\le P_{G,i}^{\max}\,,\quad 0\le AGC_i\le AGC_i^{\max}\,,\quad 0\le SR_i\le SR_i^{\max}\,,\quad P_{RE,r}^{\min}\le P_{RE,r}\le P_{RE,r}^{\max}\,,$$

and

$$P_{G,i}+AGC_i+SR_i\le P_{G,i}^{\max}\,,\ i=1,\ldots,NG\,, \quad (6.12)$$

$$\sum_{i=1}^{NG}AGC_i\ge\%AGCR\left(\sum_{i=1}^{NG}P_{G,i}+\sum_{r=1}^{NRE}P_{RE,r}\right), \quad (6.13)$$

$$\sum_{i=1}^{NG}SR_i\ge\%SRR\left(\sum_{i=1}^{NG}P_{G,i}+\sum_{r=1}^{NRE}P_{RE,r}\right), \quad (6.14)$$

Table 6.1 Market study cases under double-side auction framework

Case	Market components	Objective function
Case 6.0	EM	Welfare maximisation with energy cost-benefit only
Case 6.1	EM+CM	Adds carbon cost into the market mechanism to internalise emissions
Case 6.2	EM+REM	Includes REC revenues and renewable energy in the market mechanism
Case 6.3	EM+ASM	Co-optimises AGC and SR procurement with energy market
Case 6.4	EM+CM+REM+ASM	Multi-dimensional framework with environmental, renewable, and security of supply to the market mechanism

6.4 Methodology

This study employs two optimisation approaches, including quadratic programming (QP) and hybrid particle swarm optimisation-quadratic programming (PSO-QP), to determine the optimal market-clearing outcomes under different policy and operational scenarios. The comparative application of these two techniques allows for assessing economic and technical efficiency in the integrated market framework. The QP-based optimisation provides an efficient means for solving the economic dispatch problem, particularly in markets where only real power generation is treated as a control variable. This method is suitable for convex quadratic cost functions and linear or mildly nonlinear constraints, making it computationally efficient and appropriate for initial benchmark studies. However, QP assumes simplified network conditions, typically DC-based formulations, and therefore cannot fully represent the nonlinear power flow and voltage-dependent characteristics of actual AC systems.

To overcome these limitations, the hybrid PSO-QP approach is introduced. In this method, PSO is employed to fine-tune nonlinear control variables, which directly influence reactive power flow, transmission losses, and system stability. These Variables significantly affect the feasible operating region of the power system and the resulting market outcomes. The QP algorithm is then embedded as a local solver within the PSO framework to optimise the generation dispatch for each candidate solution proposed by PSO. This hybrid structure enables the model to combine the global exploration capability of PSO with the fast convergence and precision of QP, achieving solutions that are both economically optimal and technically feasible under realistic AC network constraints. As a result, the hybrid PSO-QP framework provides a more accurate representation of system operations in integrated electricity markets that include environmental, renewable, and reliability considerations. The subsequent sections detail the implementation of each method. Section 6.4.1 presents the QP optimisation process, while Section 6.4.2 explains the hybrid PSO-QP approach and its computational procedure.

6.4.1 Quadratic Programming Optimisation

QP optimisation is applied to determine the optimal energy dispatch that maximises total social welfare within a convex optimisation framework. The objective function is quadratic, while all equality and inequality constraints are linear. This structure allows for efficient computation and ensures convergence to a unique global solution. The general quadratic programming structure is given as in Equation (5.24). So, the procedural steps for the QP optimisation are as follows:

(1) Case 6.0: Baseline Case

Step 1: Gather all required system data.

Step 2: Perform a power flow analysis to determine the $P_{G,i}$ and $P_{D,j}$.

Step 3: Define the control variables are $P_{G,i}$ and $P_{D,j}$ as in Equation (5.26) and

$$\mathbf{x}_{P_D} = [P_{D,1}, \ldots, P_{D,ND}] \tag{6.15}$$

Step 4: Minimise the objective function, as in Equation (6.6), using QP as follows:

$$\mathbf{H}_{6.0} = \begin{bmatrix} \mathbf{H}_{P_G} & 0_{ND\times ND} \\ 0_{ND\times ND} & \mathbf{H}_{P_D} \end{bmatrix}_{(NG+ND)\times(NG+ND)}, \tag{6.16}$$

$$\mathbf{f}_{6.0} = [B_{G,1} \ldots B_{G,NG} \;\; S_1 \ldots S_{ND}]^T, \tag{6.17}$$

where:

$$\mathbf{H}_{P_G} = \begin{bmatrix} 2A_{G,1} & \dots & 0 \\ \vdots & \ddots & \vdots \\ 0 & \dots & 2A_{G,NG} \end{bmatrix}_{NG \times NG}, \tag{6.18}$$

$$\mathbf{H}_{P_D} = \begin{bmatrix} 2T_1 & \dots & 0 \\ \vdots & \ddots & \vdots \\ 0 & \dots & 2T_{ND} \end{bmatrix}_{ND \times ND}, \tag{6.19}$$

$$\mathbf{x}_{6.0} = \left[\mathbf{x}_{P_G} \ \mathbf{x}_{P_D} \right], \tag{6.20}$$

$$A_{G,i} = a_i,\ B_{G,i} = b_i,\ i = 1,\dots,NG, \tag{6.21}$$

$$T_j = d_j,\ S_j = e_j,\ j = 1,\dots,ND, \tag{6.22}$$

Step 5: Verify that the optimised values satisfy the power balance constraint, reserve requirements, and operational limits for $P_{G,i}$ and $P_{D,j}$. If any constraints are violated, refine the QP setup and resolve.

(2) Case 6.1: Carbon Pricing Mechanism

Step 1: Gather all required system data.

Step 2: Perform a power flow analysis to determine the $P_{G,i}$ and $P_{D,j}$.

Step 3: Define the control variables are $P_{G,i}$ and $P_{D,j}$ as in Equations (5.26) and (6.15).

Step 4: Minimise the objective function, as in Equation (6.7), using QP as follows:

$$\mathbf{H}_{6.1} = \begin{bmatrix} \mathbf{H}_{5.1a,1} & 0_{ND \times ND} \\ 0_{ND \times ND} & \mathbf{H}_{P_D} \end{bmatrix}_{(NG+ND) \times (NG+ND)}, \tag{6.23}$$

$$\mathbf{f}_{6.1} = [B_1 \dots B_{NG} \ \ S_1 \dots S_{ND}]^T, \tag{6.24}$$

where:

$$\mathbf{x}_{6.1} = \left[\mathbf{x}_{P_G} \ \mathbf{x}_{P_D} \right]. \tag{6.25}$$

Step 5: Verify that the optimised values satisfy the power balance constraint, reserve requirements, and operational limits for $P_{G,i}$ and $P_{D,j}$. If any constraints are violated, refine the QP setup and resolve.

(3) Case 6.2: Renewable Energy Market

Step 1: Gather all required system data.

Step 2: Perform a power flow analysis to determine the $P_{G,i}$ and $P_{D,j}$.

Step 3: Define the control variables are $P_{G,i}$, $P_{D,j}$, and $P_{RE,r}$ as in Equations (5.26), (6.15), and

$$\mathbf{x}_{P_{RE}} = [P_{RE,1}, \ldots, P_{RE,NRE}] \tag{6.26}$$

Step 4: Minimise the objective function, as in Equation (6.8), using QP as follows:

$$\mathbf{H}_{6.2} = \begin{array}{c} \begin{array}{ccc} \quad P_G \quad & \overbrace{\qquad\qquad}^{P_{RE} \text{ and } REC} & \overbrace{\qquad}^{P_D} \end{array} \\ \begin{bmatrix} \mathbf{H}_{P_G} & 0_{(NRE+1)\times(NRE+1)} & 0_{ND\times ND} \\ 0_{(NRE+1)\times(NRE+1)} & \mathbf{H}_{P_{RE}} & 0_{ND\times ND} \\ 0_{ND\times ND} & 0_{ND\times ND} & \mathbf{H}_{P_D} \end{bmatrix}_{(NG+NRE+1+ND)\times(NG+NRE+1+ND)} \end{array} ,\tag{6.27}$$

$$\mathbf{f}_{6.2} = [B_{G,1} \ldots B_{G,NG} \quad K_1 \ldots K_{RE} \quad RECR \quad S_1 \ldots S_{ND}]^T , \tag{6.28}$$

where:

$$\mathbf{H}_{P_{RE}} = \begin{array}{c} \begin{array}{cc} \overbrace{\qquad\qquad\qquad}^{P_{RE}} & REC \end{array} \\ \begin{bmatrix} 2R_1 & \ldots & 0 & 0 \\ \vdots & \ddots & \vdots & \vdots \\ 0 & \ldots & 2R_{NRE} & 0 \\ 0 & \ldots & 0 & 0 \end{bmatrix}_{(NRE+1)\times(NRE+1)} \end{array} , \tag{6.29}$$

$$\mathbf{x}_{6.2} = \left[\mathbf{x}_{P_G} \ \mathbf{x}_{P_{RE}} \ \mathbf{x}_{P_D} \right], \ K_r = f_r , \ r = 1, \ldots, NRE . \tag{6.30}$$

Step 5: Verify that the optimised values satisfy the power balance constraint, reserve requirements, and operational limits for $P_{G,i}$ and $P_{D,j}$. If any constraints are violated, refine the QP setup and resolve.

(4) Case 6.3: Ancillary Services Market

Step 1: Gather all required system data.

Step 2: Perform a power flow analysis to determine the $P_{G,i}$ and $P_{D,j}$.

Step 3: Define the control variables are $P_{G,i}$, AGC_i, SR_i, and $P_{D,j}$, as in Equations (5.26), (5.27), (5.28), and (6.15).

Step 4: Minimise the objective function, as in Equation (6.9), using QP as follows:

$$\mathbf{H}_{6.3}=\begin{array}{c}\begin{array}{cccc} P_G & \overbrace{\phantom{0_{ND\times ND}}}^{P_D} & \overbrace{\phantom{0_{NG\times NG}}}^{AGC} & \overbrace{\phantom{0_{NG\times NG}}}^{SR} \end{array}\\ \begin{bmatrix} \mathbf{H}_{P_G} & 0_{ND\times ND} & 0_{NG\times NG} & 0_{NG\times NG}\\ 0_{ND\times ND} & \mathbf{H}_{P_D} & 0_{NG\times NG} & 0_{NG\times NG}\\ 0_{NG\times NG} & 0_{NG\times NG} & 0_{NG\times NG} & 0_{NG\times NG}\\ 0_{NG\times NG} & 0_{NG\times NG} & 0_{NG\times NG} & 0_{NG\times NG} \end{bmatrix}_{(3\cdot NG+ND)\times(3\cdot NG+ND)}\end{array}, \tag{6.31}$$

$$\mathbf{f}_{6.3}=[B_{G,1}\ldots B_{G,NG}\;\; S_1\ldots S_{ND}\;\; AGCP_1\ldots AGCP_{NG}\;\; SRP_1\ldots SRP_{NG}]^T, \tag{6.32}$$

where:

$$\mathbf{x}_{6.3}=\left[\mathbf{x}_{P_G}\;\; \mathbf{x}_{P_D}\;\; \mathbf{x}_{AGC}\;\; \mathbf{x}_{SR}\right]. \tag{6.33}$$

Step 5: Verify that the optimised values satisfy the power balance constraint, reserve requirements, and operational limits for $P_{G,i}$ and $P_{D,j}$. If any constraints are violated, refine the QP setup and resolve.

(5) Case 6.4: Multi-Dimensional Market Mechanism

Step 1: Gather all required system data.

Step 2: Perform a power flow analysis to determine the $P_{G,i}$ and $P_{D,j}$.

Step 3: Define the control variables are $P_{G,i}$, AGC_i, SR_i, $P_{RE,r}$ and $P_{D,j}$, as in Equations (5.26), (5.27), (5.28), (6.26), and (6.15).

Step 4: Minimise the objective function, as in Equation (6.10), using QP as follows:

$$\mathbf{H}_{6.4} = \begin{array}{c} \begin{array}{ccccc} \overbrace{\qquad}^{P_G \text{ and Carbon}} & \overbrace{\qquad}^{AGC} & \overbrace{\qquad}^{SR} & \overbrace{\qquad}^{P_{RE} \text{ and } REC} & \overbrace{\qquad}^{P_D} \end{array} \\ \left[\begin{array}{ccccc} \mathbf{H}_{5.1a,1} & 0_{NG\times NG} & 0_{NG\times NG} & 0_{(NRE+1)\times(NRE+1)} & 0_{ND\times ND} \\ 0_{NG\times NG} & 0_{NG\times NG} & 0_{NG\times NG} & 0_{(NRE+1)\times(NRE+1)} & 0_{ND\times ND} \\ 0_{NG\times NG} & 0_{NG\times NG} & 0_{NG\times NG} & 0_{(NRE+1)\times(NRE+1)} & 0_{ND\times ND} \\ 0_{(NRE+1)\times(NRE+1)} & 0_{(NRE+1)\times(NRE+1)} & 0_{(NRE+1)\times(NRE+1)} & \mathbf{H}_{P_{RE}} & 0_{ND\times ND} \\ 0_{ND\times ND} & 0_{ND\times ND} & 0_{ND\times ND} & 0_{ND\times ND} & \mathbf{H}_{P_D} \end{array}\right]_{(3\cdot NG+(NRE+1)+ND)\times(3\cdot NG+(NRE+1)+ND)} \end{array}, \tag{6.34}$$

$$\mathbf{f}_{6.4} = [B_1 \ldots B_{NG} \quad AGCP_1 \ldots AGCP_{NG} \quad SRP_1 \ldots SRP_{NG} \quad K_1 \ldots K_{RE} \quad RECR \quad S_1 \ldots S_{ND} \;]^T, \tag{6.35}$$

where:

$$\mathbf{x}_{6.4} = \left[\mathbf{x}_{P_G} \;\; \mathbf{x}_{AGC} \;\; \mathbf{x}_{SR} \;\; \mathbf{x}_{P_{RE}} \;\; \mathbf{x}_{P_D}\right]. \tag{6.36}$$

Step 5: Verify that the optimised values satisfy the power balance constraint, reserve requirements, and operational limits for $P_{G,i}$ and $P_{D,j}$. If any constraints are violated, refine the QP setup and resolve.

6.4.2 Hybrid Particle Swarm Optimisation-Quadratic Programming

The hybrid PSO-QP method integrates the global search capability of PSO with the precision and convergence efficiency of QP. This hybrid structure is designed to overcome the local optimality limitations of conventional QP while maintaining computational robustness in solving complex non-linear optimisation problems. In this approach, the control variables encompass the complete set of parameters from the AC-OPF framework, including generator active power, voltage magnitudes, transformer tap-changing, and reactor reactances. The PSO algorithm first performs a global exploration of the solution space to identify promising candidate solutions, which are then refined using the QP module for local optimisation under precise constraint satisfaction. So, the procedural steps for the Hybrid PSO-QP optimisation are as follows:

Step 1: Gather all required system data. Define upper and lower bounds for all control variables related to network and market optimisation.

Step 2: Specify the optimisation architecture and performance metric, set the PSO parameters, and configure the QP solver settings.

Step 3: Define PSO control variables as follows:

$$\mathbf{x}_{PSO} = \left[V_1,\ldots,V_{NG},T_1,\ldots,T_{NL},X_{C,1},\ldots,X_{C,NC}\right]. \tag{6.37}$$

And define QP control variables for Cases 6.0, 6.1, 6.2, 6.3, and 6.4 are as in Equations (6.20), (6.25), (6.30), (6.33), and (6.36).

Step 4: Formulate the objective function representing social welfare maximisation according to Equations (6.6)-(6.14), integrating all relevant cost and benefit components.

Step 5: Initialise the PSO parameters, including particle positions and velocities, randomly within the specified bounds of V, T, and X_C.

Step 6: Execute the PSO process incorporating power flow analysis. For each particle i at iteration k, apply particle control settings to the network model and perform an AC power flow to update the network admittance and determine system states such as voltage profiles, line flows, and transmission losses.

Step 7: Formulate the QP sub-problem conditional on the current particle's network configuration, representing the inner optimisation for market-clearing variables under given system states.

Step 8: Solve the inner QP to obtain QP control variables. If the solver returns an infeasible solution, apply a penalty or modify constraint limits and attempt a remedial re-solve.

Step 9: Evaluate the fitness function for each particle by computing the financial social welfare from the QP results combined with the particle's network variables. Include penalty terms for any constraint violations.

Step 10: Update each particle's personal best and the global best based on the evaluated fitness. Subsequently, update particle velocities and positions using the standard PSO update equations, ensuring all control variables remain within their respective bounds.

Step 11: Check for constraint violations across the current iteration. If any violation exceeds the defined tolerance, apply adaptive penalties or correction mechanisms and return to Step 6 to re-evaluate the adjusted particle.

Step 12: If iteration count k reaches the maximum iteration or improvement in gbest < tolerance, proceed to final refinement. Otherwise, increment k and repeat Steps 6-11.

Step 13: Fix the best control variables (V, T, and X_C) obtained from PSO and perform a high-precision QP refinement with tightened tolerances to compute the final optimised solution vector. Verify the KKT residuals and solver diagnostics to ensure optimality and feasibility.

Step 14: Conduct a final AC power flow validation using the complete optimised set (P_G, P_D, P_{RE}, AGC, SR, V, T, and X_C). If any constraint is violated, apply targeted and return to Step 13.

Step 15: Record the final optimal results, including total generation, losses, emissions, financial social welfare, and computation time.

6.5 Simulation Results and Discussions

This study evaluates the proposed integrated market framework on the 160-bus equivalent Thai power system, which represents a realistic and complex system suitable for policy-oriented market analysis. The framework integrates energy, carbon, renewable, and ancillary service markets under a double-sided auction mechanism. The following subsections describe the test system and the market scenarios considered in the analysis. The test system comprises 42 conventional generating units, including one reference unit, five dispatchable renewable energy resources, and 59 demand bidding areas, all interconnected through 85 AC transmission lines, 100 on-load tap-changing transformers, and 22 shunt devices that provide local reactive compensation. The system also models ancillary services with requirements for AGC and SR, each set at 5% of total system demand. Policy parameters include a carbon tax rate of 200 THB/tCO_2 and a REC price of 200 THB/REC, ensuring that environmental and renewable incentives are explicitly incorporated into the optimisation process. The characteristics of the test system are summarized in Table 6.2. This analysis employs and compares two distinct optimisation approaches. The simulation results are presented in the subsequent subsections: Section 6.5.1 details the outcomes derived using QP optimisation. In contrast, Section 6.5.2 presents the results from a hybrid PSO-QP algorithm.

Table 6.2 The 160-bus equivalent Thai power system data

Parameter	Value	Description
Total generation offers	20,986 MW	Maximum capacity for all conventional units
Total demand bids	22,093 MW	Aggregated demand offers across 59 bidding areas
Dispatchable renewable energy capacity	2,520 MW	Available renewable power from 5 sites
AGC capacity	3,450 MW	Total AGC available from participating generators
SR capacity	3,450 MW	Maximum spinning reserve contribution
AGC requirement	5% of demand	Minimum proportion of demand allocated to AGC
SR requirement	5% of demand	Minimum proportion of demand allocated to SR
Carbon tax rate	200 THB/tCo_2	Cost imposed on generator emissions
REC price	200 THB/REC	Market price for renewable energy certificates

6.5.1 Simulation Results using QP Optimisation

The proposed model presents five market scenarios, as shown in Table 6.3, where dispatch, generation costs, emissions, and policy-related revenues are reported. The results provide a quantitative foundation for understanding which alternative market designs reshape operational efficiency, environmental performance, and welfare distribution. By progressively introducing carbon taxation, renewable incentives, and ancillary service requirements, the scenarios reveal the isolated and combined effects of policy instruments on market outcomes.

The baseline energy-only case (Case 6.0) yields the highest dispatch of 18,792 MW and the highest emissions of 10,774 tCO_2/h, reflecting the absence of environmental regulation and reserve obligations. This benchmark highlights the efficiency of unconstrained operation but also exposes its ecological cost. When a carbon tax is introduced in Case 6.1, dispatch declines marginally to 18,735 MW, accompanied by a modest reduction in emissions of approximately 0.3%. Although the system-wide change is limited, the policy alters welfare allocation by transferring a portion of producer surplus to government revenue, thereby internalising part of the environmental externality.

The addition of renewable incentives in Case 6.2, through REC trading, leaves dispatch and emissions virtually unchanged at 18,730 MW and 10,739 tCO_2/h, respectively. Nevertheless, financial flows are significantly affected, producer surplus and overall welfare increase due to the revenues from REC. This suggests that REC mechanisms primarily operate as financial instruments that enhance welfare distribution without altering the operational merit order. In Case 6.3, the procurement of ancillary services fundamentally changes the allocation of capacity. The total dispatch reduction to 18,204 MW from the generation fleet is reserved for AGC and SR requirements. While this strengthens system reliability, the associated reserve costs reduce consumer and producer surpluses, resulting in a total decline in overall welfare compared to previous scenarios. The multi-dimensional market (Case 6.4) produces the most balanced outcome. Dispatch decreases further to 17,872 MW, while emissions decline by nearly 5% relative to the baseline. At the same time, the joint activation of carbon pricing, REC trading, and ancillary service procurement generates multiple revenue streams, diversifying welfare distribution across stakeholders. Although total costs are higher, the complementarities among policy instruments mitigate adverse distributional effects, yielding a more sustainable welfare configuration.

In terms of welfare decomposition, economic and financial social welfares reveal significant differences across scenarios. In Case 6.0, both coincide at 49.1 billion THB/h, reflecting the absence of policy effects. With carbon taxation in Case 6.1, SW_{eco} declines to 46.9 billion THB/h, while SW_{post} remains stable as fiscal revenues offset efficiency losses. In Case 6.2, REC incentives yield the highest SW_{eco} of 55.9 billion THB/h, though SW_{post} is slightly lower at 55.4 billion THB/h. Ancillary service procurement in Case 6.3 reduces both measures to 46.3 billion THB/h, highlighting the economic burden of reserve requirements. The multi-dimensional design in Case 6.4 restores SW_{eco} to 50.7 billion THB/h and further raises SW_{post} to 52.2 billion THB/h, demonstrating that combined policy instruments balance efficiency trade-offs with financial redistribution.

These comparative results demonstrate the policy relevance of a multi-dimensional market design that incorporates environmental costs, renewable incentives, and reliability services within a unified welfare-maximising framework. The multi-dimensional scenario demonstrates that market structures can be aligned with broader policy objectives rather than focusing solely on efficiency or short-term cost minimisation. Moreover, it illustrates a pathway to balance economic performance with emission reduction and system adequacy. This highlights the potential of multi-dimensional electricity markets to support sustainable energy transitions while ensuring a more even distribution of welfare among stakeholders.

Table 6.3 Simulation results from QP method [Part I]

Case	Total P_G (MW)	CG (THB/h)	CE (tCO_2/h)	CCE (THB/h)	Total P_{RE} (MWh)	CRE (THB/h)	$RECR$ (THB/h)
Case 6.0	18,792.1	18,622,750	10,773.78	0	0	0	0
Case 6.1	18,735.09	18,445,308	10,741.96	2,148,393	0	0	0
Case 6.2	18,730.45	18,431,145	10,739.38	0	2,520	1,514,566	504,000
Case 6.3	18,203.71	17,359,255	10,437.78	0	0	0	0
Case 6.4	17,872	16,655,174	10,248.47	2,049,693	2,520	1,514,566	504,000

Table 6.3 Simulation results from QP method [Part II]

Case	Total AGC (MW)	$CAGC$ (THB/h)	Total SR (MW)	CSR (THB/h)	Total P_D (MW)	B (THB/h)	SW_{eco} (THB/h)	SW_{post} (THB/h)
Case 6.0	0	0	0	0	18,792.1	67,721,650	49,098,900	49,098,900
Case 6.1	0	0	0	0	18,735.09	67,541,027	46,947,326	49,095,719
Case 6.2	0	0	0	0	21,250.45	75,366,381	55,924,670	55,420,670
Case 6.3	910.19	1,115,100	910.19	1,040,730	18,203.71	65,856,992	46,341,907	46,341,907
Case 6.4	1,019.6	1,208,840	1,019.6	1,126,057	20,392	72,746,680	50,696,349	52,242,043

Note: Detailed simulation results are addressed in Table B.2 (Appendix B.2)

(1) Welfare Redistribution and Stakeholder Impacts

An essential dimension of the simulation results concerns the redistribution of welfare among consumers, producers, government, and renewable participants. Figure 6.2 illustrates the decomposition of post-transfer social welfare across scenarios. In the baseline, welfare is derived entirely from consumer and producer surplus. With the introduction of a carbon tax in Case 6.1, government revenue emerges as a new component, while producer surplus declines. In Case 6.2, REC trading increases producer surplus through additional renewable income, leaving consumer surplus largely unaffected. The inclusion of ancillary services in Case 6.3 reallocates part of welfare to reserve providers but reduces the overall level due to higher costs. Case 6.4 illustrates a more balanced configuration that incorporates contributions from consumers, producers, the government, and REC revenues. The incremental effects are more clearly illustrated in Figure 6.3, which compares welfare changes relative to the baseline. Carbon taxation (Case 6.1) reduces overall welfare due to compliance costs, whereas REC incentives (Case 6.2) increase welfare by adding renewable revenues without increasing system costs. Ancillary service procurement (Case 6.3) again reduces welfare, reflecting the cost of reliability requirements. However, the multi-dimensional framework in Case 6.4 yields a net positive effect, confirming that complementarities among instruments can offset their individual drawbacks.

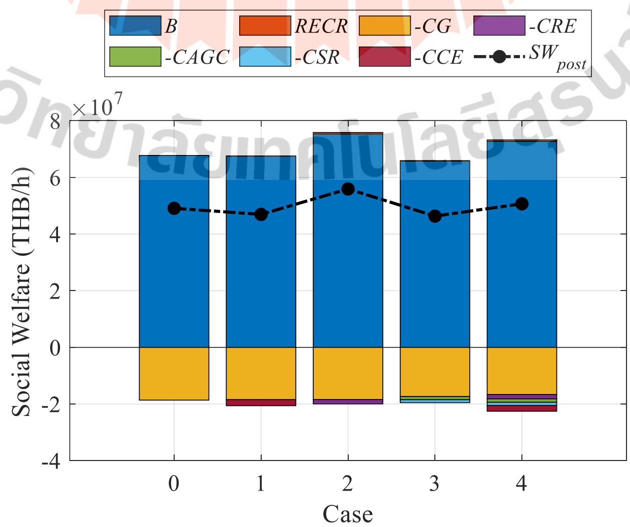

Figure 6.2 Decomposition of post-transfer social welfare

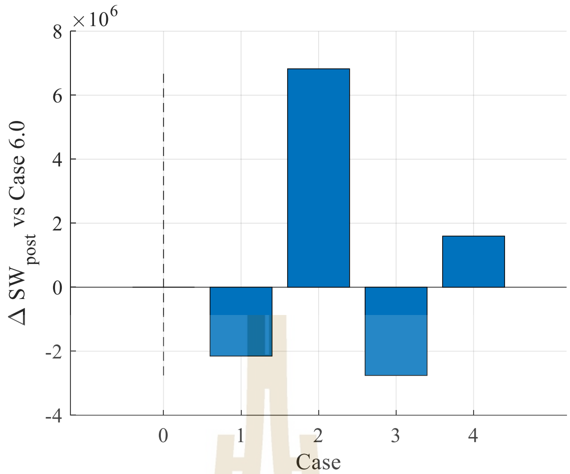

Figure 6.3 Incremental decomposition of post-transfer social welfare across market cases

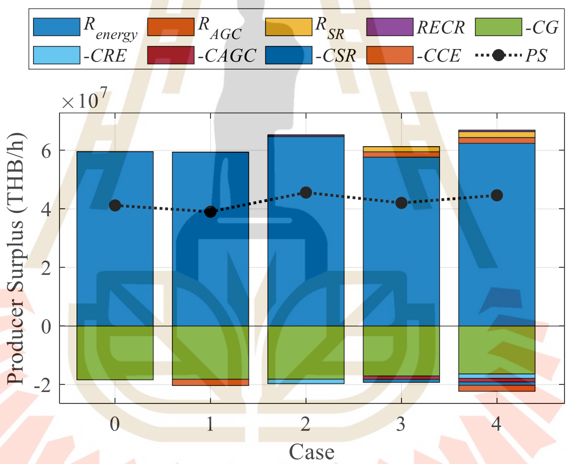

Figure 6.4 Producer surplus across market cases

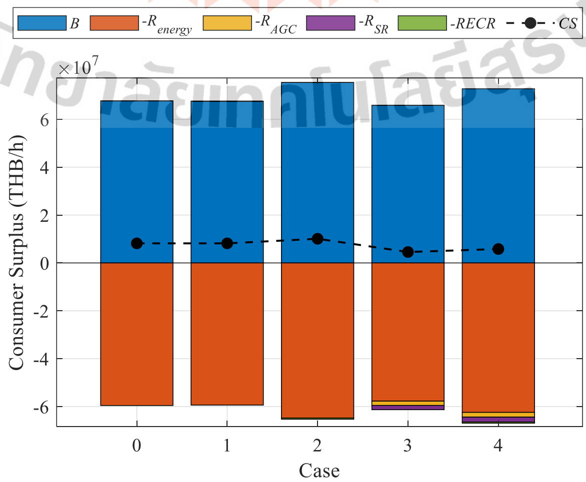

Figure 6.5 Consumer surplus across market cases

Producer surplus, shown in Figure 6.4, declines in Case 6.1 as carbon costs erode profitability, but increases sharply in Case 6.2 owing to REC revenues. It decreases again in Case 6.3 due to reserve obligations, while Case 6.4 recovers part of the loss, yielding a moderate but more stable outcome. Figure 6.5 illustrates that consumer surplus remains relatively unchanged between Cases 6.0 and 6.1, as the burden of carbon taxation is absorbed mainly by producers. In Case 6.2, it reaches its maximum level, reflecting efficiency gains from renewable incentives; however, it decreases in Case 6.3 as ancillary service costs are partially passed through to consumers. Case 6.4 achieves a positive but moderate surplus, striking a balance between consumer benefits, environmental objectives, and reliability. The fiscal implications of carbon pricing are captured in Figure 6.6, where government revenue increases substantially under Cases 6.1 and 6.4. This revenue source could be recycled to support renewable investment or grid modernisation, underscoring its policy relevance. Figure 6.7 extends the analysis to total market revenue, which remains stable between Cases 6.0 and 6.1, increases with the introduction of REC transactions in Case 6.2, and further shifts upward when ancillary services are procured in Case 6.3. The multi-dimensional market achieves the highest revenue, reflecting the simultaneous internalisation of energy, environmental, and reliability payments. Furthermore, Figure 6.8 highlights the evolution of market share in social welfare. In the baseline, producers dominate distribution, while consumers hold a smaller share, and government revenue is absent. Carbon taxation reallocates part of producer surplus to the state, REC trading strengthens producer positions, and ancillary services reduce the shares of both consumers and producers. The multi-dimensional scenario results in a more diversified structure, reducing concentration and promoting a more equitable distribution of welfare across stakeholders.

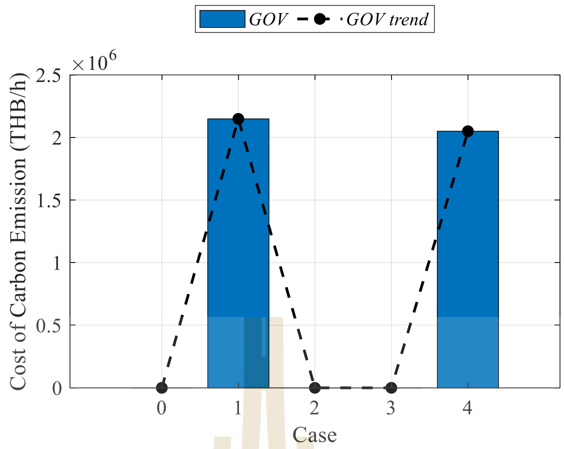

Figure 6.6 Government revenue

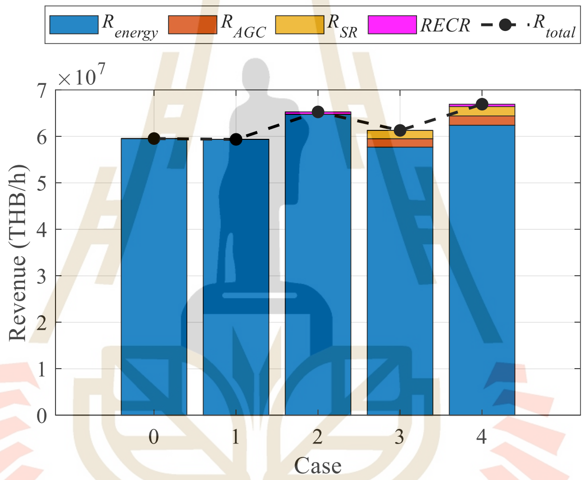

Figure 6.7 Total revenue across market cases

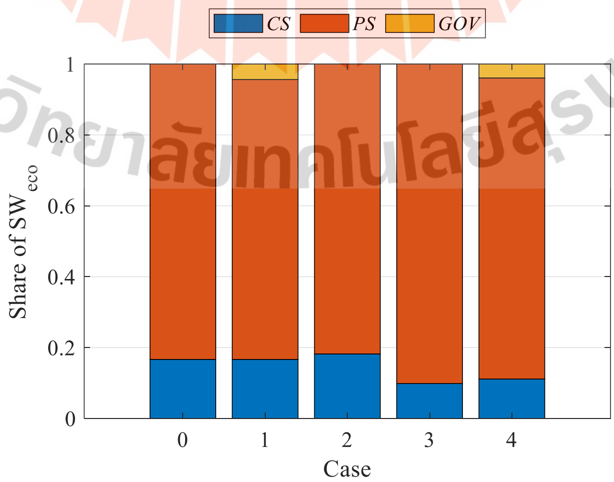

Figure 6.8 Market share of social welfare across cases

(2) Sensitivity Analysis of Carbon Tax

Sensitivity analyses were conducted to assess the influence of variations in carbon tax and REC prices on system operation and welfare outcomes. Tables 6.4 and 6.5 present the detailed results for Cases 6.1 and 6.2, respectively. Figures 6.10 to 6.13 extend the analysis by contrasting these results with those of Case 6.4, thereby illustrating the relative performance of single-instrument and multi-dimensional policy frameworks. Table 6.4 presents the carbon tax sensitivity in Case 6.1. As the tax rate increases from 0 to 1,000 THB/tCO_2, dispatch declines modestly from 18,792 MW to 18,507 MW, while emissions decrease from 10,774 to 10,615 tCO_2/h. Government revenue rises almost linearly, surpassing 10.6 million THB/h at the highest rate, but social welfare decreases from 49.1 to 38.4 billion THB/h. These results confirm that carbon pricing is effective in reducing emissions and generating fiscal revenues, although it imposes significant welfare losses.

Table 6.4 Sensitivity analysis of carbon tax rate

Carbon tax rate (THB/tCO_2)	*Dispatch (MW)*	*CE (tCO_2/h)*	*GOV(THB/h)*	SW_{post} *(THB/h)*
0	18,792.10	10,773.78	0	49,098,899.81
100	18,763.60	10,757.87	1,075,787.04	48,022,317.50
200	18,735.09	10,741.96	2,148,392.99	46,947,325.74
300	18,706.59	10,726.06	3,217,817.86	45,873,924.51
400	18,678.09	10,710.15	4,284,061.65	44,802,113.83
500	18,649.58	10,694.25	5,347,124.35	43,731,893.69
600	18,621.08	10,678.34	6,407,005.98	42,663,264.09
700	18,592.57	10,662.44	7,463,706.52	41,596,225.03
800	18,564.07	10,646.53	8,517,225.98	40,530,776.51
900	18,535.56	10,630.63	9,567,564.36	39,466,918.54
1000	18,507.06	10,614.72	10,614,721.65	38,404,651.10

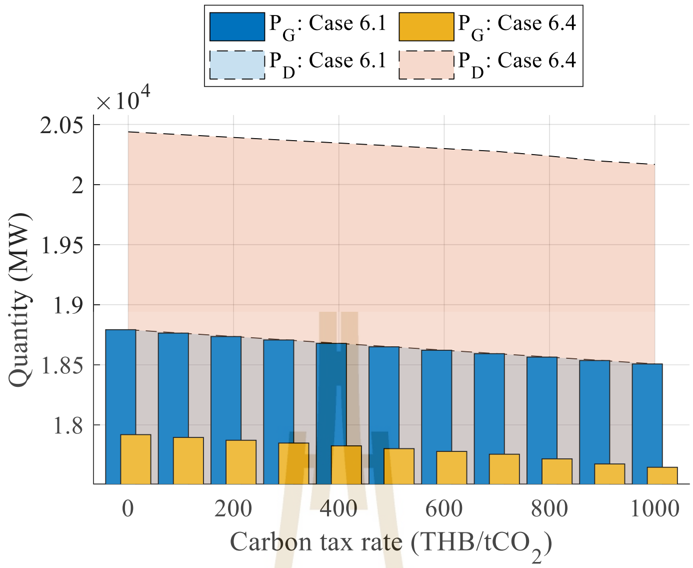

Figure 6.9 Sensitivity of carbon tax rate compared with power generation and power demand

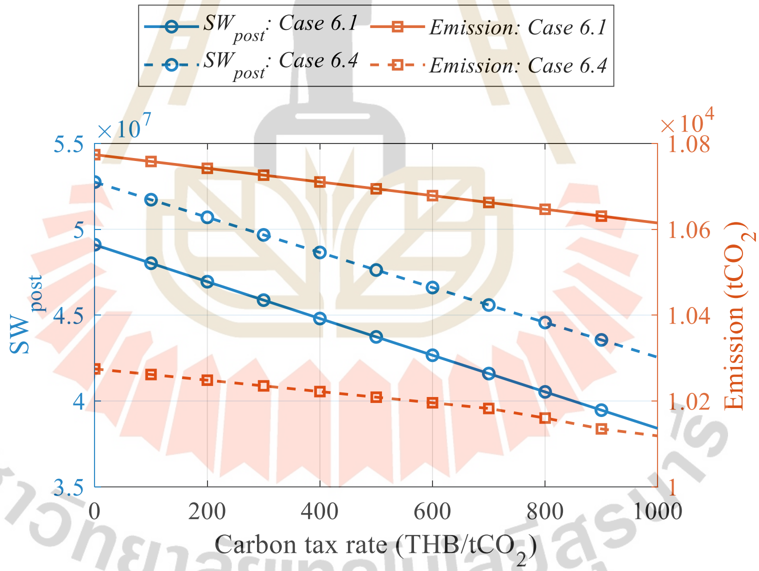

Figure 6.10 Sensitivity of carbon tax rate compared with post-transfer social welfare and emissions

Figure 6.9 compares the results, contrasting Cases 6.1 and 6.4. In both cases, dispatch decreases as the carbon tax rises, but the decline is sharper in Case 6.4, where the integration of renewable and ancillary markets amplifies the operational response to taxation. Demand remains relatively stable across both cases, indicating limited demand-side bidding. Figure 6.10 confirms that emissions decrease with higher carbon taxes in both scenarios. At the same time, welfare declines more steeply in Cases 6.1 and 6.4 as REC and ancillary revenues mitigate part of the welfare loss.

(3) Sensitivity Analysis of REC price

The REC price sensitivity in Case 6.2 is demonstrated in Table 6.5. Across the full range of REC prices, dispatch and emissions remain unchanged at 18,730 MW and 10,739 tCO_2/h, respectively. Nevertheless, producer surplus increases steadily from 44.8 to 47.3 billion THB/h, while total social welfare rises from 55.4 to 57.9 billion THB/h. This suggests that REC trading primarily functions as a financial redistribution mechanism, enhancing producer revenues and overall welfare without altering system operation or environmental outcomes.

Table 6.5 Sensitivity analysis of REC price

REC price (THB/REC)	*Dispatch (MW)*	*CE (tCO_2/h)*	*PS (THB/h)*	SW_{post} *(THB/h)*
0	18,730.45	10,739.38	44,820,442.34	55,420,669.55
100	18,730.45	10,739.38	45,072,442.34	55,672,669.55
200	18,730.45	10,739.38	45,324,442.34	55,924,669.55
300	18,730.45	10,739.38	45,576,442.34	56,176,669.55
400	18,730.45	10,739.38	45,828,442.34	56,428,669.55
500	18,730.45	10,739.38	46,080,442.34	56,680,669.55
600	18,730.45	10,739.38	46,332,442.34	56,932,669.55
700	18,730.45	10,739.38	46,584,442.34	57,184,669.55
800	18,730.45	10,739.38	46,836,442.34	57,436,669.55
900	18,730.45	10,739.38	47,088,442.34	57,688,669.55
1000	18,730.45	10,739.38	47,340,442.34	57,940,669.55

Figure 6.11 compares the outcomes of Cases 6.2 and 6.4. In Case 6.2, rising REC prices translate directly into higher producer revenues, while renewable dispatch remains constant. In the multi-dimensional framework, however, revenues are consistently higher across all REC price levels due to the complementary

contributions of carbon and ancillary service markets. Figure 6.12 confirms the same pattern for social welfare. Although both scenarios show steady increases with higher REC prices, the gains are markedly greater in Case 6.4, reflecting the synergistic effect of combining REC incentives with carbon pricing and ancillary revenues. This demonstrates that while REC trading alone supports producer viability, its welfare-enhancing potential is significantly amplified under market integration.

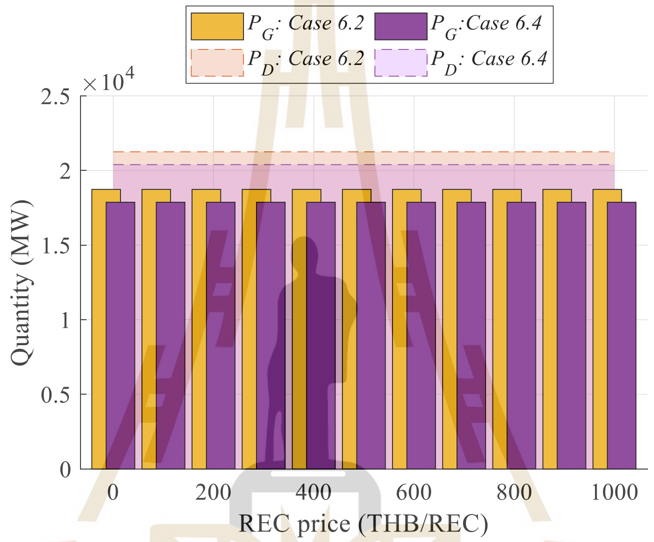

Figure 6.11 Sensitivity of REC price compared with quantity

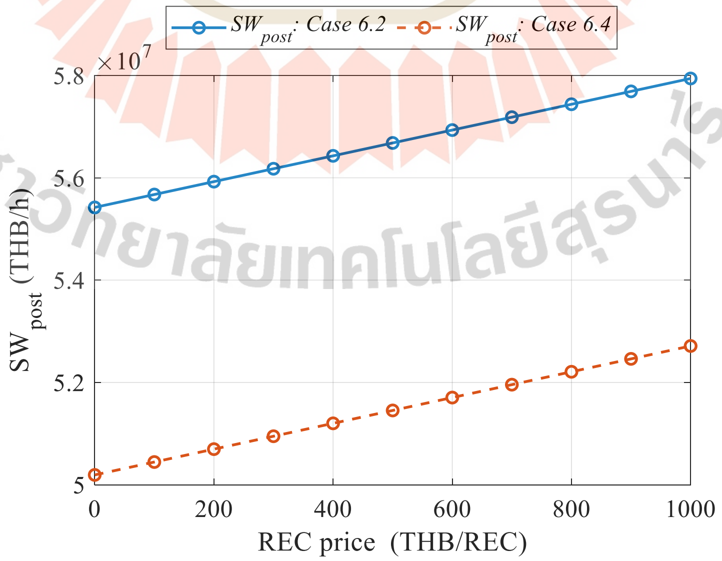

Figure 6.12 Sensitivity of REC rate compared with post-transfer social welfare

As a result, the sensitivity analyses reveal the distinct complementary functions of the two instruments. Carbon pricing delivers measurable emission reductions and fiscal revenues, but reduces short-term welfare. In contrast, REC trading improves financial redistribution and strengthens producer incentives without operational effects. Multi-dimensional market mechanisms interact to mitigate individual shortcomings, achieving a more balanced alignment of efficiency, sustainability, and equity.

6.5.2 Simulation Results using Hybrid PSO-QP Optimisation

The simulation results obtained from the hybrid PSO-QP optimisation, summarised in Tables 6.6 and 6.7, demonstrate the effectiveness of the proposed multi-dimensional market framework in improving both economic and environmental performance across different market configurations. A comparative analysis of Cases 6.0 - 6.4 reveals the progressive impacts of integrating carbon pricing, renewable incentives, and ancillary service co-optimisation as illustrated in Table 6.6. The baseline case (Case 6.0), representing a conventional energy-only market, yields a total generation output of 15,799.96 MW with a post-transfer social welfare of THB 51.87 million/h. When a carbon pricing mechanism is introduced in Case 6.1, total emissions decline from 9,104.16 tCO_2/MWh to 9,068.40 tCO_2/MWh, demonstrating effective internalisation of environmental externalities. However, this emission reduction is accompanied by a decrease in post-transfer welfare to THB 50.06 million/h, primarily due to the redistributive effect of carbon tax payments.

The inclusion of renewable generation and REC trading in Case 6.2 enhances producer revenues and overall market performance, improving post-transfer welfare to THB 58.71 million/h. This result highlights the contribution of renewable incentives in stimulating clean energy investment and increasing producer participation. In contrast, Case 6.3, which incorporates ancillary service co-optimisation, yields a lower total generation of 18,203.71 MWh but provides significant reliability benefits, as indicated by the allocation of 910.19 MW of spinning reserve and 1,115,099.94 THB/h of reserve payments. Despite slightly reduced welfare, the inclusion of ancillary services strengthens system adequacy and operational stability. Case 6.4, which co-optimises all policy instruments, achieves the most balanced and realistic outcome. Total generation is reduced to 14,872.03 MW, while emissions reach their lowest level of 8,574.48

tCO_2/MWh, representing a substantial improvement in environmental performance. Post-transfer social welfare attains a value of THB 53.82 million/h, outperforming all single-policy cases. The combined implementation also secures 1,019.6 MW of reserve capacity with an associated reserve cost of 1,208,840 THB/h, maintaining high system security at a reasonable cost.

Thirty independent trials of Case 6.4 were conducted to ensure robustness and consistency of the optimisation results, as shown in Table 6.7. The statistical outcomes show negligible variation among trials, with a standard deviation of only 288.66 THB/h, confirming the stability and convergence reliability of the hybrid PSO-QP approach. The average computation time of approximately 3,356 seconds indicates that the method achieves an acceptable balance between computational burden and optimisation precision for a large-scale system. Moreover, Figure 6.13 shows the distribution of post-transfer social welfare values across the 30 trial solutions for Case 6.4.

The comparison between QP and hybrid PSO-QP optimisation highlights apparent differences in technical representation and welfare outcomes. The hybrid PSO-QP method produces a slightly lower total dispatched generation compared with the QP approach, primarily because the PSO component optimises voltage magnitudes, transformer tap-changing, and compensator reactances, non-convex control variables that directly affect network losses, voltage profiles, and reactive power flows. Simultaneously, the QP module determines active generation, renewable output, AGC, SR, and demand, ensuring coordinated optimisation between market and system variables. The lower dispatch level obtained by the hybrid method reflects a more realistic and physically feasible operating condition, as it accounts for actual AC network losses and voltage-dependent constraints often neglected in conventional QP formulations. Despite this, the hybrid PSO-QP approach achieves a higher post-transfer social welfare, indicating more efficient resource utilisation once technical effects are integrated into the optimisation. By jointly considering economic objectives and system conditions, the hybrid framework delivers solutions that are both economically optimal and technically consistent, offering a more accurate representation of real-world power system operations under integrated market mechanisms.

Table 6.6 Simulation results from hybrid PSO-QP method [Part I]

Case	Total P_G (MW)	CG (THB/h)	CE (tCO_2/MWh)	CCE (THB/h)	Total P_{RE} (MWh)	CRE (THB/h)	$RECR$ (THB/h)
Case 6.0	15,799.96	15,873,916.70	9,104.16	0	0	0	0
Case 6.1	15,735.87	15,689,998.18	9,068.40	1,813,679.83	0	0	0
Case 6.2	15,734.68	15,678,992.26	9,067.73	0	2,520	1,514,566	504,000
Case 6.3	15,206.44	14,605,737.15	8,765.31	0	0	0	0
Case 6.4	14,872.03	13,899,177.02	8,574.48	1,714,896.35	2,520	1,514,566	504,000

Table 6.6 Simulation results from hybrid PSO-QP method [Part II]

Case	Total AGC (MW)	$CAGC$ (THB/h)	Total SR (MW)	CSR (THB/h)	Total P_D (MW)	B (THB/h)	SW_{post} (THB/h)
Case 6.0	0	0	0	0	18,792.10	67,746,643.91	51,872,727.20
Case 6.1	0	0	0	0	18,735.09	67,565,832.49	50,062,154.48
Case 6.2	0	0	0	0	21,250.45	75,398,412.41	58,708,854.15
Case 6.3	910.19	1,115,099.94	910.19	1,040,730	18,203.71	65,880,858.07	49,119,290.60
Case 6.4	1,019.6	1,208,840.19	1,019.6	1,126,057	20,392.00	72,777,612.46	53,818,075.82

Note: Detailed simulation results are addressed in Table B.3 (Appendix B.2)

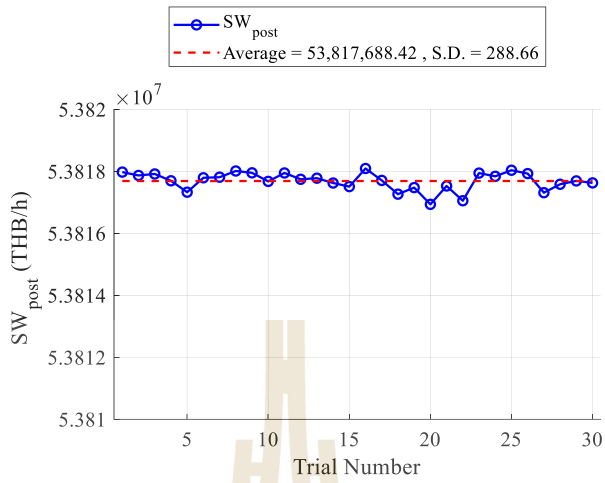

Figure 6.13 The solution with 30 trials of the hybrid PSO-QP method run for Case 6.4

Table 6.7 The best, worst, average, median and standard deviation of post-transfer social welfare and average computation times from 30 trial solutions of Case 6.4

The proposed multi-dimensional market mechanism (Case 6.4)					
	Best	*Worst*	*Average*	*Median*	*S.D.*
SW_{post} (THB/h)	53,818,090.37	53,816,936.9	53,817,688.42	53,817,726.42	288.66
Average time (s)			3,356.0939		

6.6 Conclusion

This research examined a multi-dimensional electricity market framework for the 160-bus equivalent Thai power system, incorporating carbon pricing, renewable incentives, and ancillary service procurement. The results demonstrate that single-policy instruments, including carbon taxation, REC, and ancillary services, exert distinct effects on operational efficiency, emissions, and welfare distribution. While carbon taxation reduces emissions and generates government revenue at the expense of economic efficiency, REC trading primarily serves as a financial mechanism that strengthens producer viability without significantly altering system dispatch. Ancillary service procurement enhances security but imposes additional costs that lower social welfare. By contrast, the multi-dimensional market design reveals strong complementarities. The combined implementation of carbon pricing, renewable incentives, and ancillary service procurement reduces emissions by nearly 5% relative to the baseline, diversifies welfare allocation across stakeholders, and mitigates the adverse impacts of individual policies. Sensitivity analyses further highlight that integration amplifies the environmental effectiveness of carbon taxation while enhancing the welfare gains from REC trading. These results underscore the policy relevance of multi-dimensional electricity markets as a tool for aligning efficiency, sustainability, and reliability objectives.

Furthermore, the hybrid PSO-QP optimisation method demonstrates superior computational performance compared with conventional QP optimisation. By jointly optimising non-convex network control variables with market-clearing variables, the hybrid approach yields more realistic, technically feasible dispatch solutions that explicitly account for power losses and voltage-dependent system constraints. Although the resulting total generation is slightly lower than that obtained by the QP method, the hybrid PSO-QP achieves higher post-transfer social welfare, reflecting improved resource utilisation and system efficiency once physical network effects are considered. This integrated computational framework bridges the gap between economic optimisation and technical feasibility, enhancing the accuracy and policy relevance of market-based decision-making in complex power systems.

From a policy perspective, these findings offer actionable insights for Thailand's carbon neutrality roadmap. The research indicates that carbon pricing alone may not suffice to achieve ambitious climate targets without imposing substantial welfare losses. However, integrated with renewable incentives, ancillary services, and technically consistent optimisation through the hybrid PSO-QP approach, the electricity market can simultaneously deliver emission reductions, ensure system adequacy, and maintain equitable welfare distribution. This multi-dimensional and technically grounded framework offers a pragmatic pathway for Thailand to reconcile short-run operational efficiency with long-term sustainability goals, thereby supporting the country's transition toward a carbon-neutral power sector.

CHAPTER VII
CONCLUSION AND RECOMMENDATION

7.1 Conclusion

This thesis aimed to develop an integrated optimal power dispatch framework that captures the complex interactions among electricity markets, carbon pricing mechanisms, renewable energy participation, REC revenues, and ancillary service requirements. The findings across Chapters 3 to 6 demonstrate that the research has successfully achieved these aims, offering both methodological advances and practical insights into the design of coordinated low-carbon electricity markets.

The mathematical framework developed in this research provides a unified optimisation structure that brings together elements typically treated in isolation: energy dispatch, carbon costs, renewable incentives, and system security obligations. By embedding these elements within a single clearing mechanism, the model overcomes the limitations of fragmented market structures and reveals the efficiency gains that arise from co-optimisation. The numerical analyses confirm that incorporating carbon emission costs directly into the dispatch process yields lower emissions and reduces overall expenditure, demonstrating the economic and environmental value of carbon-aware market operations.

The integration of renewable energy certificates and demand-side bidding further enriches market interactions. The results show that when renewable incentives and demand flexibility are jointly optimised with conventional generation and carbon pricing, the system achieves substantially higher cost savings and social welfare improvements. This highlights the crucial role of multi-dimensional coordination, across both supply and demand, in shaping efficient and equitable market outcomes.

The extended framework involving ancillary service co-optimisation illustrates the additional reliability and environmental benefits gained when system security requirements are integrated into the broader market mechanism rather than treated as a separate process. Coordinated procurement of reserves, combined with stepwise demand response incentives, enhances operational flexibility and supports deeper emission reductions without compromising system stability.

Applying the model to the 160-bus equivalent Thai power system further demonstrates its practical relevance. The integrated approach consistently outperforms single-policy or sequential mechanisms across economic, environmental, and reliability dimensions, offering clear evidence that coordinated multi-market designs can produce superior system-wide outcomes. Moreover, the hybrid PSO-QP method effectively captures non-convex operational characteristics, producing dispatch solutions that are both technically feasible and economically efficient, an essential requirement for real-world implementation.

The research establishes that unified market-clearing mechanisms, which jointly consider carbon pricing, renewable incentives, ancillary services, and demand-side participation, can deliver significant improvements in efficiency, sustainability, and system security. The integrated optimisation framework and methodological innovations presented in this thesis therefore contribute a robust foundation for advancing low-carbon electricity market reform and support the long-term transition toward a more efficient, resilient, and environmentally responsible power sector.

7.1.1 Comparative Analysis of Single-Sided and Double-Sided Auctions

To further contextualise the implications of the proposed integrated framework, Table 7.1 presents a comparative assessment of Single-Sided Auction (SSA) and Double-Sided Auction (DSA) mechanisms. The comparative summary reveals that the transition from SSA to DSA fundamentally shifts the market paradigm from a supply-driven model to a more holistic, elastic structure. While the SSA is limited by fixed demand and partial welfare representation, the DSA enhances economic efficiency by endogenously reflecting demand elasticity. This shift not only maximises total social welfare but also yields significant environmental and operational dividends, specifically through reduced carbon emissions and lower ancillary service requirements. Ultimately, the DSA framework provides a more robust and responsive mechanism for managing the complexities of a low-carbon power system.

Table 7.1 Comparative summary of single-side auction and double-side auction schemes

Dimension	Single-Sided Auction	Double-Sided Auction
Economic Efficiency	• Demand fixed (inelastic) • Dispatch determined solely by supply bids • Higher reliance on marginal units	• Demand bids introduce elasticity • Improved price responsiveness • More efficient resource allocation
Social Welfare	• Only producer surplus represented • Consumer surplus cannot be measured • Welfare outcome is partial	• Both consumer and producer surplus included • Welfare maximised through joint optimisation • More accurate welfare representation
Carbon Impact	• Higher total dispatch levels • Greater use of high-emission marginal units	• Lower dispatch due to DR elasticity • Reduced reliance on marginal units • Lower carbon emissions
Ancillary Services	• Higher AS requirement • Larger ramping and flexibility needs	• Lower AS requirement • Reduced ramping due to demand-side participation

7.2 Recommendation

Building upon the findings presented in Chapters 3 to 6, several promising directions for future research can be identified as follows:

(1) The integrated market framework could be extended to incorporate uncertainties from renewable energy sources, such as wind and solar generation variability, through stochastic or robust optimisation methods. This would enhance the model's applicability to real-world systems with high renewable penetration.

(2) Future studies should explore the temporal and spatial dynamics of carbon pricing and emission trading, including inter-regional carbon markets and time-varying emission factors. Such extensions would enable a more accurate representation of long-term decarbonisation pathways and the impacts of cross-border electricity trade.

(3) The integration of energy storage systems and flexible loads into the optimisation framework offers a valuable avenue for improving system flexibility, reducing curtailment, and enhancing the reliability of renewable integration. Advanced coordination mechanisms between storage, demand response, and ancillary service markets could further strengthen market efficiency and resilience.

(4) Expanding the framework to include multi-energy systems, such as the coupling of electricity, heat, hydrogen, and gas networks, would provide a holistic view of energy system decarbonisation. This approach could reveal additional synergies among sectors and improve overall energy utilisation efficiency.

(5) Integrating advanced machine learning methods to capture user behaviour, strategic or gaming bidding patterns, and other market dynamics. Such behavioural modelling, when combined with hybrid optimisation algorithms, could further improve market efficiency, robustness, and adaptability under uncertainty.

(6) From a policy perspective, future research could focus on market design under evolving carbon-neutrality targets, assessing how dynamic policy instruments, such as flexible carbon caps, renewable portfolio standards, and demand-side incentives, interact within integrated market frameworks. Pilot-scale implementation studies in actual market environments, such as Thailand's evolving power sector, would provide valuable insights into the feasibility and effectiveness of the proposed models in guiding low-carbon market reforms.

Therefore, advancing these directions will deepen the understanding of integrated market operations, strengthen the connection between policy and technical optimisation, and support the global transition toward sustainable, carbon-neutral power systems.

REFERENCE

Aggarwal, R., Ayhan, S. H., Jakob, M., & Steckel, J. C. (2025). Carbon pricing and household welfare: evidence from Uganda. Environment and Development Economics, 30(1), 1-25. https://doi.org/10.1017/S1355770X24000214

Alvarado, F., Hu, Y., Ray, D., Stevenson, R., & Cashman, E. (1991). Engineering foundations for the determination of security costs. IEEE Transactions on Power Systems, 6(3), 1175-1182. https://doi.org/10.1109/59.119263

Andersson, J. J. (2019). Carbon Taxes and CO_2 Emissions : Sweden as a Case Study [research-article]. American Economic Journal: Economic Policy, 11(4), 1-30.

Baig, A. M., Badesa, L., & Strbac, G. (2021). Importance of linking inertia and frequency response procurement: The great britain case. 2021 IEEE Madrid PowerTech,

Banshwar, A., Sharma, N. K., Sood, Y. R., & Shrivastava, R. (2017). Market based procurement of energy and ancillary services from Renewable Energy Sources in deregulated environment. Renewable Energy, 101, 1390-1400.

Baughman, M. L., & Siddiqi, S. N. (1991). Real-time pricing of reactive power: theory and case study results. IEEE Transactions on Power Systems, 6(1), 23-29. https://doi.org/10.1109/59.131043

Baughman, M. L., Siddiqi, S. N., & Zarnikau, J. W. (1997). Advanced pricing in electrical systems. II. Implications. IEEE Transactions on Power Systems, 12(1), 496-502. https://doi.org/10.1109/59.575803

Berger, A. W., & Schweppe, F. C. (1989). Real time pricing to assist in load frequency control. IEEE Transactions on Power Systems, 4(3), 920-926. https://doi.org/10.1109/59.32580

Bunn, D. W. (2000). Forecasting loads and prices in competitive power markets. Proceedings of the IEEE, 88(2), 163-169.

Caramanis, M. C., Bohn, R. E., & Schweppe, F. C. (1987). System security control and optimal pricing of electricity. International Journal of Electrical Power & Energy Systems, 9(4), 217-224. https://doi.org/10.1016/0142-0615(87)90003-2

Chen, L., Zhong, J., & Gan, D. (2007). Optimal Automatic Generation Control (AGC) Dispatching and Its Control Performance Analysis for the Distribution Systems with DGs. 2007 IEEE Power Engineering Society General Meeting,

Chen, Y.-h., Wang, C., Nie, P.-y., & Chen, Z.-r. (2020). A clean innovation comparison between carbon tax and cap-and-trade system. Energy Strategy Reviews, 29, 100483. https://doi.org/10.1016/j.esr.2020.100483

Chen, Z.-y., & Nie, P.-y. (2016). Effects of carbon tax on social welfare: A case study of China. Applied Energy, 183, 1607-1615. https://doi.org/10.1016/j.apenergy.2016.09.111.

Deng, Y., Mae, M., & Matsuhashi, R. (2024). Dynamic Pricing and System Optimization of Integrated Energy System in Industrial Parks Based on Carbon Tax. 2024 20th International Conference on the European Energy Market (EEM).

Dorband, I. I., Jakob, M., Kalkuhl, M., & Steckel, J. C. (2019). Poverty and distributional effects of carbon pricing in low- and middle-income countries – A global comparative analysis. World Development, 115, 246-257. https://doi.org/10.1016/j.worlddev.2018.11.015.

Dutta, S., Paul, B., Kundu, B., & Chanda, C. K. (2024). Co-optimization of Reserves in Energy Market to mitigate Congestion. 2024 6th International Conference on Energy, Power and Environment (ICEPE).

Fang, Y., Zhao Yang, D., Ke, M., Zhao, X., Iu, H. H., & Kit Po, W. (2012). Quantum-Inspired Particle Swarm Optimization for Power System Operations Considering Wind Power Uncertainty and Carbon Tax in Australia [Periodical]. IEEE Transactions on Industrial Informatics, Industrial Informatics, IEEE Transactions on, IEEE Trans. Ind. Inf., 8(4), 880-888. https://doi.org/10.1109/TII.2012.2210431.

Fu, J., Núñez, A., & De Schutter, B. (2023). A bidding mechanism for maintenance of generation units considering inter-ISO power exchange. International Journal of Electrical Power & Energy Systems, 144, 108595. https://doi.org/10.1016/j.ijepes.2022.108595.

Gedra, T. W. (1999). On transmission congestion and pricing. IEEE Transactions on Power Systems, 14(1), 241-248.

Gjengedal, T., Gjerde, J. O., & Flolo, R. (1998). Ancillary services in deregulated power systems; what are they; who needs them and who pays. POWERCON'98. 1998 International Conference on Power System Technology. Proceedings (Cat. No. 98EX151).

Gugler, K., Haxhimusa, A., & Liebensteiner, M. (2023). Carbon pricing and emissions: Causal effects of Britain's carbon tax. Energy Economics, 121. https://doi.org/10.1016/j.eneco.2023.106655.

Hayyolalam, V., & Pourhaji Kazem, A. A. (2020). Black Widow Optimization Algorithm: A novel meta-heuristic approach for solving engineering optimization problems. Engineering Applications of Artificial Intelligence, 87, 103249. https://doi.org/10.1016/j.engappai.2019.103249.

He, H., Wang, P., Wang, Y., & Wang, H. (2023, 7-9 July 2023). Ancillary Service Market Equilibrium Analysis for Multi-Agent Load Aggregators in Distribution System. 2023 IEEE/IAS Industrial and Commercial Power System Asia (I&CPS Asia).

Hustveit, M., Frogner, J. S., & Fleten, S.-E. (2017). Tradable green certificates for renewable support: The role of expectations and uncertainty. Energy, 141, 1717-1727. https://doi.org/10.1016/j.energy.2017.11.013.

Ilyas, M. A., Abbas, G., Alquthami, T., Awais, M., & Rasheed, M. B. (2020, 01/01/). Multi-Objective Optimal Power Flow With Integration of Renewable Energy Sources Using Fuzzy Membership Function [Periodical]. IEEE Access, Access, IEEE, 8, 143185-143200. https://doi.org/10.1109/ACCESS.2020.3014046.

Jay, D., & Swarup, K. S. (2021). A comprehensive survey on reactive power ancillary service markets. Renewable and Sustainable Energy Reviews, 144, 110967. https://doi.org/10.1016/j.rser.2021.110967.

Jin, Y., Wang, Z., Jiang, C., & Zhang, Y. (2015). Dispatch and bidding strategy of active distribution network in energy and ancillary services market. Journal of Modern Power Systems and Clean Energy, 3(4), 565-572. https://doi.org/10.1007/s40565-015-0161-8.

Kaye, R. J., Wu, F. F., & Varaiya, P. (1995). Pricing for system security [power tariffs]. IEEE Transactions on Power Systems, 10(2), 575-583. https://doi.org/10.1109/59.387891.

Kennedy, J., & Eberhart, R. (1995). Particle swarm optimization. Proceedings of ICNN'95 - International Conference on Neural Networks.

Khastar, M., Aslani, A., & Nejati, M. (2020). How does carbon tax affect social welfare and emission reduction in Finland? Energy Reports, 6, 736-744. https://doi.org/10.1016/j.egyr.2020.03.001.

Kirschen, D. S., & Strbac, G. (2004). Fundamentals of power system economics [BibliographiesFiction]. John Wiley & Sons.

Li, S., Gong, W., Wang, L., & Gu, Q. (2022). Multi-objective optimal power flow with stochastic wind and solar power. Applied Soft Computing, 114, 108045. https://doi.org/10.1016/j.asoc.2021.108045.

Lin, B., & Jia, Z. (2019). Impacts of carbon price level in carbon emission trading market. Applied Energy, 239, 157-170. https://doi.org/10.1016/j.apenergy.2019.01.194.

Lin, W.-M., Yang, C.-Y., Tsai, M.-T., & Wang, Y.-H. (2021). Unit commitment with ancillary services in a day-ahead power market. Applied Sciences, 11(12), 5454.

Litvinov, E. (2010). Design and operation of the locational marginal prices-based electricity markets. IET GENERATION TRANSMISSION AND DISTRIBUTION, 4(2), 315-323.

Liu, H., Tesfatsion, L., & Chowdhury, A. A. (2009). Locational marginal pricing basics for restructured wholesale power markets. 2009 IEEE Power & Energy Society General Meeting.

Lou, K. (2023). Pricing Models for a Two-Period Manufacturing and Remanufacturing Process Under Carbon Cap and Trade Mechanism. IEEE Access, 11, 56142-56151. https://doi.org/10.1109/ACCESS.2023.3283437.

Lu, Z., Wang, J., Shahidehpour, M., Bai, L., & Li, Z. (2024). Convex-Hull Pricing of Ancillary Services for Power System Frequency Regulation With Renewables and Carbon-Capture-Utilization-and-Storage Systems. IEEE Transactions on Power Systems, 39(5), 6615-6635. https://doi.org/10.1109/TPWRS.2024.3368338.

Maneesha, A., & Swarup, K. S. (2022). Optimal Double Auction Bidding Strategy Considering Ancillary Services and Demand Response. 2022 22nd National Power Systems Conference (NPSC).

Mirjalili, S., & Lewis, A. (2016). The Whale Optimization Algorithm. Advances in Engineering Software, 95, 51-67. https://doi.org/10.1016/j.advengsoft.2016.01.008.

Mirjalili, S., Mirjalili, S. M., & Lewis, A. (2014). Grey Wolf Optimizer. Advances in Engineering Software, 69, 46-61. https://doi.org/10.1016/j.advengsoft.2013.12.007.

Muangkhiew, P., & Chayakulkheeree, K. (2024). Carbon-Accounted Optimal Power Dispatch and Spot Pricing. 2024 IEEE/IAS Industrial and Commercial Power System Asia (I&CPS Asia).

Muangkhiew, P., & Chayakulkheeree, K. (2024). Optimizing social welfare: A double-sided auction approach for low-carbon emission power systems with renewable energy certificates. Journal of Renewable and Sustainable Energy, 16(5). https://doi.org/10.1063/5.0213399.

Muangkhiew, P., & Chayakulkheeree, K. (2025). Enhanced Carbon-Accounted Auction-Based Dispatch and Spot Pricing Using Stochastic Optimizations. IEEE Transactions on Industry Applications, 61(6), 8555-8569. https://doi.org/10.1109/TIA.2025.3571832.

Ohlendorf, N., Jakob, M., Minx, J. C., Schröder, C., & Steckel, J. C. (2021). Distributional Impacts of Carbon Pricing: A Meta-Analysis. Environmental and Resource Economics, 78(1), 1-42. https://doi.org/10.1007/s10640-020-00521-1.

Ouyang, T., Li, Y., Xie, S., Wang, C., & Mo, C. (2024). Low-carbon economic dispatch strategy for integrated power system based on the substitution effect of carbon tax and carbon trading. Energy, 294, 130960. https://doi.org/10.1016/j.energy.2024.130960.

Pollitt, M. G., & Anaya, K. L. (2021). Competition in Markets for Ancillary Services? The Implications of Rising Distributed Generation. The Energy Journal, 42(1), 1-28. https://doi.org/10.5547/01956574.42.SI1.mpol.

Rahmani, A. M., Khorsandi, A., & Hosseinian, S. H. (2024). Implementing Demand Response to reduce spinning Reserve Costs in the Electricity Market. 2024 9th International Conference on Technology and Energy Management (ICTEM).

Rebours, Y. G., Kirschen, D. S., Trotignon, M., & Rossignol, S. (2007). A Survey of Frequency and Voltage Control Ancillary Services—Part I: Technical Features. IEEE Transactions on Power Systems, 22(1), 350-357. https://doi.org/10.1109/TPWRS.2006.888963.

Reddy, S. S., Bijwe, P. R., & Abhyankar, A. R. (2015). Optimum day-ahead clearing of energy and reserve markets with wind power generation using anticipated real-time adjustment costs. International Journal of Electrical Power & Energy Systems, 71, 242-253. https://doi.org/10.1016/j.ijepes.2015.03.002.

Schweppe, F. C., Caramanis, M. C., Tabors, R. D., & Bohn, R. E. (1988). Spot Pricing of Electricity. Springer US.

Siddiqi, S. N., & Baughman, M. L. (1995). Reliability differentiated pricing of spinning reserve. IEEE Transactions on Power Systems, 10(3), 1211-1218. https://doi.org/10.1109/59.466535.

Singh, H., & Papalexopoulos, A. (1999). Competitive procurement of ancillary services by an independent system operator. IEEE Transactions on Power Systems, 14(2), 498-504.

Tan, Q., Ding, Y., Zheng, J., Dai, M., & Zhang, Y. (2021). The effects of carbon emissions trading and renewable portfolio standards on the integrated wind–photovoltaic–thermal power-dispatching system: Real case studies in China. Energy, 222, 119927. https://doi.org/10.1016/j.energy.2021.119927.

Tao, Y., Qiu, J., Lai, S., & Zhao, J. (2021). Renewable energy certificates and electricity trading models: Bi-level game approach. International Journal of Electrical Power & Energy Systems, 130, 106940. https://doi.org/10.1016/j.ijepes.2021.106940.

Tian, J., Huang, B., Wang, Q., Du, P., Zhang, Y., & He, B. (2023). A Multi-Agent Integrated Energy Trading Strategy Based on Carbon Emission/Green Certificate Equivalence Interaction. Sustainability, 15(22). https://doi.org/10.3390/su152215766.

Viola, L., Mohammadi, S., Dotta, D., Hesamzadeh, M. R., Baldick, R., & Flynn, D. (2024). Ancillary services in power system transition toward a 100% non-fossil future:

Market design challenges in the United States and Europe. Electric Power Systems Research, 236, 110885.

Wang, G., Ma, H., Qin, L., Wu, S., & Ren, B. (2022). Optimal Power Flow of Low Carbon Power System Based on NSGA2 Algorithm and Carbon Flow Theory. 2022 IEEE 2nd International Conference on Digital Twins and Parallel Intelligence (DTPI).

Wang, G., Ma, H., Wang, B., Alharbi, A. M., Wang, H., & Ma, F. (2023). Multi-Objective Optimal Power Flow Calculation Considering Carbon Emission Intensity. Sustainability, 15(24), 16953. https://www.mdpi.com/2071-1050/15/24/16953.

Wang, J., Wang, X., & Wu, Y. (2005). Operating reserve model in the power market. IEEE Transactions on Power Systems, 20(1), 223-229.

Wang, M., Song, Y., Sui, B., Wu, H., Zhu, J., Jing, Z., & Rong, Y. (2022). Comparative study of pricing mechanisms and settlement methods in electricity spot energy market based on multi-agent simulation. Energy Reports, 8, 1172-1182. https://doi.org/10.1016/j.egyr.2022.02.078.

Wang, R., Dada, M., & Sahin, O. (2019). Pricing Ancillary Service Subscriptions. Management Science, 65(10), 4712-4732. https://doi.org/10.1287/mnsc.2018.3168.

Wang, Y., Yang, Z., Yu, J., & Liu, J. (2023). An optimization-based partial marginal pricing method to reduce excessive consumer payment in electricity markets. Applied Energy, 352, 121935. https://doi.org/10.1016/j.apenergy.2023.121935.

Wang, Z., Zhao, J., & Li, M. (2017). Analysis and optimization of carbon trading mechanism for renewable energy application in buildings. Renewable and Sustainable Energy Reviews, 73, 435-451. https://doi.org/10.1016/j.rser.2017.01.094.

Wood, A. J., & Wollenberg, B. F. (2014). Power generation, operation, and control (3rd ed.). J. Wiley & Sons.

Xuan, A., Shen, X., Guo, Q., & Sun, H. (2023). Two-Stage Planning for Electricity-Gas Coupled Integrated Energy System With Carbon Capture, Utilization, and Storage Considering Carbon Tax and Price Uncertainties. IEEE Transactions on Power Systems, 38(3), 2553-2565. https://doi.org/10.1109/TPWRS.2022.3189273

Yang, J., Dong, Z. Y., & Wen, F. (2021). A comparative study of marginal loss pricing algorithms in electricity markets. IET Generation, Transmission & Distribution, 15(3), 576-588.

Yang, M., Xue, Y., Cai, B., & Xue, F. (2025). Co-Optimization of Carbon Reduction and Carbon Sequestration in Power Sector Toward Carbon Neutrality. Journal of Modern Power Systems and Clean Energy, 13(5), 1481-1494. https://doi.org/10.35833/MPCE.2024.001135.

Yang, Z., Bose, A., Zhong, H., Zhang, N., Lin, J., Xia, Q., & Kang, C. (2017). LMP revisited: A linear model for the loss-embedded LMP. IEEE Transactions on Power Systems, 32(5), 4080-4090.

Ying, Z., & Xin-gang, Z. (2021). The impact of Renewable Portfolio Standards on carbon emission trading under the background of China's electricity marketization reform. Energy, 226, 120322. https://doi.org/10.1016/j.energy.2021.120322.

Yu, X., Dong, Z., Zhou, D., Sang, X., Chang, C.-T., & Huang, X. (2021). Integration of tradable green certificates trading and carbon emissions trading: How will Chinese power industry do? Journal of Cleaner Production, 279, 123485. https://doi.org/10.1016/j.jclepro.2020.123485.

Zeng, R., Zhang, X., Deng, Y., Li, H., & Zhang, G. (2019). An off-design model to optimize CCHP-GSHP system considering carbon tax. Energy Conversion and Management, 189, 105-117. https://doi.org/10.1016/j.enconman.2019.03.062.

Zhao, X., Wen, F., Gan, D., Huang, M., Yu, C., & Chung, C. (2004). Determination of AGC capacity requirement and dispatch considering performance penalties. Electric Power Systems Research, 70(2), 93-98.

Zheng, T., & Litvinov, E. (2006). Ex post pricing in the co-optimized energy and reserve market. IEEE Transactions on Power Systems, 21(4), 1528-1538.

Zhou, Z., Levin, T., & Conzelmann, G. (2016). Survey of US ancillary services markets.

Zuo, Y. (2022). Tokenizing Renewable Energy Certificates (RECs)—A Blockchain Approach for REC Issuance and Trading. IEEE Access, 10, 134477-134490. https://doi.org/10.1109/ACCESS.2022.3230937.

APPENDIX A
TEST SYSTEM DATA

A.1 IEEE 30-bus Test System

Appendix A.1 provides the detailed data of the IEEE 30-bus test system used in this study. These standard benchmark parameters are widely adopted in the literature and serve as a reference dataset for validating the proposed optimisation framework. Table A.1 presents the bus load and power injection data of the IEEE 30-bus test system, in which Type 1, 2, and 3 represent the slack bus, the PV bus, and the PQ bus, respectively. Table A.2 summarises the transmission line parameters of the IEEE 30-bus test system, including line impedances and capacity limits. Table A.3 reports the generation cost parameters, emission coefficients, and capacity constraints of the generating units in the IEEE 30-bus test system. The AGC and SR offered prices and quantities of IEEE 30-bus test system are shown in Table A.4.

Table A.1 Bus load and injection data of IEEE 30-bus test system

Bus No.	Bus type	Load (MW)	Bus No.	Bus type	Load (MW)	Bus No.	Bus type	Load (MW)
1	1	0	11	2	0	21	3	17.5
2	2	21.7	12	3	11.2	22	3	0
3	3	2.4	13	2	0	23	3	3.2
4	3	7.6	14	3	6.2	24	3	8.7
5	2	94.2	15	3	8.2	25	3	0
6	3	0	16	3	3.5	26	3	3.5
7	3	22.8	17	3	9	27	3	0
8	2	30	18	3	3.2	28	3	0
9	3	0	19	3	9.5	29	3	2.4
10	3	5.8	20	3	2.2	30	3	10.6

Table A.2 Line parameter of IEEE 30-bus test system

From Bus	To Bus	R (p.u.)	X (p.u.)	B/2 (p.u.)	Tap Ratio	Limit MVA
1	2	0.0192	0.0575	0.0264		2.6428
1	3	0.0452	0.1652	0.0204		2.9309
2	4	0.057	0.1737	0.0184		0.8224
3	4	0.0132	0.0379	0.0042		2.7255
2	5	0.0472	0.1983	0.0209		1.2383
2	6	0.0581	0.1763	0.0187		0.9997
4	6	0.0119	0.0414	0.0045		1.7064
4	12		0.256		0.932	0.6202
5	7	0.046	0.116	0.0102		1.0603
6	7	0.0267	0.082	0.0085		1.2994
6	8	0.012	0.042	0.0045		0.316
6	9		0.208		0.978	0.5078
6	10		0.556		0.969	0.281
9	11		0.208			0.1771
9	10		0.11			0.4983
12	13		0.14			0.331
12	14	0.1231	0.2559			0.1714
12	15	0.0662	0.1304			0.2579
12	16	0.0945	0.1987			0.1584
14	15	0.221	0.1997			0.1029
16	17	0.0524	0.1923			0.1779
15	18	0.1073	0.2185			0.1582
18	19	0.0639	0.1292			0.1221
19	20	0.034	0.068			0.1726
10	20	0.0936	0.209			0.1986
10	17	0.0324	0.0845			0.2585
10	21	0.0348	0.0749			0.2653
10	22	0.0727	0.1499			0.2412

Table A.2 Line parameter of IEEE 30-bus test system (Continued)

From Bus	To Bus	R (p.u.)	X (p.u.)	B/2 (p.u.)	Tap Ratio	Limit MVA
21	22	0.0116	0.0236			0.2034
15	23	0.1	0.202			0.1215
22	24	0.115	0.179			0.2099
23	24	0.132	0.27			0.1103
24	25	0.1885	0.3292			0.194
25	26	0.2544	0.38			0.0428
25	27	0.1093	0.2087			0.1415
27	29	0.2198	0.4153			0.1443
27	30	0.3202	0.6027			0.1424
28	27		0.369		0.968	0.248
29	30	0.2399	0.4533			0.1122
8	28	0.0636	0.2	0.0214		0.3083
6	28	0.0169	0.0599	0.0065		0.4734

Table A.3 Generation cost parameters, emission coefficients, and capacity limits for generating units in the IEEE 30-bus test system

Bus No.	Generation cost			Carbon emission			P_G^{min}	P_G^{max}
	a (\$/MW^{2}h)	b (\$/MWh)	c (\$/h)	α (t/p.u^{2}h)	β (t/p.u.h)	ω (t/h)	(MW)	(MW)
1	0.00375	2.00	0.00	0.06490	-0.05554	0.04091	50	200
2	0.01750	1.75	0.00	0.05638	-0.06047	0.02543	20	80
5	0.06250	1.00	0.00	0.04586	-0.05094	0.04258	15	50
8	0.00834	3.25	0.00	0.03380	-0.03550	0.05326	10	35
11	0.02500	3.00	0.00	0.04586	-0.05094	0.04258	10	30
13	0.02500	3.00	0.00	0.05151	-0.55550	0.06131	12	40

Table A.4 AGC and SR offered prices and quantities of IEEE 30-bus test system

Bus No.	AGC		SR	
	MW	$/MW	MW	$/MW
1	6	7	4	8
2	8	11	6	11
5	5	12	5	8
8	4	13	6	10
11	3	14	5	14
13	4	5	4	12

A.2 160 bus Equivalent Thai Power System

Appendix A.2 provides the data for the 160-bus equivalent Thai power system developed for this study. This system is a simplified, aggregated representation constructed for research purposes and does not fully replicate the Thai power grid. However, it captures the essential structural characteristics and generator operating ranges required for large-scale optimisation and electricity market analysis. Table A.5 presents the bus load and power injection data of the 160-bus equivalent Thai power system. Table A.6 summarises the transmission line parameters of the 160-bus equivalent Thai power system. Table A.7 presents the cost coefficients and emission coefficients of the generating units considered in this study. The emission coefficients for each generator are derived from the emission factors reported in the Emission Factor CFP Report (July 2022) published by the Thailand Greenhouse Gas Management Organization (TGO). Specifically, the emission coefficient assigned to each generating unit corresponds to its primary fuel type by matching the generator's fuel characteristics with the relevant emission factors provided in the TGO report. This approach ensures that the emission modelling accurately reflects fuel-specific carbon intensities in the Thai power system context. The AGC and SR offered prices and quantities of 160-bus equivalent Thai power system are shown in Table A.8.

Table A.5 Bus load and injection data of the 160-bus equivalent Thai power system

Bus No.	Bus type	Load (MW)	Bus No.	Bus type	Load (MW)	Bus No.	Bus type	Load (MW)
1	1	0	28	2	60.64	55	3	0
2	2	0	29	2	0	56	3	0
3	2	0	30	2	23.29	57	3	0
4	2	0	31	2	0	58	3	0
5	2	16.57	32	2	0.23	59	3	0
6	2	0	33	2	0.08	60	3	297.8
7	2	23.15	34	2	0.18	61	3	640.4
8	2	0	35	2	0	62	3	662.5
9	2	0	36	2	98.05	63	3	837.5
10	2	26.13	37	2	0	64	3	359.4
11	2	0	38	2	0	65	3	486.9
12	2	0.98	39	2	0	66	3	340.8
13	2	0.98	40	2	9.6	67	3	0
14	2	1.36	41	2	0	68	3	0
15	2	0.38	42	2	0	69	3	241.5
16	2	24.26	43	3	51.51	70	3	0
17	2	0	44	3	553.3	71	3	0
18	2	0.55	45	3	0	72	3	0
19	2	0.28	46	3	0	73	3	0
20	2	22.61	47	3	0	74	3	0
21	2	0	48	3	0	75	3	0
22	2	0	49	3	0	76	3	0
23	2	0	50	3	0	77	3	0
24	2	0	51	3	0	78	3	0
25	2	36.46	52	3	0	79	3	0
26	2	0	53	3	0	80	3	29.3
27	2	0	54	3	0	81	3	0

Table A.5 Bus load and injection data of the 160-bus equivalent Thai power system (Continued)

Bus No.	Bus type	Load (MW)	Bus No.	Bus type	Load (MW)	Bus No.	Bus type	Load (MW)
82	3	0	109	3	29.8	136	3	184.5
83	3	0	110	3	30.2	137	3	462.4
84	3	0	111	3	249.4	138	3	168.6
85	3	0	112	3	80.5	139	3	302.1
86	3	49.6	113	3	248	140	3	60.9
87	3	0	114	3	137.2	141	3	110.4
88	3	0	115	3	42.2	142	3	146.2
89	3	0	116	3	3.3	143	3	281.4
90	3	0	117	3	42.8	144	3	126.6
91	3	0	118	3	198	145	3	70
92	3	0	119	3	161	146	3	95.9
93	3	0	120	3	341.1	147	3	515.2
94	3	0	121	3	69.7	148	3	0
95	3	0	122	3	280.2	149	3	0
96	3	0	123	3	238.2	150	3	0
97	3	0	124	3	180.3	151	3	0
98	3	0	125	3	137.6	152	3	0
99	3	0	126	3	87.9	153	3	0
100	3	0	127	3	245.4	154	3	0
101	3	122.1	128	3	119.3	155	3	0
102	3	121.9	129	3	50.8	156	3	0
103	3	48.2	130	3	50.5	157	3	0
104	3	151.7	131	3	45.8	158	3	0
105	3	231.4	132	3	45.6	159	3	177.1
106	3	177.8	133	3	196	160	3	0
107	3	-27.3	134	3	208.8			
108	3	72.8	135	3	86			

Table A.6 Line parameter of the 160-bus equivalent Thai power system

From Bus	To Bus	R (p.u.)	X (p.u.)	B/2 (p.u.)	Tap Ratio	Limit MVA
60	61	0.0007	0.005	0.0052		500
60	65	0.0018	0.0146	0.0134		500
60	66	0.0019	0.014	0.0145		500
61	62	0.0002	0.0027	0.0223		500
61	66	0.0017	0.0128	0.0132		500
62	68	0.0001	0.0012	0.0389		500
62	69	0.0002	0.0011	0.0044		500
63	44	0.0004	0.0041	0.0347		500
63	68	0.0005	0.0041	0.0184		500
63	43	0.0011	0.0116	0.0945		500
44	64	0.00026	0.0027	0.0501		500
64	65	0.0001	0.0018	0.0149		500
64	100	0.0009	0.0102	0.0215		500
65	45	0.00147	0.01429	0.03442		500
65	100	0.0005	0.006	0.0127		500
45	66	0.0012	0.0087	0.0393		500
45	87	0.0035	0.0251	0.1129		500
45	96	0.0026	0.021	0.0791		500
66	67	0.0019	0.0214	0.0397		500
66	46	0.0019	0.0214	0.0397		500
67	94	0.0017	0.0179	0.0365		500
67	55	0.0021	0.0222	0.0453		500
67	68	0.0009	0.0096	0.0196		500
68	46	0.0009	0.0096	0.0196		500
68	55	0.0024	0.0148	0.1212		500
46	94	0.0017	0.0179	0.0365		500
46	55	0.0021	0.0222	0.0453		500
70	71	0.0052	0.0372	0.1673		500
70	88	0.0059	0.0432	0.1892		500

Table A.6 Line parameter of the 160-bus equivalent Thai power system (Continued)

From Bus	To Bus	R (p.u.)	X (p.u.)	B/2 (p.u.)	Tap Ratio	Limit MVA
71	72	0.0049	0.0347	0.1557		500
71	82	0.0079	0.0584	0.2629		500
72	47	0.0008	0.0088	0.0738		500
72	73	0.0057	0.0413	0.0196		500
72	74	0.0005	0.0036	0.0158		500
72	84	0.0087	0.0632	0.2797		500
48	75	0.0025	0.0214	0.0759		500
75	49	0.0038	0.03	0.1132		500
75	58	0.014	0.1032	0.4603		500
49	76	0.0048	0.0383	0.1444		500
76	77	0.0044	0.0352	0.1325		500
77	78	0.0044	0.0346	0.1303		500
79	153		0.0001			500
153	154	0.0026	0.0326	1.75205		500
154	59		0.0001			500
79	155		0.0001			500
155	156	0.0026	0.0326	1.75205		500
156	59		0.0001			500
79	157		0.0001			500
157	158	0.00265	0.03589	1.67202		500
158	59		0.0001			500
79	151		0.0001			500
79	152		0.0001			500
151	91	0.00169	0.02298	1.06595		500
152	91	0.00169	0.02298	1.06595		500
50	80	0.0054	0.0438	0.0406		500
50	81	0.0107	0.0833	0.3253		500
80	81	0.0159	0.1284	0.1189		500
81	82	0.0024	0.0277	0.0718		500

Table A.6 Line parameter of the 160-bus equivalent Thai power system (Continued)

From Bus	To Bus	R (p.u.)	X (p.u.)	B/2 (p.u.)	Tap Ratio	Limit MVA
81	83	0.0107	0.0538	0.1982		500
81	87	0.0049	0.0381	0.1503		500
82	86	0.0072	0.0525	0.2354		500
82	90	0.0032	0.0341	0.2784		500
82	53	0.0041	0.077	0.1956		500
51	83	0.009	0.0454	0.1671		500
83	84	0.006	0.045	0.1841		500
83	52	0.0079	0.0593	0.2428		500
52	85	0.0058	0.0424	0.1867		500
86	89	0.0024	0.0176	0.0788		500
87	90	0.0025	0.0185	0.0829		500
88	90	0.0015	0.011	0.0494		500
89	53	0.0006	0.0068	0.0556		500
43	94	0.0002	0.0021	0.0173		500
92	54	0.0025	0.0184	0.0828		500
92	93	0.0014	0.0103	0.0463		500
92	55	0.0026	0.0192	0.0877		500
54	93	0.0022	0.0159	0.0715		500
95	55	0.0018	0.0197	0.1667		500
96	97	0.002	0.0163	0.0617		500
97	56	0.0027	0.0213	0.3219		500
97	98	0.0196	0.1545	0.1456		500
97	99	0.0111	0.0883	0.0886		500
98	58	0.0029	0.0216	0.0945		500
56	57	0.0041	0.0325	0.1228		500
99	98	0.0084	0.0689	0.0673		500
53	67	0.00127	0.0172	0.03588		500
59	52	0.0014	0.0208		1.052	900
79	148	0.0014	0.02231		1.0165	600

Table A.6 Line parameter of the 160-bus equivalent Thai power system (Continued)

From Bus	To Bus	R (p.u.)	X (p.u.)	B/2 (p.u.)	Tap Ratio	Limit MVA
148	82		0.02514		1.05217	600
79	149	0.0014	0.02231		1.0165	600
149	82		0.02514		1.05217	600
79	150	0.0014	0.02231		1.0165	500
150	82		0.02514		1.05217	500
91	67	0.0014	0.0208		1	500
91	46	0.0014	0.0208		1	500
44	101	0.0006	0.0645		1	200
44	102	0.0006	0.0645		1	200
45	103	0.0006	0.0705		0.9	300
46	104	0.0006	0.0705		0.9244	200
47	105	0.0003	0.03255		0.9625	200
48	106	0.0003	0.0364		1.05	200
49	107	0.0014	0.131		1.075	100
50	108	0.0014	0.1417		1.025	100
51	109	0.0014	0.1685		1.025	66.7
51	110	0.0014	0.1535		1.025	66.7
52	111	0.0003	0.03376		0.95	400
52	112	0.0014	0.17583		0.9025	100
54	113	0.00012	0.0137		0.9875	1000
55	114	0.0003	0.02629		1	400
56	115	0.0014	0.14283		1.025	100
57	116	0.0014	0.16447		1.025	66.7
58	117	0.0003	0.03625		1	400
66	118	0.0002	0.0215		1.01	600
67	119	0.0006	0.0705		1.0882	200
70	120	0.0002	0.0217		0.975	600
71	121	0.0006	0.0651		0.975	200
73	122	0.0003	0.03255		0.9625	400

Table A.6 Line parameter of the 160-bus equivalent Thai power system (Continued)

From Bus	To Bus	R (p.u.)	X (p.u.)	B/2 (p.u.)	Tap Ratio	Limit MVA
74	123	0.0002	0.022		0.9875	600
75	124	0.00047	0.04683		1.0375	300
76	125	0.0003	0.0364		0.9875	100
77	126	0.0006	0.07279		1	200
78	127	0.0002	0.02426		1	600
81	128	0.0014	0.063		1.025	200
82	129	0.0006	0.0651		1	200
82	130	0.0006	0.066		1	200
83	131	0.0014	0.063		1	200
84	132	0.0014	0.1417		1.025	100
85	133		0.03255		0.9875	400
86	134	0.0003	0.03377		1.03342	400
87	135	0.0003	0.03103		0.96386	400
88	136	0.0002	0.02251		0.988	600
89	137	0.00015	0.01688		0.9505	800
90	138	0.0002	0.0217		0.975	600
92	139	0.0002	0.02092		1	600
93	140	0.0002	0.02092		0.9875	600
94	141	0.0002	0.02092		1	600
95	142	0.0003	0.03138		0.9625	400
96	143		0.02417		1.0125	600
97	144	0.0003	0.03582		0.975	400
98	145	0.0007	0.06675		0.9875	200
99	146	0.0006	0.0725		0.964	200
100	147	0.00015	0.01813		0.925	800
43	1		0.0174		0.95	680
43	2		0.0174		0.95	680
43	3		0.0326		0.95	340
43	4		0.02766		1	368

Table A.6 Line parameter of the 160-bus equivalent Thai power system (Continued)

From Bus	To Bus	R (p.u.)	X (p.u.)	B/2 (p.u.)	Tap Ratio	Limit MVA
44	5		0.0383		0.95	225
44	6		0.0383		0.95	225
44	7		0.0317		0.95	370
44	8		0.0317		0.95	370
44	9		0.0317		0.95	370
44	10		0.02608		0.95	425
44	11		0.02608		0.95	425
45	12		0.12987		1	125
46	13		0.06523		0.95	170
47	14		0.013		0.95	850
48	15		0.0442		0.95	270
49	16		0.04246		0.95	425
49	17		0.04246		0.95	425
50	18		0.01738		0.975	696
51	19		0.03613		1	450
52	20		0.0731		0.95	171
52	21		0.0731		0.95	171
52	22		0.0731		0.95	171
53	23		0.01276		1	750
53	24		0.01276		1	750
54	25		0.01956		0.95	570
54	26		0.01956		0.95	570
54	27		0.01956		0.95	570
55	28		0.0174		1.1	680
55	29		0.0174		1.1	680
55	30		0.02174		0.95	510
55	31		0.02174		0.95	510
56	32		0.02805		0.97	300
56	33		0.0291		0.95	440

Table A.6 Line parameter of the 160-bus equivalent Thai power system (Continued)

From Bus	To Bus	R (p.u.)	X (p.u.)	B/2 (p.u.)	Tap Ratio	Limit MVA
57	34		0.03077		0.975	333.3
58	35		0.0397		0.975	300
59	36		0.0317		0.975	370
59	37		0.0317		0.975	370
59	38		0.0317		0.975	370
59	39		0.0317		0.975	370
159	40		0.11		0.975	90
159	41		0.1144		0.975	90
159	42		0.1133		0.975	105
159	160		0.00721		1.0507	200
159	60	0.0006	0.07246		1.025	200

Table A.7 Modified generation cost and emission coefficients for generating units in the 160-bus equivalent Thai power system

Bus No.	Generation cost			Carbon emission			P_G^{min} (MW)	P_G^{max} (MW)
	a (\$/MW^{2}h)	b (\$/MWh)	c (\$/h)	α (t/p.u.^{2}h)	β (t/p.u.h)	ω (t/h)		
1	43519.17	914.926	0.0012	0	0.558	0	240	3100
2	48211.38	913.503	0.0011	0	0.558	0	100	510
3	-21402.9	1186.901	0.0297	0	0.558	0	100	500
4	-23886.2	1202.975	0.0322	0	0.558	0	100	410
5	20825.59	969.934	0.1732	0	0.558	0	80	150
6	19623.75	989.860	0.1306	0	0.558	0	80	150
7	23407.79	980.789	0.0127	0	0.558	0	186	250
8	23376.01	979.458	0.0127	0	0.558	0	186	225
9	23396.59	980.323	0.0127	0	0.558	0	186	400
10	34072.57	-298.463	3.9100	0	0.558	0	120	250
11	-13071.1	917.5457	0.3649	0	0.558	0	120	450
12	34072.57	-298.463	3.9100	0	0.558	0	18	2030
13	34072.57	-298.463	3.9100	0	0.73	0	18	340

Table A.7 Modified generation cost and emission coefficients for generating units in the 160-bus equivalent Thai power system (Continued)

Bus No.	Generation cost			Carbon emission			P_G^{min} (MW)	P_G^{max} (MW)
	a (\$/MW^{2}h)	b (\$/MWh)	c (\$/h)	α (t/p.u^{2}h)	β (t/p.u.h)	ω (t/h)		
14	43519.17	914.926	0.0012	0	0.558	0	100	460
15	0	0	0	0	0	0	100	100
16	7576.921	876.873	0.3888	0	0.558	0	220	381
17	9215.791	958.689	0.6816	0	0.558	0	220	796
18	0	0	0	0	0	0	150	150
19	0	0	0	0	0	0	200	200
20	3058.372	441.381	0.0462	0	0.876	0	100	203
21	3082.437	444.742	0.0466	0	0.876	0	100	472
22	3071.661	443.200	0.0465	0	0.876	0	100	316
23	0	922.151	0.3476	0	0.558	0	100	500
24	0	982.104	0.4344	0	0.558	0	220	500
25	-53553.5	1380.261	1.1955	0	0.558	0	100	250
26	-55517.6	1408.05	1.3486	0	0.558	0	200	250
27	-13154.4	984.040	0.4014	0	0.558	0	184	250
28	36843.24	858.008	0.0623	0	0.558	0	300	320
29	36782.98	856.602	0.0622	0	0.558	0	320	1300
30	-55760.9	1362.416	1.3033	0	0.558	0	120	1300
31	-32118	1149.104	0.8689	0	0.558	0	120	575
32	0	0	0	0	0	0	200	200
33	0	0	0	0	0	0	300	300
34	0	0	0	0	0	0	200	200
35	0	0	0	0	0.558	0	0	0
36	20963.1	278.445	0.2309	0	0.876	0	180	550
37	20801.48	276.301	0.2291	0	0.876	0	180	350
38	20746.63	275.568	0.2285	0	0.876	0	180	403
39	20856.76	277.034	0.2297	0	0.876	0	180	445
40	9011.999	925.424	1.02	0	0.558	0	60	400
41	6906.259	1019.99	0.1553	0	0.558	0	60	700
42	7430.474	953.987	0.3381	0	0.558	0	60	350

Table A.8 AGC and SR offered prices and quantities of 160-bus equivalent Thai power system

Bus No.	AGC		SR		Bus No.	AGC		SR	
	MW	$/MW	MW	$/MW		MW	$/MW	MW	$/MW
1	480	122	480	197	22	63	124	63	137
2	48	153	48	179	23	44	78	44	159
3	32	104	32	106	24	61	196	61	108
4	20	91	20	112	25	40	100	40	145
5	20	68	20	60	26	66	59	66	147
6	20	102	20	153	27	40	140	40	193
7	95	177	95	80	28	64	109	64	159
8	51	150	51	185	29	260	182	260	200
9	78	68	78	171	30	260	59	260	195
10	34	123	34	65	31	115	114	115	77
11	43	141	43	76	32	0	0	0	0
12	406	74	406	73	33	0	0	0	0
13	68	56	68	159	34	0	0	0	0
14	32	157	32	80	35	0	0	0	0
15	0	0	0	0	36	110	95	110	79
16	76	194	76	134	37	70	86	70	103
17	159	114	159	165	38	81	152	81	92
18	0	0	0	0	39	89	148	89	94
19	0	0	0	0	40	80	168	80	144
20	41	53	41	176	41	140	200	140	143
21	94	117	94	188	42	70	99	70	141

APPENDIX B
ADDITIONAL SIMULATION RESULTS

B.1 Hyperparameter Sensitivity Analyses

The hyperparameter sensitivity analyses were conducted for all four stochastic optimisation algorithms, which are summarised in Table 3.2 of Chapter 3. Each algorithm was simulated under systematically varied hyperparameter settings, such as the inertia weight for PSO, control coefficients for BWO, leadership and encircling parameters for GWO, and exploration–exploitation factors for WOA, to evaluate their influence on convergence behaviour, solution quality, and computational robustness. The resulting performance patterns from these simulations are illustrated in Figure B.1, which presents a comprehensive comparison of the algorithms under the full range of tested configurations. This appendix, therefore, serves to supplement the main chapter by offering detailed visual and analytical insights into how hyperparameter adjustments affect algorithmic performance.

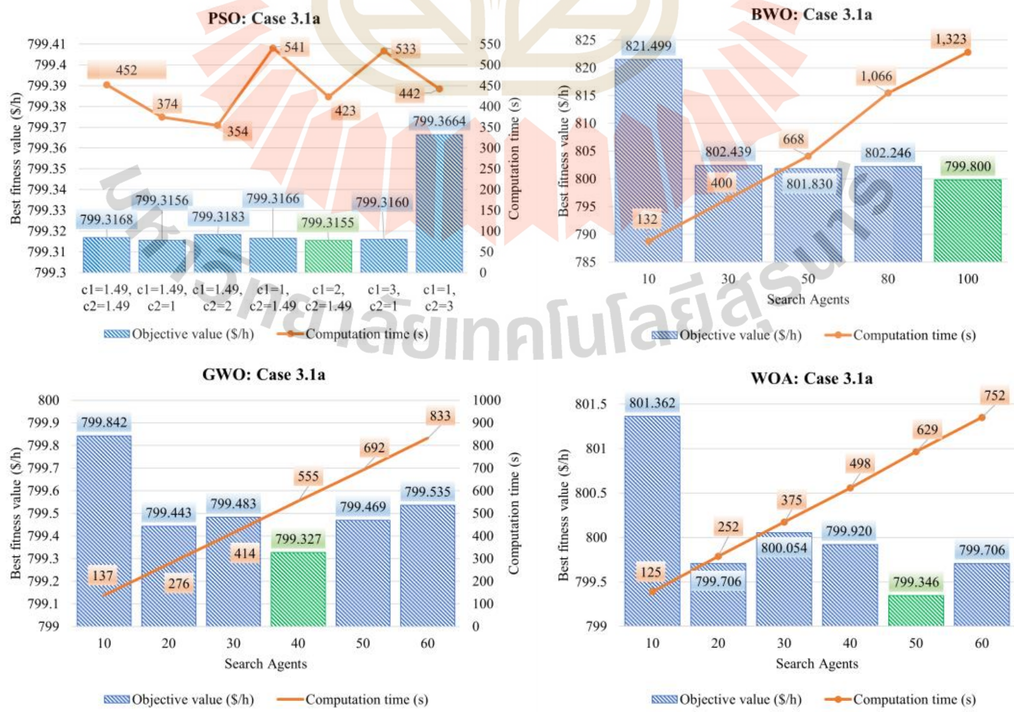

(a) Case 3.1a: Conventional single-side auction scheme

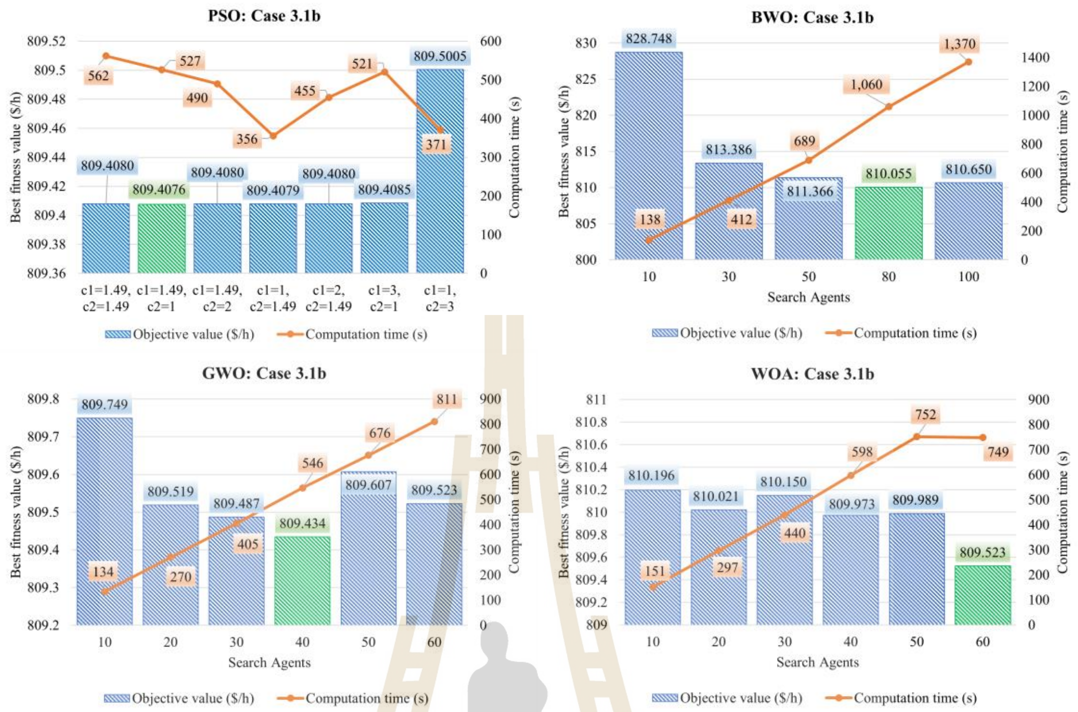

(b) Case 3.1b: Carbon-accounted single-side auction scheme

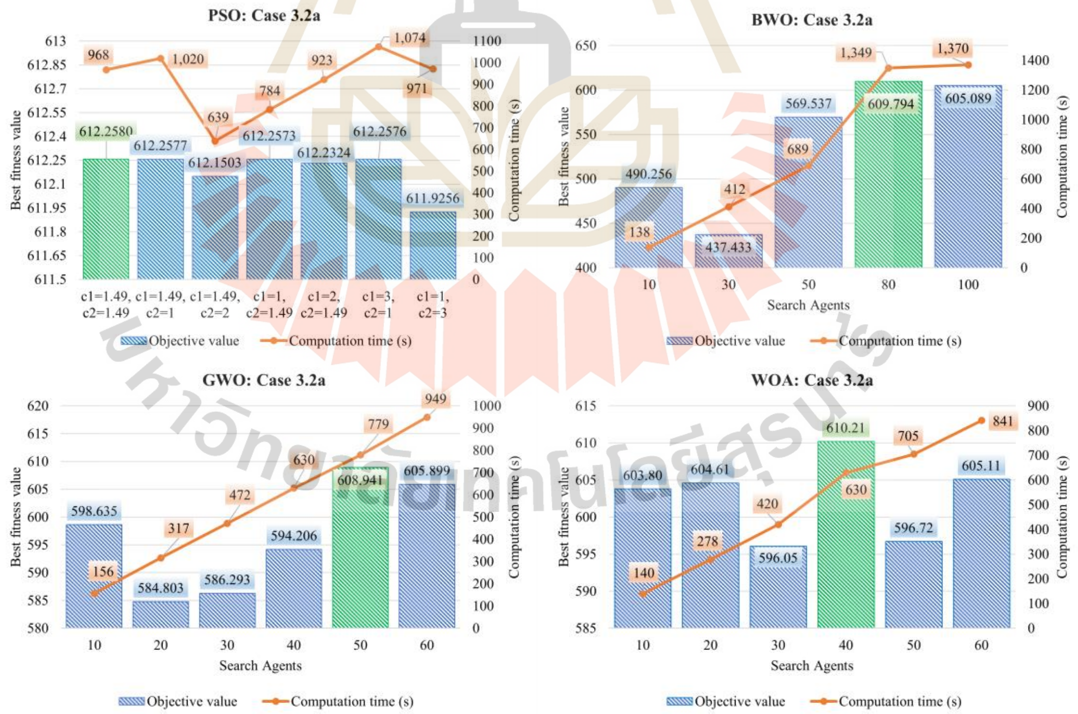

(c) Case 3.2a: Conventional double-side auction scheme

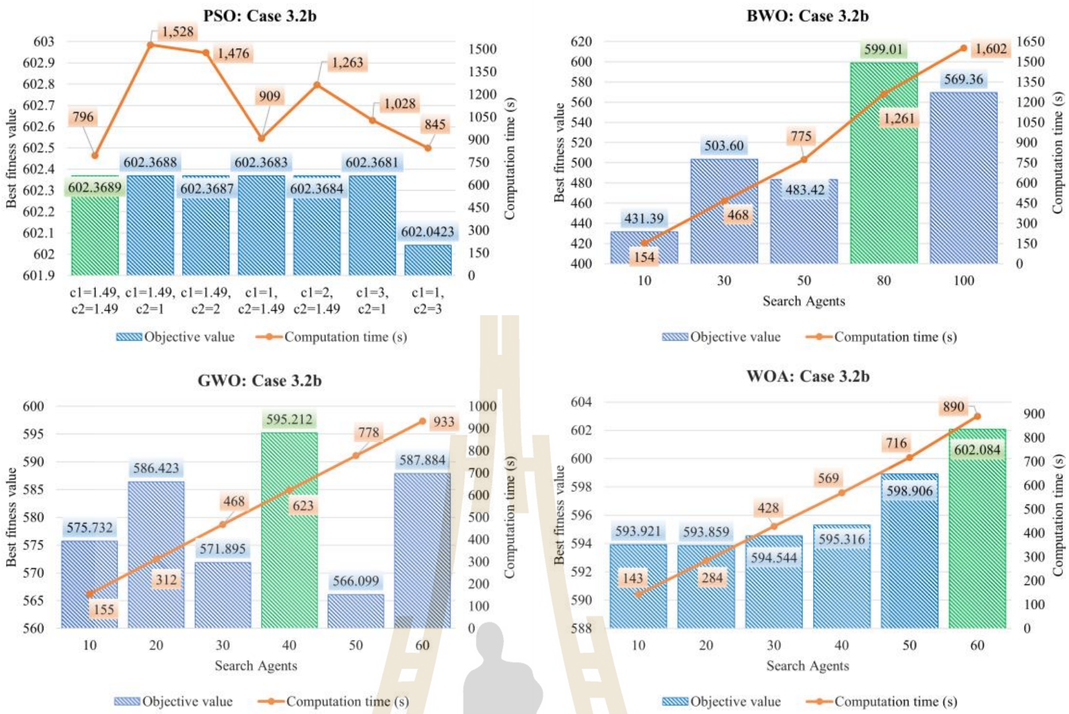

(d) Case 3.2b: Carbon-accounted double-side auction scheme

Figure B.1 Hyperparameter sensitivity analysis in different optimisation algorithms

B.2 Additional Simulation Results

This appendix presents supplementary optimisation results for the multi-dimensional market framework. The tables report the final values of the control variables obtained from two solution approaches, (i) QP method and (ii) the hybrid PSO-QP method. These results complement the summary tables in Chapter 6 by providing full optimised outputs for all decision variables under each method, thereby enabling a more detailed comparison of solution performance. Table B.1 reports the complete set of optimised control variables derived from the QP-based solution, illustrating the deterministic behaviour of the convex optimisation model. Moreover, Table B.2 presents the corresponding results from the hybrid PSO-QP method, highlighting the improvements achieved when combining stochastic search with deterministic refinement.

Table B.1 Optimised control variable results obtained using QP method for the multi-dimensional market framework

Variable	Case 6.0	Case 6.1	Case 6.2	Case 6.3	Case 6.4	Variable	Case 6.0	Case 6.1	Case 6.2	Case 6.3	Case 6.4
$P_{G,1}$ (MW)	3100	3100	3100	3100	3100	$P_{G,18}$ (MW)	150	150	150	150	150
$P_{G,2}$ (MW)	510	510	510	510	510	$P_{G,19}$ (MW)	200	200	200	200	200
$P_{G,3}$ (MW)	500	500	500	500	500	$P_{G,20}$ (MW)	203	203	203	203	203
$P_{G,2}$ (MW)	410	410	410	410	410	$P_{G,21}$ (MW)	472	472	472	472	472
$P_{G,5}$ (MW)	150	150	150	150	150	$P_{G,22}$ (MW)	316	316	316	316	316
$P_{G,6}$ (MW)	150	150	150	150	150	$P_{G,23}$ (MW)	500	500	500	500	500
$P_{G,7}$ (MW)	250	250	250	250	250	$P_{G,24}$ (MW)	500	500	500	500	500
$P_{G,8}$ (MW)	225	225	225	225	225	$P_{G,25}$ (MW)	250	250	250	250	250
$P_{G,9}$ (MW)	400	400	400	400	400	$P_{G,26}$ (MW)	250	250	250	200	200
$P_{G,10}$ (MW)	250	250	250	241.5045	217.9716	$P_{G,27}$ (MW)	250	250	250	250	250
$P_{G,11}$ (MW)	450	450	450	450	450	$P_{G,28}$ (MW)	320	320	320	320	320
$P_{G,12}$ (MW)	443.318	429.065	427.905	418.311	390.092	$P_{G,29}$ (MW)	1300	1300	1300	1300	1300
$P_{G,13}$ (MW)	340	340	340	295.415	270.862	$P_{G,30}$ (MW)	692.786	650.029	646.550	617.765	533.109
$P_{G,14}$ (MW)	460	460	460	460	460	$P_{G,31}$ (MW)	575	575	575	433.310	345
$P_{G,15}$ (MW)	100	100	100	100	100	$P_{G,32}$ (MW)	200	200	200	200	200
$P_{G,16}$ (MW)	381	381	381	381	381	$P_{G,33}$ (MW)	300	300	300	300	300
$P_{G,17}$ (MW)	796	796	796	552.400	478	$P_{G,34}$ (MW)	200	200	200	200	200

Table B.1 Optimised control variable results obtained using QP method for the multi-dimensional market framework (Continued)

Variable	Case 6.0	Case 6.1	Case 6.2	Case 6.3	Case 6.4	Variable	Case 6.0	Case 6.1	Case 6.2	Case 6.3	Case 6.4
$P_{G,35}$ (MW)	0	0	0	0	0	$P_{D,10}$ (MW)	452.813	452.813	452.813	452.813	452.813
$P_{G,36}$ (MW)	550	550	550	550	550	$P_{D,11}$ (MW)	54.938	54.938	54.938	54.938	54.938
$P_{G,37}$ (MW)	350	350	350	350	350	$P_{D,12}$ (MW)	93	93	93	93	93
$P_{G,38}$ (MW)	403	403	403	403	403	$P_{D,13}$ (MW)	228.938	228.938	228.938	228.938	228.938
$P_{G,39}$ (MW)	445	445	445	445	445	$P_{D,14}$ (MW)	228.563	228.563	228.563	228.563	228.563
$P_{G,40}$ (MW)	400	400	400	400	391.967	$P_{D,15}$ (MW)	90.375	90.375	90.375	90.375	90.375
$P_{G,41}$ (MW)	700	700	700	700	700	$P_{D,16}$ (MW)	284.438	284.438	284.438	284.438	284.438
$P_{G,42}$ (MW)	350	350	350	350	350	$P_{D,17}$ (MW)	433.875	433.875	433.875	433.875	433.875
$P_{D,1}$ (MW)	96.581	96.581	96.581	96.581	96.581	$P_{D,18}$ (MW)	333.375	333.375	333.375	333.375	333.375
$P_{D,2}$ (MW)	1037.438	1037.438	1037.438	1037.438	1037.438	$P_{D,19}$ (MW)	136.5	136.5	136.5	136.5	136.5
$P_{D,3}$ (MW)	558.375	558.375	558.375	558.375	558.375	$P_{D,20}$ (MW)	55.875	55.875	55.875	55.875	55.875
$P_{D,4}$ (MW)	1200.75	1200.75	1200.75	1200.75	1200.75	$P_{D,21}$ (MW)	56.625	56.625	56.625	56.625	56.625
$P_{D,5}$ (MW)	0	0	623.124	0	0	$P_{D,22}$ (MW)	0	0	467.625	0	467.625
$P_{D,6}$ (MW)	662.835	605.826	1570.313	74.437	1570.313	$P_{D,23}$ (MW)	150.938	150.938	150.938	150.938	150.938
$P_{D,7}$ (MW)	673.875	673.875	673.875	673.875	673.875	$P_{D,24}$ (MW)	465	465	465	465	465
$P_{D,8}$ (MW)	912.938	912.938	912.938	912.938	912.938	$P_{D,25}$ (MW)	257.25	257.25	257.25	257.25	257.25
$P_{D,9}$ (MW)	639	639	639	639	639	$P_{D,26}$ (MW)	79.125	79.125	79.125	79.125	79.125

Table B.1 Optimised control variable results obtained using QP method for the multi-dimensional market framework (Continued)

Variable	*Case 6.0*	*Case 6.1*	*Case 6.2*	*Case 6.3*	*Case 6.4*	*Variable*	*Case 6.0*	*Case 6.1*	*Case 6.2*	*Case 6.3*	*Case 6.4*
$P_{D,27}$ (MW)	6.188	6.188	6.187	6.187	6.188	$P_{D,44}$ (MW)	367.5	367.5	367.5	367.5	367.5
$P_{D,28}$ (MW)	80.25	80.25	80.25	80.25	80.25	$P_{D,45}$ (MW)	391.5	391.5	391.5	391.5	391.5
$P_{D,29}$ (MW)	371.25	371.25	371.25	371.25	371.25	$P_{D,46}$ (MW)	161.25	161.25	161.25	161.25	161.25
$P_{D,30}$ (MW)	301.875	301.875	301.875	301.875	301.875	$P_{D,47}$ (MW)	345.938	345.938	345.938	345.938	345.938
$P_{D,31}$ (MW)	639.563	639.563	639.563	639.563	639.563	$P_{D,48}$ (MW)	867	867	867	867	867
$P_{D,32}$ (MW)	130.688	130.688	130.688	130.688	130.688	$P_{D,49}$ (MW)	316.125	316.125	316.125	316.125	316.125
$P_{D,33}$ (MW)	525.375	525.375	525.375	525.375	525.375	$P_{D,50}$ (MW)	566.438	566.438	566.438	566.438	566.438
$P_{D,34}$ (MW)	446.625	446.625	446.625	446.625	446.625	$P_{D,51}$ (MW)	114.188	114.188	114.188	114.188	114.188
$P_{D,35}$ (MW)	338.063	338.063	338.063	338.063	338.063	$P_{D,52}$ (MW)	207	207	207	207	207
$P_{D,36}$ (MW)	258	258	258	258	258	$P_{D,53}$ (MW)	274.125	274.125	274.125	274.125	274.125
$P_{D,37}$ (MW)	164.813	164.813	164.813	164.813	164.813	$P_{D,54}$ (MW)	527.625	527.625	527.625	527.625	527.625
$P_{D,38}$ (MW)	0	0	460.125	0	224.795	$P_{D,55}$ (MW)	237.375	237.375	237.375	237.375	237.375
$P_{D,39}$ (MW)	0	0	0	0	0	$P_{D,56}$ (MW)	131.25	131.25	131.25	131.25	131.25
$P_{D,40}$ (MW)	95.25	95.25	95.25	95.25	95.25	$P_{D,57}$ (MW)	179.813	179.813	179.813	179.813	179.813
$P_{D,41}$ (MW)	94.688	94.688	94.688	94.688	94.688	$P_{D,58}$ (MW)	966	966	966	966	966
$P_{D,42}$ (MW)	85.875	85.875	85.875	85.875	85.875	$P_{D,59}$ (MW)	332.063	332.063	332.063	332.063	332.063
$P_{D,43}$ (MW)	85	85	85	85	85	AGC_1 (MW)	0	0	0	0	0

Table B.1 Optimised control variable results obtained using QP method for the multi-dimensional market framework (Continued)

Variable	Case 6.0	Case 6.1	Case 6.2	Case 6.3	Case 6.4	Variable	Case 6.0	Case 6.1	Case 6.2	Case 6.3	Case 6.4
AGC_2 (MW)	0	0	0	0	0	AGC_{19} (MW)	0	0	0	0	0
AGC_3 (MW)	0	0	0	0	0	AGC_{20} (MW)	0	0	0	0	0
AGC_4 (MW)	0	0	0	0	0	AGC_{21} (MW)	0	0	0	0	0
AGC_2 (MW)	0	0	0	0	0	AGC_{22} (MW)	0	0	0	0	0
AGC_6 (MW)	0	0	0	0	0	AGC_{23} (MW)	0	0	0	0	0
AGC_7 (MW)	0	0	0	0	0	AGC_{24} (MW)	0	0	0	0	0
AGC_8 (MW)	0	0	0	0	0	AGC_{25} (MW)	0	0	0	0	0
AGC_9 (MW)	0	0	0	0	0	AGC_{26} (MW)	0	0	0	50	46.433
AGC_{10} (MW)	0	0	0	8.495	32.028	AGC_{27} (MW)	0	0	0	0	0
AGC_{11} (MW)	0	0	0	0	0	AGC_{28} (MW)	0	0	0	0	0
AGC_{12} (MW)	0	0	0	406	406	AGC_{29} (MW)	0	0	0	0	0
AGC_{13} (MW)	0	0	0	0	1.1383	AGC_{30} (MW)	0	0	0	260	260
AGC_{14} (MW)	0	0	0	0	0	AGC_{31} (MW)	0	0	0	26.690	115
AGC_{15} (MW)	0	0	0	0	0	AGC_{32} (MW)	0	0	0	0	0
AGC_{16} (MW)	0	0	0	0	0	AGC_{33} (MW)	0	0	0	0	0
AGC_{17} (MW)	0	0	0	159	159	AGC_{34} (MW)	0	0	0	0	0
AGC_{18} (MW)	0	0	0	0	0	AGC_{35} (MW)	0	0	0	0	0

Table B.1 Optimised control variable results obtained using QP method for the multi-dimensional market framework (Continued)

Variable	Case 6.0	Case 6.1	Case 6.2	Case 6.3	Case 6.4	Variable	Case 6.0	Case 6.1	Case 6.2	Case 6.3	Case 6.4
AGC_{36} (MW)	0	0	0	0	0	SR_{11} (MW)	0	0	0	0	0
AGC_{37} (MW)	0	0	0	0	0	SR_{12} (MW)	0	0	0	406	406
AGC_{38} (MW)	0	0	0	0	0	SR_{13} (MW)	0	0	0	44.585	68
AGC_{39} (MW)	0	0	0	0	0	SR_{14} (MW)	0	0	0	0	0
AGC_{40} (MW)	0	0	0	0	0	SR_{15} (MW)	0	0	0	0	0
AGC_{41} (MW)	0	0	0	0	0	SR_{16} (MW)	0	0	0	0	0
AGC_{42} (MW)	0	0	0	0	0	SR_{17} (MW)	0	0	0	84.6	159
SR_{1} (MW)	0	0	0	0	0	SR_{18} (MW)	0	0	0	0	0
SR_{2} (MW)	0	0	0	0	0	SR_{19} (MW)	0	0	0	0	0
SR_{3} (MW)	0	0	0	0	0	SR_{20} (MW)	0	0	0	0	0
SR_{4} (MW)	0	0	0	0	0	SR_{21} (MW)	0	0	0	0	0
SR_{5} (MW)	0	0	0	0	0	SR_{22} (MW)	0	0	0	0	0
SR_{6} (MW)	0	0	0	0	0	SR_{23} (MW)	0	0	0	0	0
SR_{7} (MW)	0	0	0	0	0	SR_{24} (MW)	0	0	0	0	0
SR_{8} (MW)	0	0	0	0	0	SR_{25} (MW)	0	0	0	0	0
SR_{9} (MW)	0	0	0	0	0	SR_{26} (MW)	0	0	0	0	3.567
SR_{10} (MW)	0	0	0	0	0	SR_{27} (MW)	0	0	0	0	0

Table B.1 Optimised control variable results obtained using QP method for the multi-dimensional market framework (Continued)

Variable	Case 6.0	Case 6.1	Case 6.2	Case 6.3	Case 6.4	Variable	Case 6.0	Case 6.1	Case 6.2	Case 6.3	Case 6.4
SR_{28} (MW)	0	0	0	0	0	SR_{38} (MW)	0	0	0	0	0
SR_{29} (MW)	0	0	0	0	0	SR_{39} (MW)	0	0	0	0	0
SR_{30} (MW)	0	0	0	260	260	SR_{40} (MW)	0	0	0	0	8.033
SR_{31} (MW)	0	0	0	115	115	SR_{41} (MW)	0	0	0	0	0
SR_{32} (MW)	0	0	0	0	0	SR_{42} (MW)	0	0	0	0	0
SR_{33} (MW)	0	0	0	0	0	$P_{RE,1}$ (MW)	0	0	400	0	400
SR_{34} (MW)	0	0	0	0	0	$P_{RE,2}$ (MW)	0	0	750	0	750
SR_{35} (MW)	0	0	0	0	0	$P_{RE,3}$ (MW)	0	0	300	0	300
SR_{36} (MW)	0	0	0	0	0	$P_{RE,4}$ (MW)	0	0	650	0	650
SR_{37} (MW)	0	0	0	0	0	$P_{RE,5}$ (MW)	0	0	420	0	420

Table B.2 Optimised control variable results obtained using the hybrid PSO-QP method for the multi-dimensional market framework

Variable	Case 6.0	Case 6.1	Case 6.2	Case 6.3	Case 6.4	Variable	Case 6.0	Case 6.1	Case 6.2	Case 6.3	Case 6.4
V_1 (p.u.)	0.95	0.990	1.009	0.996	0.955	V_{18} (p.u.)	0.965	0.95	0.956	0.975	1.012
V_2 (p.u.)	0.960	1.043	0.969	0.95	1.003	V_{19} (p.u.)	0.95	0.968	1.027	1.05	1.022
V_3 (p.u.)	0.95	0.984	1.007	0.978	0.994	V_{20} (p.u.)	0.95	1.035	1.05	1.05	1.003
V_4 (p.u.)	1.05	0.955	0.970	0.95	0.988	V_{21} (p.u.)	1.013	0.996	0.969	0.968	0.994
V_5 (p.u.)	0.95	1.032	0.971	0.970	0.961	V_{22} (p.u.)	0.95	1.024	0.956	1.037	0.973
V_6 (p.u.)	1.006	0.986	1.046	1.003	1.004	V_{23} (p.u.)	1.028	0.95	0.973	1.025	0.990
V_7 (p.u.)	1.046	0.976	0.95	1.012	1.004	V_{24} (p.u.)	1.045	0.969	1.028	0.991	0.994
V_8 (p.u.)	0.971	0.95	0.95	0.984	1.004	V_{25} (p.u.)	1.035	0.957	1.001	1.033	0.994
V_9 (p.u.)	0.95	1.042	0.95	0.965	0.993	V_{26} (p.u.)	1.041	0.956	1.003	1.05	0.994
V_{10} (p.u.)	0.95	0.961	0.957	0.95	1.019	V_{27} (p.u.)	1.05	0.972	1.001	0.968	0.950
V_{11} (p.u.)	1.05	0.954	1.040	1.016	1.004	V_{28} (p.u.)	0.95	1.026	1.044	1.041	1.004
V_{12} (p.u.)	0.959	0.993	0.978	0.95	0.995	V_{29} (p.u.)	0.955	0.963	0.999	1.05	0.995
V_{13} (p.u.)	0.95	0.958	1.001	1.016	1.002	V_{30} (p.u.)	1.016	0.986	1.012	1.022	1.005
V_{14} (p.u.)	1.05	0.950	0.996	1.05	1.004	V_{31} (p.u.)	1.05	1.027	1.011	1.008	0.995
V_{15} (p.u.)	0.95	0.985	1.011	1.030	0.995	V_{32} (p.u.)	0.957	0.95	1.05	0.978	0.993
V_{16} (p.u.)	0.961	0.95	0.960	0.95	0.995	V_{33} (p.u.)	0.95	0.982	0.988	1.026	0.994
V_{17} (p.u.)	1.017	1.019	0.967	0.95	0.995	V_{34} (p.u.)	1.007	1.004	1.048	1.005	1.006

Table B.2 Optimised control variable results obtained using the hybrid PSO-QP method for the multi-dimensional market framework (Continued)

Variable	Case 6.0	Case 6.1	Case 6.2	Case 6.3	Case 6.4	Variable	Case 6.0	Case 6.1	Case 6.2	Case 6.3	Case 6.4
V_{35} (p.u.)	0.95	0.956	1.002	1.028	1.038	T_{9} (p.u.)	0.945	0.941	1.036	0.914	1.014
V_{36} (p.u.)	0.936	1.1	1.041	1.081	0.990	T_{10} (p.u.)	0.972	1.003	0.965	0.919	0.994
V_{37} (p.u.)	0.921	0.907	0.958	1.016	1.053	T_{11} (p.u.)	0.939	1.044	0.915	0.987	1.031
V_{38} (p.u.)	0.925	1.021	0.936	0.996	1.010	T_{12} (p.u.)	1.024	1.1	1.085	1.064	0.985
V_{39} (p.u.)	0.958	0.966	1.020	1.026	0.998	T_{13} (p.u.)	1.000	1.028	1.039	0.930	0.989
V_{40} (p.u.)	0.943	1.035	0.960	1.041	1.052	T_{14} (p.u.)	1.036	1.065	0.974	1.073	0.966
V_{41} (p.u.)	1.020	1.1	1.066	1.1	1.057	T_{15} (p.u.)	0.9	0.946	1.1	1.042	0.948
V_{42} (p.u.)	1.016	1.084	1.013	1.060	0.962	T_{16} (p.u.)	0.922	0.931	1.067	0.971	0.947
T_{1} (p.u.)	1.055	1.008	0.927	1.044	0.943	T_{17} (p.u.)	1.028	1.060	0.989	0.9	1.043
T_{2} (p.u.)	0.948	0.931	1.077	0.908	0.991	T_{18} (p.u.)	1.1	1.042	0.936	1.012	1.084
T_{3} (p.u.)	1.001	0.927	1.035	0.935	0.936	T_{19} (p.u.)	1.003	1.080	1.022	0.979	0.987
T_{4} (p.u.)	1.053	1.057	1.049	1.036	0.987	T_{20} (p.u.)	0.999	1.003	0.924	1.1	0.987
T_{5} (p.u.)	1.059	0.993	1.064	0.921	0.989	T_{21} (p.u.)	1.062	0.956	1.053	0.994	0.957
T_{6} (p.u.)	1.062	1.001	1.014	0.908	0.991	T_{22} (p.u.)	1.1	1.028	1.034	0.9	1.037
T_{7} (p.u.)	0.945	1.024	1.044	1.1	0.987	T_{23} (p.u.)	0.995	0.905	0.923	1.007	0.986
T_{8} (p.u.)	1.022	1.051	0.947	0.946	0.994	T_{24} (p.u.)	1.088	1.013	1.011	0.983	0.995

Table B.2 Optimised control variable results obtained using the hybrid PSO-QP method for the multi-dimensional market framework (Continued)

Variable	Case 6.0	Case 6.1	Case 6.2	Case 6.3	Case 6.4	Variable	Case 6.0	Case 6.1	Case 6.2	Case 6.3	Case 6.4
T_{25} (p.u.)	0.955	1.020	1.008	0.923	0.988	T_{41} (p.u.)	0.903	0.988	1.026	0.9	0.949
T_{26} (p.u.)	1.083	0.900	0.930	1.053	0.968	T_{42} (p.u.)	0.9	0.9	1.1	1.040	1.053
T_{27} (p.u.)	1.073	1.054	1.076	0.983	1.035	T_{43} (p.u.)	1.1	1.062	1.1	1.031	0.985
T_{28} (p.u.)	1.021	0.943	1.085	0.985	0.990	T_{44} (p.u.)	0.9	1.093	1.041	0.907	1.024
T_{29} (p.u.)	1.025	0.923	1.007	0.983	0.976	T_{45} (p.u.)	0.937	0.908	0.902	0.962	1.009
T_{30} (p.u.)	0.902	1.064	1.037	1.017	0.990	$X_{C,1}$ (p.u.)	-4.503	-5	-2.419	-3.869	-4.028
T_{31} (p.u.)	1.073	0.9	0.987	1.010	1.042	$X_{C,2}$ (p.u.)	-4.133	-2.514	-3.666	-3.566	-3.354
T_{32} (p.u.)	1.006	1.018	1.033	0.9	0.922	$X_{C,3}$ (p.u.)	-5	-4.785	-2.856	-2	-2.304
T_{33} (p.u.)	0.931	1.057	0.989	1.0	0.928	$X_{C,4}$ (p.u.)	-5	-2.099	-2.608	-3.739	-2.999
T_{34} (p.u.)	1.022	1.100	1.070	1.1	0.988	$X_{C,5}$ (p.u.)	-4.663	-2.593	-3.713	-2.716	-4.019
T_{35} (p.u.)	1.072	1.049	1.055	0.939	1.009	$X_{C,6}$ (p.u.)	-5	-2.075	-3.435	-4.196	-4.025
T_{36} (p.u.)	1.1	0.937	1.059	1.1	1.008	$X_{C,7}$ (p.u.)	-4.110	-4.915	-4.622	-2.452	-3.999
T_{37} (p.u.)	1.025	1.036	0.977	0.974	1.010	$X_{C,8}$ (p.u.)	-3.851	-3.049	-3.225	-4.507	-3.004
T_{38} (p.u.)	0.977	1.018	0.948	0.973	1.010	$X_{C,9}$ (p.u.)	-3.795	-2.166	-4.809	-3.749	-3.873
T_{39} (p.u.)	0.978	1.1	0.976	0.990	0.990	$X_{C,10}$ (p.u.)	-5	-3.017	-2.830	-3.792	-3.992
T_{40} (p.u.)	0.991	1.058	1.028	1.005	0.999	$X_{C,11}$ (p.u.)	-4.835	-2	-2.257	-3.047	-3.094

Table B.2 Optimised control variable results obtained using the hybrid PSO-QP method for the multi-dimensional market framework (Continued)

Variable	Case 6.0	Case 6.1	Case 6.2	Case 6.3	Case 6.4	Variable	Case 6.0	Case 6.1	Case 6.2	Case 6.3	Case 6.4
$X_{C,12}$ (p.u.)	-2.403	-4.3942	-3.994	-3.153	-4.001	$P_{G,14}$ (MW)	460	460	460	460	460
$X_{C,13}$ (p.u.)	-3.466	-2.4851	-5	-4.714	-2.002	$P_{G,15}$ (MW)	100	100	100	100	100
$X_{C,14}$ (p.u.)	-4.379	-4.3394	-2.3810	-4.594	-4.003	$P_{G,16}$ (MW)	381	381	381	381	381
$P_{G,1}$ (MW)	107.855	100.7782	104.2273	102.736	100.013	$P_{G,17}$ (MW)	796	796	796	552.4	478
$P_{G,2}$ (MW)	510	510	510	510	510	$P_{G,18}$ (MW)	150	150	150	150	150
$P_{G,3}$ (MW)	500	500	500	500	500	$P_{G,19}$ (MW)	200	200	200	200	200
$P_{G,2}$ (MW)	410	410	410	410	410	$P_{G,20}$ (MW)	203	203	203	203	203
$P_{G,5}$ (MW)	150	150	150	150	150	$P_{G,21}$ (MW)	472	472	472	472	472
$P_{G,6}$ (MW)	150	150	150	150	150	$P_{G,22}$ (MW)	316	316	316	316	316
$P_{G,7}$ (MW)	250	250	250	250	250	$P_{G,23}$ (MW)	500	500	500	500	500
$P_{G,8}$ (MW)	225	225	225	225	225	$P_{G,24}$ (MW)	500	500	500	500	500
$P_{G,9}$ (MW)	400	400	400	400	400	$P_{G,25}$ (MW)	250	250	250	250	250
$P_{G,10}$ (MW)	250	250	250	241.505	217.972	$P_{G,26}$ (MW)	250	250	250	200	200
$P_{G,11}$ (MW)	450	450	450	450	450	$P_{G,27}$ (MW)	250	250	250	250	250
$P_{G,12}$ (MW)	443.318	429.065	427.905	418.311	390.092	$P_{G,28}$ (MW)	320	320	320	320	320
$P_{G,13}$ (MW)	340	340	340	295.415	270.862	$P_{G,29}$ (MW)	1300	1300	1300	1300	1300

Table B.2 Optimised control variable results obtained using the hybrid PSO-QP method for the multi-dimensional market framework (Continued)

Variable	Case 6.0	Case 6.1	Case 6.2	Case 6.3	Case 6.4	Variable	Case 6.0	Case 6.1	Case 6.2	Case 6.3	Case 6.4
$P_{G,30}$ (MW)	692.786	650.029	646.550	617.765	533.109	$P_{D,4}$ (MW)	1200.750	1200.750	1200.750	1200.750	1200.750
$P_{G,31}$ (MW)	575	575	575	433.31	345	$P_{D,5}$ (MW)	0	0	623.124	0	0
$P_{G,32}$ (MW)	200	200	200	200	200	$P_{D,6}$ (MW)	662.835	605.826	1570.313	74.437	1570.313
$P_{G,33}$ (MW)	300	300	300	300	300	$P_{D,7}$ (MW)	673.875	673.875	673.875	673.875	673.875
$P_{G,34}$ (MW)	200	200	200	200	200	$P_{D,8}$ (MW)	912.938	912.938	912.938	912.938	912.938
$P_{G,35}$ (MW)	0	0	0	0	0	$P_{D,9}$ (MW)	639	639	639	639	639
$P_{G,36}$ (MW)	550	550	550	550	550	$P_{D,10}$ (MW)	452.813	452.813	452.813	452.813	452.813
$P_{G,37}$ (MW)	350	350	350	350	350	$P_{D,11}$ (MW)	54.938	54.938	54.938	54.938	54.938
$P_{G,38}$ (MW)	403	403	403	403	403	$P_{D,12}$ (MW)	93	93	93	93	93
$P_{G,39}$ (MW)	445	445	445	445	445	$P_{D,13}$ (MW)	228.938	228.938	228.938	228.938	228.938
$P_{G,40}$ (MW)	400	400	400	400	391.967	$P_{D,14}$ (MW)	228.563	228.563	228.563	228.563	228.563
$P_{G,41}$ (MW)	700	700	700	700	700	$P_{D,15}$ (MW)	90.375	90.375	90.375	90.375	90.375
$P_{G,42}$ (MW)	350	350	350	350	350	$P_{D,16}$ (MW)	284.438	284.438	284.438	284.438	284.438
$P_{D,1}$ (MW)	96.581	96.581	96.581	96.581	96.581	$P_{D,17}$ (MW)	433.875	433.875	433.875	433.875	433.875
$P_{D,2}$ (MW)	1037.438	1037.438	1037.438	1037.438	1037.438	$P_{D,18}$ (MW)	333.375	333.375	333.375	333.375	333.375
$P_{D,3}$ (MW)	558.375	558.375	558.375	558.375	558.375	$P_{D,19}$ (MW)	136.5	136.5	136.5	136.5	136.5

Table B.2 Optimised control variable results obtained using the hybrid PSO-QP method for the multi-dimensional market framework (Continued)

Variable	Case 6.0	Case 6.1	Case 6.2	Case 6.3	Case 6.4	Variable	Case 6.0	Case 6.1	Case 6.2	Case 6.3	Case 6.4
$P_{D,20}$ (MW)	55.875	55.875	55.875	55.875	55.875	$P_{D,36}$ (MW)	258	258	258	258	258
$P_{D,21}$ (MW)	56.625	56.625	56.625	56.625	56.625	$P_{D,37}$ (MW)	164.813	164.813	164.813	164.813	164.813
$P_{D,22}$ (MW)	0	0	467.625	0	467.625	$P_{D,38}$ (MW)	0	0	460.125	0	224.795
$P_{D,23}$ (MW)	150.938	150.938	150.938	150.938	150.938	$P_{D,39}$ (MW)	0	0	0	0	0
$P_{D,24}$ (MW)	465	465	465	465	465	$P_{D,40}$ (MW)	95.25	95.25	95.25	95.25	95.25
$P_{D,25}$ (MW)	257.25	257.25	257.25	257.25	257.25	$P_{D,41}$ (MW)	94.688	94.688	94.688	94.688	94.688
$P_{D,26}$ (MW)	79.125	79.125	79.125	79.125	79.125	$P_{D,42}$ (MW)	85.875	85.875	85.875	85.875	85.875
$P_{D,27}$ (MW)	6.188	6.188	6.187	6.187	6.188	$P_{D,43}$ (MW)	85	85	85	85	85
$P_{D,28}$ (MW)	80.25	80.25	80.25	80.25	80.25	$P_{D,44}$ (MW)	367.5	367.5	367.5	367.5	367.5
$P_{D,29}$ (MW)	371.25	371.25	371.25	371.25	371.25	$P_{D,45}$ (MW)	391.5	391.5	391.5	391.5	391.5
$P_{D,30}$ (MW)	301.875	301.875	301.875	301.875	301.875	$P_{D,46}$ (MW)	161.25	161.25	161.25	161.25	161.25
$P_{D,31}$ (MW)	639.563	639.563	639.563	639.563	639.563	$P_{D,47}$ (MW)	345.938	345.938	345.938	345.938	345.938
$P_{D,32}$ (MW)	130.688	130.688	130.688	130.688	130.688	$P_{D,48}$ (MW)	867	867	867	867	867
$P_{D,33}$ (MW)	525.375	525.375	525.375	525.375	525.375	$P_{D,49}$ (MW)	316.125	316.125	316.125	316.125	316.125
$P_{D,34}$ (MW)	446.625	446.625	446.625	446.625	446.625	$P_{D,50}$ (MW)	566.438	566.438	566.438	566.438	566.438
$P_{D,35}$ (MW)	338.063	338.063	338.063	338.063	338.063	$P_{D,51}$ (MW)	114.188	114.188	114.188	114.188	114.188

Table B.2 Optimised control variable results obtained using the hybrid PSO-QP method for the multi-dimensional market framework (Continued)

Variable	Case 6.0	Case 6.1	Case 6.2	Case 6.3	Case 6.4	Variable	Case 6.0	Case 6.1	Case 6.2	Case 6.3	Case 6.4
$P_{D,52}$ (MW)	207	207	207	207	207	AGC_{9} (MW)	0	0	0	0	0
$P_{D,53}$ (MW)	274.125	274.125	274.125	274.125	274.125	AGC_{10} (MW)	0	0	0	8.495	32.028
$P_{D,54}$ (MW)	527.625	527.625	527.625	527.625	527.625	AGC_{11} (MW)	0	0	0	0	0
$P_{D,55}$ (MW)	237.375	237.375	237.375	237.375	237.375	AGC_{12} (MW)	0	0	0	406	406
$P_{D,56}$ (MW)	131.25	131.25	131.25	131.25	131.25	AGC_{13} (MW)	0	0	0	0	1.1383
$P_{D,57}$ (MW)	179.813	179.813	179.813	179.813	179.813	AGC_{14} (MW)	0	0	0	0	0
$P_{D,58}$ (MW)	966	966	966	966	966	AGC_{15} (MW)	0	0	0	0	0
$P_{D,59}$ (MW)	332.063	332.063	332.063	332.063	332.063	AGC_{16} (MW)	0	0	0	0	0
AGC_{1} (MW)	0	0	0	0	0	AGC_{17} (MW)	0	0	0	159	159
AGC_{2} (MW)	0	0	0	0	0	AGC_{18} (MW)	0	0	0	0	0
AGC_{3} (MW)	0	0	0	0	0	AGC_{19} (MW)	0	0	0	0	0
AGC_{4} (MW)	0	0	0	0	0	AGC_{20} (MW)	0	0	0	0	0
AGC_{2} (MW)	0	0	0	0	0	AGC_{21} (MW)	0	0	0	0	0
AGC_{6} (MW)	0	0	0	0	0	AGC_{22} (MW)	0	0	0	0	0
AGC_{7} (MW)	0	0	0	0	0	AGC_{23} (MW)	0	0	0	0	0
AGC_{8} (MW)	0	0	0	0	0	AGC_{24} (MW)	0	0	0	0	0

Table B.2 Optimised control variable results obtained using the hybrid PSO-QP method for the multi-dimensional market framework (Continued)

Variable	Case 6.0	Case 6.1	Case 6.2	Case 6.3	Case 6.4	Variable	Case 6.0	Case 6.1	Case 6.2	Case 6.3	Case 6.4
AGC_{25} (MW)	0	0	0	0	0	AGC_{41} (MW)	0	0	0	0	0
AGC_{26} (MW)	0	0	0	50	46.433	AGC_{42} (MW)	0	0	0	0	0
AGC_{27} (MW)	0	0	0	0	0	SR_{1} (MW)	0	0	0	0	0
AGC_{28} (MW)	0	0	0	0	0	SR_{2} (MW)	0	0	0	0	0
AGC_{29} (MW)	0	0	0	0	0	SR_{3} (MW)	0	0	0	0	0
AGC_{30} (MW)	0	0	0	260	260	SR_{4} (MW)	0	0	0	0	0
AGC_{31} (MW)	0	0	0	26.690	115	SR_{5} (MW)	0	0	0	0	0
AGC_{32} (MW)	0	0	0	0	0	SR_{6} (MW)	0	0	0	0	0
AGC_{33} (MW)	0	0	0	0	0	SR_{7} (MW)	0	0	0	0	0
AGC_{34} (MW)	0	0	0	0	0	SR_{8} (MW)	0	0	0	0	0
AGC_{35} (MW)	0	0	0	0	0	SR_{9} (MW)	0	0	0	0	0
AGC_{36} (MW)	0	0	0	0	0	SR_{10} (MW)	0	0	0	0	0
AGC_{37} (MW)	0	0	0	0	0	SR_{11} (MW)	0	0	0	0	0
AGC_{38} (MW)	0	0	0	0	0	SR_{12} (MW)	0	0	0	406	406
AGC_{39} (MW)	0	0	0	0	0	SR_{13} (MW)	0	0	0	44.585	68
AGC_{40} (MW)	0	0	0	0	0	SR_{14} (MW)	0	0	0	0	0

Table B.2 Optimised control variable results obtained using the hybrid PSO-QP method for the multi-dimensional market framework (Continued)

Variable	Case 6.0	Case 6.1	Case 6.2	Case 6.3	Case 6.4	Variable	Case 6.0	Case 6.1	Case 6.2	Case 6.3	Case 6.4
SR_{15} (MW)	0	0	0	0	0	SR_{31} (MW)	0	0	0	115	115
SR_{16} (MW)	0	0	0	0	0	SR_{32} (MW)	0	0	0	0	0
SR_{17} (MW)	0	0	0	84.6	159	SR_{33} (MW)	0	0	0	0	0
SR_{18} (MW)	0	0	0	0	0	SR_{34} (MW)	0	0	0	0	0
SR_{19} (MW)	0	0	0	0	0	SR_{35} (MW)	0	0	0	0	0
SR_{20} (MW)	0	0	0	0	0	SR_{36} (MW)	0	0	0	0	0
SR_{21} (MW)	0	0	0	0	0	SR_{37} (MW)	0	0	0	0	0
SR_{22} (MW)	0	0	0	0	0	SR_{38} (MW)	0	0	0	0	0
SR_{23} (MW)	0	0	0	0	0	SR_{39} (MW)	0	0	0	0	0
SR_{24} (MW)	0	0	0	0	0	SR_{40} (MW)	0	0	0	0	8
SR_{25} (MW)	0	0	0	0	0	SR_{41} (MW)	0	0	0	0	0
SR_{26} (MW)	0	0	0	0	3.567	SR_{42} (MW)	0	0	0	0	0
SR_{27} (MW)	0	0	0	0	0	$P_{RE,1}$ (MW)	0	0	400	0	400
SR_{28} (MW)	0	0	0	0	0	$P_{RE,2}$ (MW)	0	0	750	0	750
SR_{29} (MW	0	0	0	0	0	$P_{RE,3}$ (MW)	0	0	300	0	300
SR_{30} (MW	0	0	0	260	260	$P_{RE,4}$ (MW)	0	0	650	0	650
						$P_{RE,5}$ (MW)	0	0	420	0	420

APPENDIX C

PUBLICATION

Muangkhiew, P., & Chayakulkheeree, K. (2024). Carbon-Accounted Optimal Power Dispatch and Spot Pricing. 2024 IEEE/IAS Industrial and Commercial Power System Asia (I&CPS Asia). Pattaya, Thailand, pp. 671-676, https://doi.org/10.1109/ICPSAsia61913.2024.10761212.

Muangkhiew, P., & Chayakulkheeree, K. (2024). Optimizing social welfare: A double-sided auction approach for low-carbon emission power systems with renewable energy certificates. Journal of Renewable and Sustainable Energy, 16(5). https://doi.org/10.1063/5.0213399.

Muangkhiew, P., & Chayakulkheeree, K. (2025). Enhanced Carbon-Accounted Auction-Based Dispatch and Spot Pricing Using Stochastic Optimizations. IEEE Transactions on Industry Applications, 61(6), 8555-8569. https://doi.org/10.1109/TIA.2025.3571832.

BIOGRAPHY

Prakaipetch Muangkhiew received the B.Eng. degree in Electrical Engineering from Suranaree University of Technology (SUT), Thailand, in 2019, graduating with First Class Honors. She completed the M.Eng. degree in Electrical Engineering at SUT in 2021, where her thesis focused on probabilistic fuzzy multi-objective optimal power flow using particle swarm optimisation. She has completed the Ph.D. degree in Electrical Engineering at SUT, supported by the Royal Golden Jubilee Ph.D. Program Scholarship.

Her research interests encompass electricity market design, carbon pricing mechanisms, ancillary service procurement, renewable energy certificates, and optimisation-based market-clearing methodologies. She has been recognised with several academic distinctions, including the Best Paper Award at the 2024 IEEE IAS Industrial and Commercial Power System Asia and the 2021 International Electrical Engineering Congress.

In addition, she completed a visiting research placement at Lancaster University, United Kingdom, from August 2025 to January 2026, during which she collaborated on research on carbon accounting and integrated electricity market optimisation. Her work contributed to advancing efficient, reliable, and environmentally responsible market frameworks for future power systems.